

PHYSICAL MODELLING INVESTIGATION OF ROCK SCOUR EXTENT DUE TO A PLUNGING JET FOR TYPICAL HIGH HEAD DAMS

By
Marie Grace UMUMARARUNGU

*Thesis presented in fulfilment of the requirements for the degree of
Master of Engineering in the Faculty of Engineering at Stellenbosch
University*



Supervisor: Mrs Bosman Adele
Lecturer: Hydraulic Engineering, Stellenbosch University

March 2016

Declaration

By submitting this dissertation electronically, I declare that the entirety of the work contained therein is my own original work, that I am the owner of the copyright thereof (unless to the extent explicitly otherwise stated), and that I have not previously submitted it, in its entirety or in part, for obtaining any qualification.

Date: March 2016

Abstract

Hydraulic structures can release high-velocity plunging jets, which can result in scouring of the rock downstream of the structure. The extent of the scour hole must be predicted and analysed to ensure the safety of hydraulic structures. Many researches had developed empirical or semi-empirical formulae based on physical or prototype assessment. These formulae have limitations in estimating the scour hole shape, i.e. determining the pressure propagation in fissure or joints of rock and the velocity of the jet as it travels through the plunge pool.

A 1:40 scaled physical hydraulic model was constructed to determine the scour hole geometry in rock material. The main objective of the study was to determine the scour hole geometry formed in rock as a result of to an impinging jet by using a physical model and analysing the factors that cause scouring. The tests were conducted in two parts, namely the assessment of the scour hole geometry and secondly the measurement of the pressures inside the rock joints and the air concentration in the plunge pool.

In this research, the Erodibility Index developed by Annandale(1995) was used to quantify the relative ability of rock to resist the scour capacity of water. The Comprehensive Scour Model developed by Bollaert (2002; 2010; 2012) was also used to evaluate the ultimate scour depth. The physical model data was obtained in the laboratory at Stellenbosch University, South Africa, and were compared to the predicted results based on scour prediction methods found in the literature, namely the Comprehensive Scour model (Dynamic Impulsion and Quasi Steady Impulsion methods) and the Erodibility Index method. There was a reasonable difference between the physical model results and the prediction method results. The differences could be readily attributed to limitations of the laboratory (available pumping capacity, physical model scale and the density of the PVC blocks used for replicating rock blocks was lower than that of rock).

I would like to dedicate this dissertation work to my beloved family.

Acknowledgements

I would like to express my sincere gratitude to The Almighty for guidance, strength and endurance to successfully complete this task.

My sincere appreciation and gratitude are extended to the following persons and organisations that assisted in various ways during the course of this study:

Mrs Adele Bosman, lecturer in the department of Civil Engineering, Stellenbosch University, South Africa and my supervisor, for her advice and motivation.

Mr Mike George, Geo-Engineering doctoral student at University of California, Berkeley, for his guidance, continuous motivation and his willingness to share his superior knowledge.

Professor Dr Anton Schleiss, from Ecole Polytechnique Fédérale de Lausanne. I am deeply appreciative for your input, practical advice and interest in this research.

My gratitude goes to the laboratory assistance personnel of Stellenbosch, especially Christiaan Visser, for his assistance during the test phase.

Thanks are also addressed to my colleagues with whom I had the chance to directly collaborate, Dr Sawadogo Ousmane and Mr Kuria Kiringu, for their significant contributions in the field of sediment transportation.

I would like to thank African Union “Mwalimu Nyerere” for the scholarship that gave me the opportunity to conduct this study. It would not have been possible without the help from the kind souls.

Last, but certainly not least, I would like to express my love and gratitude for my parents, my sisters, my fiancé, in-laws, my friends and brethren of the Emmanuel community for your prayers and encouragement. Without their unconditional love and support, I would not have made it to where I am today.

“Nyagasani abahe umugisha usendereye”

Contents

DECLARATION	I
ABSTRACT	II
ACKNOWLEDGEMENTS	IV
LIST OF FIGURES	VIII
LIST OF TABLES	XI
LIST OF SYMBOLS	XIII
LIST OF ABBREVIATIONS	XVII
<u>CHAPTER 1 : INTRODUCTION</u>	<u>1</u>
1.1. BACKGROUND	1
1.2. ASPECTS OF ROCK SCOUR.....	1
1.3. ASPECT OF SCOUR TECHNOLOGY.....	1
1.4. STUDY OBJECTIVE.....	2
1.5. THEORETICAL FRAME WORK	2
1.6. LAYOUT OF THE RESEARCH.....	3
<u>CHAPTER 2. LITERATURE REVIEW</u>	<u>4</u>
2.1. BACKGROUND OF ROCK SCOURING.....	4
2.1.1. TYPES OF SCOUR	4
2.1.2. ROCK MASS.....	4
2.2. MAIN SCOUR PROCESS AND PARAMETERS OF ROCK SCOUR.....	5
2.2.1 FREE FALLING JET	6
2.2.2 JET DIFFUSION WITHIN THE PLUNGE POOL.....	8
2.2.3 SEDIMENT CHARACTERISTICS.....	12
2.3. PHASES OF SCOUR DEVELOPMENT	12
2.4. ROCK SCOUR PREDICTIONS METHODS	13
2.4.1 EMPIRICAL METHODS.....	14
2.4.2 SEMI-EMPIRICAL METHODS	18
2.4.2.1. ERODIBILITY INDEX (EI).....	18
2.4.2.2. STREAM POWER.....	19
2.4.3 PHYSICAL-MECHANICAL METHOD (COMPREHENSIVE SCOUR MODEL)	20
2.4.3.1. COMPREHENSIVE FRACTURE MECHANICS METHOD.....	28
2.4.3.2. DYNAMIC IMPULSION METHOD	30
2.4.3.3. QUASI-STEADY IMPULSION METHOD	33
2.5. PRACTICAL APPLICATION OF SCOUR PREDICTION METHODS.....	36
2.6.1 KARIBA DAM.....	36
2.6. SCALE PHYSICAL MODEL TEST FOR SPILLWAY	38
2.7.1 LIMITATION OF SCALING	39
2.7. SUMMARY	39
<u>CHAPTER 3. TESTING SETUP AND INVESTIGATION OF ROCK SCOUR</u>	<u>41</u>
3.1. MODEL SETUP.....	41

3.2	MEASUREMENT EQUIPMENT	44
3.2.1	MEASUREMENT OF WATER LEVELS	44
3.2.2	DISCHARGE MEASUREMENT.....	44
3.2.3	JET AIR ENTRAINMENT MEASUREMENT	45
3.3	HYDRAULIC PARAMETERS	45
3.3.1	FALLING JET	45
3.3.2	PLUNGE POOL AERATION	47
3.3.3	ROCK MASS.....	49
3.3.3.1	ROCK SIZE, SHAPE AND DENSITY	49
3.3.3.2	SETTLING VELOCITY.....	50
3.3.3.3	SPECIFIC GRAVITY.....	50
3.3.3.4	THE DRAG COEFFICIENT	51
3.4	EXPERIMENTAL PROCEDURE.....	51
CHAPTER 4. PHYSICAL LABORATORY TEST RESULTS		55
4.1	DETERMINATION OF SCOUR SHAPE.....	55
4.2	PRESSURE MEASURED IN THE PLUNGE POOL	61
4.3	EFFECT OF JET AIR CONTENT ON SCOUR	63
4.4	SUMMARY	66
CHAPTER 5. EVALUATING THE DEVELOPMENT OF ULTIMATE ROCK SCOUR HOLE.....		67
5.1.	ERODIBILITY INDEX METHOD (ANNANDALE’S METHOD)	67
5.2.	COMPREHENSIVE SCOUR MODEL (CSM).....	69
5.2.1.	FALLING JET.....	70
5.2.2.	PLUNGE POOL MODULE.....	70
5.2.3.	THE ROCK MASS	71
5.2.3.1.	MAXIMUM DYNAMIC PRESSURE C_{pmax}	71
5.2.3.2.	DYNAMIC IMPULSION (DI) METHODS.....	74
5.2.3.3.	EVALUATING ROCK SCOUR BY USING QUASI-STEADY IMPULSION MODEL.....	76
5.2.3.4.	RESULTS OF QUASI STEADY SCOUR SHAPE AGAINST LABORATORY TEST.....	79
5.3.	SUMMARY	81
CHAPTER 6. CONCLUSION AND RECOMMENDATION.....		82
6.1.	CONCLUSION.....	82
6.2.	RECOMMENDATION FOR THE FURTHERS RESEARCH	83
REFERENCES		84
APPENDIX A GEOLOGICAL PARAMETERS		88
APPENDIX B SEDIMENT CHARACTERISTICS CALCULATION		93
APPENDIX C DYNAMIC IMPULSION COMPUTATION.....		94
APPENDIX D: WORK SHEET AND GRAPHS OF QSI METHOD		106

**APPENDIX E PARAMETERS, WORK SHEET OF PRACTICAL APPLICATION OF DI METHOD AND
ADDITION FORMULA205**

APPENDIX F SURVEYING DATA GRAPHS208

List of Figures

Figure 1-1. Research methodology to understand the equilibrium scour hole geometry.....	2
Figure 2-1. Rock mass layer situations: 1. intermittently jointed rock 2. Completely jointed rock (adapted from Bollaert & Schleiss, 2001).	5
Figure 2-2. Representation of physical-mechanical processes occurring in spillway system showing the water, air and rock phases (adapted from Bollaert & Schleiss, 2001)	6
Figure 2-3. Types of spillways that affect impinging jet flow (adapted from Whittaker & Schleiss, 1984).....	7
Figure 2-4. Illustration of three jet regions present during the normal impingement of jet on a flat plate (adapted from Bollaert, 2002)	8
Figure 2-5. Core and developed jet impact in relation to the plunge pool (adapted from Bollaert, 2002).	8
Figure 2-6. Diffusion of round jets in plunge pools. (a) Submerged jet (b) Almost laminar plunging jet (c) Smooth turbulent plunging jet (d) Highly turbulent plunging jet (adapted from Ervine & Falvey, 1987).	9
Figure 2-7. Conceptual model depicting the three stages in the rock scour process (adapted from Annandale, 1995).	13
Figure 2-8. Erosion Threshold for variety of earth material between stream power and EI (adapted from Annandale, 2006).	20
Figure 2-9. Schematic diagram of the parameters of a falling jet (adapted from Bollaert, 2002)	21
Figure 2-10. Jet diffusion in a pool with maximum dynamic pressure at the bottom (adapted from Melo, 2002).....	22
Figure 2-11. Reduction factor F of fluctuating dynamic pressure coefficient (adapted from Castillo & Carrillo, 2014)	26
Figure 2-12. Brittle fracture failure of rock (adapted from Annandale, 2006).	29
Figure 2-13. Fatigue failure of rock (adapted from Annandale, 2006).	30
Figure 2-14 Block removal failure of rock (adapted from Annandale, 2006).	31
Figure 2-15. Bollaert's (2002) simplified rock mass.....	32
Figure 2-16. Peeling of rock blocks at the surface of the rock during flow (adapted from Bollaert, 2010).	33
Figure 2-17. Plane jet deflection on a flat bottom (adapted from Bollaert, 2012).	34
Figure 2-18. Summary of uplift pressures coefficients over and under protruding rock blocks subjected to high-velocity of wall jet flow adapted by Reinius (1986).	35
Figure 2-19. Sub-vertical lines of calculation of QSI model (adapted by Bollaert 2012).....	36
Figure 2-20. Longitudinal section of Kariba plunge (adapted from Sanyanga, 2012).	37
Figure 3-1. Model of experimental spillway in action.	41
Figure 3-2. Adjustable gate to adjust tailwater level.....	42
Figure 3-3. Cross section of spillway model in laboratory.	43
Figure 3-4 Plan of plunge pool (top view)	43
Figure 3-5. Point gauge for measuring the water depth in the rectangular issuance canal	44
Figure 3-6. Tailwater gauge (manometer) for measuring the tailwater depth.....	44
Figure 3-7. Proline Promag 50W, 53W flow meter	45

Figure 3-8. Air probe conductivity for measuring air concentration.....	45
Figure 3-9 (a) and (b) Jet length “L” of different discharge at different height and different water depths “TW”	47
Figure 3-10. Jet impact into plunge pool with turbulent shear layer developed	48
Figure 3-11. Calibrated digital scale for measuring mass PVC blocks	49
Figure 3-12. Drag coefficient as function of Reynolds number and particle shape (adapted from Wu & Wang, 2006).....	51
Figure 3-13. PVC cubes filled up in the plunge pool before start the experiment	52
Figure 3-14. Grid for surveying or mapping of scouring area	52
Figure 3-15. Micro-sensors for measuring the pressure inside the test box.	54
Figure 3-16. A schematic diagram (plan view) of the arrangement of pressure sensors within the test box.....	54
Figure 4-1 Scour profile in 3D of the test system with $Q=20\text{l/s}$, $H=3\text{m}$ and $TW=0,25\text{m}$).	55
Figure 4-2. Contour line map of scour test system of $Q=20\text{l/s}$, $H=3\text{m}$ and $TW=0.25\text{m}$).	55
Figure 4-3. Rock Scour in model for $Q=20\text{l/s}$, $H=3\text{m}$ and TW of 0.25m	55
Figure 4-4. Lateral Section of $Q=20\text{l/s}$, $TW=0.5\text{m}$ at different height of spillway.....	57
Figure 4-5. Longitudinal Section of $Q=20\text{l/s}$, $TW=0.5\text{m}$ at different height of spillway	57
Figure 4-6. Lateral Section of $Q=20\text{l/s}$, $TW=0.25\text{m}$ at different height of spillway.....	58
Figure 4-7. Longitudinal Section of $Q=20\text{l/s}$, $TW=0.25\text{m}$ at different height of spillway	58
Figure 4-8. Lateral Section of $Q=10\text{l/s}$, $TW=0.5\text{m}$ at different height of spillway.....	59
Figure 4-9. Longitudinal Section of $Q=10\text{l/s}$, $TW=0.5\text{m}$ at different height of spillway	59
Figure 4-10. Lateral Section of $Q=10\text{l/s}$, $TW=0.25\text{m}$ at different height of spillway.....	60
Figure 4-11. Longitudinal Section of $Q=10\text{l/s}$, $TW=0.25\text{m}$ at different height of spillway	60
Figure 4-12. Rock scour view for 10 l/s of discharge, 4 m drop height and 0.5 m water depth	61
Figure 4-13. Pressure sensor inside the test box placed at the centre of the PVC rock blocks under test conditions	61
Figure 4-14. PLW (PicoLog Recorder Graph) graph of pressure at the plunge pool under jet impact of 10l/s of discharge and 0.25 m of water depth and 2m of height	62
Figure 4-15. General view of contour plot of air concentration of four scenarios (Test with discharge of 20l/s with 4m and 2 m of height and two different of tailwater depth)	64
Figure 4-16. The comparison of air concentration and scour depth.....	65
Figure 5-1: Schematic sketch of joint length.....	74
Figure 5-2. Plane jet deflection on a flat bottom (adapted from Bollaert, 2012).	76
Figure 5-3. Wall jet velocity in the plunge pool for different tailwater depths for a 2 m drop height	77
Figure 5-4. Calculated velocity decline along plunge pool centreline (y-direction).....	78
Figure 5-5. Velocity along jet wall against quasi-steady lift pressure at 3 m of height of spillway and 10 l/s along different distance row of block z . ($z\text{ (m)}$ are row of block)	78
Figure 5-6. Longitudinal section for $Q=20\text{l/s}$, $H=2\text{m}$ and $TW=0.25\text{m}$ at the maximum point of observed scour profile compare to the QSI scour hole.....	79
Figure 5-7. Longitudinal section for $Q=10\text{l/s}$, $H=4\text{m}$ and $TW=0.25\text{m}$ at the maximum point of observed scour profile compare to the QSI scour hole.....	80

Figure A 0-1. The presentation of rock joint set (left to right: One joint set, one joint set with random joints, two joint sets)	89
Figure D 0-1. Longitudinal section for $Q=20\text{l/s}$, $H=2\text{m}$ and $TW=0.5\text{m}$ at the maximum point of observed scour profile compare to the QSI scour hole	106
Figure D 0-2. Longitudinal section for $Q=10\text{l/s}$, $H=2\text{m}$ and $TW=0.5\text{m}$ at the maximum point of observed scour profile compare to the QSI scour hole	106
Figure D 0-3. Longitudinal section for $Q=10\text{l/s}$, $H=2\text{m}$ and $TW=0.25\text{m}$ at the maximum point of observed scour profile compare to the QSI scour hole.	107
Figure D 0-4. Longitudinal section for $Q=10\text{l/s}$, $H=3\text{m}$ and $TW=0.5\text{m}$ at the maximum point of observed scour profile compare to the QSI scour hole.	107
Figure D 0-5. Longitudinal section for $Q=10\text{l/s}$, $H=3\text{m}$ and $TW=0.25\text{m}$ at the maximum point of observed scour profile compare to the QSI scour hole.	108
Figure D 0-6. Longitudinal section for $Q=20\text{l/s}$, $H=3\text{m}$ and $TW=0.5\text{m}$ at the maximum point of observed scour profile compare to the QSI scour hole.	108
Figure D 0-7. Longitudinal section for $Q=20\text{l/s}$, $H=3\text{m}$ and $TW=0.25\text{m}$ at the maximum point of observed scour profile compare to the QSI scour hole.	109
Figure D 0-8. Longitudinal section for $Q=10\text{l/s}$, $H=4\text{m}$ and $TW=0.25\text{m}$ at the maximum point of observed scour profile compare to the QSI scour hole.	109
Figure D 0-9. Longitudinal section for $Q=20\text{l/s}$, $H=4\text{m}$ and $TW=0.5\text{m}$ at the maximum point of observed scour profile compare to the QSI scour hole.	110
Figure D 0-10. Longitudinal section for $Q=20\text{l/s}$, $H=4\text{m}$ and $TW=0.25\text{m}$ at the maximum point of observed scour profile compare to the QSI scour hole.	110
Figure D 0-11. General view of contour plot of air concentration of four scenarios	112
Figure F. 0-1. Scour profile and contour line of 20 l/s , $H=3\text{m}$ and $TW=0.5\text{m}$	208
Figure F. 0-2. Scour profile and contour line of 10 l/s , $H=3\text{m}$ and $TW=0.25\text{m}$	209
Figure F.0-3. Scour profile and contour line of 10 l/s , $H=3\text{m}$ and $TW=0.5\text{m}$	210
Figure F. 0-4. Scour profile and contour line of 10 l/s , $H=4\text{m}$ and $TW=0.25\text{m}$	211
Figure F 0-5. Scour profile and contour line of 20 l/s , $H=4\text{m}$ and $TW=0.5\text{m}$	212
Figure F. 0-6. Scour profile and contour line of 20 l/s , $H=4\text{m}$ and $TW=0.25\text{m}$	213
Figure F.0-7. Scour profile and contour line of 20 l/s , $H=2\text{ m}$ and $TW=0.5\text{ m}$	214
Figure F. 0-8. Scour profile and contour line of 20 l/s , $H=2\text{ m}$ and $TW=0.25\text{ m}$	215
Figure F.0-9. Scour profile and contour line of 10 l/s , $H=2\text{m}$ and $TW=0.5\text{m}$	216
Figure F.0-10. Scour profile and contour line of 10 l/s , $H=2\text{m}$ and $TW=0.25\text{m}$	217

List of Tables

Table 2.1. Approximate values of K given under varying jet and turbulence conditions (Ervin & Falvey, 1987)	11
Table 2.2. Coefficients proposed for equation 7	14
Table 2.3. Coefficient values of dynamic pressure coefficient C_{pa} formula (Castillo & Carrillo, 2014)	24
Table 2.4. Coefficient values of root-mean-square pressure fluctuations coefficient C_{pa'} formula with $Y/D_j \leq 14$ (Castillo & Carrillo, 2014)	25
Table 2.5. Coefficient values of root-mean-square pressure fluctuations coefficient C_{pa'} formula with $Y/D_j \geq 14$ (Castillo & Carrillo, 2014)	25
Table 2.6. Criteria to assess rock scour by DI (Bollaert, 2002)	33
Table 2.7. The deviation of up- and downstream parts of the total flow for different jet angles δ (adapted by Bollaert, 2012)	35
Table 2.8. Scour depth for Kariba Dam based on empirical methods with different authors in 1978	37
Table 2.9. Froude Law Model Scale Relationships (Castillo & Carrillo, 2013)	39
Table 3.1. Characteristics of model of spillway	42
Table 3.2. Typical value of Issuance Turbulence Intensity (Bollaert, 2002)	46
Table 3.3. Jet break-up length and distance from issuance to the jet impact	46
Table 3.4. Main characteristics of plunging rectangular shaped jets	48
Table 3.5. Test program (model values)	53
Table 3.6. Summary of test of the velocities at the jet issuance and the jet impact	53
Table 4.1. Summary of maximum erodible region survey considering discharge rate, height and water depth	56
Table 4.2. Results of pressure sensors at rock mass for different discharge rates, heights and tailwater depths	63
Table 4.3. Summary of jet mean density and air concentration measured at the impact with the plunge pool	65
Table 5.1. Stream power of different prototype	68
Table 5.2. Summary of parameters to calculate the erodibility index (prototype)	69
Table 5.3. Falling Jet module parameter calculations at impact with tailwater level	70
Table 5.4. Dynamic pressure and RMS pressure fluctuation coefficients	71
Table 5.5. Maximum and minimum pressure P_{max} in closed rock joint calculated at different heights and with different discharges	73
Table 5.6. The positive extreme pressure C_+ coefficients and Pressure inside the blocks results	73
Table 5.7. Summary of ultimate scour depths based on DI method for the different test scenarios	75
Table 5.8. Comparison of scour depth model and empirical computation of DI method	75
Table A 0.1. Mass strength number for rock (Annandale, 2006)	88
Table A 0.2. Joint set number (Annandale, 1995)	88
Table A 0.3. Joint roughness number J_r (Annandale, 2006)	89
Table A 0.4. Joint alteration number (Annandale, 2006)	90

Table A 0.5. Relative ground structure number J_s (Annandale, 2006).	91
Table A 0.6. Value of C and m various Rock Types (Annandale, 2006).	92
Table B 0.1. Specific gravity calculation of PVC blocks	93
Table B. 0.2. The Settling velocity and effective diameter of PVC blocks	93
Table C 0.1. The ultimate scour depth for $Q=10$ l/s, $H=2$ m, $TW=0.5$ m computed by DI	94
Table C 0.2. The ultimate scour depth for $Q=10$ l/s, $H=2$ m, $TW=0.25$ m computed by DI	95
Table C 0.3. The ultimate scour depth for $Q=20$ l/s, $H=2$ m, $TW=0.5$ m computed by DI	96
Table C 0.4. The ultimate scour depth for $Q=20$ l/s, $H=2$ m, $TW=0.25$ m computed by DI	97
Table C 0.5. The ultimate scour depth for $Q=10$ l/s, $H=3$ m, $TW=0.5$ m computed by DI	98
Table C 0.6. The ultimate scour depth for $Q=10$ l/s, $H=3$ m, $TW=0.25$ m computed by DI	99
Table C 0.7. The ultimate scour depth for $Q=20$ l/s, $H=3$ m, $TW=0.5$ m computed by DI	100
Table C 0.8. The ultimate scour depth for $Q=20$ l/s, $H=3$ m, $TW=0.25$ m computed by DI	101
Table C 0.9. The ultimate scour depth for $Q=10$ l/s, $H=4$ m, $TW=0.5$ m computed by DI	102
Table C 0.10. The ultimate scour depth for $Q=10$ l/s, $H=4$ m, $TW=0.25$ m computed by DI	103
Table C 0.11. The ultimate scour depth for $Q=20$ l/s, $H=4$ m, $TW=0.5$ m computed by DI	104
Table C 0.12. The ultimate scour depth for $Q=20$ l/s, $H=4$ m, $TW=0.25$ m computed by DI	105
Table D 0.1. Quasi-steady method of $Q=10$ l/s, $H=2$ m and $TW=0.5$ m	114
Table D 0.2. Quasi-steady method of $Q=20$ L l/s, $H=2$ m and $TW= 0.5$ m.....	122
Table D 0.3. Quasi-steady method of $Q=10$ l/s, $H=2$ m and $TW=0.25$ m	131
Table D 0.4. Quasi-steady method of $Q=10$ l/s, $H=3$ m and $TW=0.5$ m	139
Table D0.5. Quasi-steady method of $Q= 10$ l/s, $H=3$ m and $TW=0.25$ m	147
Table D 0.6. Quasi-steady method of $Q=10$ l/s, $H=4$ m and $TW=0.5$ m	154
Table D 0.7. Quasi-steady method of $Q=10$ l/s, $H=4$ m and $TW=0.25$ m	161
Table D 0.8. Quasi-steady method of $Q=20$ l/s, $H=2$ m and $TW=0.25$	168
Table D 0.9. Quasi-steady method of $Q=20$ l/s, $H=3$ m and $TW=0.5$ m	175
Table D 0.10. Quasi-steady method of $Q=20$ l/s, $H=3$ m and $TW=0.25$ m	183
Table D 0.11. Quasi-steady method of $Q=20$ l/s, $H=4$ m and $TW=0.5$ m	190
Table D 0.12. Quasi-steady method of $Q=20$ l/s, $H=4$ m and $TW=0.25$ m	197
Table E 0.1. Parameters used for calculation of DI method for Kariba Dam.	205
Table E.0.2. The ultimate scour depth of Kariba Dam based on the adapted DI method	207

List of Symbols

- A** : Area perpendicular to the flow. (m^2).
- C_d** : Drag coefficient.
- C_I** : The net dynamic impulsion coefficient.
- C_I^{max}** : Maximum dynamic impulsion coefficient.
- C_r** : Material parameters.
- C'_{pa}** : The fluctuation dynamic pressure coefficient.
- C_{pa}** : The mean dynamic pressure.
- C_p^{max}** : Maximum dynamic pressure coefficient.
- D** : Pipe diameter (m).
- D_i** : The jet diameter at issuance.
- D_j** : The jet diameter at the impact in plunge pool.
- D_s** : Depth of scour (m).
- F** : Froude number (-).
- F_o** : Force over the block.
- F_{sh}** : The shear and interlocking forces.
- F_u** : Force under the block.
- G** : Specific gravity of bed sediment
- G_b** : The immersed weight of the block.
- H** : Elevation difference between reservoir and Tailwater (m).
- H_n** : Elevation difference between reservoir and Tailwater (m).
- J_a** : Degree of alteration of materials.
- J_n** : The joint set number which is a function of the number of joint sets in a rock mass.
- J_r** : Degree of roughness of opposing faces of rock discontinuity.
- J_s** : Factor representing the impact of the relative shape.
- K_b** : Block or particle size factor.
- K_d** : Shear strength factor.

- K_h** : Erodibility index.
- K_I** : Stress intensity (MPa \sqrt{m}).
- K_{IC}** : Fracture toughness.
- L** : The plunge length through the atmosphere (m).
- L_b** : The jet break-up length (m).
- M_s** : Mass strength Factor for granular soil.
- N** : The number of pressure cycles.
- Q** : Total discharge (m³/s).
- Re** : Reynolds number.
- RQD** : Rock Quality Designation number, a standard parameter in drill core logging.
- R_r** : Hydraulic radius.
- S_r** : Slope.
- T** : Tensile strength of the rock (MPa).
- T_u** : Initial turbulence intensity (-).
- UCS** : Unconfined compressive strength of the rock (MPa).
- V_i** : The jet velocity at issuance.
- V_j** : The jet velocity at the impact in plunge pool.
- ν** : Kinematic viscosity of water.
- V** : Mean flow velocity (m/s).
- V_e** : Minimum velocity required to entrain air (m/s).
- V_i** : Nappe velocity at impact (m/s).
- V_r** : Relative velocity (m/s).
- V_s** : Volume of sediments.
- V_{SS}** : Settling velocity (m/s).
- V_v** : Volume of voids.
- X_L** : the distance along the jet trajectory.
- Y** : The plunge pool depth.

- b** : Jet width (m).
- c** : The shortest of the three perpendicular axes (a, b, c) of the particle.
- d** : Median grain size of bed material (m).
- d_i** : The nozzle diameter.(Pa).
- d_m** : Characteristic sediment size of bed material (m).
- d_{out}** : The jet's outer diameter.
- e** : Voids ratio.
- f** : A factor that accounts for the shape of the close-ended fissure.
- f_c** : Characteristics frequency of pressure cycles.
- g** : Gravitational constant (m/s²).
- g** : Acceleration of gravity (9.81 m²/s).
- h** : Tailwater depth (m).
- k₁** : Coefficient (-).
- k₂** : Coefficient (-).
- m_r** : material parameters.
- n** : Sediment Porosity.
- n** : Manning's n value for grain roughness (-).
- p_e** : Jet perimeter (m).
- q** : Unit discharge (m²/s).
- q_{a1}** : rate of air entrainment per unit jet width (m²/s).
- q_{a2}** : rate of air entrainment per unit jet width (m²/s).
- q_{a3}** : rate of air entrainment per unit jet width (m²/s).
- q_w** : Discharge per unit width (m²/s).
- a** : Crack length (m).
- β** : Air-water relationship (-).
- σ_{water}** : Stress introduced by turbulent fluctuating pressures in a close-ended fissure (MPa).
- σ_i** : Confining stress in the rock (MPa).

- ρ : Density of submerged particle (kg/m^3).
- ρ_s : Density of sediment (kg/m^3).
- ρ_w : Water density (kg/m^3).
- γ : The unit weight of water (N/m^3).
- θ : Jet angle with horizontal at impact in plunge pool.
- Θ_T : Angle of incidence from vertical of the jet.
- ΔK_I : The difference of maximum and minimum stress intensity factors.
- Δp_c : Characteristic amplitude of pressure cycles.
- Γ^+ : An amplification factor.
- ψ : Shape factor of sediment.
- ν : Kinematic viscosity (m^2/s).

List of Abbreviations

CFM:	Comprehensive Fracture Mechanics
CSM:	Comprehensive Scour Model
DI:	Dynamic Impulsion
EI :	Erodibility Index
FQSI:	Quasi-steady uplift pressure
m.a.s.l.	Metres above sea level
TW :	Tailwater
RQD :	Rock Quality Designation number
QSI :	Quasi-Steady Impulsion
UCS :	Uni-axial Compressive Strength
USBR :	United States Bureau of Reclamation
PLW :	PicoLog Recorder Graph

Chapter 1 : Introduction

1.1. Background

The last century has been characterised by a huge evolution of hydraulic dams. By 1950, about 5000 large dams had been constructed worldwide with three-quarters in industrialised countries (Yogendra & Gopalakrishnan, 2000). Dams are built for different purposes, i.e. irrigation, hydropower generation, flood controls and domestic use.

Even with the different purposes of dams, they are still exposed to downstream rock scour, due to the energy dissipation of the high-velocity plunging water jet. Therefore, many researchers have developed methods to predict rock scour to determine whether the ultimate scour hole would undermine the stability and foundations of the dam wall.

1.2. Aspects of Rock Scour

It has been found that rock scour could endanger the stability of the dam wall and its pertinent structures'. The removal of rock blocks is one of the principal mechanisms by which scour occur. It is a critical issue because of its destabilisation action at the foundation of hydraulic structures. Rock scour occurs when the erosive capacity of the water flowing over the rock exceeds the ability of the bed to resist it (Annandale, 1995).

The high-velocity water jet, created by the transfer of water from the reservoir level to the downstream tailwater level, impinges onto the plunge pool bottom and results in the scour of the bedrock, which has contributed to the failure of different dams worldwide. For example, the Kariba Dam (Zambia-Zimbabwe) designed with a discharge capacity of 9 000 m³/s and 128 m in height; has a scour hole deeper than 80 m, nearly as tall as the dam height (Bollaert, 2002). Similarly, the Cahora-Bassa Dam (Mozambique) consists of five turbines and eight sluice gates designed with a storage capacity of 63x10⁹ m³ and a maximum height of 171 m has a 68 m deep scour hole (Whittaker & Schleiss, 1984).

Similarly, the same problem was experienced at the Srisailem Dam situated across the Krishna River in India, which has a maximum design discharge of 28370 m³/s at the maximum reservoir level of 271.88 m.a.s.l. During construction that started in 1963, a deep scour hole was observed near the toe of the dam (Bollaert and Mason, 2006).

1.3. Aspect of Scour Technology

Over the past decades, many researchers have developed empirical and semi-empirical expressions based on physical model tests and prototype observations, in order to evaluate the ultimate scour depth of the scour hole (Mason, 1984; Mason & Arumugan, 1985; Spurr, 1985). Most of these expressions have been carried out to determine the extent of the scour. In recent work, researchers have been attempting to quantify pressures within a plunge pool that is subjected to a free falling jet (Annandale, 1995; Elvine, et al., 1997). Most research (Annandale, 1995; Elvine, et al., 1997) has shown that it is difficult to estimate plunge pool scour, as there are numerous interrelated physical processes involved that need to be considered. These are plunging jet diffusion, fluctuation pressure distribution on the plunge pool floor, fracturing and dislodgment of the bed material, the abrasion process, the downstream sediment transport capacity and induced shear on scour hole boundaries.

Hence, the major issue regarding the rock scour considering all the above scour technologies and combination of the given examples of serious erosion cases of dams observed in different areas of the world, highlighted the need for this research. Moreover, understanding the energy dissipation of the jet in the atmosphere and in the plunge pool is important and research has used simplified one and two-dimensional rock joints to prove that the formation of scour is caused by transient water pressures between the rock joints (Bollaert, 2002). Therefore, the challenge is to determine the scour on a multiple three-dimensional rock block and a complex network of regular shapes.

1.4. Study Objective

The main purpose of this study was to determine the equilibrium scour hole geometry by means of constructing a physical model which operates according to the Froude law. This was accomplished through:

- determining and emphasising the conceptual understanding of rock scour by focusing on the physical hydraulic model results involved in the interaction between free falling jets, plunge pool aeration and turbulence and fractured solid mass;
- understanding different rock scour assessment methods by including the characteristics of turbulent flows;
- the analysis of the influence of pool geometry on pressure propagation inside rock joints and the influence of air concentration in the plunge pool and
- estimating the maximum rock scour depth and the extent (dimensions) of the rock scour hole.

1.5. Theoretical Frame Work

The analysis of this study was based on the analytical triangular process. It required integration of experimental data obtained from the laboratory compared against a physical-mechanical based model and semi-empirical methods found in the literature as shown in Figure 1-1. The following variables were investigated in the physical model study as:

- different pressure in plunge pool inside blocks
- different air concentration in plunge pool
- rock scour characteristics.

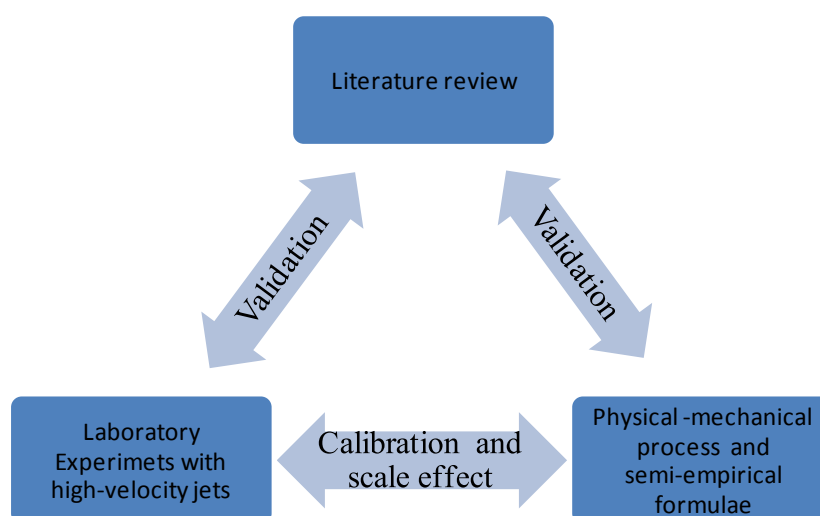


Figure 1-1. Research methodology to understand the equilibrium scour hole geometry

1.6. Layout of the Research

This thesis is structured in accordance with the broad objectives of the study, namely to determine the equilibrium scour hole geometry. This report is organised into three parts with a total of six chapters and appendices.

The first part, the objectives and the methodology used in this research is presented in two chapters, namely:

- Chapter Two includes the literature review of the physical phenomena involved in this study, specifically covering scour development and scour assessment with the different methods used.
- Chapter Three explains the model and experimental laboratory tests. This chapter deals with the experimental facility, measurement equipment, parametric analysis and detailed test programme.

The second part is the core of the research study and comprises the following:

- Chapter Four is divided into two sub-sections. The first is devoted to the influence of the height of a spillway, the tailwater depth, the discharge and the evaluation of the effect of bed material. The second section outlines the dynamic pressure fluctuation measured at the plunge pool floor and air concentration results.
- Chapter Five evaluates the development of the ultimate rock scour hole by highlighting a detailed application model and a comparison of the different methods used.

The third part of the report, Chapter six, summarises the research project and followed by a conclusion of this research project, and makes recommendations for future research.

Chapter 2. Literature Review

This chapter contains the general overview of the scour process with the basic information required for assessing the scour hole geometry, including the scale limitation. It also defines the keywords and introduces the literature, research and discussion of different authors regarding the essential and practical methods that are used to determine the scour hole geometry.

2.1. Background of Rock Scouring

Scour is a natural phenomenon caused by the erosive action of a flowing stream on rock beds, which breaks up and removes the sediment in the impingement zone. Due to this phenomenon, dam safety requires assessment of the foundation scour that might result from overtopping events, scour of auxiliary spillways, and the effects of fuse-plug scour according to Annandale (2006). The erosive capacity of water flowing over dams and through spillways can have a very high discharge as described by Annandale (2006).

According to Schleiss (2002), a rock scour hole is progressively formed until an equilibrium condition is reached at the ultimate scour depth, which is dependent on the duration and discharge of spilling. When the equilibrium has been reached, the energy of the jet is effectively dissipated by the plunge pool so that further block ejection does not occur (Duarte, 2014). If the ultimate scour hole geometry is excessive, it can cause the dam and pertinent structures to fail that can lead to the loss of life and property.

2.1.1. Types of Scour

The scour that may occur at a structure can be divided into general scour and local scour.

General scour is caused by natural processes and/or human interaction, but it can further be broken down into four sub-categories as stated by Armitage (2002):

- 1) Overall degradation occurs as a river adjusts to changes in the water or sediment flow. The changes may be natural or as a results of human interference such as flow rate variation, construction of weirs or dams, or inter-basin water transfers.
- 2) Constriction scour is a special, localised case of overall degradation and occurs if a structure causes the narrowing of a watercourse or the rechanneling of berm or flood plain flow.
- 3) Bend scour occurs in response to the large coherent flow structures or secondary currents that are set up whenever the flow is forced to follow a path.
- 4) Confluence scour occurs when two branches of a river meet.

Local scour is the removal of sediment such as sand and rocks from around hydraulic structures. It is caused by swiftly moving water that can scoop out scour holes, and therefore compromising the integrity of a structure. Local scour is superimposed on the general scour. The type of scour investigated in this study could be defined as local scour.

2.1.2. Rock Mass

Rock could be described in several ways. For example, rock is represented by the geology, the mineralogical texture, and the quantitative material properties (Bollaert, 2002). The three main rock type groups are igneous, sedimentary, and metamorphic. Bollaert and Schleiss (2001) grouped them into two group properties of rocks: rock intrinsic material properties and rock mass characteristics. The rock type and its discontinuities play a role mainly in the initial stage of scour, influencing the rock mass and its

strength, durability and permeability. Almost all igneous rocks offer resistance to erosion, similar to metamorphic rock.

Considering the rock mass discontinuities, the rock can be classified as intermittently jointed, completely jointed, and intact as referred to in Figure 2-1. Bollaert and Schleiss (2001) explain that hydrodynamic fracturing and fatigue play an important role in the scour process in intermittently jointed rocks. The hydrodynamic uplift forces are responsible for rock scour in completely jointed rock. They summarise the most important parameters that are necessary to resist scouring of completely jointed rock such as dimension, size, shape, weight of the blocks, and friction force along joint. These parameters describe how the rock resists against tensile forces.

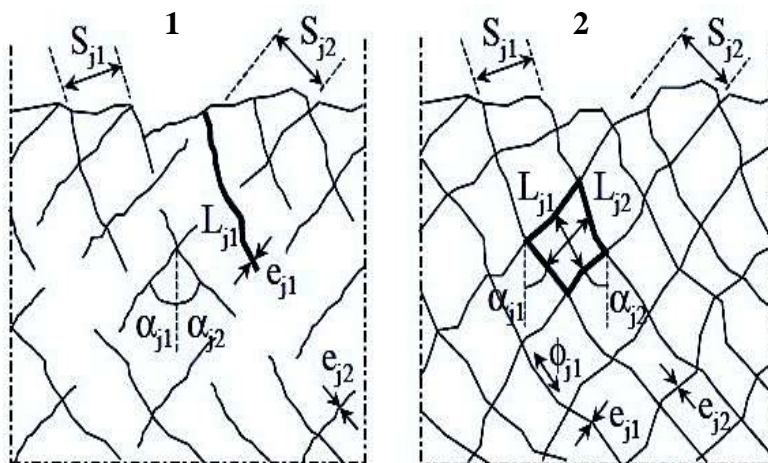


Figure 2-1. Rock mass layer situations: 1. intermittently jointed rock 2. Completely jointed rock (adapted from Bollaert & Schleiss, 2001).

To conclude, the assessment of rock scour needs the understanding of a series of physical-mechanical processes, specifically how hydrodynamic fracturing and uplift are responsible for destruction of the rock mass (Figure 2-2). Similarly, it is also necessary to understand the type of rock and the characteristics of turbulent flows that lead to scour.

2.2. Main Scour Process and Parameters of Rock Scour

Rock scour, due to plunging water jets, is comprised of a series of processes that occur consecutively. The evolution of the subsequent plunge pool geometry is a dynamic phenomenon that is governed by a physical-mechanical interaction between three phases involved in the process; namely water, air and rock.

In the analysis, one must consider every parameter in the physical-mechanical process. Figure 2-2 shows the physical process that is described by a series of processes: aerated jet impingement, plunge pool turbulent flow, pressure fluctuations at the water-rock interface, hydrodynamic fracturing of closed-end rock joints by pressure propagation, hydrodynamic uplift of the formed rock block and finally, rock block ejection (Bollaert, 2002).

Furthermore, the Figure 2-2 explains this process whereby the aerated jet impingement depends on the jet velocity at impact, the initial turbulence intensity of the jet, and the degree of aeration. The flow conditions in the plunge pool are divided into a high-velocity, two-phase turbulent shear layer flow and a macro-turbulent flow. The transfer of pool bottom pressures into rock joints results in transient flow that

is governed by the propagation of pressure waves. Therefore, the rock block can be ejected from the rock mass as a result of the pressure exerted on its top and pass through the fissures and also of the resistance against the displacement (Fedzespiel, et al., 2011).

The scouring hole is formed progressively as a function of discharges and the duration of time until the equilibrium scour depth is found (Schleiss, 2002). Thus, the rock mass is capable of dissipating the jet energy.

2.2.1 Free Falling Jet

A free falling (plunging) jet shown in Figure 2-2 has different characteristics that can be further explained to improve the understanding of scour processes. The free-falling jet is the first process of scour formation and determines the energy and turbulence conditions at the plunge pool section as stated by Bollaert (2002). The parameters that describe the jet that travels through the air are the water discharge, velocity, issuance jet diameter, issuance turbulence intensity and issuing angle.

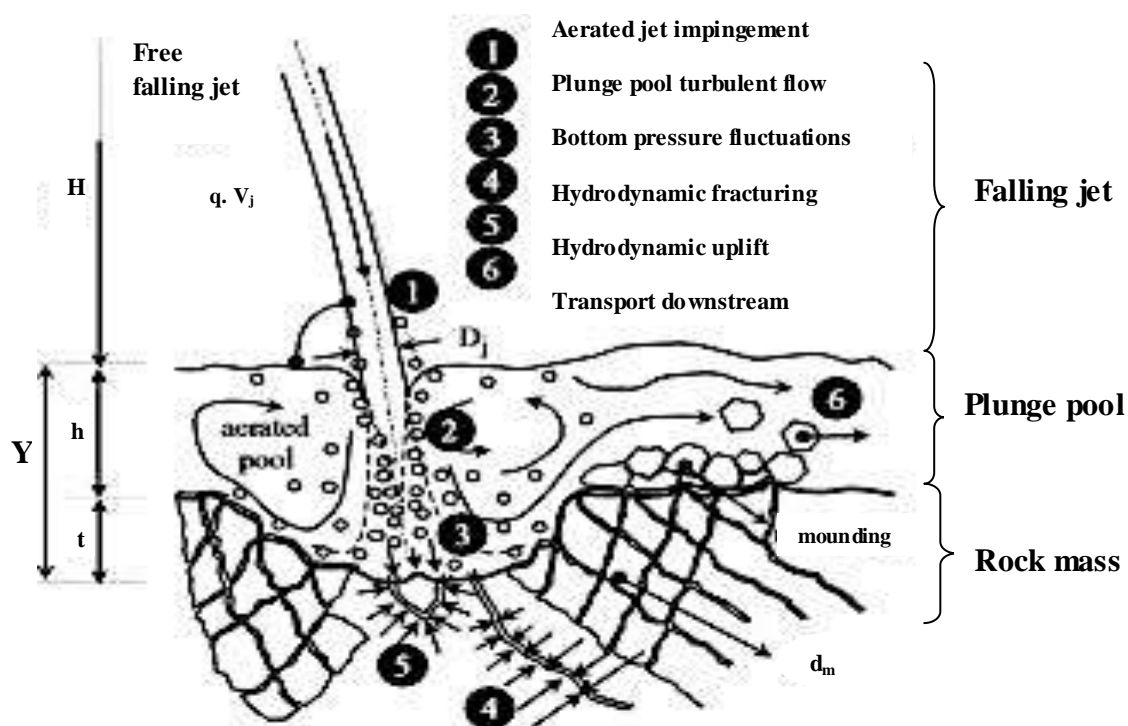


Figure 2-2. Representation of physical-mechanical processes occurring in spillway system showing the water, air and rock phases (adapted from Bollaert & Schleiss, 2001)

During the free-fall through the air, the jet is governed by ballistics and the jet core diameter decreases while disturbances in the outer layer are created by the jet's internal turbulence, thus increasing the outer diameter. Thus, gravitational acceleration and travel length must be considered. Two distinct jet regions exist, namely the developed and undeveloped region, when comparing the trajectory and break-up lengths, which allow the assessment of the state of the jet when it plunges into the pool (Ervine & Falvey, 1987). Monfette (2004) defined the break-up length as the free falling distance from issuance to the point where the jet core has dissipated.

An undeveloped jet is defined as a jet with the core still intact. Lewis et al (1999) stated that "when an undeveloped jet falls a sufficient distance, the jet loses its coherence due to turbulence and becomes a developed jet". Therefore, developed jets are fully aerated and composed of discrete water segments.

In addition, it is necessary to consider the jet trajectory by understanding the effect of air drag, jet break-up in the air and aeration to evaluate the scour caused by the free falling jets as pointed out by Whittaker and Schleiss (1984). Generally, scour associated with energy dissipaters of high head structures can be caused by two different flows, namely: vertical or oblique free jets and horizontal flow. Typical spillways creating impinging jets are shown in Figure 2-3.

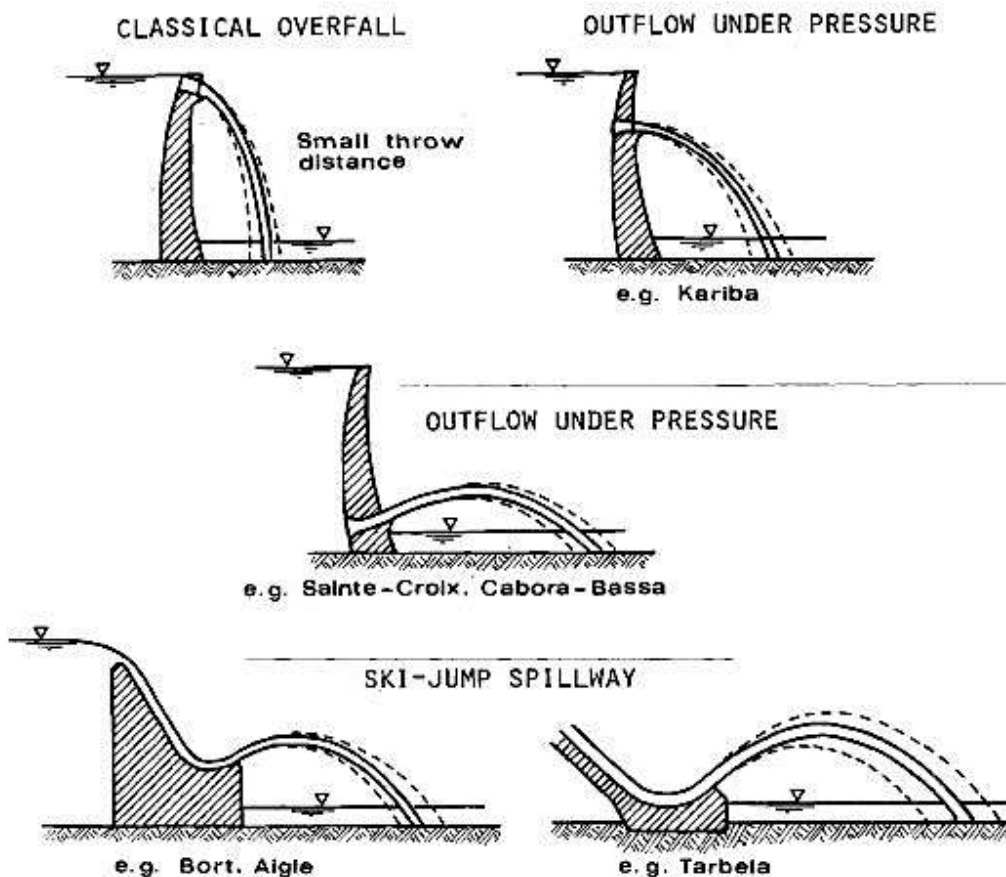


Figure 2-3. Types of spillways that affect impinging jet flow (adapted from Whittaker & Schleiss, 1984)

Whittaker and Schleiss (1984) stated that the bed material erode immediately downstream of a structure due to the horizontal flow, while the vertical or oblique jets are obtained with different types of spillways shown in Figure 2-3. The jet follows its trajectory along the spillway through the air, and disturbances are progressively formed on its surface as turbulence due to aeration. The jet is subjected to gravity as it falls through the air and the solid water core of the jet contracts causing the jet to entrain air at its outer boundary. This leads to internal turbulence and jet breakup (Bollaert, 2002; Ervine & Falvey, 1987). Ervine and Falvey (1987) define three main jet regions: the free jet region, the impingement region and the wall jet region, as shown in Figure 2-4.

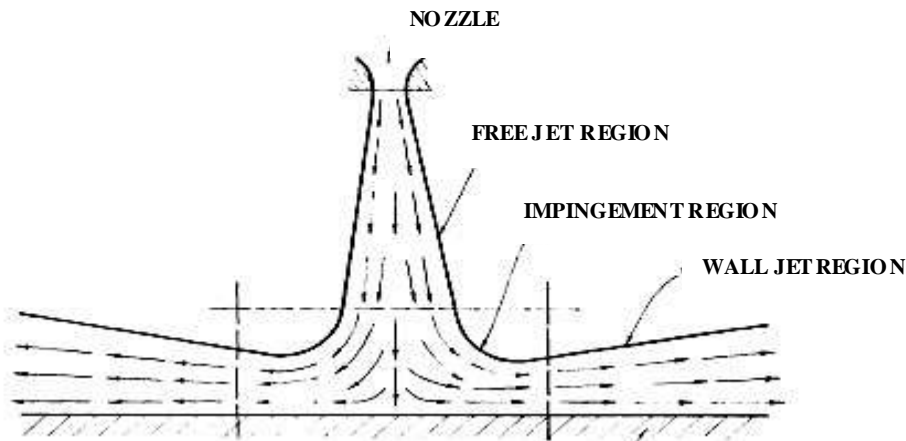


Figure 2-4. Illustration of three jet regions present during the normal impingement of jet on a flat plate (adapted from Bollaert, 2002)

The free jet region is a zone where the jet is classified as an outflow from a core into a large stagnant environment. The impingement zone is created where the bottom influences the uniform flow field of the incoming jet, and the wall jet region is a result of jet deflection creating a flow parallel to the bottom (Ervine & Falvey, 1987).

2.2.2 Jet Diffusion within the Plunge Pool

Several studies have used the behaviour of a plunging jet to derive the possible extent of scour caused by a free falling jet (Harting & Hausler, 1973). The free falling jet determines the energy and turbulence condition at the plunge pool. Thus, turbulence is the most significant air-entraining mechanism of a plunging jet (Ervine & Falvey, 1987). It is a factor that can vary significantly for various issuing conditions (Mason, 1989).

The jet (air-water) dissipation in plunge pools is influenced by the geometry of the pool bottom. For the flat bottom, the impingement of the jet deflected radially at the water-rock interface and produces a wall jet parallel to the bottom (Duarte, 2014). For the laterally bottom, the jet is deflected back towards the pool surface. These deflected jets increase the energy dissipation. Further diffusion of the jet occurs in the plunge pool and can also be classified as developed or underdeveloped (Figure 2-5) depending on the coherence of the jet core at the moment of impact with the bedrock. Gravitational effects on the jet would be minimal once it enters the plunge pool, and the jet would tend to follow a straight line rather than a free falling jet trajectory (Johnson, 1974).

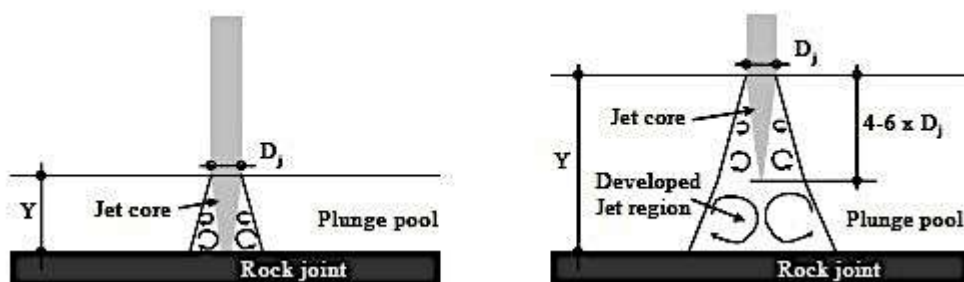


Figure 2-5. Core and developed jet impact in relation to the plunge pool (adapted from Bollaert, 2002).

As the jet core is diffused as it travels through the plunge pool, the energy of the jet (scour potential) is dissipated. Ervine and Falvey (1987) and Ervine et al (1997) found that the outer spread angles of round jets in pools differ for various jet conditions (i.e. smooth laminar or turbulent jet) as shown Figure 2-6.

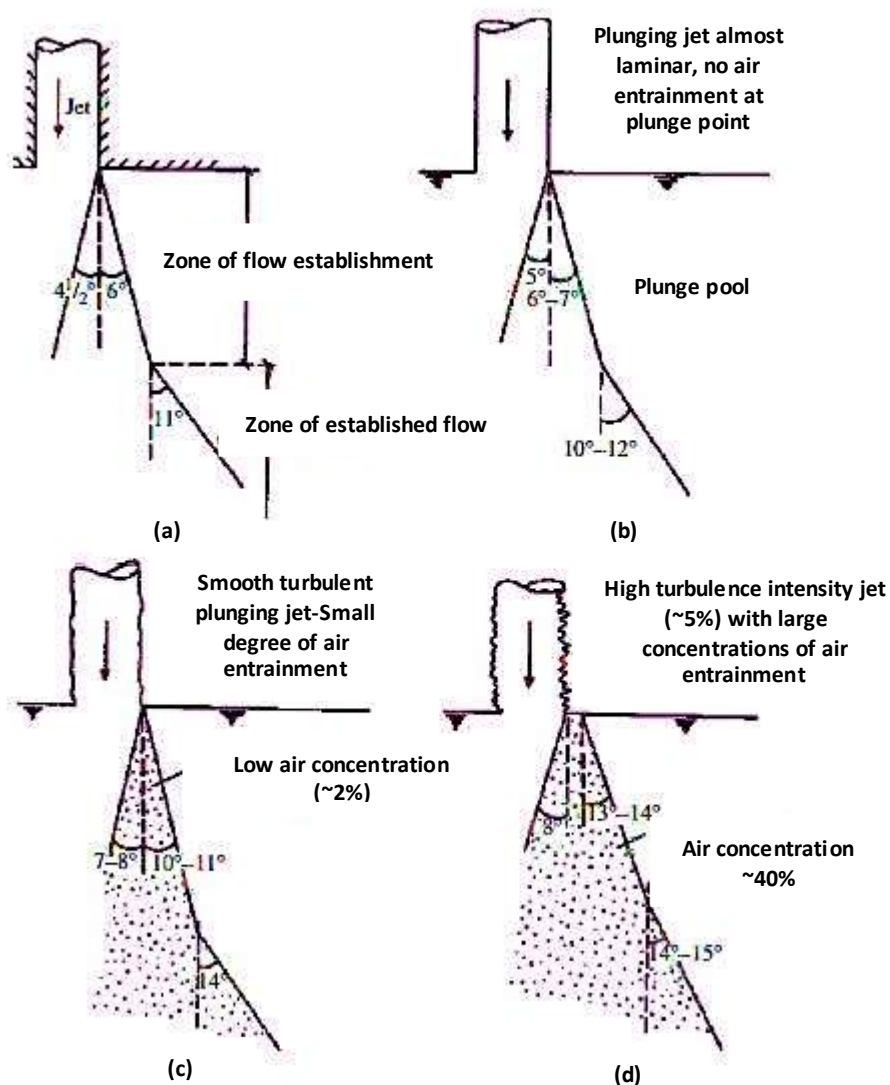


Figure 2-6. Diffusion of round jets in plunge pools. (a) Submerged jet (b) Almost laminar plunging jet (c) Smooth turbulent plunging jet (d) Highly turbulent plunging jet (adapted from Ervine & Falvey, 1987).

The jet diameter expands with depth until it reaches the rock-water interface (bedrock). Great quantities of air are entrained at the tailwater level as the jet plunges into the pool, and the jet diffuses almost linearly until it reaches the rock-bed and is deflected sideways forming wall jets.

This first mechanism to determine the rate of air entrainment at the point of impact with the tailwater level depends on the jet at impact velocity, V_j , and turbulence, T_u (Ervine, 1998). The rate of air entrainment can be expressed as follows:

$$q_{a1} = k_1 \left(\frac{V_j^3}{g} \right) T_u^2 \quad [1]$$

Where

q_{a1} : Rate of air entrainment per unit jet width (m^2/s).

g : Acceleration of gravity ($9.81 m/s^2$).

T_u : The turbulence intensity (-).

k_1 : Coefficient (-).

The air boundary layer that is entrained by the jet into the pool independently of the existence of a disturbed outer region represents the second mechanism. This mechanism determines the rate of air entrainment at the point of impact with the tailwater level. Air entrainment is caused by a discontinuity in the water between the perimeter of the jet and the plunge pool. Ervine (1998) expresses this as:

$$q_{a2} = 1.73(v/2g)^{1/2}V_j^{3/2} \quad [2]$$

Where

q_{a2} : Rate of air entrainment per unit jet width (m^2/s).

g : Acceleration of gravity ($9.81 m/s^2$).

v : Kinematic viscosity (m^2/s)

The third mechanism to determine the rate of air entrainment at the point of impact with the tailwater level is represented by the aeration provided by the foamy surface of the plunge pool. This air entrainment process is caused by the intense turbulence and vorticity at the impacted water surface, enabling additional air to enter to the pool. Ervine (1998) expresses this as:

$$q_{a3} = k_2 \frac{D - d_i}{\sin \theta} V_j \quad [3]$$

Where

q_{a3} : Rate of air entrainment per unit jet width (m^2/s).

k_2 : Coefficient (-).

D : Pipe diameter (m).

d_i : The nozzle diameter (m)

V_j : Jet velocity at impact in plunge pool (m^2/s)

θ : Jet angle with horizontal at impact in plunge pool ($^\circ$).

Ervine (1987) expresses the value of air/water ratio at jet impact as follows:

$$\beta_i = K \left(\frac{L}{d_i} \right)^{1/2} \quad [4]$$

Where

L : The plunge length through the atmosphere (m)

d_i : The nozzle diameter (m)

For vertical jets, the value of K is given in Table 2.1.

Table 2.1. Approximate values of K given under varying jet and turbulence conditions (Ervine & Falvey, 1987)

	Circular Jets	Rectangular Jets	Valid range
Rough turbulence	0.4	0.2	$L/d_i \leq 50$
Moderate turbulence	0.3	0.15	$L/d_i \leq 100$
Smooth turbulence	0.2	0.1	$L/d_i \leq 200$

Ervine et al (1997) also proposed an empirical relationship to express the air-water ratio for circular jets:

$$\beta = K \left(1 - \frac{V_e}{V_i}\right) \sqrt{\frac{L}{d_i}} \quad [5]$$

Where

V_e : Minimum velocity required to entrain air (m/s).

V_i : Nappe velocity at impact (m/s).

L : The plunge length through the atmosphere (m).

d_i : The nozzle diameter.(Pa).

For rectangular jets, Ervine and Elsayw (1975) developed an empirical equation that predicts the relative quantity of air taken into the water by jets, which is as follows:

$$\beta = 0.26 \left(\frac{b}{p_e}\right) \left(\frac{L}{d_i}\right)^{0.446} \quad [6]$$

Where

b : Jet width (m).

p_e : Jet perimeter (m).

L : The plunge length through the atmosphere (m).

d_i : The nozzle diameter (Pa).

The ratio L/d_i accounts for the degree of the jet development, which is, to a certain extent, an indicator of the jet turbulence.

2.2.3 Sediment Characteristics

Scour geometry depends not only on the characteristics of the jet but also on the rock characteristics. Annandale (2006) stated that "the principal rock characteristics playing a role in resisting the erosive capacity of water are mass strength, block size, shape and discontinuity characteristics." Bed materials, from the point of view of erosivity, may be loosely classified as non-cohesive and cohesive sediments. As the term implies, non-cohesive sediments are those consisting of discrete particles, the movement of which, for given erosive forces, depends only on particle properties (e.g. shape, size, type and density) and on the relative position of the particle with respect to surrounding particles. Annandale (2006) illustrated two types of rock shapes, namely equi-sided and elongated, which has an impact on its erosion resistance. When the rock shape is equi-sided, it will be easier to remove it than the elongated shapes rocks. Similarly, Annandale (2006) indicates that "the principal increase in erosion resistance is offered by the increase in the effective particle size".

Various observations indicate that a common method in plunge pool scour hole reproduction models is the use of non-cohesive or cohesive material as the movable bed. For a physical model, the use of gravel as a non-cohesive bed material is considered practical for rock scour hole geometry studies according to Attari, et al. (2002). Most plunge pool research has been conducted with uniform grain size material to evaluate the performance. Rajaratnam and Mazurek (2003) presented test results from experiments with non-cohesive bed material and provided an empirical formula for the scour profile and its evolution over time, for different jet velocities and angles of impact. The use of cohesive material, such as the mixing of sand, cement and water, could provide more realistic scour as reported by Sokchhay et al. (2009). Other researchers have built a riverbed test without cohesion, where blocks were made of cement/sand mortar, and it gave realistic results in terms of the ultimate scour depth (Martins, 1973).

2.3. Phases of Scour Development

According to Akmedov (1988), there are three conceptual models to describe the scour process:

1. Removal of fragments by the hydrodynamic forces of the flow: the rock fragments are removed when the hydraulic force exceeds the resistance force of the rock block.
2. Destabilisation of rock mass by vibration-induced hydrodynamic pressure fluctuations: the energy of water flowing over the unit area decreases as the scour process proceeds due to the increase in the flow area.
3. Abrasion of the scour hole walls by the recirculation of trapped material: here the strength of the rock mass is considered as the most important factor.

In a similar way Annandale (1995; 1994) describes the process of progressive dislodgement of fragments from the rock mass based on a rational correlation between the energy of flow and the resistance of the earth material to erosion. These three processes are depicted in Figure 2-7:

- Jacking,
- Dislodgement and
- Displacement.

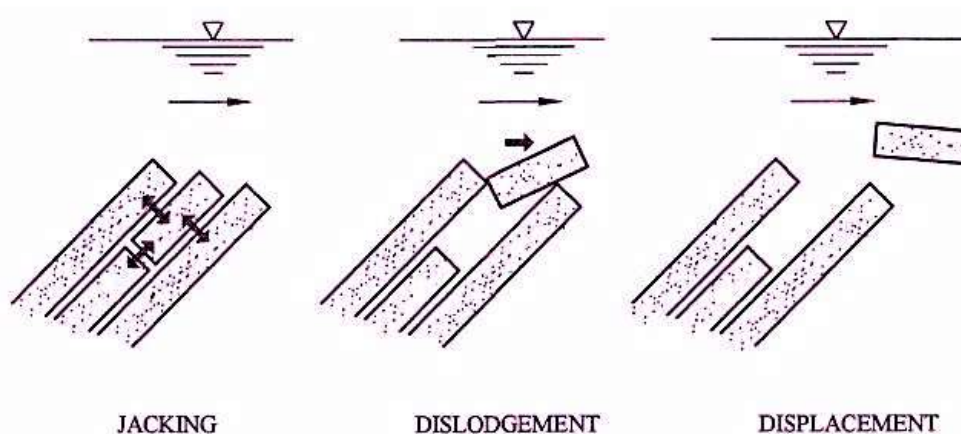


Figure 2-7. Conceptual model depicting the three stages in the rock scour process (adapted from Annandale, 1995).

The instantaneous pressure fluctuations applied on the upper and bottom surfaces of rock blocks cause the jacking effect as the first stage of the scour process. The dislodgement effect is caused by the combination of the plucking forces normal to the loose block and the tangential drag forces induced by the local boundary flows (Spurr, 1985). The characteristics of the rock that influence its erosive resistance are the mass strength, block size, shape and orientation. Smaller sizes and equi-sided shapes rock blocks provide less resistance to erosion than larger and elongated shaped blocks. The orientation of the material relative to the direction of flow also has an impact on its capacity to resist erosion, i.e. when the rock is dipped in the direction of the flow it is easier to remove it compared to the situation where it is dipped against the direction of the flow (Annandale, 1995). Finally, the material is displaced downstream of the scour hole.

Rock scour can occur through three processes, namely brittle fracture, fatigue failure and dynamic impulsion (Bollaert, 2002). These different rock scour mechanisms are further explained in Section 2.4.3.

2.4. Rock Scour Predictions Methods

Rock scour in plunge pools results from the interaction between an aerated turbulent flow environment and a fractured solid mass (Bollaert, 2010). Manso et al (2006) also defines rock scour as a function of the jet type and distance it travels through the air, the discharge time series, the downstream pool depth, and the riverbed's resistance to scour (Manso, 2006).

Based on these definitions, a series of different methods have been developed to evaluate the scour of rock in plunge pools downstream of dams. However, these methods considered a degree of uncertainty in each of these variables. Therefore, in most practical cases, the priority is to estimate the ultimate scour depth and spatial extent that is likely to be reached during the lifetime of the dam. The research demonstrates numerous methods to predict the scour, which can be divided into three methods focusing on the removal of rock blocks, namely:

- empirical methods derived from model or prototype observations (Mason & Arumugan, 1985; Martins, 1973),
- semi-empirical methods (Annandale, 1995) and
- physical-mechanical based methods (Bollaert, 2002; Bollaert & Schleiss, 2005).

2.4.1 Empirical Methods

Empirical formulae used to determine the ultimate scour depth have been derived from laboratory model studies and observation in prototypes. The experiments done by Veronese (1937) as reported by Monfette (2004) lead to the development of empirical formulae that are recommended by the United States Bureau of Reclamation (USBR). These formulae are limited to small-scale tests on non-cohesive beds using vertically falling jets (Monfette, 2004).

Comprehensive reviews have been made by Schleiss and Whittaker (1984), which were updated by Mason and Arumugan (1985) and discussed by Bollaert (2002). The most widely known and used empirical formulae are those of Mason and Arumugan (1985). It was found that the most accurate formula is Equation 7:

$$D = K \frac{q^x H_n^y}{d^z} h^w \quad [7]$$

Where:

D : Depth of scour (m)

q : Unit discharge (m²/s).

H_n: The head drop between reservoir and tailwater levels (m)

h : Tailwater depth (m).

d : The characteristic size of bed material (m)

K, x, y, z and w: Constants proposed by different authors as capsulated in Table 2.2

Table 2.2. Coefficients proposed for equation 7

Author	Year	K	X	Y	z	w
Veronese	1937	1.9	0.54	0.225	0	0
Jaeger	1939	0.6	0.5	0.25	0.333	0.333
Chee and Kung	1974	1.663	0.6	0.2	0.1	0
Damle	1966	0.543	0.5	0.5	0	0
Schoklitsch	1935	0.521	0.57	0.2	0.32	0
Martins	1975	1.5	0.6	0.1	0	0

Scour development downstream of a dam spillway based on different observations of the researchers deals with various materials, flow velocities, and geometry. The equilibrium scour depth measured from the tailwater surface is a function of the unit discharge, the total head, tailwater depth, mean sediment size, acceleration due to gravity, density of the water and the rock. The different formulae developed are discussed as follows:

a) Veronese (1937)

Veronese has considered sediments with $91\text{mm} < d_{50} < 26.2\text{mm}$. The hydraulic heads varied as $0.05\text{ m} < H < 0.50\text{ m}$ and $0.65\text{ m} < H < 1.32\text{ m}$ respectively, and unit discharges were $0.003\text{m}^2/\text{s} < q < 0.10\text{ m}^2/\text{s}$, and $0.001\text{ m}^2/\text{s} < q < 0.083\text{ m}^2/\text{s}$. The Veronese equation yields an estimation of erosion measured from the tailwater surface to the bottom of the scour hole. This equation is given as:

$$D_s = 1.32 H^{0.225} q^{0.54} \quad [8]$$

This formula was modified in 1994 by Yildiz and Uzupek as follows:

$$D_s = 1.90 H^{0.225} q^{0.54} \sin \theta_T \quad [9]$$

Where

D_s : Depth of scour (m).

H : Elevation difference between reservoir and Tailwater (m).

q : Unit discharge (m^2/s).

θ_T : Angle of incidence from vertical of the jet.

b) Jaeger (1939)

Jaeger (1939) reanalysed Schoklitsch's equation (Table 2.2) with coarse sediment in the range $D_{90} = 9$ to 36mm to arrive the following scour depth equation for plunging jets (Dargahi, 2003):

$$D_s = 0.6 q^{0.5} H_n^{0.25} \left(\frac{h}{d_m} \right)^{0.333} \quad [10]$$

Where

D_s : Depth of scour (m).

H_n : Elevation difference between reservoir and Tailwater (m).

q : Unit discharge (m^2/s).

h : Tailwater depth (m).

d_m : Characteristic sediment size of bed material (m).

c) Damle (1966)

Damle et al (1966) used model and prototype data from Indian dams with ski-jumps spillways and developed the following equation to calculate the scour depth:

$$D_s = 0.55 q^{0.50} H^{0.50} \quad [11]$$

Where

D_s : Depth of scour (m).

H : Elevation difference between reservoir and Tailwater (m).

q : Unit discharge (m²/s).

d) Chee and Kung (1974)

Chee and Kung (1974) (as cited in Mason and Arumugan 1985) proposed the following empirical equation to calculate the scour depth that is mostly suited for prototypes:

$$D_s = 1.663q^{0.60}H^{0.20} \quad [12]$$

Where

D_s : Depth of scour (m).

H : Elevation difference between reservoir and Tailwater (m).

q : Unit discharge (m²/s).

e) Martin (1975)

Through prototype observation, Martin (1975) built a riverbed test facility using equally sized cubic blocks that yielded the following equation (Mason & Arumugan, 1985):

$$D_s = 1.5q^{0.60}H^{0.10} \quad [13]$$

Where

D_s : Depth of scour (m).

H : Elevation difference between reservoir and Tailwater (m).

q : Unit discharge (m²/s).

f) Mason (1985)

Mason and Arumugan (1985) developed the following equation for scour depth for estimating the depth of scour under a jet:

$$D_s = \frac{3.27 q^{0.60} H^{0.05} h^{0.15}}{g^{0.30} d^{0.10}} \quad [14]$$

Where

D_s : Depth of scour (m).

H : Elevation difference between reservoir and Tailwater (m).

q : Unit discharge (m²/s).

g : Acceleration of gravity (9.81 m²/s).

d : Median grain size of bed material (m).

Mason (1989) presented a new expression (Equation 15) for calculating the scour depth by considering the effect air entrainment has on scour for a jet with an impact angle of 45°. The air entrainment replaces the use of elevation difference between reservoir and tailwater level (drop height H) used in the empirical formulae developed by Mason and Arumugan (1985) (Equation 14). The empirical expression is suited for prototype and models. The equation is:

$$D_s = 3.39 \frac{q^{0.60} (1 + \beta)^{0.30} h^{0.16}}{g^{0.30} d_m^{0.06}} \quad [15]$$

Where

- D_s**: Depth of scour (m).
- q**: Unit discharge (m²/s).
- h**: Tailwater depth (m).
- d_m**: Characteristic sediment size of bed material (m).
- g**: Gravitational acceleration (9.81 m²/s).
- β**: Air-water relationship (-).

g) **Bombardelli and Gioia (2006)**

Bombardelli and Gioia (2006) developed the following empirical expression for calculating scour depth by considering another parameter known as specific gravity of sediment:

$$D_s = K \frac{q^{0.67} H_n^{0.67} h^{0.15}}{g^{0.33} d_{90}^{0.33}} \left(\frac{\rho}{\rho_s - \rho} \right) \quad [16]$$

Where

- D_s**: Depth of scour (m).
- q**: Unit discharge (m²/s).
- h**: Tailwater depth (m).
- d_m**: Characteristic sediment size of bed material (m).
- H_n**: Elevation difference between reservoir and Tailwater (m).
- g**: Gravitational acceleration (m²/s).
- ρ**: Water density (kg/m³).
- ρ_s**: Density of sediment (kg/m³).

2.4.2 Semi-empirical Methods

Semi-empirical methods can also be used to evaluate rock scour. The Erodibility Index method developed by Annandale (1995) was developed in order to investigate the scour threshold of the earth material ranging from granular sediment to rock mass formation. The method is based on quantification of the relative ability of the earth material to resist the erosion capacity of water and the relative magnitude of the erosive capacity of water (stream power) (Annandale, 2006). This method does not take into account the rate at which the scour hole forms.

2.4.2.1. Erodibility Index (EI)

The Erodibility Index is used to quantify the relative ability of earth material to resist the scour capacity of the water proved by Annandale (1995). It takes into account the mass strength, block size, inter-particle or block friction and relative shape and orientation of the rock blocks. The Erodibility Index can be calculated by the following equation:

$$K_h = M_s K_b K_d J_s \quad [17]$$

Where

K_h : Erodibility Index.

K_b : Block or particle size factor.

K_d : Shear strength factor.

J_s : Factor representing the impact of the relative shape and relative orientation of rock that is exposed to the erosive power of water.

M_s : Mass strength Factor for granular soil

The mass strength (M_s) number equals the product of a material's uni-axial compressive strength (UCS) and its coefficient of relative density as stated by Annandale (2006). It represents the potential of the rock to scour because of brittle fracture or fatigue failure. Typical M_s -values are repeated in Table A 0.1 in Appendix A. It can be also calculated by:

$$M_s = c_r 0.78 UCS^{1.05} \text{ when } UCS \leq 10\text{pa} \quad [18]$$

$$M_s = C_r UCS \text{ when } UCS > 10\text{Mpa} \quad [19]$$

The C_r (N/m^3) is a coefficient of relative density. It is defined by the acceleration of gravity (g in m/s^2) and the density of rock (ρ in kg/m^3). This coefficient is calculated in equation 20.

$$C_r = \frac{g \rho_r}{27 \times 10^3} \quad [20]$$

The particle size number (K_b) is a function of the rock joint spacing and the number of joint sets that represents the potential for block removal (Annandale, 2006). The rock joint spacing can be calculated through the Rock Quality Designation (**RQD**). For rock materials, the equation is:

$$K_b = \frac{RQD}{J_n} \quad [21]$$

Where

RQD: Rock Quality Designation number.

J_n : The joint set number which is a function of the number of joint sets in a rock mass refer to Table A 0.2 in Appendix A and the rock joint set is provide in Figure A 0-1.

The shear strength factor (**K_d**) relates to the different surface characteristics of the joints and represents the friction developed between the blocks. According to Annandale (2006), the discontinuity shear strength factor is determined as a ratio between the joint wall roughness (**J_r**) and wall alteration (**J_a**):

$$K_d = \frac{J_r}{J_a} \quad [22]$$

Where

J_r : Degree of roughness of opposing faces of rock discontinuity.

J_a : Degree of alteration of materials.

The values of **J_r** and **J_a** can be found in Table A 0.3 and Table A 0.4 in Appendix A.

Annandale (2006) defines the orientation and shape factor (**J_s**) as “relative ground structure number which represents the relative ability of rock to resist erosion because of the structure of the rock formation and its direction to the flow.” It is a function of the angle between the rock joints and the horizontal plane and the ratio of the joint spacing (Annandale, 1995). The concepts of this factor are illustrated in Table A 0.5 Appendix A. The shear strength factor, orientation and shape factor represents the strength of the eroded rock and block orientation.

2.4.2.2. Stream Power

The ability of the flow to generate erosion, stream power (**P**), can be expressed in terms of velocity **v** and energy loss **ΔE** such as (Annandale, 1995):

$$P = \frac{\gamma Q \Delta E}{A} = \gamma v \Delta E \quad [23]$$

Where

γ: The unit weight of water (N/m³).

Q : Total discharge (m³/s).

A : Area perpendicular to the flow (m²).

Annandale (1995) established a relationship known as the erosion threshold between stream power and the Erodibility Index by analysing published and field data for a wide variety of earth material types and flow conditions. The relationship shown in Figure 2-8 compares the Erodibility Index with the erosive capacity of the water (stream power) to determine whether scour would occur.

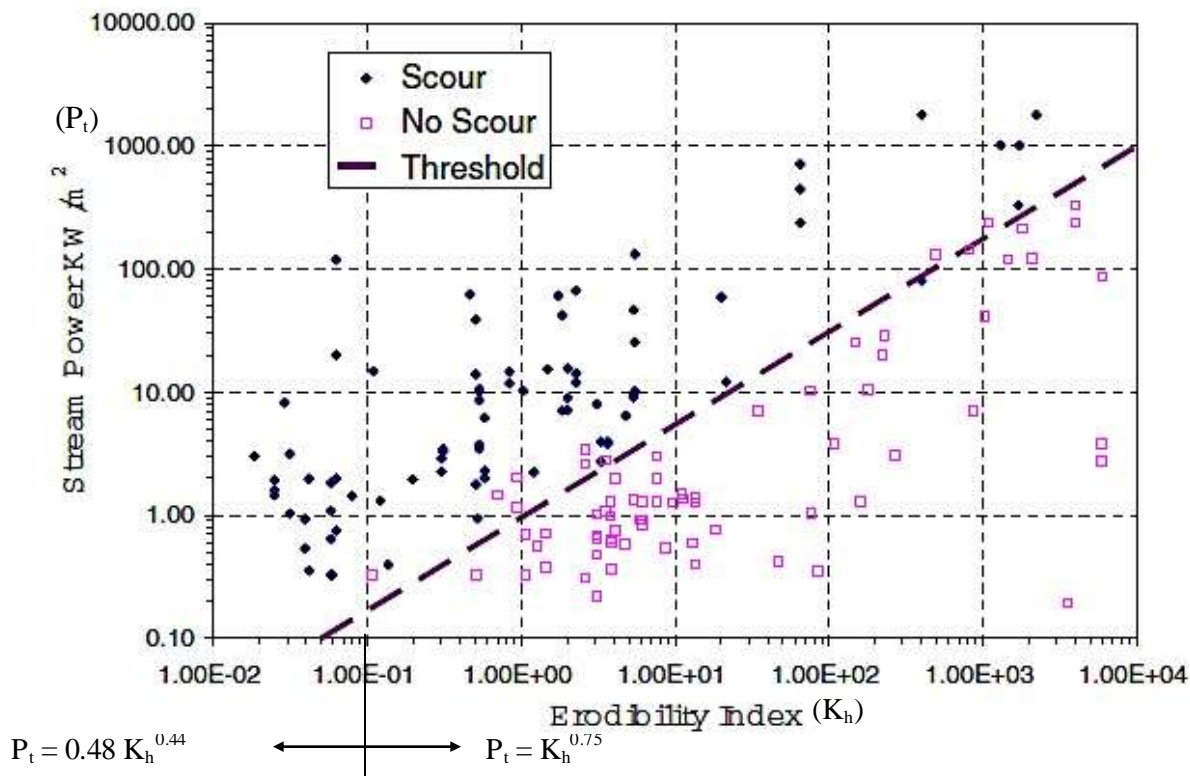


Figure 2-8. Erosion Threshold for variety of earth material between stream power and EI (adapted from Annandale, 2006).

The threshold stream power for a particular earth material is determined (dashed line on Figure 2-8) by using either of the following equation (Annandale, 1995; 2006; Castillo & Carrillo, 2014):

$$P_{rock} = 0.48K^{0.44} \text{ if } K \leq 0.1 \quad [24]$$

$$P_{rock} = K^{0.75} \text{ if } K > 0.1$$

It is evident from Figure 2-8 that as long as the available stream power exceeds the required stream power for erosion, the bedrock would begin to scour. The Erodibility Index method can determine the equilibrium scour depth and not the extent of the scour hole and the scour rate.

2.4.3 Physical-Mechanical Method (Comprehensive Scour Model)

A new method, the Comprehensive Scour Model, was proposed by Bollaert (2002) for ultimate scour depth evaluation. It is based on the experimental and numerical investigation of dynamic water pressure in rock joints.

The structural model of the comprehensive scour is entirely physical-mechanically based and considers pressure fluctuations acting on the water-rock interface and inside rock fissures. The structural model consists of three modules: the falling jet, the plunge pool and the fractured rock as illustrated in Figure 2-9 (Bollaert, 2012). The rock module evaluates scour formation due to plunging jets by means of three methods, namely:

- Comprehensive Fracture mechanics (CFM) method
- Dynamic Impulsion (DI) method
- Quasi-Steady Impulsion method (QSI)

The Comprehensive Fracture mechanics (CFM) determines the ultimate scour depth by expressing instantaneous or time-dependent joint propagation due to water pressures inside the joint as pointed out by Bollaert (2004). In this method, hydrodynamic fracturing of closed-end joints means that the joints are not yet completely formed (intact rock). The Dynamic Impulsion (DI) method describes the ejection of rock blocks from their mass because of sudden uplift forces (Bollaert, 2004). This means that the joint network has completely formed. The Quasi-Steady Impulsion method (QSI) describes the peeling-off of protruding blocks generated by the turbulent jet generating a high-velocity flow oriented upstream and parallel to protruding blocks (Bollaert, 2012). Figure 2-9 summarises the main parameters of the falling jet module.

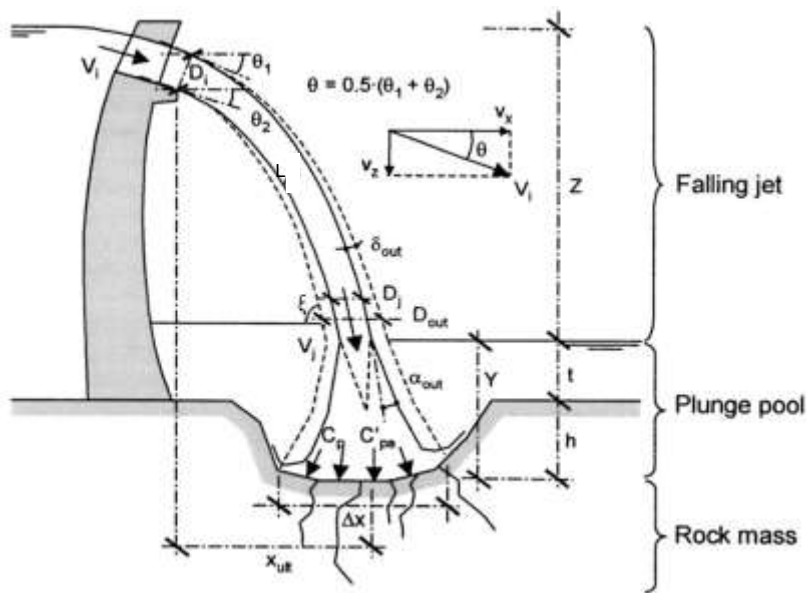


Figure 2-9. Schematic diagram of the parameters of a falling jet (adapted from Bollaert, 2002)

A. Falling Jet Module

The falling jet describes how the hydraulic and geometric characteristics of a jet are transformed from the point of issuance down to the plunge pool (Figure 2-9 and Figure 2-2). Three parameters characterise the jet at issuance, namely the velocity V_i , the core diameter D_i , and the initial turbulence intensity T_u . The jet module computes the longitudinal location of impact x_{ult} , the total trajectory length L and the velocity V_j , outer later jet spread δ_{out} and the diameter D_j at impact. The velocity V_j and core diameter D_j at impact with the pool surface can be calculated with equation 25 and 26 respectively.

$$V_j = \sqrt{V_i^2 + 2gz} \quad [25]$$

$$D_j = D_i \sqrt{\frac{V_i}{V_j}} \quad [26]$$

Ervin et al (1997) depicts two opposed properties that govern the flow of water jets in the air, namely the stability and internal turbulence. The turbulence intensity T_u is defined as the ratio of velocity fluctuations to the mean velocity. Ervin and Falvey (1987) determined the relationship between the jet's outer diameter d_{out} (circular jet) or jet's outer width B_{out} (rectangular jet) and the distance along the jet

trajectory X_L which relates to the turbulence intensity and the half lateral spread of the jet (δ_{out}) as it travels through the air:

$$B_{out} = B_i + 2\delta_{out}L \quad \text{where} \quad \frac{\delta_{out}}{x_L} = 0.38T_u \quad [27]$$

Where

x_L is the distance from the issuance section

B_i is the width of the jet at issuance

B. Plunge Pool Module

Bollaert (2004) describes the plunge pool module as the characteristics of the jet when traversing through the plunge pool and it defines the water pressures at the water-rock interface. Diffusion of the jet core in the plunge pool dissipates a part of the jet's energy (scour potential). The behaviour of a turbulent water jet, in the air and inside a plunge pool, was investigated by Ervine and Falvey (1987) and they found that the outer turbulent zone of the jet expands at a different angle than that at which the inner core contracts. Whittaker and Schleiss (1984) reveal that the remaining energy that was not dissipated by the "water cushion" in the plunge pool is responsible for the dynamic pressures applied on the pool bottom. Figure 2-10 shows the jet diffusion in plunge pool with maximum dynamic pressure at the bottom at the rock interface.

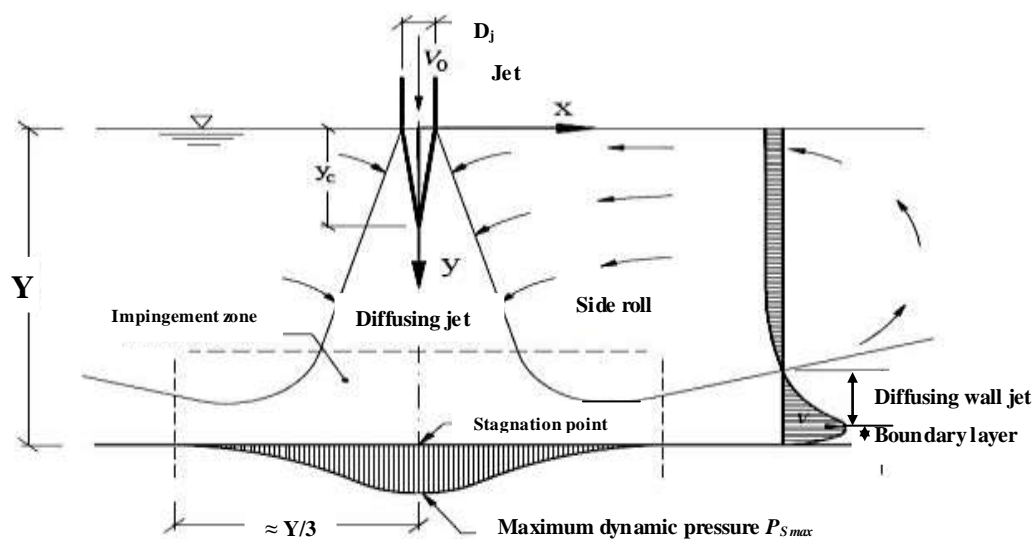


Figure 2-10. Jet diffusion in a pool with maximum dynamic pressure at the bottom (adapted from Melo, 2002)

As mentioned in section 2.2.2, the jet diffuses almost linearly and as it plunges into the pool and air is entrained at the tailwater level. When the jet impinges on the rock-bed (Figure 2-10), it generates dynamic pressures inside the rock joints. The plunge pool water depth Y is essential in this plunge pool module. The ratio Y/D_j is determined by the water depth Y and the jet core diameter at impact D_j . This ratio relates to the jet diffusion characteristics in the plunge pool. The pressures measured are the mean dynamic pressure coefficient C_{pa} and the root-mean-square coefficient of fluctuating dynamic pressures C'_{pa} under the centreline of the jet (Bollaert, 2002). Moreover, the jet large entrains quantities of air into

the plunge pool, which strongly effect in diffusion properties. The mean density of air-to-water jet inside the plunge pool ρ_{aw} , Ervine and Falvey (1987) proposed:

$$\rho_{aw} = \frac{1}{1 + \beta} \rho_w + \frac{\beta}{1 + \beta} \rho_a \quad [28]$$

Where ρ_a and ρ_w are the air and water densities. Therefore, the dissipation process of the jet begins when the jet aeration was plunging into the pool with air-water ratio β , density ρ_{aw} and kinetic energy E_k . The kinetic energy is given by the equation 29 (Elvine, et al., 1997).

$$E_k = 1/2 \rho_{aw} V_i^2 \quad [29]$$

Furthermore, the time-averaged pressure coefficient is defined as C_p , which is reproduced by the following relationship as reported by Duarte (2014):

$$C_p = \psi \left(0.926 - 0.0779 \frac{Y - Y_c}{B_j} \right)^2 \quad \text{if } Y > Y_c \quad [30]$$

$$\psi = \frac{1}{1 + \exp \left\{ -5.37 \times 10^{-6} \left(\frac{V_i B_j}{\nu} - 6.63 \times 10^5 \right) \right\}} \quad [31]$$

If $Y < Y_c$, the core of the jet effects directly on the rock bottom, the C_p equals to 0.86. Hence, Y_c is the core development length and can calculated by the equation 32. The parameter ψ defines the loss of energy that takes place at the impingement region formed at the vicinity of the intersection of the jet centerline with the pool bottom (Beltaos & Rajaratnam, 1977).

$$\begin{aligned} \frac{Y_c}{B_i} &= 7.74 \times 10^{-6} \frac{V_i B_j}{\nu} & \text{if } \frac{Y_c}{B_i} \leq A' \\ \frac{Y_c}{B_j} &= A' & \text{if } \frac{Y_c}{B_i} > A' \end{aligned} \quad [32]$$

Where ν is the kinematic viscosity of fluid and parameter A' is 3.5 for submerged jets and 7.8 for plunging jets. In addition, the Y/D_j ratio, H/L_b ratio where L_b is the jet break-up length, the velocity of the jet at impact V_j in the plunge pool and air concentration at impact in the pool α_i define the mean dynamic pressure coefficient C_{pa} :

For circular jet (Elvine, et al., 1997):

$$C_{pa} = 38.4 (1 - \alpha_i) \left(\frac{D_j}{Y} \right)^2 \quad \text{for } Y/D_j > 4 - 6 \quad [33]$$

$$C_{pa} = 0.85 \quad \text{for } Y/D_j < 4 - 6 \quad [34]$$

Where the air concentration at the impact in the pool α_i is calculated as a function of the volumetric air to water ratio β :

$$\alpha_i = \frac{\beta}{1 + \beta} \quad [35]$$

The expressions of the volumetric air to water ratio β are summarised in section 2.2.2.

For Rectangular jet (Castillo & Carrillo, 2014):

1. $Y \leq 5.5 B_j$

$$C_{pa} = 1 - 0.0014e^{5.755(H/L_b)} \text{ for } \frac{H}{L_b} < 1.00 \quad [36]$$

$$C_{pa} = 14.643e^{-3.244(H/L_b)} \text{ for } \frac{H}{L_b} > 1.00 \quad [37]$$

2. $Y \geq 5.5 B_j$

$$C_{pa} = ae^{-b(Y/D_j)} \quad [38]$$

Where a, b, c and d are the coefficients for calculating the dynamic pressure and root-mean-square pressure fluctuations coefficients and are dependent on the degree of the jet development, H/L_b , as shown in Table 2.3, Table 2.4 (for $0 \leq Y/D_j \leq 14$) and Table 2.5 (for $Y/D_j \geq 14$).

Table 2.3. Coefficient values of dynamic pressure coefficient C_{pa} formula (Castillo & Carrillo, 2014)

H/L_b	a	b
≤ 0.85	2.50	0.20
0.90-1.00	1.70	0.18
1.00-1.10	1.35	0.18
1.10-1.20	1.00	0.17
1.20-1.30	0.88	0.18
1.30-1.40	0.39	0.15
1.40-1.60	0.24	0.14
≥ 1.60	0.14	0.12

The root-mean-square pressure fluctuations C'_{pa} at the water-rock interface depends on the Y/D_j ratio and the initial turbulence intensity of the jet T_u (Castillo & Carrillo, 2014):

$$C'_{pa} = a \left(\frac{Y}{D_j} \right)^3 - b \left(\frac{Y}{D_j} \right)^2 + c \left(\frac{Y}{D_j} \right) + d \text{ for } Y/D_j \leq 14, \text{ polynomial fit} \quad [39]$$

Table 2.4. Coefficient values of root-mean-square pressure fluctuations coefficient C'_{pa} formula with $Y/D_j \leq 14$ (Castillo & Carrillo, 2014).

	$0 \leq Y/D_j \leq 14$			
H/L_b	a	B	c	d
≤ 0.80	0.00030	-0.01000	0.0815	0.08
0.80-1.00	0.00030	-0.01000	0.0790	0.13
1.00-1.30	-0.00001	-0.00220	0.0160	0.35
1.30-1.60	0.00003	-0.00180	0.0100	0.21
1.60-1.80	0.00005	-0.00195	0.0098	0.16
≥ 1.80	0.00005	-0.00190	0.0100	0.11

For $Y/D_j \geq 14$, Coefficient values of root-mean-square pressure fluctuation can be determined by the following relationship (Castillo & Carrillo, 2014):

$$C'_{pa} = ae^{-b\left(\frac{Y}{D_j}\right)} \quad [40]$$

Table 2.5. Coefficient values of root-mean-square pressure fluctuations coefficient C'_{pa} formula with $Y/D_j \geq 14$ (Castillo & Carrillo, 2014).

	$Y/D_j \geq 14$	
H/L_b	a	b
≤ 0.80	1.50	0.21
0.80-1.00	1.80	0.21
1.00-1.30	1.00	0.15
1.30-1.60	0.40	0.12
1.60-1.80	1.33	0.23
≥ 1.80	2.50	0.35

Hence, the dynamic pressures are a function of the fall height (H) to disintegration height (L_b) ratio (H/L_b) and water cushion (Y) to impingement jet thickness (B_j) ratio (Y/B_j), thus the total dynamic pressure is expressed as (Castillo & Carrillo, 2014):

$$P_{Total} = C_p \left(\frac{Y}{B_j} \right) P_{jet} + FC'_p \left(\frac{Y}{B_j} \right) P_{jet} \quad [41]$$

Where $C_p(Y/B_j)$ is the mean dynamic pressure coefficient, $C'_p(Y/B_j)$ the fluctuation dynamic pressure coefficient, P_{jet} the stream power per unit of area and F the reduction factor of the fluctuating dynamic pressure coefficient. Castillo and Carrillo (2014) were adjusted the formulae by using new laboratory data for rectangular jet (Figure 2-11).

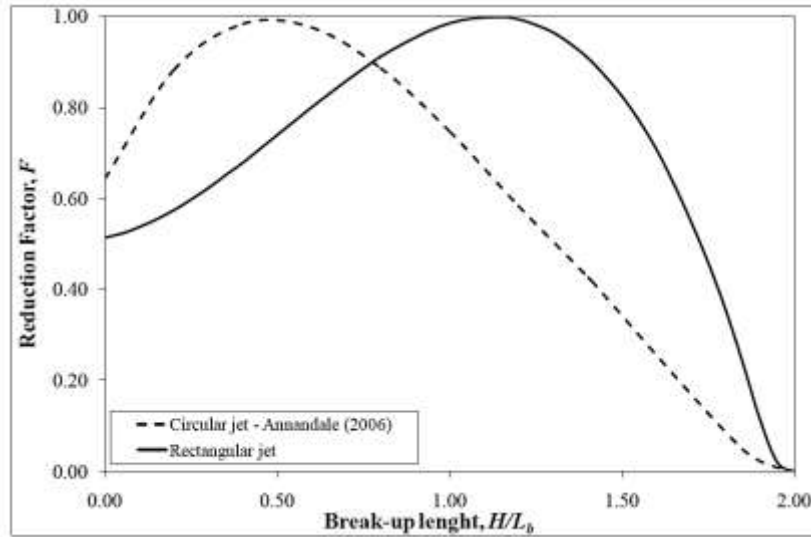


Figure 2-11. Reduction factor F of fluctuating dynamic pressure coefficient (adapted from Castillo & Carrillo, 2014)

The tests with submerged jets could assess the influence of jet aeration β on the C_p values and the time-averaged pressure coefficients for aerated jets C_p^a divided by the corresponding C_p value for non-aerated jet are expressed as function of β (Duarte, 2014):

$$\frac{C_p^a}{C_p} = 1 + 0.4\beta \quad [42]$$

Bollaert (2002) recommends that to relate the choice of mean dynamic pressure coefficient C_{pa} to the choice of root-mean-square pressure fluctuation C'_{pa} "the higher the chosen curve of root-mean-square values, the lower the choice for the mean pressure value". Bollaert (2002) illustrated that the three parameters, such as Y/D_j ratio, mean dynamic pressure coefficient C_{pa} and root-mean-square pressure fluctuation C'_{pa} are used to define the ultimate scour depth under the jet's centerline. In addition, the determination of the shape and the extent of the ultimate scour hole need these aforementioned parameters, as well as the radial pressure coefficient C_{pr} and the radial pressure fluctuations C'_{pr} .

Bollaert (2002) described that "the radial distribution of the non-dimensional fluctuating dynamic pressure coefficient C'_{pa} is of great significance for the radial shape and extension of the scour hole". He proposed the following expressions to determine the C'_{pa} -value:

$$\frac{C'_{pr}}{C'_{pa}} = e^{-3\left(\frac{r}{r_{max}}\right)^2} \text{ for developed and all } r \text{ values} \quad [43]$$

$$\frac{C'_{pr}}{C'_{pa}} = e^{-3\left(\frac{r}{r_{max}} - 0.5\right)^2} \text{ for core jets and } r > 0.5 r_{max} \quad [44]$$

$$\frac{C'_{pr}}{C'_{pa}} = 1 \text{ for jets and } r < 0.5 r_{max} \quad [45]$$

For the practice of the radial mean dynamic pressure coefficient, Bollaert (2002) proposed the following expressions:

$$\frac{C_{pr}}{C_{pa}} = e^{-3\left(\frac{r}{r_{max}}\right)^2} \text{ for core jets (undeveloped)} \quad [46]$$

$$\frac{C_{pr}}{C_{pa}} = e^{-6\left(\frac{r}{r_{max}}\right)^2} \text{ for developed jet} \quad [47]$$

Bollaert (2002) concluded that it is important to know that the radial decay of the mean dynamic pressures is much higher than the radial decay of the corresponding root-mean-square pressures, because the root-mean-square pressures generate peak pressure inside underlying rock joints.

C. The Rock Mass Module

Bollaert (2002) defines the pressure at the bottom of the pool as used for determination of transient pressures inside open-end or closed-end rock joints. Bollaert and Schleiss (2003) show that inside rock joints, pressures propagate as pressure waves in pressurised flows. Bollaert and Schleiss (2003) conducted an experiment of high-velocity impinging jets and examined two processes of rock erosion: crack propagation and block uplift. Bollaert (2002) and Bollaert and Schleiss (2003) have highlighted how brittle fracture and fatigue failure modes occurring inside the rock fissures break up the rock into smaller pieces. Short-duration pressures peaks generate brittle failure, whereas failure by fatigue is time dependent.

The main parameters for this module that define the hydrodynamic loading inside open-end or close-end rock joints are (Bollaert, 2002):

1. Maximum dynamic pressure coefficient C_p^{max}
2. Characteristic amplitude of pressure cycles Δp_c
3. Characteristics frequency of pressure cycles f_c
4. Maximum dynamic impulsion coefficient C_I^{max}

The maximum dynamic pressure coefficient C_p^{max} is applicable to brittle propagation of closed-end rock joints. Bollaert (2002) developed an amplification factor Γ^+ that is applied to the fluctuation dynamic pressure coefficient C'_{pa} and by superposition with the mean dynamic pressure C_{pa} to determine the maximum dynamic pressure coefficient C_p^{max} as:

$$P_{max} (Pa) = \gamma C_p^{max} \frac{\phi V_j^2}{2g} = \gamma (C_{pa} + \Gamma^+ C'_{pa}) \frac{\phi V_j^2}{2g} \quad [48]$$

Where γ is the specific weight of water (N/m^3), ϕ is a coefficient of non-uniform velocity profile, P_{max} is maximum pressure (Pa) and amplification factor Γ^+ which is defined by means of theoretical curves for the maximum and minimum shown below:

$$\begin{array}{l}
\Gamma^+ = 4 + 2 \frac{Y}{B_j} \quad \text{for } \frac{Y}{B_j} < 8 \\
\Gamma^+ = 20 \quad \text{for } 8 \leq \frac{Y}{B_j} \leq 10 \\
\Gamma^+ = 40 - 2 \frac{Y}{B_j} \quad \text{for } \frac{Y}{B_j} > 10
\end{array}
\left. \vphantom{\begin{array}{l} \Gamma^+ = 4 + 2 \frac{Y}{B_j} \\ \Gamma^+ = 20 \\ \Gamma^+ = 40 - 2 \frac{Y}{B_j} \end{array}} \right\} \begin{array}{l} \text{Curve of} \\ \text{maximum} \\ \text{values} \end{array}$$

$$\begin{array}{l}
\Gamma^+ = -8 + 2 \frac{Y}{B_j} \quad \text{for } \frac{Y}{B_j} < 8 \\
\Gamma^+ = 8 \quad \text{for } 8 \leq \frac{Y}{B_j} \leq 10 \\
\Gamma^+ = 28 - 2 \frac{Y}{B_j} \quad \text{for } \frac{Y}{B_j} > 10
\end{array}
\left. \vphantom{\begin{array}{l} \Gamma^+ = -8 + 2 \frac{Y}{B_j} \\ \Gamma^+ = 8 \\ \Gamma^+ = 28 - 2 \frac{Y}{B_j} \end{array}} \right\} \begin{array}{l} \text{Curve of} \\ \text{minimum} \\ \text{values} \end{array} \quad [49]$$

The characteristic amplitude of pressure cycles Δp_c is determined by the characteristic maximum and minimum pressures of the cycles as stated by Bollaert (2002). Minimum pressures are considered equal to the standard atmospheric pressure and the maximum pressure is chosen to be equal to the C_p^{max} value according to the shape of the pressure spikes (Bollaert, 2004). Therefore, the average value of the maximum pressures is needed and it can be obtained by counting the number of peaks and by making the average of all the peaks values.

Bollaert (2002) illustrated that the characteristic frequency of pressure cycles f_c follows the assumption of a perfect resonator system and depends on the air concentration in the joint α_i and on the length of the joint L . An assumption has to be made on the length of the joint. The air content inside the joint can be related to the air content in the plunge pool.

The characteristic amplitude of pressure cycles Δp_c and the characteristic frequency of pressure cycles f_c express the time-dependent propagation of closed-end rock joints. The maximum dynamic impulsion coefficient C_I^{max} is used to define dynamic uplift of rock blocks formed by an open-end rock joint and the calculation thereof is discussed under the Dynamic Impulsion method in section 2.4.3.2.

2.4.3.1. Comprehensive Fracture mechanics method

Brittle friction causes the rock to breakup into smaller pieces over a short time period. It is also an instantaneous failure that occurs as soon as the shear intensity becomes larger than the fracture roughness of the rock as illustrated in Figure 2-12.

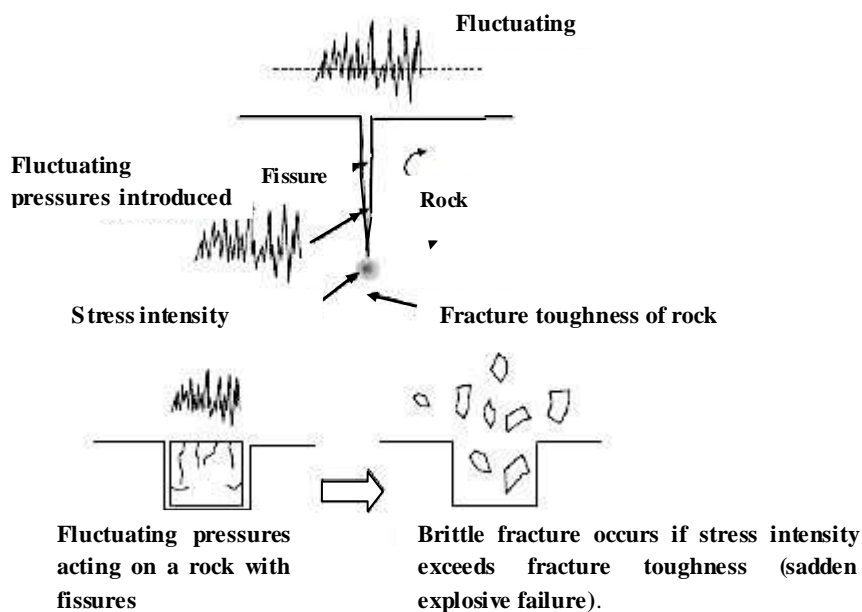


Figure 2-12. Brittle fracture failure of rock (adapted from Annandale, 2006).

Bollaert (2002) proposed a method that describes joint propagation by fatigue stresses occurring at the tip of a joint. This method is applicable to any partially jointed rock (Bollaert, 2004). The stress intensity factor K_I described the pure tensile pressure loading inside the rock joint, representing the amplitude of the rock mass stresses generated by water pressures at the tip of the joint (Bollaert, et al., 2015). The corresponding resistance of the rock mass against joint propagation is expressed by its fracture toughness K_{IC} . Brittle fracture of the rock would occur when the stress intensity (K_I) in the close-ended rock fissure is greater than the fracture toughness (K_{IC}) of the rock, i.e.

$$K_I > K_{IC} \quad [50]$$

The stress intensity is expressed as:

$$K_I = \sigma_{water} \sqrt{\pi a f} \quad [51]$$

Where

σ_{water} : Stress introduced by turbulent fluctuating pressures in a close-ended fissure (MPa).

a : Crack length (m).

f : A factor that accounts for the shape of the close-ended fissure.

K_I : Stress intensity ($MPa\sqrt{m}$).

The fracture toughness is related to the mineralogical type of rock and to the unconfined compressive strength (UCS). The fracture toughness of rock can be determined by equations 52 and 53 as developed by Bollaert (2002):

$$K_{I,insitu,T} = (0.105 \text{ to } 0.132)T + (0.054\sigma_i) + 0.5276 \quad [52]$$

$$K_{I,insitu,UCS} = (0.008 \text{ to } 0.010)UCS + (0.054\sigma_i) + 0.42 \quad [53]$$

Where

T : Tensile strength of the rock (MPa).

UCS : Unconfined compressive strength of the rock (MPa).

σ_i : Confining stress in the rock (MPa).

Fatigue failure refers to the time-dependent breakup of rock mass along existing close-ended fissures. Therefore, when the stress intensity caused by the fluctuating pressure does exceed the fracture toughness of rock, fatigue failure occurs after a period time as shown in Figure 2-13.

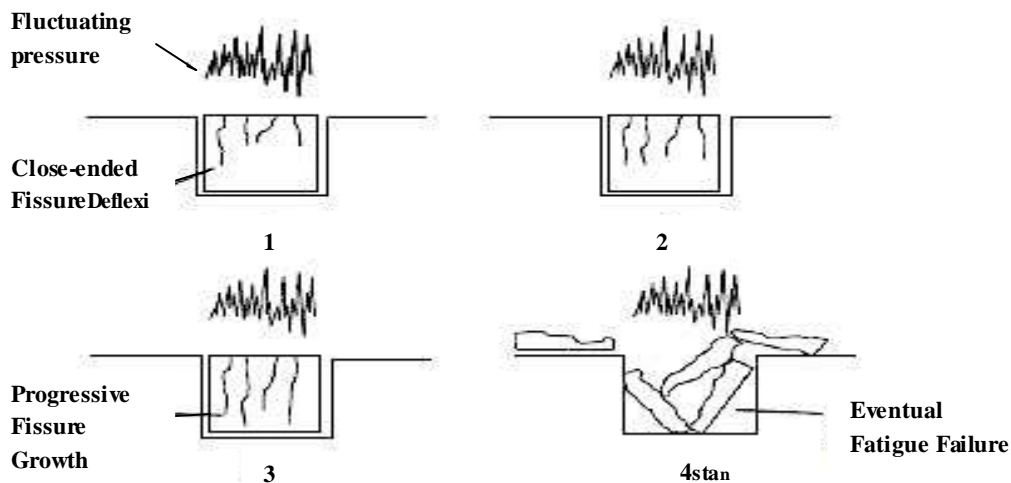


Figure 2-13. Fatigue failure of rock (adapted from Annandale, 2006).

Bollaert (2002) calculated the time to propagate a fissure through a certain distance by the time-dependent joint propagation. This is expressed by equation 54 that was originally proposed to describe fatigue growth in metals:

$$\frac{dL_f}{dN} = C_r (\Delta K_I / K_{IC})^{m_r} \quad [54]$$

Where N is the number of pressure cycles. C_r and m_r are material parameters that are determined by fatigue tests and ΔK_I represents the difference between maximum and minimum stress intensity factors. To implement time-dependent joint propagation into the model, C_r and m_r have to be known as they depend on the rock type and quality. Table A 0.6 in Appendix A presents different values of C_r and m_r . They represent the vulnerability of rock to fatigue and have been derived from available literature and data on the sensitivity of rock to quasi-steady break-up by water pressure in a joint (Bollaert, 2004).

2.4.3.2. Dynamic Impulsion method

The Dynamic Impulsion method aims to evaluate the scour potential of plunging jets by means of their capacity to remove the individual rock blocks from the pool bottom by analysing the forces that works onto the blocks (Bollaert & Schleiss, 2005). Figure 2-14 shows a schematic of a rock block and the forces acting onto it. This method is only applicable when the rock mass has been completely fractured by brittle fracture or fatigue failure. The method does not consider the evolution in time of the scour hole, but instead computes the equilibrium or ultimate scour depth.

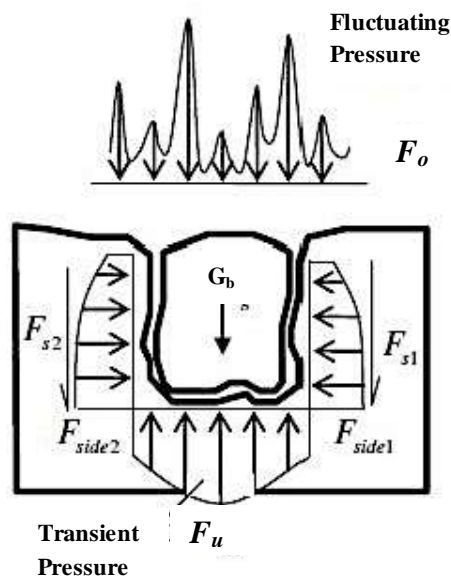


Figure 2-14 Block removal failure of rock (adapted from Annandale, 2006).

Bollaert (2002) described that the impulse on a rock corresponds to a time integration of the net forces (Figure 2-14) on the rock block. It is expressed by equation 55:

$$I_{\Delta tpulse} = \int_0^{\Delta tpulse} (F_u - F_o - G_b - F_{sh}) dt = mV_{\Delta tpulse} \quad [55]$$

Where

F_u : Force under the block.

F_o : Force over the block.

G_b : The immersed weight of the block.

F_{sh} : The shear and interlocking forces.

m : mass of block.

$V_{\Delta tpulse}$: Uplift velocity

The Dynamic Impulsion method is also defined by the maximum dynamic pressure impulsion coefficient and the characteristics of a rock block. As already mentioned in section 2.4.3 C, the dynamic impulsion coefficient C_I^{max} is defined as the non-dimensional uplift force (Newton) acting on the rock block during a given time period. The maximum dynamic impulsion coefficient can be computed by the maximum impulse I^{max} through dividing it by the period of the pressure waves inside the joints $T_p = \frac{2L_f}{c}$ (Bollaert & Schleiss, 2005). It is expressed as the following:

$$C_I^{max} = \frac{I^{max} c}{x_b^2 \rho_{aw} V_j^2 L_f} \quad [56]$$

Where

L_f : The fissure length (m)

c : Wave celerity (-)

x_b^2 : The square base of side of rock block (m)

V_j^2 : Velocity of the jet at the plunge section (m/s)

ρ_{aw} : Density of the air-water mixture (Kg/m³)

In addition, Bollaert (2002) has expressed the maximum dynamic impulsion coefficient C_I^{max} in terms of the dimensionless depth Y/D_j in a plunge pool, where Y is the plunge pool depth and D_j or B_j is the diameter or width of a circular or rectangular jet respectively at the water surface of the plunge pool. Hence, the non-dimensional impulsion coefficient C_I is used to obtain the maximum net impulsion by multiplying it with $V^2L/g.c$. Its magnitude can also be calculated with Equation 57:

$$C_I^{max} = 0.0035 \left(\frac{Y}{D_j} \right)^2 - 0.119 \left(\frac{Y}{D_j} \right) + 1.22 \quad [57]$$

Bollaert and Schleiss (2005) simplified the block geometry to a rectangular block (Figure 2-15), based on case study data. The increase of the pressure at the bottom of the block (F_u) is caused by the application force induced by fluctuating pressures (F_o). If the uplift forces are greater than the fluctuating pressures, the submerged weight (G_b) and side friction forces (F_S) of the rock block, failure in jointed rock occurs. The height of the block displaced (h_{up}) can be calculated by using:

$$h_{up} = \frac{V_{\Delta t pulse}^2}{2g} \quad [58]$$

Where $V_{\Delta t pulse}$ is the uplift velocity (refer to equation 55) and the immersed weight of the block G_b can be calculated as follows:

$$G_b = \forall (\gamma_r - \gamma_w) = x_b^2 \cdot z_b (\gamma_r - \gamma_w) \quad [59]$$

Where

$(\gamma_r - \gamma_w)$: The specific weight of the rock respectively to that of water

x_b : The side length of rock block (m) (Figure 2-15)

z_b : The vertical side of the block (m) (Figure 2-15)

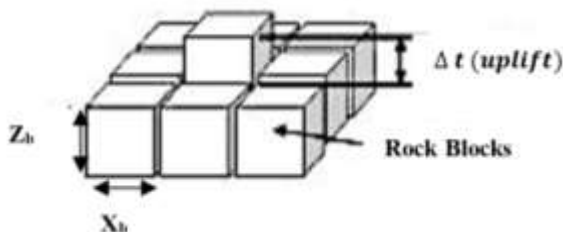


Figure 2-15. Bollaert's (2002) simplified rock mass

Bollaert (2002) have proposed the criteria shown in Table 2.6 for determining whether a rock block from a jointed mass would experience incipient motion.

Table 2.6. Criteria to assess rock scour by DI (Bollaert, 2002)

$H_{up}/Z_b \leq 0.1$	Rock block remains in place
$0.1 < H_{up}/Z_b < 0.5$	Rock block vibrates and most likely remains in place
$0.5 \leq H_{up}/Z_b < 1$	Rock block vibrates and is likely to be removed depending of ambient flow conditions
$H_{up}/Z_b > 1$	Rock block is definitely removed from its matrix

2.4.3.3. Quasi-steady Impulsion method

Bollaert (2012) describes the quasi-steady impulsion method (QSI) as the flow parallel to the bottom, outside of the impingement region of the jet that causes the scour. Particularly, it is a specific combination of brittle or fatigue fracturing and quasi-steady forces which define the peeling-off of rock blocks from their mass. Bollaert (2012) and Reinius (1986) described the diffusion and bottom deflection of a high-velocity jet through a plunge pool. As explained in Section 2.4.3, so far, the free jet region and the jet impingement have been discussed with other methods such as CFM and DI. However, QSI deals with the wall jet region (refer to Figure 2-4). Because of the flow deviation, it generates drag and lift forces on the blocks and the net uplift displacement governed by the protrusion (e) of the block into the flow and by the local quasi-steady flow velocity (V_x) (Figure 2-16).

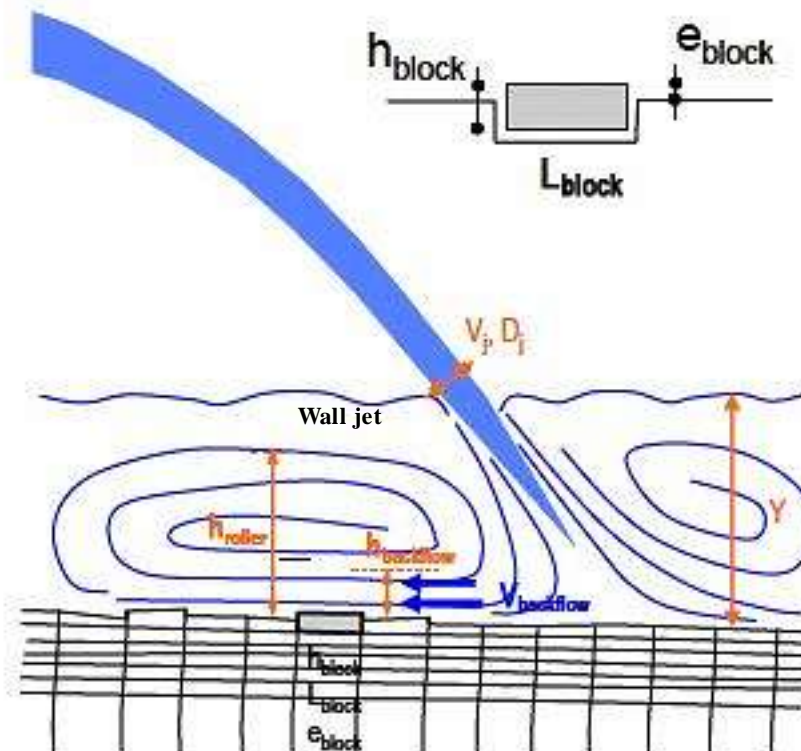


Figure 2-16. Peeling of rock blocks at the surface of the rock during flow (adapted from Bollaert, 2010).

Figure 2-17 describes the jet diffusion that starts in the free jet region through the plunge pool water depth, where pressure and velocity profiles are valid, as explained in section 2.4.3.A. The jet is not influenced by the presence of the pool bottom. Hartung et al. (1973) studied the velocity and pressure distributions in this area. However, the jet impingement region generates stagnation pressures due to the deflection of the turbulent shear layer of the jet at the bottom. Bollaert (2012) described the wall jet region as the area of flow parallel to the bottom, outside of the impingement region. In this case, the flow is deflected by rock blocks along the bottom, which generates turbulent pressure fluctuations. The deflection of the jet at the pool bottom occurs in both the upstream and downstream directions.

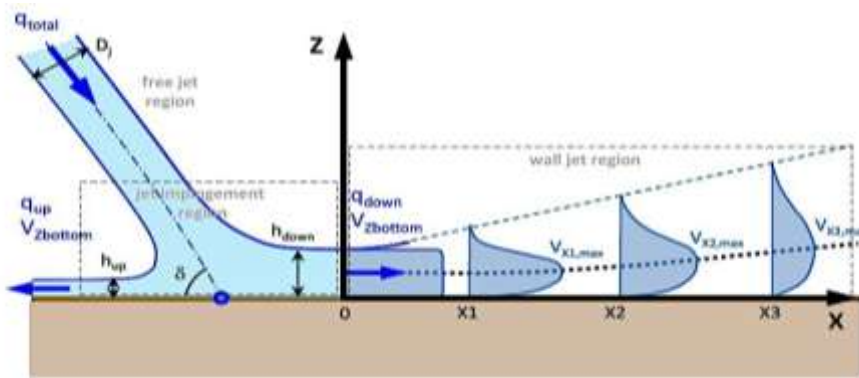


Figure 2-17. Plane jet deflection on a flat bottom (adapted from Bollaert, 2012).

Bollaert (2012) based on the application of the CSM, noted that the wall jets were characterised by their initial flow velocity $V_{zbottom}$ and their initial thickness h_{up} or h_{down} at the point of deflection. $V_{zbottom}$ depends on the diffusion angle of the impinging jet and on its development length through the water depth Z . During the scour formation, the $V_{zbottom}$ changes continuously. The wall jets develop radially outwards following self-preserving velocity profiles $V(z)$ in plunge pool for the rectangular jet given by the following equation:

$$\frac{V(Z)}{V_i} = \sqrt{\frac{Z_{core}}{Z}} \quad [60]$$

Where the **Zcore** stands for the distance required for the jet's core to diffuse completely through the plunge pool. The deflections of the jet depend on the jet impinging angle δ , a theoretical approach for plane jets with initial discharge q_{total} and thickness B_j impinging on a flat plan relates the respective discharges q_{up} and q_{down} (refer to Table 2.8) and wall jet thicknesses h_{up} and h_{down} by means of the cosines of the jet angle with horizontal δ , as shown in Figure 2-17:

$$\frac{q_{up}}{q_{total}} = \frac{h_{up}}{D_j} = \frac{1}{2}(1 - \cos \delta) \quad [61]$$

$$\frac{q_{down}}{q_{total}} = \frac{h_{down}}{D_j} = \frac{1}{2}(1 + \cos \delta) \quad [62]$$

Table 2.7. The deviation of up- and downstream parts of the total flow for different jet angles δ (adapted by Bollaert, 2012)

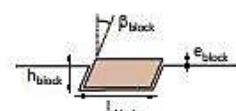
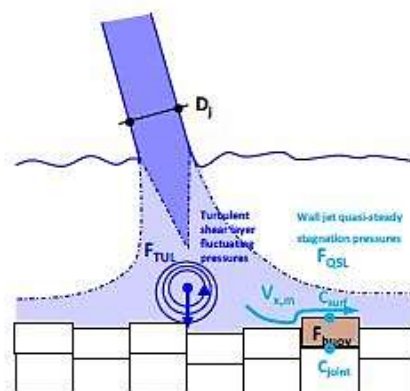
Jet angle δ	10°	20°	30°	40°	90°
q_{up}	1.5%	6%	7%	12%	50%
q_{down}	98.5%	94%	93%	88%	50%

The wall generated after jet deflection characterised by the flow velocity $V_{zbottom}$ and its velocity profiles computed by the equation 63. $V_{x,max}$ is the decay of the maximum cross-sectional jet velocity with the relative distance from the beginning of the wall jet and $h_{up/down}$ is the initial thickness of the deflected jet (Figure 2-6).

$$\frac{V_{x,max}}{V_{zbottom}} = \frac{3.5}{\sqrt{X/h_{down}}} \quad [63]$$

Bollaert (2012) has confirmed that the jet profile flattens and the jet thickness increases when the distance from the jet deflection increases. Furthermore, the quasi-steady flow deviations were generated by the net uplift pressure coefficients. Reinius (1986) has summarised uplift pressure coefficient C_{uplift} depending on the degree of protrusion of the blocks and on the shape of blocks (Figure 2-18) (Bollaert, 2012). The protrusion scenarios with its corresponding C-coefficients encircled were assumed to represent the physical model and are discussed further in Figure 2-18.

	h_{block}/e_{block}	β_{block}	C_{surf}	C_{joint}	C_{uplift}	Comment
	17-29	0°	0.030	0.250	0.220	
	17-29	0°	0.030	0.250	0.220	
	17-29	0°	0.020	0.105	0.085	
	17-34	0°	-0.010	0.145	0.155	
	4-9	0°	0.075	-0.110	-0.070	block stabilizing forces
	4-10	3°	0.030	0.350	0.310	
	2-4	9°	-0.10-0.17	0.36-0.55	0.37-0.47	
	1.0-2.5	18°	-0.15-0.00	0.23-0.40	0.25-0.45	
	4.2-8.7	-3°	0.02-0.13	-0.105	-0.070	block stabilizing forces
	1.0-2.3	-18°	-0.10-0.16	-0.075	-0.150	block stabilizing forces



Quasi-steady lift force F_{QSL}

$$F_{QSL} = (C_{joint} - C_{surf})L_{block} \frac{V_{x,m}^2}{2g}$$

$$V_{x,m} = f(X, h_{down}, V_{zbottom})$$

Figure 2-18. Summary of uplift pressures coefficients over and under protruding rock blocks subjected to high-velocity of wall jet flow adapted by Reinius (1986).

The QSI method allows the estimation of the shape of the scour hole and not just the depth. The computations of scour are performed along a vertical 2D-plane and distinct computational grid, thus determining the scour depth in a step-wise manner. The scour developed considers the main angle of impact of the jet δ (Figure 2-19).

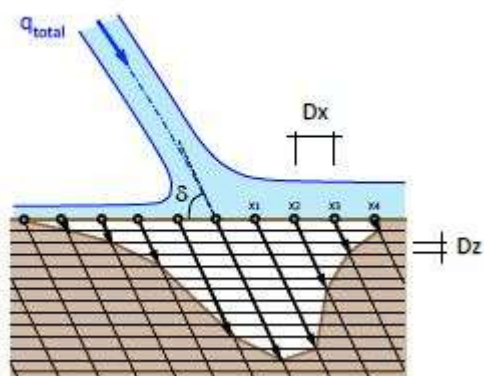


Figure 2-19. Sub-vertical lines of calculation of QSI model (adapted by Bollaert 2012)

2.5. Practical Application of Scour Prediction Methods

A number of rock scour technologies for spillways have been developed over the years around the world. The Kariba Dam is an example of the different spillways that were assessed by using rock scour technology.

2.6.1 Kariba Dam

Kariba Dam is located at the Zambezi River between Zambia and Zimbabwe. It is an arch dam designed with a discharge capacity of 9000 m³/s and 130m high double curvature. The plunge pool has experienced significant scour over the years. The indication of the pool bottom level was 306 m.a.s.l (80 m deep) in 1981 as visually depicted in Figure 2-20. Table 2.8 shows the scour depth calculated for the Kariba Dam in 1981 by means of the empirical formulae discussed in section 2.4.1.

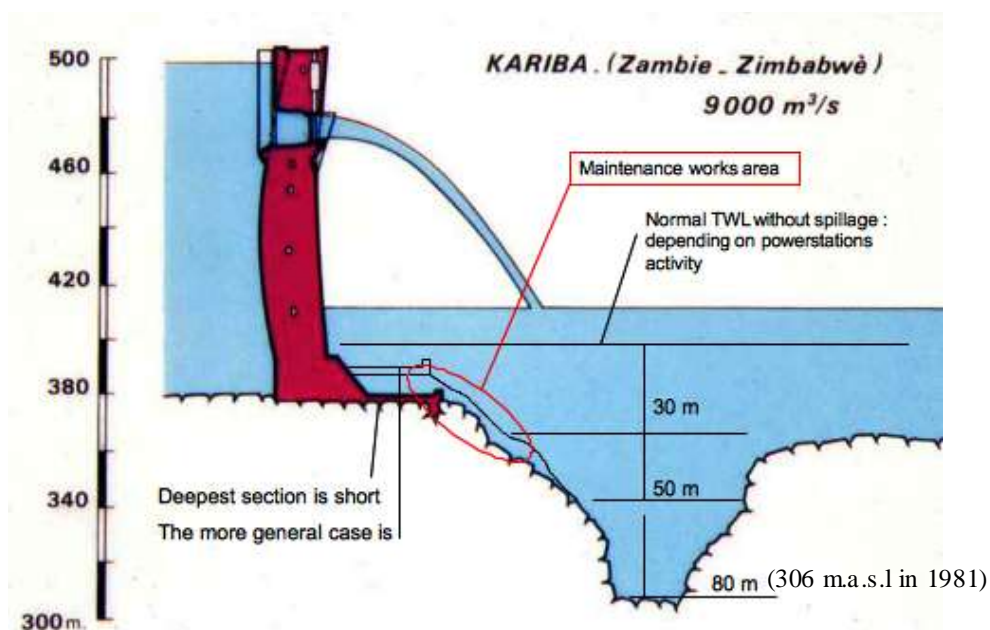


Figure 2-20. Longitudinal section of Kariba plunge (adapted from Sanyanga, 2012).

The relevant parameters for Kariba Dam were obtained from Whittaker and Schleiss (1984) as given in Table 2.8. The predicted maximum depth of the scour hole was determined by different methods as summarised in Table 2.8.

Table 2.8. Scour depth for Kariba Dam based on empirical methods with different authors in 1978

Kariba Dam started in 1959			
Characteristics		Formula	Sour depth (m) in 1981
q (m ² /s)	96	Mason and Arguman (1985) ¹	54.6
H (m)	91.5	Mason and Arguman (1985) ²	79.8
h _d (m)	16	Chee and Kung (1974)	71.6
D (m)	0.3	Veronese (1937)	61.7
Θ (°)	59	Martins (1973)	36.4
Cr	0.86	Jaeger (1939)	68.1

¹. Equation obtained from model data

². Equation obtained from model and prototype data.

Furthermore, Duarte (2014) has used the Comprehensive Scour model proposed by Bollaert (2002) for determining the ultimate scour depth of the Kariba Dam by using the Dynamic Impulsion method (DI). Duarte (2014) found that by taking the influence of jet air entrainment into consideration the results were similar to that of the prototype. The issuance velocity V_i equals 18.5 m/s and the velocity at impact with the tailwater level V_j equals to 41.4 m/s (equation 25) and the jet air concentration into the plunge pool C_a was 48% (equation 76). Hence, the pressure wave celerity is reduced by the air content and by the block

vibration. Duarte (2014) assumed a pressure wave celerity of 70 m/s according to a highly aerated high velocity jet. Duarte (2014) has determined the degree of displacement of the block (h_{up}/z) inside the rock mass cavity as equal to one. This degree of displacement of the block helps to determine the threshold below which the rock bottom is stable. Thus, if the rock bottom is not stable, scour would occur and the scour hole would become deeper. The calculations based on the parameters and intermediate results are described in Table E.0.1 and Table E.0.2 in Appendix E. The scour results calculated by the physical-mechanical methods of the CSM were similar to the actual bottom levels surveyed in 1981 and 2001.

Regarding different criteria (Table 2.6), the results of the ultimate scour depth computed by adapting Dynamic Impulsion (DI) method are close to the deepest point of the pool bottom, as measured in 1981. In fact, the criterion $0.1 < H_{up}/Z_b < 0.5$ where the block vibrates and most likely remains in place resulted in exactly the same pool bottom elevation of 306 m.a.s.l. (Table E.0.2).

2.6. Scale Physical Model test for spillway

These tests are normally conducted as reduced-scale models of dams to refine engineering design and to assess the hydraulic behaviour of structures. They are also normally conducted under Froude's similarity because of the governing effect of gravitational forces (Bollaert, 2002). As such, many scaled physical model studies have been made, resulting in a significant amount of empirical expression (Bollaert, 2002).

Reduced-scale model results are often conservative, meaning that the scour depth is deeper and achieved faster than observed in reality (Manso, 2006). Throughout the spillway, free surface flow exists and dynamic similitude between the model and prototype is based solely on Froude's Law of Similarity, which assumes gravity and inertia to be the dominant forces (Sokchay, et al., 2009). Using subscripts "m" and "p" to denote model and prototype respectively. The equal Froude number between model and prototype is as follows:

$$F_m = F_p \text{ or } \frac{V_m}{\sqrt{g_m L_m}} = \frac{V_p}{\sqrt{g_p L_p}} \quad [64]$$

Where

F : Froude number (-).

V : Mean flow velocity (m/s).

L : Characteristic length (m).

g : Gravitational acceleration (9.81 m/s^2).

Following the Froude number similarity, the scale relationships between model and prototype are shown in Table 2.9.

Table 2.9. Froude Law Model Scale Relationships (Castillo & Carrillo, 2013)

Parameter	Scale relation
Length, L	$\frac{L_p}{L_m} = L_r$
Velocity, V	$V_r = L_r^{1/2}$
Discharge, Q	$Q_r = L_r^{5/2}$
Pressure head, h	$h_r = L_r$
Time, t	$t_r = L_r^{1/2}$

2.7.1 Limitation of scaling

There are three primary limitations in modelling plunge pool scour. Firstly, there is the issue of accurately representing the riverbed geology at a model scale. In order to use model data for predicting scour depths associated with a plunge pool, the model sediment bed type and size must be chosen carefully to allow scaling (Schleiss & Whittaker, 1984). The typical approach is to examine the rock on site and to estimate, from joint and fissure patterns and from the strength of the rock, the individual block size to which the rock will break down (Mason, 1984). Furthermore, grain size differs and not all are appropriate for model tests, and so choosing the right particle size to represent the material becomes complicated. Nevertheless, "if the bed material is chosen carefully, good predictive results for scour depth can be obtained by using non-cohesive material", as pointed out by Schleiss and Whittaker (1984).

The second limitation is that air entrainment cannot be scaled appropriately. The aeration is governed by the initial jet turbulence intensity (Tu) and this cannot be represented appropriately by Froude-based scaling laws (Bollaert, 2002). Thus, to assess the effect of aeration is a challenge in the evaluation of scour depth. Moreover, Ervine and Falvey (1987) developed an empirical expression of the volumetric air-to-water ratio β that would be used. The Ervine and Falvey's (1987) formula is accurate for model data and predicts reasonably accurately the scour depth for prototype conditions (Bollaert, 2002).

Thirdly, there is a limitation based on scale effects, as hydraulic model studies is required as a common way of predicting plunge pool performance but such predictions can be incorrect because of the scaled spillway discharge to identify possible areas of concern downstream of hydraulic structures and assess expected plunge pool development (Whittaker & Schleiss, 1984). The mechanism of scour is still a complex process as a result of the influence of various hydraulic, hydrological and geological factors and these factors are difficult to assess theoretically and are therefore limited at a model scale.

2.7. Summary

The literature review introduced the basic concepts relating to the understanding of the scour process. Scour estimation is of specific concern and it is defined by jets being issued from hydraulic schemes. The high velocity water jet created by the transfer of water from reservoir level to the downstream tailwater level, impinges onto plunge pool bottom and results in scour of bedrock.

Different authors have discussed different methods and approaches. These include empirical methods developed by Veronese (1937), Damle (1966), Martins (1975) and Masons (1985), to represent a comprehensive tool that allows the evaluation of ultimate scour depth.

The semi-empirical methods were developed by the combination of an analytical description of hydrodynamic and geomechanic characteristics. This theory consists of the jet diffusion theory, the initiation of motion concept applied to rock blocks, and the use of conservation formulae. The latest approach is the Erodibility Index Method (EIM) by Annandale (1995) which is helpful to assess the scour hole geometry and is a useful indicator of the relative magnitude of pressure fluctuations.

Bollaert (2002) has considered the pressure fluctuations acting on a water-rock interface and inside rock fissures. These pressure fluctuations cause brittle failure on rock fissures, and they play an important role on block uplift and erosion process. Hence, Bollaert (2002) presented the Comprehensive Scour Method (CSM), which comprises of an assessment of the major geo-mechanical processes that are responsible for rock mass destruction by turbulent flow impingement. It recognises that impulse forces and the rate of imparting energy to the boundary influence the presence of pressure fluctuations in turbulent flow. Ultimately, pressure fluctuation and air concentration assist in prediction of ultimate scour depth.

Chapter 3. Testing setup and Investigation of Rock Scour

The main objective of the experimental tests was to determine the geometry of the rock scour subjected to water pressure and high-velocity jet impact. This chapter presents the experimental facility and the tests undertaken to improve the understanding of rock scour technology and the explanation given in the last chapter. It also discusses the structural equipment needed to simulate the jet, the plunge pool, rock mass and the measurement equipment, focusing on velocity measurement and air concentration.

Furthermore, parametric details, based on factors such as size, shape, settling velocity and specific gravity played the main role to validate the tests. The work performed under this study consisted of the development of a methodology for rock scour geometry focused on the mechanism of failure including crack propagation because of the pressure fluctuations within rock joints and block uplift. The explanation of the model set-up and methodology followed, are divided into four categories. The first category describes the model set-up including the measurement equipment, the second category the hydraulic parameters, the third category the geometry of the rockbed, and the last category explains the methodology followed during the experiment.

3.1. Model Setup

A 1:40 scaled physical model was constructed in the hydraulic laboratory at Stellenbosch University, South Africa, to model rock scour downstream of high dams (Figure 3-1). The experimental equipment included the jet, plunge pool, rock mass and devices for measuring the discharges and water level.

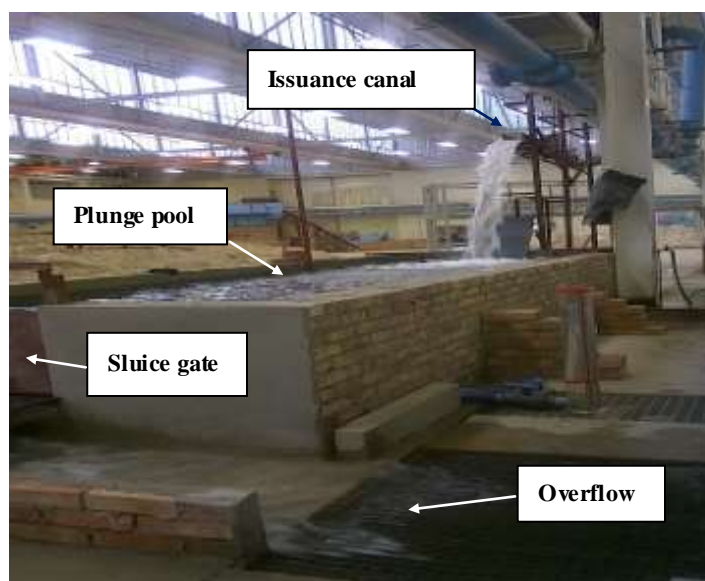


Figure 3-1. Model of experimental spillway in action.

The model spillway consisted of a 0.2m wide rectangular issuance canal that was fixed for the specific drop height under evaluation (2m, 3m or 4m – model values). The plunge pool was constructed by means of a brick wall 8.40m long, 2.45m wide and 1 m in depth. The inside of the plunge pool was plastered and sealed to prevent any leakages. PVC blocks (25mm by 25mm by 25mm – model dimensions) represented the jointed rock were used to simulate the mobile bed downstream of the spillway. It was therefore assumed that the joint network has already formed completely. It is also relatively light and can easily be removed by flow of water (Sawadogo, 2010). The PVC blocks were packed into a smaller steel box (1.24m long, 1.22m wide and 0.35m of depth) inside the bricked plunge pool. This steel box could be

moved to the jet's impingement zone. At the downstream side of the bricked plunge pool, a sluice gate was used to adjust the tailwater level to the required depth as seen in Figure 3-2.



Figure 3-2. Adjustable gate to adjust tailwater level

The purpose of the model study is to determine the effect the drop height, discharge, and tailwater depth have on the geometry of the scour hole. Based on the gravitational and inertial forces for the hydraulic performance, the Froude law was used to scale the model. The main characteristics of the 1:40 scale model are given in Table 3.1, Figure 3-3 and Figure 3-4.

Table 3.1. Characteristics of model of spillway

	Unit	Prototype	Model
Dam height	m	160	4
		120	3
		80	2
Tailwater level (Y_T)	m	20	0.50
		10	0.25
Discharge	m^3/s	232,743	0.023
		121,431	0.012
Diameter of block	mm	1	0.025
Density	kg/m^3	2650	1152

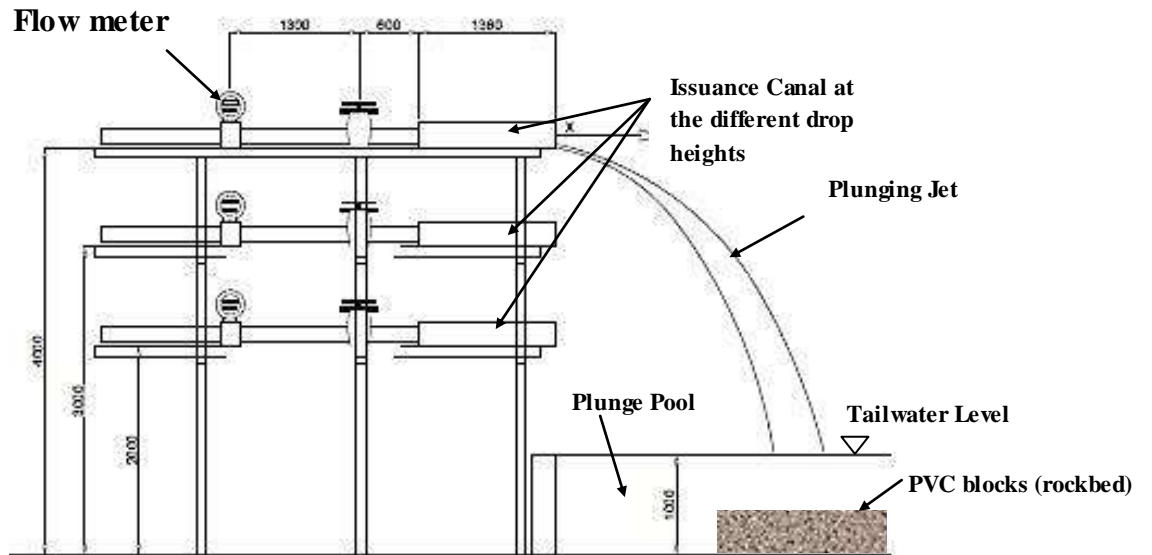


Figure 3-3. Cross section of spillway model in laboratory.

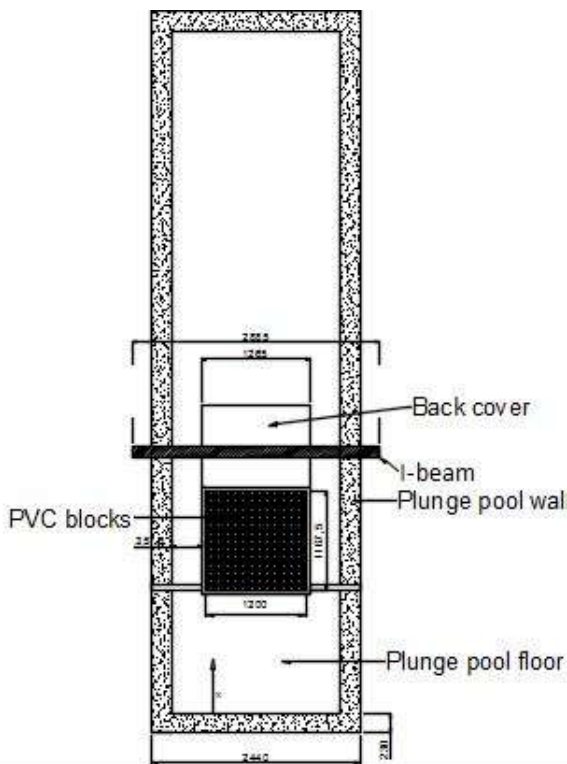


Figure 3-4 Plan of plunge pool (top view)

3.2 Measurement Equipment

3.2.1 Measurement of water levels

During the physical model investigation, accurate measurement of the water level in the issuance canal and the tailwater level were needed. From Figure 3-5 it can be seen that a point gauge was used to measure the water depth in the issuance canal. A manometer was connected to the plunge pool (see Figure 3-6), for measuring the tailwater level.



Figure 3-5. Point gauge for measuring the water depth in the rectangular issuance canal



Figure 3-6. Tailwater gauge (manometer) for measuring the tailwater depth

3.2.2 Discharge Measurement

Before setting the desired discharge rate that could be passed over the spillway, the correct tailwater level had to be obtained by adjusting the sluice gate. At first, a low discharge was passed over the crest to obtain the correct tailwater level and to ensure that no premature scouring occur or an alternative was to fill the plunge pool with water supplied from an outside source. Once the desired tailwater has been obtained, the specified discharge could pass over the spillway. The discharge was measured with a Proline Promag 50W electromagnetic flow meter with a minimum conductivity of $\geq 5 \mu\text{s/cm}$. (refer to Figure 3-7).



Figure 3-7. Proline Promag 50W, 53W flow meter

3.2.3 Jet Air Entrainment Measurement

Air probe conductivity (Figure 3-8) was used to record air concentration of the falling jet. The probe consists of a needle probe, TNP device connectors and computer. The software TNP 2 control 2.4.0.4 was used for data analysis with additional software Void wizard. The measurements were taken at different points in the impingement zone in the plunge pool. The sampling interval was 10 mm, the sampling rate was 10 kHz and the sampling period was 1 minute.



Figure 3-8. Air probe conductivity for measuring air concentration

3.3 Hydraulic Parameters

The hydraulic parameters of the jet at issuance and as it travels through the air and in the plunge pool influence its scour potential. Sections 3.3.1 to 3.3.3 discuss the falling jet, jet in the plunge pool and the rock mass parameters used in the physical model.

3.3.1 Falling Jet

The jet trajectory must be determined in order to analyse the scour caused by a free falling jet (Jeffrey & Anton, 1984). As the jet travels through the air it is subjected to gravity and the solid water core contracts and the jet begins to entrain air at its outer boundary. This leads to internal turbulence and jet breakup (Bollaert, 2002; Ervine & Falvey, 1987). A free falling jet plunging through the atmosphere entrains a

certain amount of air because of its turbulent character. Its analysis is governed by gravity, surface tension and internal turbulence effects. The break-up length can be determined with equation 65.

$$L_b = 6. q_w^{0.32} \quad [65]$$

Where

L_b : The jet break-up length (m)

q_w : Discharge per unit width (m²/s)

The initial turbulence intensity reflects the amount of air entrainment experienced by the jet. Table 3.2 shows the value of issuance turbulence intensity at various outlet structure types.

Table 3.2. Typical value of Issuance Turbulence Intensity (Bollaert, 2002)

Types of outlet structure	Turbulence Intensity Tu
Free overfall	0.00-0.03
Ski jump outlet	0.03-0.05
Valve	0.03-0.08

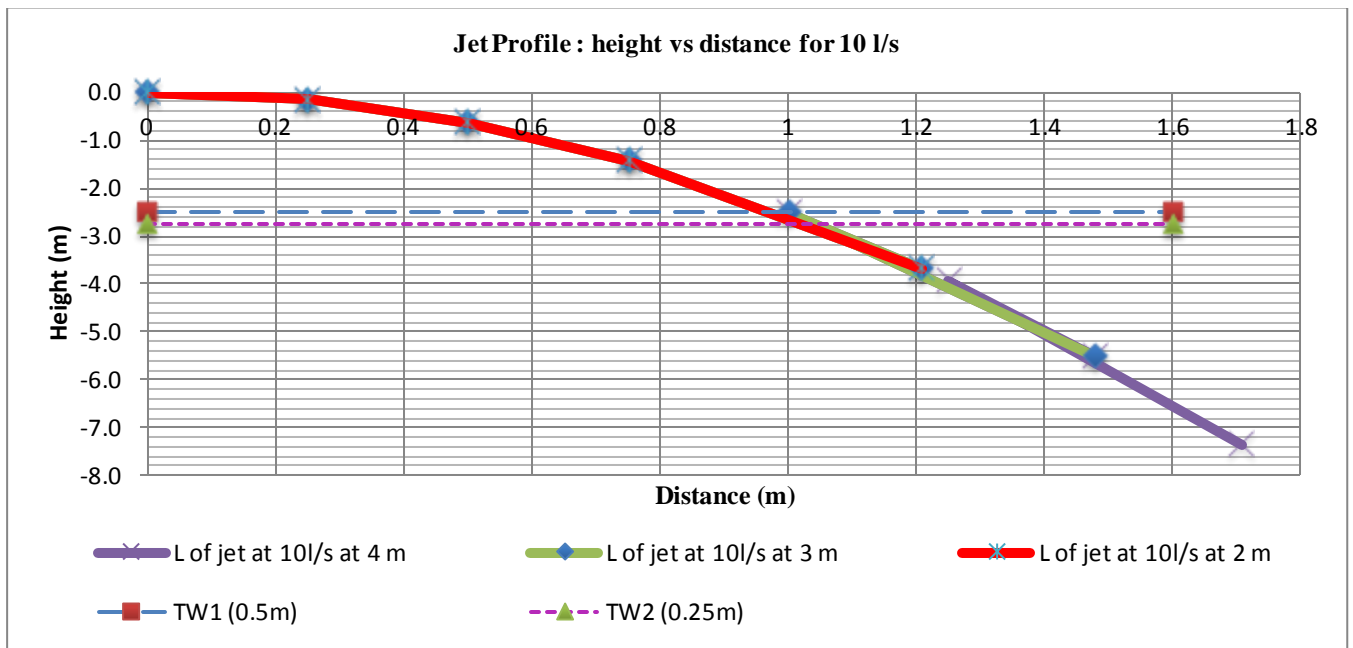
The prediction of the jet trajectory is necessary to localise where the jet impact will be, in order to know where the scour hole will form. It allows also determining the degree of development of turbulent eddies due to the gravitational acceleration. The jet trajectory has been calculated based on ballistic equations. The jet trajectory depends on the initial velocity of the jet, the difference in elevation between water surface in plunge pool (drop height), the gravitational acceleration, the deflection angle of the flow and air resistance. The break-up length of jet, trajectory length and the horizontal distance between the point of issuance and the jet impact are presented in Table 3.3 for the three different drop heights inspected.

Table 3.3. Jet break-up length and distance from issuance to the jet impact

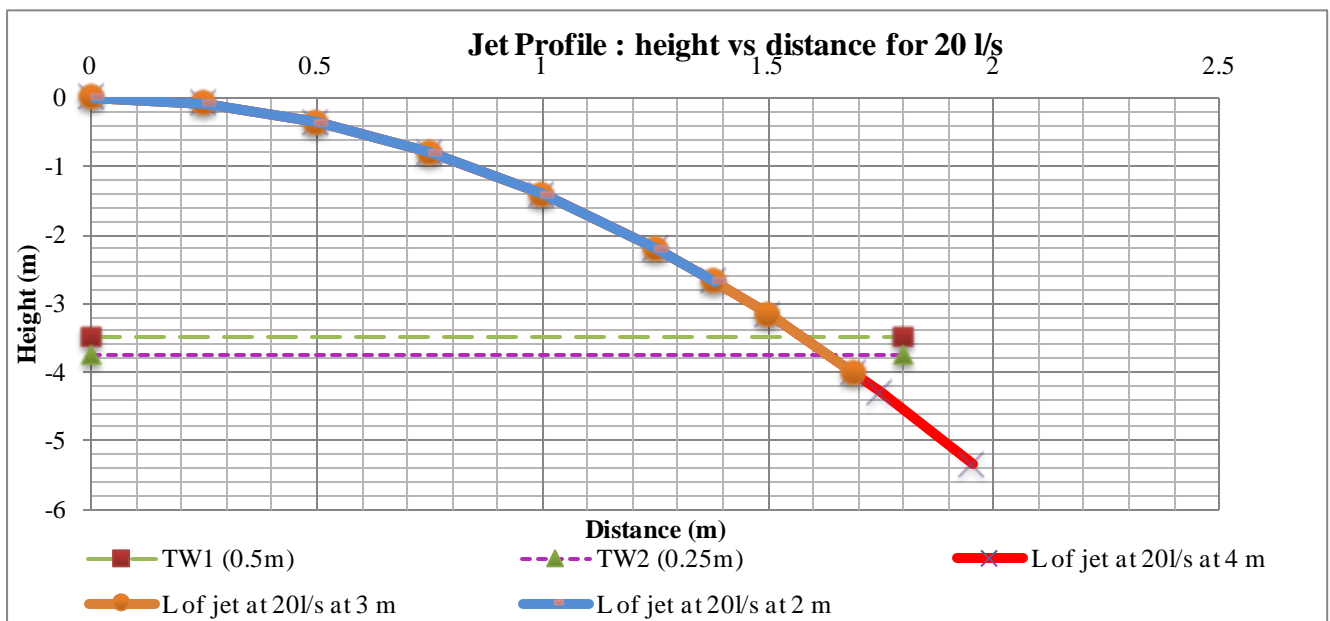
Height (m)	Discharge					
	20 l/s			10 l/s		
	Trajectory length L (m)	Break-up length L_b (m)	Horizontal distance X (m)	Trajectory length L (m)	Break-up length L_b (m)	Horizontal distance X (m)
	L^1	Eq. 65	measured	L^1	Eq. 65	measured
4	4.630	1.715	1.952	4.418	1.374	1.707
3	3.541	1.715	1.691	3.355	1.374	1.479
2	2.512	1.715	1.38	2.332	1.374	1.207

1. $L = X \tan \theta + (X^2 / 4K \cos^2 \theta)$ with $K = 0.9$ for air and $\theta = 0^\circ$

Figure 3-9 depicts the jet trajectory length (L) for the three different drop heights and two different discharges.



(a)



(b)

Figure 3-9 (a) and (b) Jet length “L” of different discharge at different height and different water depths “TW”

3.3.2 Plunge Pool Aeration

As mentioned before, air entrainment effects the pressure fluctuations at the plunge pool and inside the rock mass. The impact of a water jet into a plunge pool is accompanied by the entrainment of large volumes of air as seen in Figure 3-10 (Bollaert, 2002). The jet core is further broken up as it travels through the plunge pool. The plunge pool depth Y and the jet diameter/width D_j (circular jet) or B_j (rectangular jet) at plunge pool impingement represent the ratio Y/B_j , and characterises the jet diffusion when travelling through the pool.

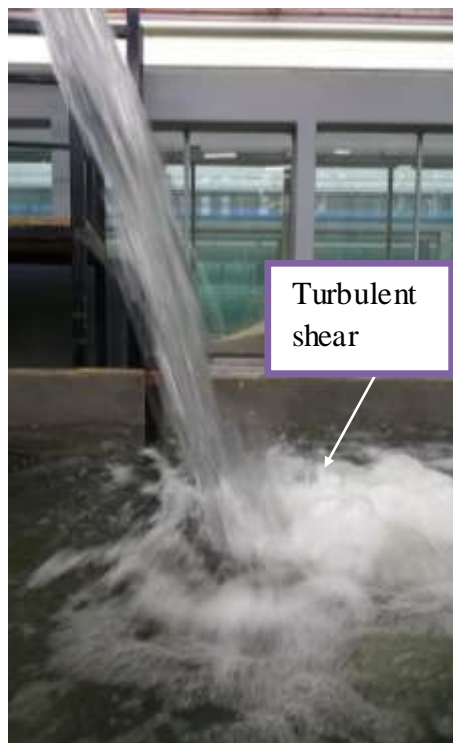


Figure 3-10. Jet impact into plunge pool with turbulent shear layer developed

The main characteristics for the 0.2 m wide rectangular jets are summarised in Table 3.4 for the various issuing parameters as tested in the laboratory. Based on the measured jet width and velocity at issuance the jet velocity at the impact, Froude number and the jet trajectory length could be calculated.

Table 3.4. Main characteristics of plunging rectangular shaped jets

Discharge	Drop height	Tail water depth	Jet width at issuance	Velocity at impact	Velocity at impact	Froude number		Jet Trajectory Length
				Calculated (Q = vA)	(Eq. 25)	initial	impact	(m)
Q (l/s)	H (m)	Y (m)	B _i (m)	V _i (m/s)	V _i (m/s)	Vi/√gB _i	Vi/√gB _i	Y ¹
Measured	Measured	Measured	Measured	Calculated (Q = vA)	(Eq. 25)	Vi/√gB _i	Vi/√gB _i	Y ¹
20	4	0.500	0.200	2.0	8.525	1.428	2.052	4.630
20	4	0.250	0.200	2.0	8.808	1.428	2.068	4.630
20	3	0.500	0.200	2.0	7.284	1.428	1.972	3.542
20	3	0.250	0.200	2.0	7.613	1.428	1.994	3.542
20	2	0.500	0.200	2.0	5.782	1.428	1.894	2.512
20	2	0.250	0.200	2.0	6.192	1.428	1.862	2.512
10	4	0.250	0.200	1.7	8.738	1.190	1,800	4.418
10	4	0.500	0.200	1.7	8.453	1.190	1.786	4.418
10	3	0.250	0.200	1.7	7.532	1.190	1.735	3.355
10	3	0.500	0.200	1.7	7.199	1.190	1.715	3.355
10	2	0.500	0.200	1.7	5.675	1.190	1.616	2.333
10	2	0.250	0.200	1.7	6.092	1.190	1.645	2.333

1. $Y=X \tan\theta - (X^2/4KH\cos^2\theta)$ with $K=0.9$ for air and $\theta=0^\circ$

3.3.3 Rock Mass

The rock blocks are characterised by the diameter, size, shape, settling velocity and specific gravity, which are summarised Appendix B Table B 0.1 and Table B. 0.2 Hence, the geo-mechanical properties of the model rockbed are described in the subsequent subsections.

3.3.3.1 Rock Size, Shape and Density

The most important physical property of rock particles is the size. It had a direct effect on the mobility of the particle. The size of the particles can be determined in different ways. Usually, it is measured by the displaced volume of submerged particles.

Apart from size, the shape of the blocks affects the transport of sediment but there is no direct quantitative way to measure shape and its effects. Simons and Sentürk (1992) proposed that particles that have very different shapes but equal volume and density could display similar behaviour in fluids. McNown (1951) suggested a shape factor as:

$$S_p = \frac{c}{\sqrt{ab}} \quad [66]$$

Where

c: The shortest of the three perpendicular axes (a, b, c) of the particle.

The shape factor of the PVC cubes had a value of one, since the bed materials for this study was considered to be uniform in size. Usually, the values below one indicate the increase in deviation.

The transport of sediment is effected due to segregation by the density of the particles. The relative density is interpreted as the ratio of relative density of the sediment to the density of the reference substance and can be determined by using the following equation:

$$Relative\ density = \frac{\rho_{Sediment}}{\rho_{Reference}} \quad [67]$$

The density of water is commonly taken as the density of reference, which equals to 1000 kg/m³. The rock density is an important parameter for stability calculation. A good estimation for riprap density in general seems to be in the order of 2650 kg/m³ (Annandale, 1999) . A calibrated digital scale as shown in Figure 3-11 measured the mass of the PVC cubes.



Figure 3-11. Calibrated digital scale for measuring mass PVC blocks

3.3.3.2 Settling Velocity

The settling velocity of sediment is a function of the sediment size, shape, specific density, and viscosity of the fluid. In general, the settling velocity V_{SS} of a particle can be determined with the following equation (Simons & Senturk, 1992):

$$V_{SS} = \frac{4g(\rho - \rho_w)d.\psi}{3\rho_w C_d} \quad [68]$$

Where

V_{SS} : Settling velocity (m/s).

ρ : Density of submerged particle (kg/m^3).

ρ_w : Water density (kg/m^3).

ψ : Shape factor of sediment.

d : Diameter of sediment (m).

C_d : Drag coefficient.

g : Gravitational constant (m/s^2).

The Reynolds number of the settling process determines whether the flow pattern around the blocks is laminar or turbulent (Zhao-Yin, et al., 2015). The Reynolds number can be determined by:

$$Re = \frac{d V_{SS}}{\nu} \quad [69]$$

Where

Re : Reynolds number.

d : Diameter of sediment (m).

V_{SS} : Settling Velocity (m/s).

ν : Kinematic viscosity (m^2/s).

The settling velocity calculated for the PVC cubes was 0.263 m/s and the Reynolds number is 6575, which is greater than 4000, i.e. it is turbulent flow. Details of the calculation can be seen in Table B. 0.2 Appendix B.

3.3.3.3 Specific Gravity

The weight of the rock bed is required to calculate the forces acting on them for example gravity, frictional resistance and kinetic energy. The ability of flowing water to transport rock blocks depends on various factors, including the specific gravity of rock. When the rock blocks are lifted up and transported downstream by the water, they acquire kinetic energy. Hence, the specific gravity is the ratio of the weight of a volume of substance to the weight of an equal volume of reference substance. For this study, the specific gravity of the PVC blocks was thus calculated to be 1.152. Detailed in Table B 0.1 Appendix B.

3.3.3.4 The Drag Coefficient

The drag coefficient C_d (required to solve equation 68) depends on the Reynolds number (equation 69) according to Turton & Levenspiel (1986). The drag coefficient is determined based on the settling velocity of the particles. Wu & Wang (2006) developed Figure 3-12, where the drag coefficients are plotted against the Reynolds number for different particle shapes. The drag coefficient was determined as 1.1 as indicated by the red line on Figure 3.12.

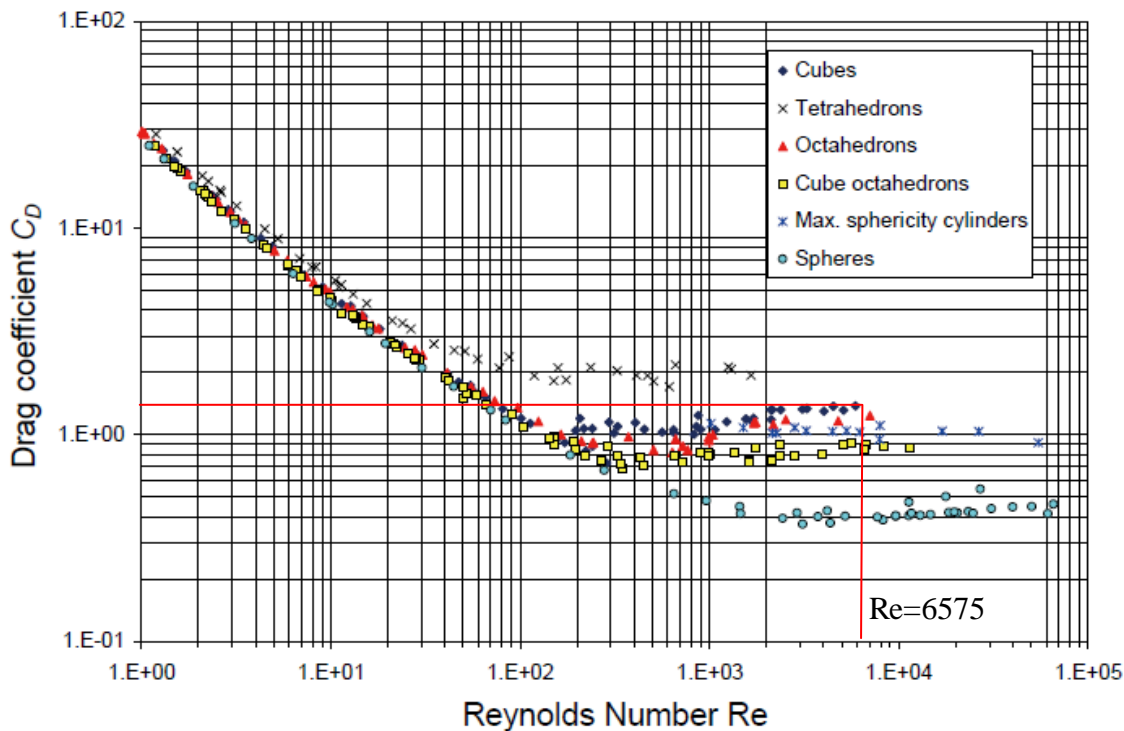


Figure 3-12. Drag coefficient as function of Reynolds number and particle shape (adapted from Wu & Wang, 2006).

3.4 Experimental Procedure

This section describes the procedures that were used to perform the experiments. Firstly, the issuance canal was fixed to the desired drop height under evaluation. The steel box, which had to contain the PVC blocks, was pushed to the correct location, namely the impingement zone. This was done by determining the jet trajectory (refer to Figure 3-9). Thereafter the steel box was filled with the PVC blocks representing the jointed rockbed material (see Figure 3-13), which had to be accurately levelled. The levelling was achieved by using a straight edge and a split level. During the surveying, many precautions had to be taken to keep the survey rod as perpendicular as possible to all three axes and not disturbing the scouring area. The monitoring facility was achieved by using "spirit bubble."



Figure 3-13. PVC cubes filled up in the plunge pool before start the experiment



Figure 3-14. Grid for surveying or mapping of scouring area

After the blocks were made level, before the experiment was started, the surveying grid (Figure 3-14) was removed and the plunge pool was filled carefully with water to the acquired tailwater level with a downstream supply at a very slow rate. Subsequently, the PVC cube bed became saturated safely and remained undisturbed. After complete saturation, the required discharge was reached by using the flow meter (see Figure 3-7). In order to obtain the correct tailwater level, the tailgate had to be adjusted to keep the tailwater at the correct level (Figure 3-2). The jet velocities at issuance and at impact with the tailwater level were recorded. The experiment was stopped when the scour depth reached the equilibrium state at which there are negligible changes in bed elevation with time.

After the experiment, the bed elevation was surveyed with the spirit level, spirit bubble and tape measure. The plunge pool was slowly drained so to not disturb the scour contours and the final bed elevations and the grid for surveying was fixed into position. The scour depth and scour contours were calculated by subtracting the bed elevation after reaching equilibrium scour depth from the initial bed elevations before starting the experiment.

The tests were carried out in two parts as summarised in Table 3.5. The first part was to assess the scour hole geometry and measure the air entrainment along the falling jet, and the second part was to record the pressures at the bottom of plunge pool. It has to be underlined that the tests for assessing the scour shape and pressures inside the blocks were not measured simultaneously, since the pressure sensors influenced the shape of the scour hole formed.

Table 3.5. Test program (model values)

Discharge (l/s)	Water depth (m)	Height of spillway (m)	Experiments
10	0.250	2, 3,4	Without pressure sensor + air concentration measurement
	0.500		
20	0.250		
	0.500		
10	0.250		Including the pressure sensor
	0.500		
20	0.250		
	0.500		

As summarised in Table 3.1 and Table 3.5, the test procedure explained above was repeated in Figure 3-1 three different drop heights (2, 3 and 4 m), two different discharges (10 and 20 l/s) and two different tailwater depths (0.25 and 0.5 m). The velocities calculated at the jet issuance and at the jet impact are summarised in Table 3.6.

Table 3.6. Summary of test of the velocities at the jet issuance and the jet impact

Discharge (l/s)	Height (m)	Water depth (m)	Velocity at jet issue (m/s)	Velocity at impact (m/s)	Angle at the jet impact (°)
Measured	Measured	Measured	$Q=AV$	Eq. 25	Measured
10	2	0.500	1.667	5.675	70
		0.250	1.667	6.092	70
20	2	0.500	2.000	5.782	70
		0.250	2.000	6.192	70
10	3	0.500	1.667	7.199	70
		0.250	1.667	7.532	70
20	3	0.500	2.000	7.284	70
		0.250	2.000	7.613	70
10	4	0.500	1.667	8.453	70
		0.250	1.667	8.738	70
20	4	0.500	2.000	8.525	70
		0.250	2.000	8.808	70

Micro-pressure sensors (pressure transmitter S-10) were used for measuring the dynamic pressure (Figure 3-15). A series of five pressure sensors was arranged as shown in Figure 3-16 and was situated in the impingement zone (0.225 m from top of blocks). The pressure sensor transmitter model S-10 has a pressure range of 0-1000 bar in all major units, non-linearity 0.2% of span, output signals of DC 0-5.0 V.

the sampling period was one hour. The software "Picolog Recorder" was used for recording, analysing and displaying the pressure data.



Figure 3-15. Micro-sensors for measuring the pressure inside the test box.

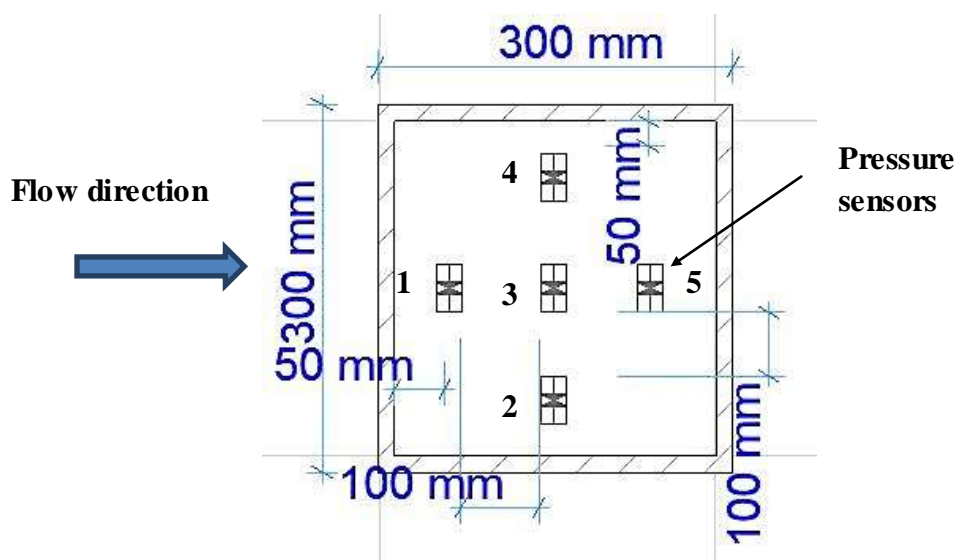


Figure 3-16. A schematic diagram (plan view) of the arrangement of pressure sensors within the test box

Chapter 4. Physical laboratory test results

This chapter explains the laboratory investigation performed to collect the scour hole data and discusses the results obtained.

4.1 Determination of scour shape

The equilibrium scour hole for each test subjected to the various hydraulic parameters (drop height, discharge and tailwater level) was surveyed and plotted. Figure 4-1 to Figure 4-3 depict an example of the scour survey results in 3D, contour line and the photograph respectively for the 20 l/s; 0.25m deep tailwater depth (TW) and 3m drop height test. Refer to Appendix F for the 3D and contour map for all the tests.

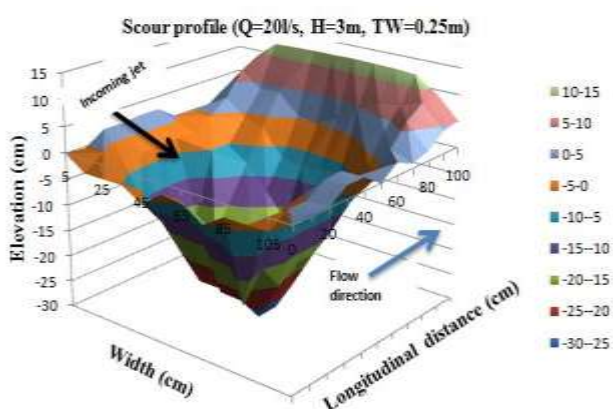


Figure 4-1 Scour profile in 3D of the test system with $Q=20\text{l/s}$, $H=3\text{m}$ and $TW=0,25\text{m}$).

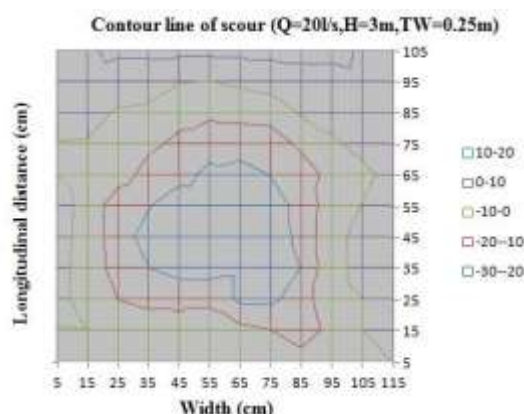


Figure 4-2. Contour line map of scour test system of $Q=20\text{l/s}$, $H=3\text{m}$ and $TW=0.25\text{m}$).



Figure 4-3. Rock Scour in model for $Q=20\text{l/s}$, $H=3\text{m}$ and TW of 0.25m

Table 4.1 gives the summary of the maximum scour depth surveyed for each test scenario by linking the maximum scour depth to the drop height and tailwater depth. It can be seen that maximum scour depths were found for the 20 l/s, 0.25 m tailwater depth at the 2 m drop height (Figure 4-6 and Figure 4-7) and the minimum was found for the 10 l/s, 0.5 m tailwater depth at the 4 m drop height (no scour).

Table 4.1. Summary of maximum erodible region survey considering discharge rate, height and water depth.

Surveyed Scour Hole Geometry							
Discharge (l/s)	Height (m)	Tailwater depth (m)	Velocity (m/s)		Max length (m)	Max width (m)	Max depth (m)
			Issuance (V_i)	Impact (V_j)			
20	2	0.50	2.0	5.78	0.60	0.70	0.129
		0.25		6.19	0.85	0.75	0.312
	3	0.50		7.28	0.60	0.60	0.075
		0.25		7.61	0.87	0.90	0.272
	4	0.50		8.53	0.30	0.40	0.026
		0.25		8.81	0.85	0.60	0.271
10	2	0.50	1.7	5.68	0.45	0.75	0.075
		0.25		6.09	0.70	0.80	0.1731
	3	0.50		7.20	0.45	0.35	0.052
		0.250		7.53	0.55	0.50	0.175
	4	0.50		8.45	0	0	0
		0.25		8.74	0.70	0.65	0.183

Table 4.1 illustrates that the scour hole depth increased as the tailwater depth decreases. The scour hole depth was also deeper with the discharge of 20l/s and it decreased with an increase in drop height. These observations are made more clearly by visual inspection from Figure 4-4 to Figure 4-11 where the surveyed scour hole depths at the point of impingement (centreline) in the longitudinal and lateral direction for each test scenario were plotted

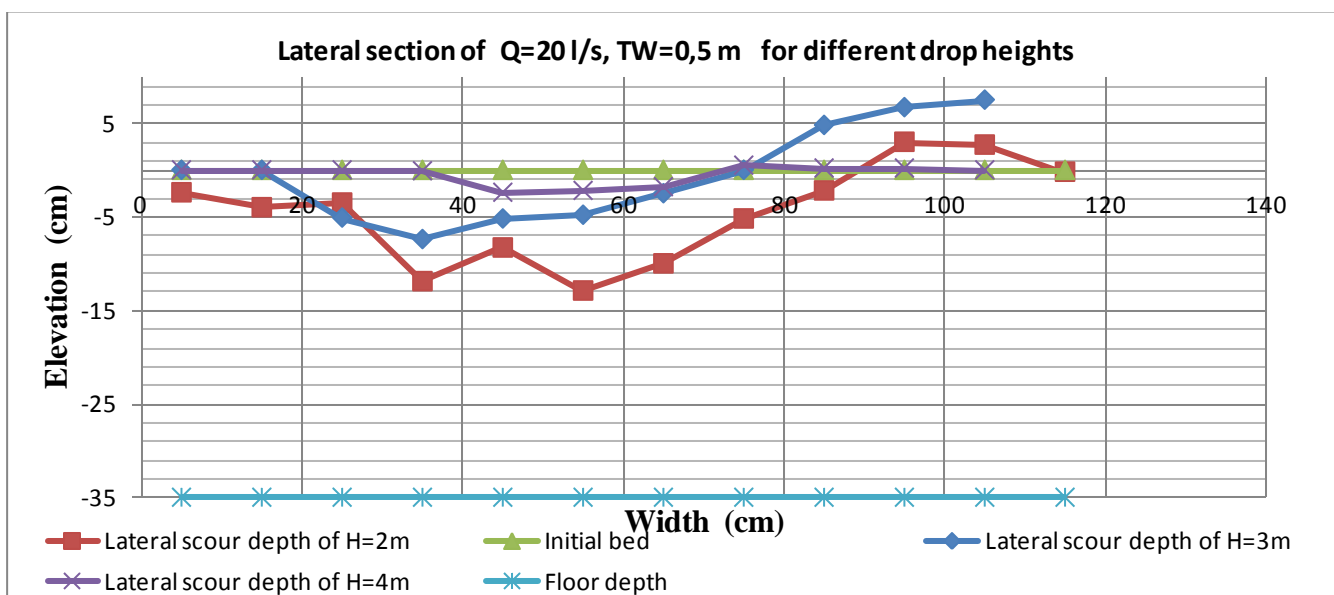


Figure 4-4. Lateral Section of $Q=20\text{l/s}$, $TW=0.5\text{m}$ at different height of spillway

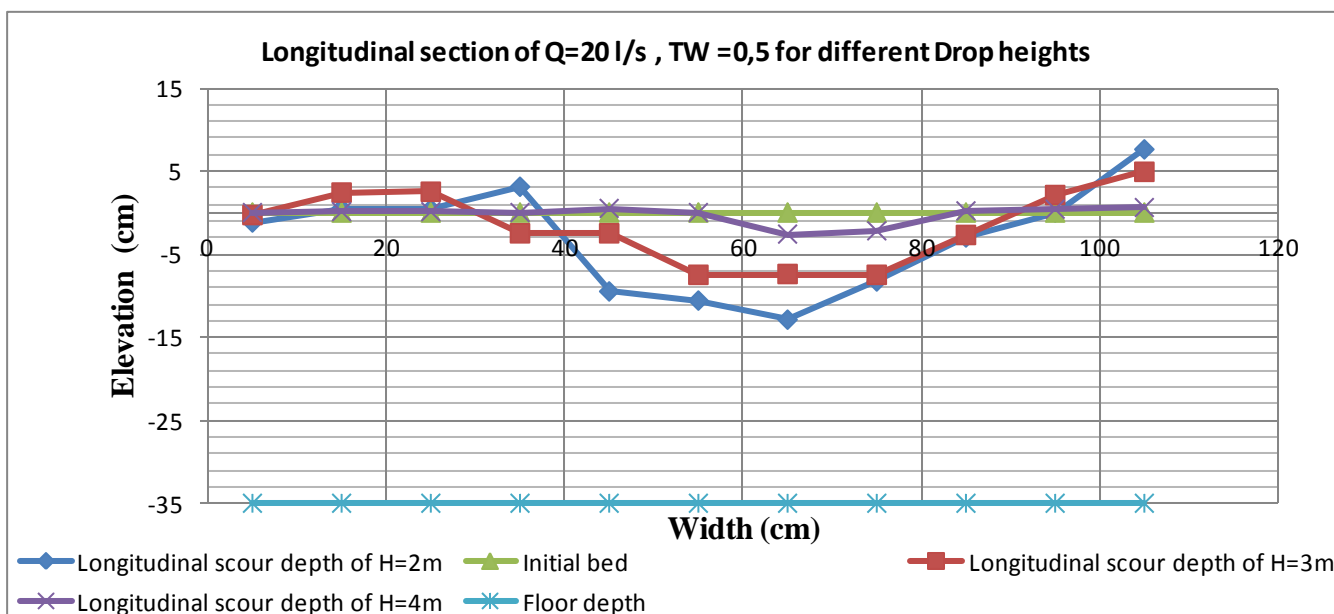


Figure 4-5. Longitudinal Section of $Q=20\text{l/s}$, $TW=0.5\text{m}$ at different height of spillway

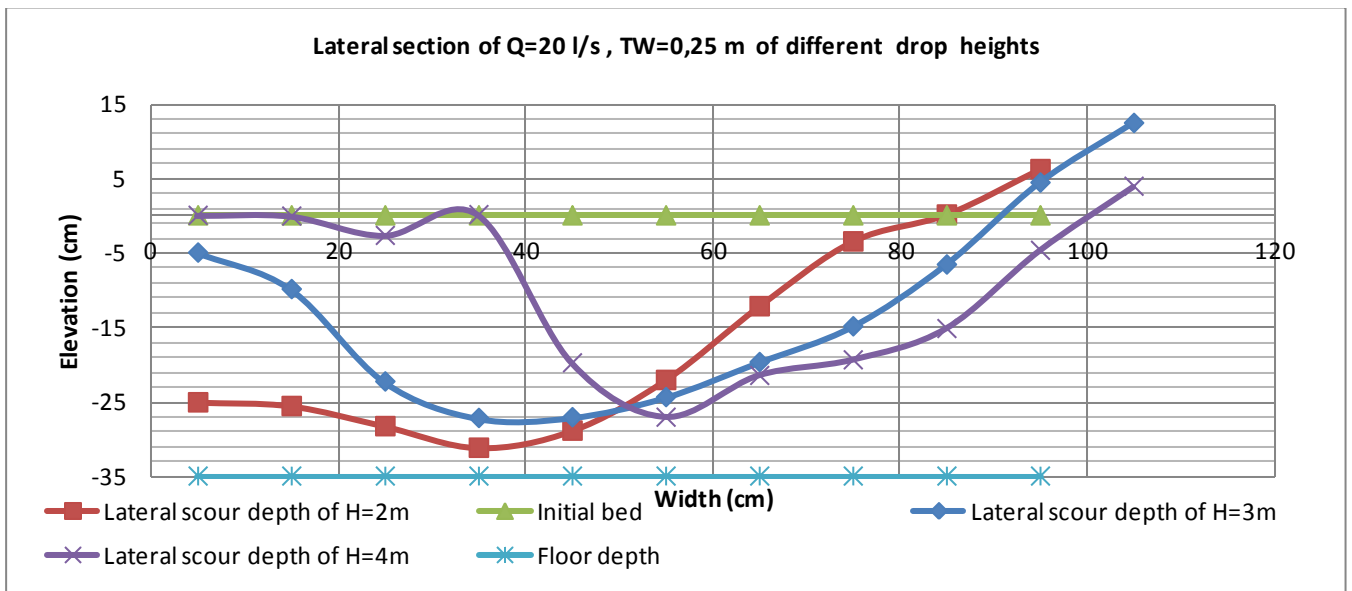


Figure 4-6. Lateral Section of $Q=20\text{ l/s}$, $TW=0.25\text{ m}$ at different height of spillway

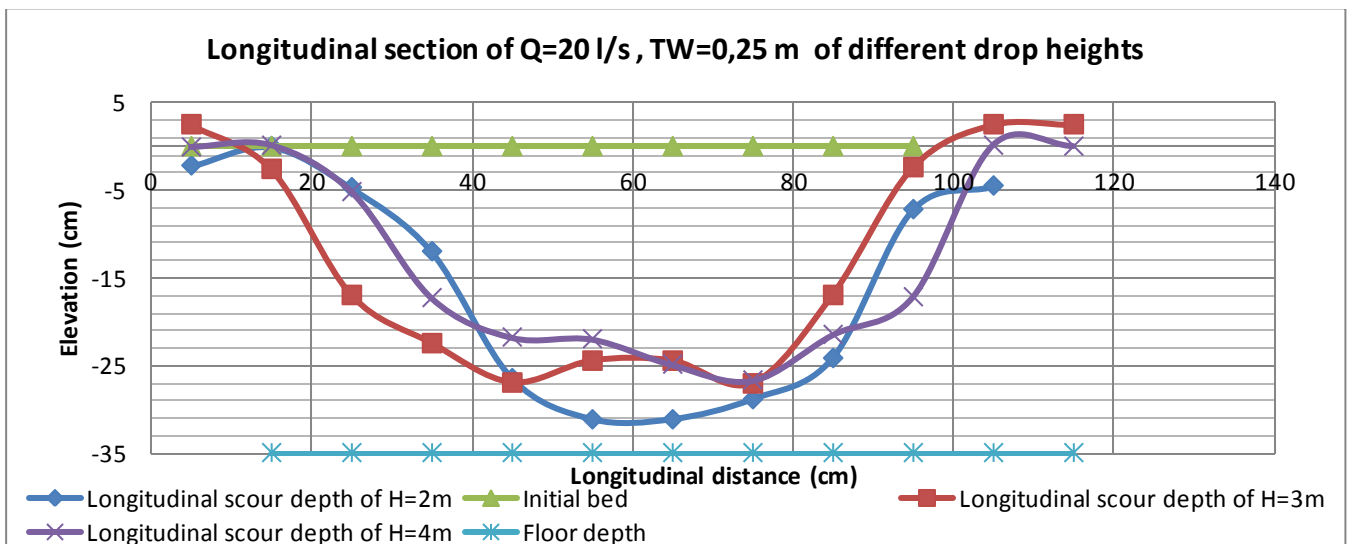


Figure 4-7. Longitudinal Section of $Q=20\text{ l/s}$, $TW=0.25\text{ m}$ at different height of spillway

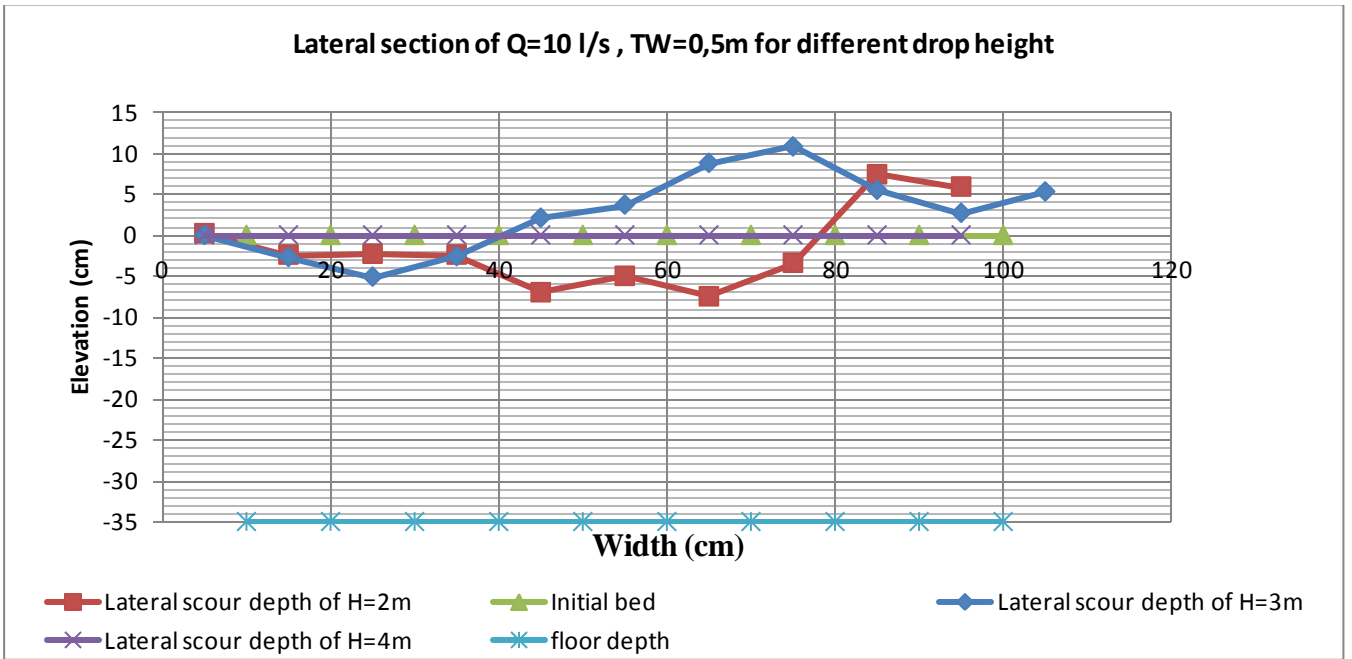


Figure 4-8. Lateral Section of $Q=10\text{l/s}$, $TW=0.5\text{m}$ at different height of spillway

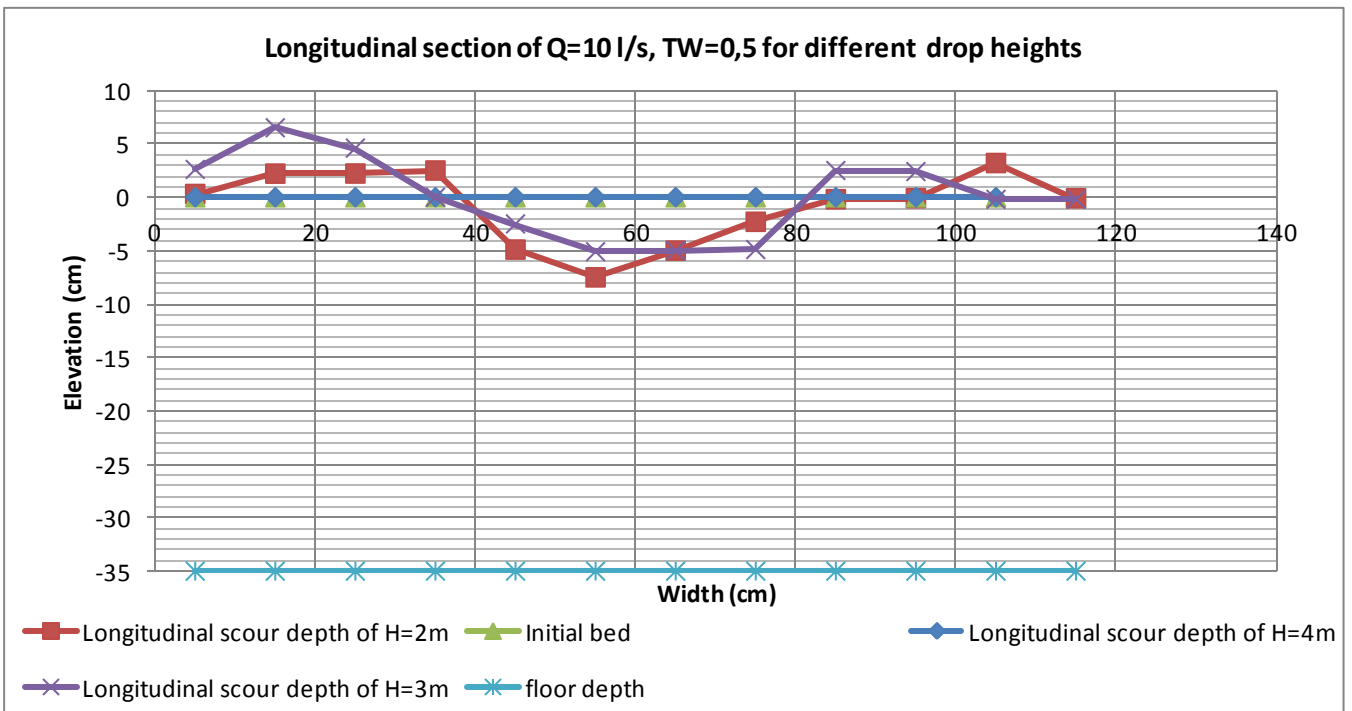


Figure 4-9. Longitudinal Section of $Q=10\text{l/s}$, $TW=0.5\text{m}$ at different height of spillway

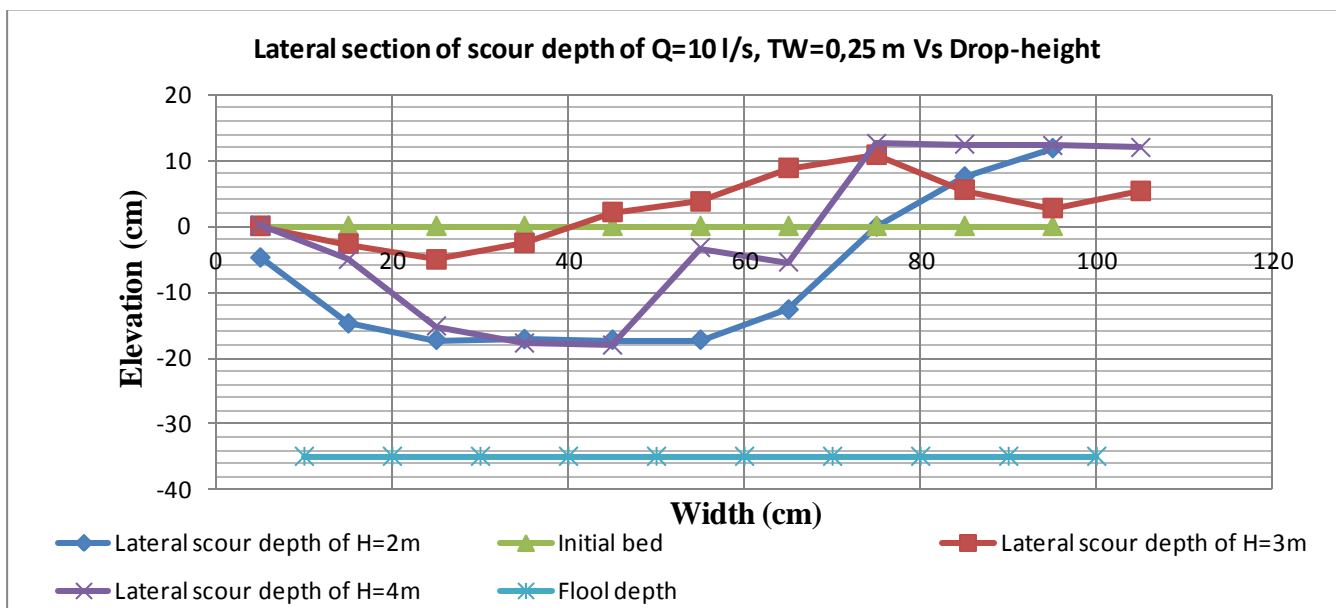


Figure 4-10. Lateral Section of $Q=10\text{ l/s}$, $TW=0.25\text{ m}$ at different height of spillway

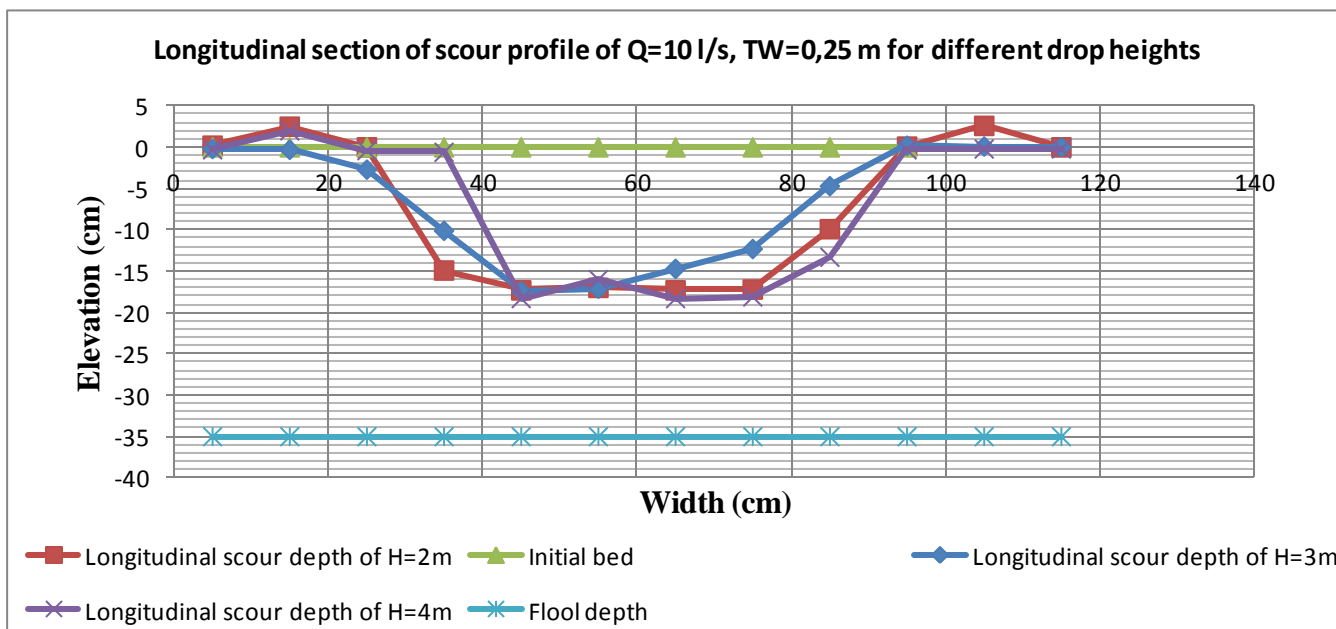


Figure 4-11. Longitudinal Section of $Q=10\text{ l/s}$, $TW=0.25\text{ m}$ at different height of spillway

From Figure 4-4 to Figure 4-11 it can be observed that the scour depth decreased as the drop height increase (when keeping the other hydraulic parameters constant). The reason for this is because the scour potential of the water jet decrease as the jet becomes developed (no core present). From the literature it was determined that the longer the travel distance is of the jet through the air, the more the jet core breaks up, thus losing its energy.

It was also observed from Figure 4-4 to Figure 4-11 that deeper, wider and longer scour holes were obtained for a shallower tailwater depth. As mentioned in the literature (section 2.4.3B) that the jet core is further diffused (scour potential decrease) by the “water cushion.” Thus, the jet is not diffused completely the shallower the tailwater depth is; therefore, the jet still has a high scour potential when compared to the scenario for a deeper tailwater depth.

The scour hole depth decreased as the discharge decreased as seen from Figure 4-4 to Figure 4-11. This is because of energy input of the scour process is at the plunge section of the jet with the pool. The test for the 10 l/s, 0.5m tailwater depth for the 4m drop height was run for eight hours, however, no scouring occurred as seen in Figure 4-12. This result indicates that the small discharge, the high drop height and deep tailwater depth generated a developed jet which scour potential was lower than that of the scour resistance of the bed material



Figure 4-12. Rock scour view for 10 l/s of discharge, 4 m drop height and 0.5 m water depth

4.2 Pressure measured in the plunge pool

The pressures at the water-rock interface were recorded during each scouring test by means of a series of five pressure sensors situated under the jet centreline as shown Figure 4-13.

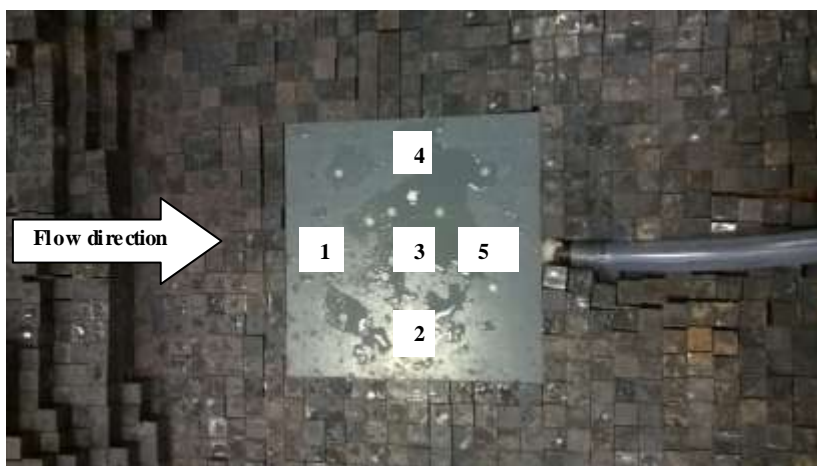


Figure 4-13. Pressure sensor inside the test box placed at the centre of the PVC rock blocks under test conditions

Figure 4-14 shows the recorded pressures at the centreline of jet at impact for the 10 l/s, 0.25m tailwater depth and 2m drop height. Pressure sensor 1 (Figure 3-16) was placed upstream of all other micro-sensors in the direction of the flow, which is the reason for the higher-pressure fluctuation record. Micro-sensor 5 was the furthest downstream when compared to the other micro-sensors and had less pressure fluctuations than the other micro-sensors.

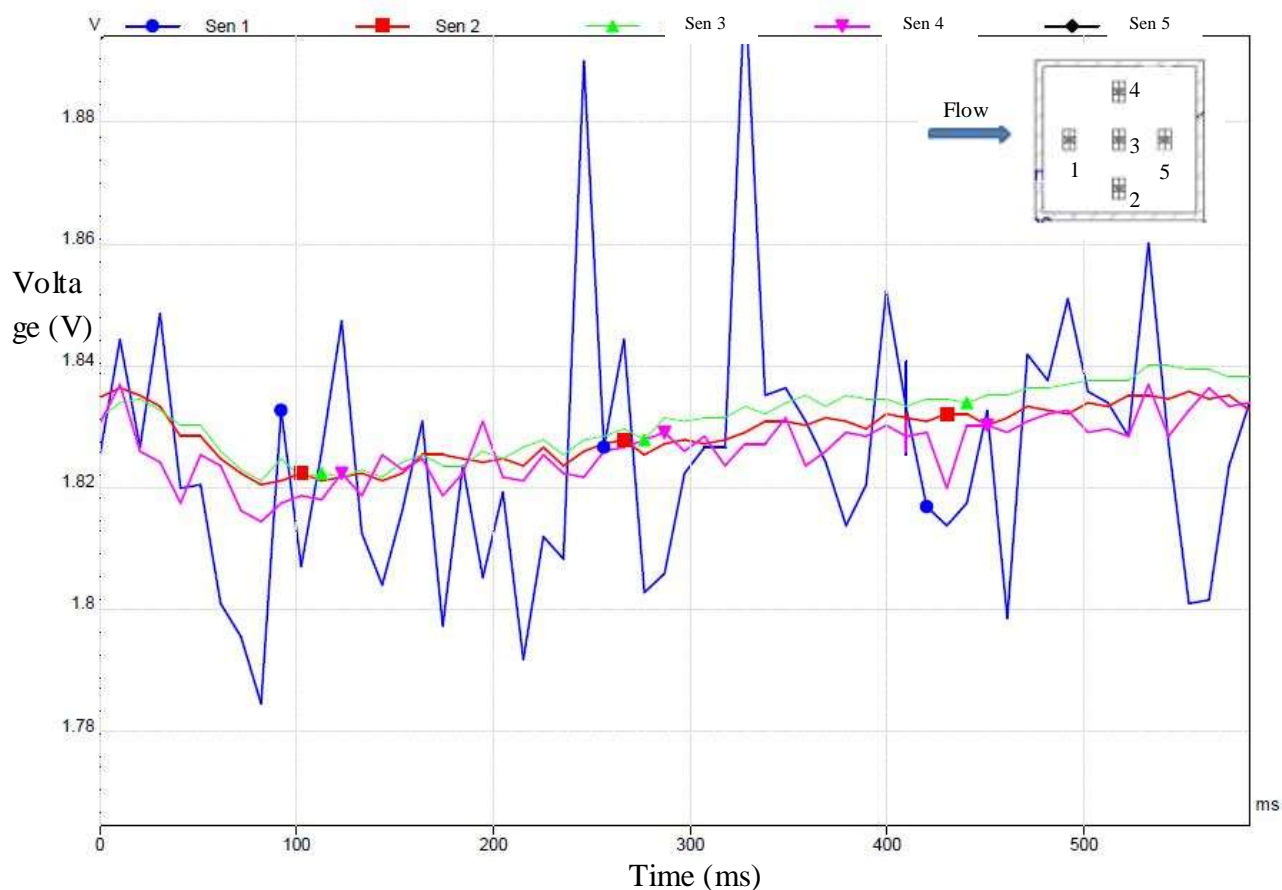


Figure 4-14. PLW (PicoLog Recorder Graph) graph of recorded pressure at the plunge pool under jet impact of 10l/s of discharge and 0.25 m of water depth and 2m of height

The maximum pressures recorded during each test is summarised in Table 4.2. Furthermore, sensor 5 was ignored because of a big difference in the recorded results when compared to the other four pressure sensors. It was further noted that the tests were taken after measuring scour, because of the size of the pressure sensors affected the rock scour (see Figure 4-13).

Table 4.2 shows the pressure distribution depending on the different discharge used during the test, different tailwater depths and different elevation heights. The highest pressure of 0.754 m was measured where the test was running for a discharge of 10 l/s, tailwater depth of 0.5 m and drop height 3 m. The lowest pressure of 0.432m was measured where the test was running with discharge of 20 l/s and tailwater depth was 0.25 m and 2 m drop height. Based on tailwater depth, the pressure has decreased and the tailwater varied from 0.5 m to 0.25 m. It was indicated that the pressures were increased when the tailwater increased as well as the drop height increased. This is explained that the pressure did not depend on the drop height only. Pressure depends also on the ratio of tailwater depth to width of jet (Y/B_j) and to the air concentration. By pointing the air concentration, adding air to discharges as discussed by Manso et al (2004), discharge generates jets with increased kinetic energy, while jets of the same total discharge and increasing aeration have lower kinetic energy. Therefore, it is evident that such a type of jet depending on the tailwater depth and the width of jet could be capable to transient energy to rock mass. This is studied more in detail in section 5.2.3.

Table 4.2. Results of pressure sensors at rock mass for different discharge rates, heights and tailwater depths.

Height (m)	Discharge (l/s)	Water depth (m)	Pressure Sensors (m)				Instant Maximum Pressure head (m)
			1	2	3	4	
4	10	0.50	0.736	0.686	0.747	0.717	0.747
		0.25	0.480	0.425	0.493	0.461	0.493
	20	0.50	0.689	0.636	0.698	0.670	0.698
		0.25	0.617	0.601	0.609	0.577	0.617
3	10	0.50	0.709	0.707	0.754	0.737	0.754
		0.25	0.500	0.471	0.515	0.491	0.515
	20	0.50	0.750	0.660	0.722	0.670	0.750
		0.25	0.611	0.432	0.495	0.492	0.611
2	10	0.50	0.676	0.630	0.689	0.662	0.689
		0.25	0.490	0.410	0.473	0.446	0.664
	20	0.50	0.688	0.622	0.686	0.659	0.490
		0.25	0.431	0.358	0.420	0.432	0.432

4.3 Effect of jet air content on scour

Scour of rock depends on the various factors, i.e. velocity, jet thickness, jet air content, water depth and bed sediments. This section discusses results related to the jet air entrainment. The different mechanism of air entrainment are discussed in the literature review (Section 2.2.2). The air probe measurements were taken in the impingement zone at 36 different points in plunge pool at 15 mm from the plunge pool water surface.

One of the objectives of the physical model study was to obtain sufficient information on air content in the plunge pool to determine the effect of air entrainment on the geometry of the scour hole. The jet characteristics are shown in Table 3.4 and the turbulent intensity Tu was assumed based on experiment of Bollaert (2002) to vary between 3% to 5% for a ski jump outlet. Contour line plots displaying the air content for the jet in the plunge pool are shown Figure 4-15 and results of air concentration and jet mean density are summarised in Table 4.3.

From Figure 4-15 it can be seen that the highest air concentration, thus air entrainment, was recorded at the point of impingement, and it decreased outwards. The highest recorded concentration was 85.304% for scenario 20 l/s, 3m drop height and tailwater depth of 0.5m. The air concentration measured during the laboratory test and the jet mean density are summarised in Table 4.3. It was revealed that at the 0.25 m tailwater depth, the air concentration was higher than the air concentration for the 0.5 m tailwater depth, with the exception for the 20 l/s, 3 m drop height and 0.5 m tailwater depth. The reason is because the air concentration along the jet centerline for submerged jets is a function of the entrained air

concentration and of the relative depth below jet impingement as Duarte (2014) revealed. The air entrainment contour maps for the other test scenarios are shown in Appendix D (Figure D 0-11).

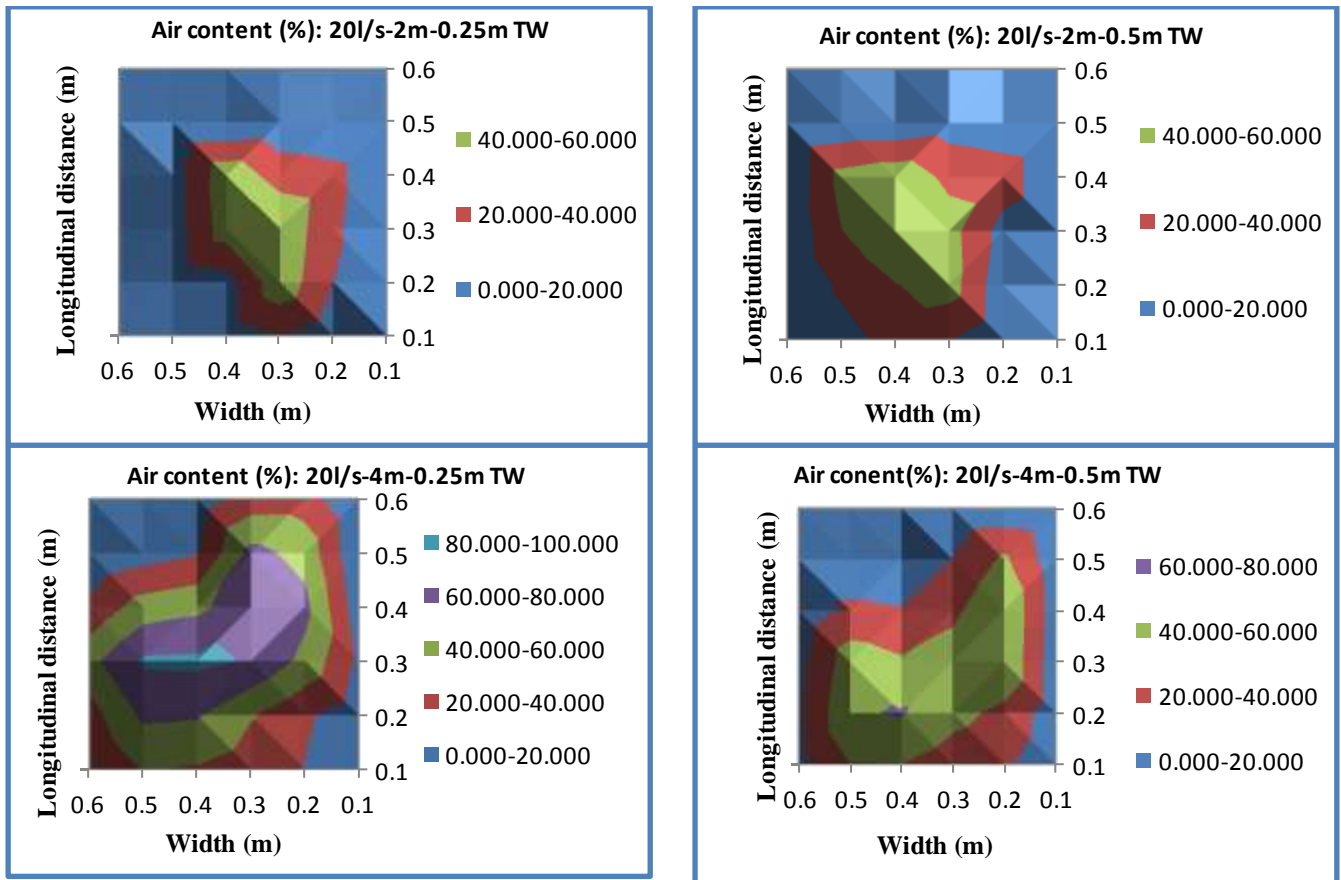


Figure 4-15. General view of contour plot of air concentration of four scenarios (Test with discharge of 20l/s with 4m and 2 m of height and two different of tailwater depth)

Table 4.3. Summary of jet mean density and air concentration measured at the impact with the plunge pool

Drop height	Discharge (l/s)	Tailwater Level	Air concentration	Air-water ratio	Density of the air-water mixture
H (m)	Q (l/s)	Y(m)	α (%)	β	ρ_{aw} (kg/m ³)
Measured	Measured	Measured	Measured	Eq. 35	Eq. 28
2	10	0.50	57.365	1.345	427.040
2	10	0.25	60.929	1.559	391.441
2	20	0.50	57.657	1.362	424.118
2	20	0.25	57.832	1.371	422.378
3	10	0.50	65.740	1.919	343.389
3	10	0.25	72.710	2.664	273.773
3	20	0.50	85.304	5.805	147.985
3	20	0.25	77.536	3.452	225.566
4	10	0.50	69.967	2.330	301.171
4	10	0.25	75.946	3.157	241.447
4	20	0.50	61.727	1.613	383.476
4	20	0.25	83.743	5.151	163.572

Figure 4-16 compares the observed air concentration and the scour hole depth. It can be seen that the air concentrations increased when the drop height increased with the corresponding scour depth decreasing, with the exception of the 20 l/s and 0.5 m pool depth scenario.

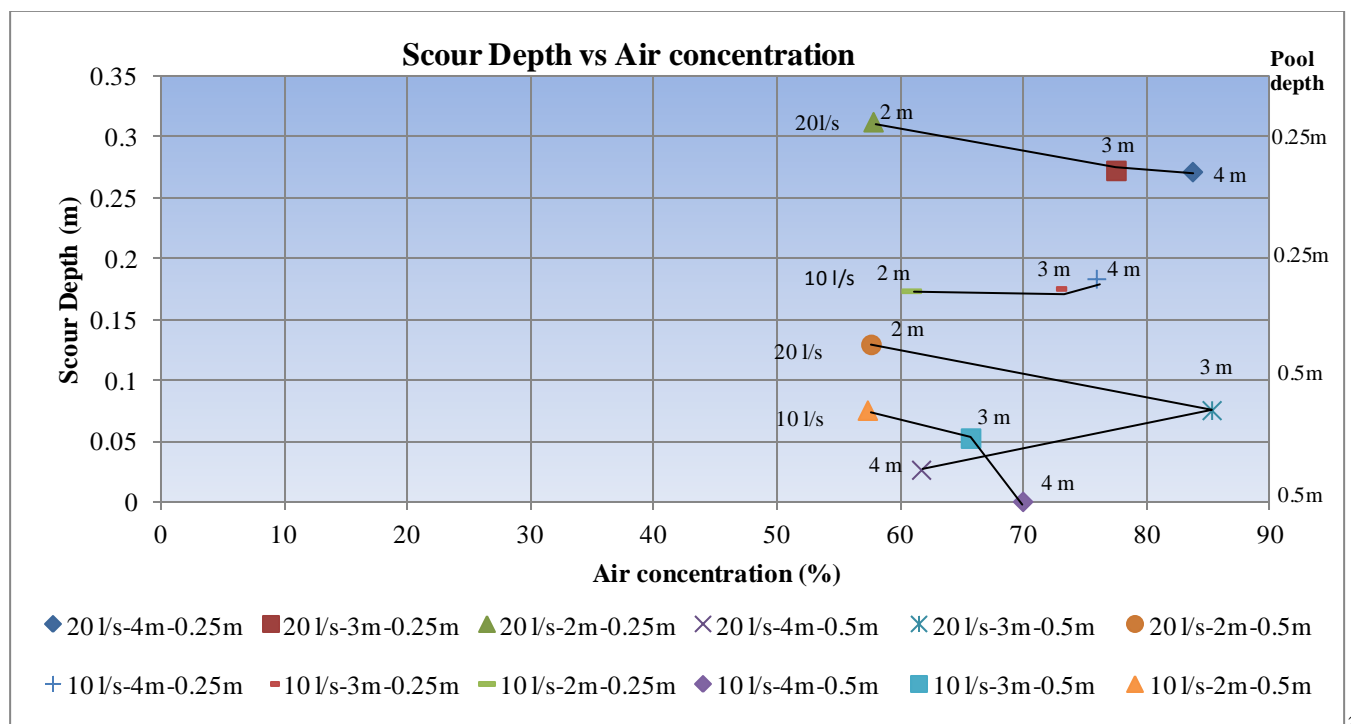


Figure 4-16. The comparison of air concentration and scour depth

4.4 Summary

From the physical model results it was found that the drop height, tailwater depth and discharge have an effect on the rock scour hole geometry. The tests proved that the scour hole depth decreased with an increase in drop height, increased with an increase in discharge and decreased for a deeper tailwater depth.

The influence of pressure on the block displacement differs with the relative pool depth. It indicates that the pressures increased with an increase in tailwater level, as well as in increase in the drop height. It should be noted that the pressures results used in the calculations were the recorded pressures with the hydrostatic pressures subtracted from it.

The air concentrations increased with an increase in drop height, corresponding to a decrease in scour depth

Chapter 5. Evaluating the development of ultimate rock scour hole

This chapter compares the physical model results with that obtained from the scour prediction methods (Erodibility Index method and Comprehensive Scour method) discussed in the literature review. The content of the chapter includes different methods developed to determine the scour hole shape. The estimation of rock scour hole shape was determined through two methods found in the literature. The first method was to determine the bed sediment's ability to resist the erosive capacity of the water by using EIM and the second method was to estimate the extent of scour by using the CSM.

5.1. Erodibility Index Method (Annandale's Method)

The first step of the Erodibility Index method (EIM) is to determine the ability of the rock bed to resist the erosive capacity of the water that is quantified by the erodibility index (K) (section 2.4.2) by using the tables in Appendix A.

The mass strength number (M_s) was determined by assuming hard rock and using Table A 0.1 to assume the UCS, since it was assumed that the rock was not easy to peel the rock with a knife. Based on the calculation and using the equation 19, the mass strength number was 12.52 regarding the UCS > 10 MPa. The joint set number (J_n) was assumed as five corresponding to multiple joint set as obtained from Table A 0.2. The rock quality designation (RQD) was estimated as 95 by using $RQD = (105 - 10/D)$ where D is the mean block diameter. The block size number (K_b) of the prototype was computed to be 19 with equation 21. Table A 0.3 and Table A 0.4 in Appendix A, summarising the joint of roughness (J_r) number and the degree of alteration (J_a) respectively, were used to determine the shear strength factor (K_d) as one by using equation 22. The joint roughness number was estimated as one for smooth planar joint conditions that corresponds to the uniform PVC blocks joints. The degree of alteration number was assumed to be one. The relative ground structure number is 1.14 where the dip angle of close spaced joint set is assumed as horizontal (0°) (Table A 0.5 in Appendix A). By substituting all the values discussed above into equation 17 (see Section 2.4.2) the erodibility index (K) for the prototype was calculated as 271.11

The stream power at the impingement zone was computed based on the equation 23 (section 2.4.2) and its values depend on the prototype of twelve scenarios. The discharges of the prototype under evaluation were calculated to be 202.38 m³/s and 101.19 m³/s. The others parameters are summarised in Table 5.1. The erodibility index parameters discussed above are summarised in the Table 5.2. Therefore, Table 5.1 and Table 5.2 were discussed based on prototype because of the Erodibility Index (EI) method is classification method applicable to rock mass as a whole, which is opposite to an analytical or numerical method based on mechanical principles

Table 5.1. Stream power of different prototype

Test Scenario	Stream Power	Discharge	Drop height	Area	Tailwater
	P	Q	H	A	Y
	kW/s ²	m ³ /s	m	m ²	m
1	18 068.6	202.38	160	15.3786	0.50
2	19 409.7	202.38	160	15.3387	0.25
3	12 768.9	202.38	120	15.5439	0.50
4	14 084.03	202.38	120	15.5018	0.25
5	7 576.27	202.38	80	15.7185	0.50
6	8 864.11	202.38	80	15.674	0.25
7	15 294.24	101.19	160	9.08419	0.50
8	16 444.39	101.19	160	9.05232	0.25
9	10 766.39	101.19	120	9.21756	0.50
10	1 188.722	101.19	120	9.18329	0.25
11	6 360.62	101.19	80	9.36133	0.50
12	7 450.17	101.19	80	9.32433	0.25

From Table 5.1 it can be seen that the applied stream power (P) increases with an increase in drop height, an increase in discharge and a decrease in tailwater level.

Table 5.2. Summary of parameters to calculate the erodibility index (prototype)

Erodibility Index		
Parameter	Prototype Magnitude	Equation & reference
Erodibility Index K	271.11	Eq 17
Mass strength		
Mass strength number M_s	12.51	Table A 0.1 & Eq 19
Coefficient of relative density Cr	0.96	Eq 20
Unconfined Compressive Strength UCS	13.5	
Acceleration due to gravity g	9.81	
Mass density of rock ρ_r	2650	
Block size number		
Block size number K_b	19	Eq. 21
Rock Quality designation RQD¹	95	
Joint set number J_n	5	Table A 0.2.
Mean block diameter D	1	
Interparticle bond shear strength		
Shear strength number K_d	1	Eq. 22
Degree of roughness J_r	1	Table A 0.3
Degree of alteration J_a	1	Table A 0.4
Relative ground structure number		
Relative ground structure J_s	1.14	Table A 0.5

Stream power defines the power of the impinging jet to cause scour. The threshold (critical) stream power, expressed in kW/m², indicates the stream power required for scour to commence and can be expressed as follows (Castillo & Carrillo, 2014):

$$P_{rock} \left(\frac{kW}{m^2} \right) = 0.48K^{0.44} \text{ if } K \leq 0.1 \quad (a)$$

[70]

$$P_{rock} \left(\frac{kW}{m^2} \right) = K^{0.75} \text{ if } K > 0.1 \quad (b)$$

Since the erodibility index (K) is greater than 0.1 (K = 271.11, refer to Table 5.2), the threshold (critical) stream power was estimated as 66.81 kW/m² by using equation 70 (b). This indicates that the rock would likely scour under these conditions (applied stream power (Table 5.1) greater than the threshold (critical) stream power). Additionally, by plotting the calculated erodibility index against the stream power on Annandale's threshold criteria graph, it is observed that the stream power values calculated in Table 5.1 are above the proposed thresholds criteria line (Figure 2-8), which confirms that scour would occur.

5.2. Comprehensive Scour Model (CSM)

As outlined in Section 2.4.3, this method consists of three modules, namely the falling jet, the plunge pool and the rock mass that influence scouring. Each module and all parameters required to estimate the scour hole geometry according to the Comprehensive Scour method are detailed below. It must be noted that the analysis was based on model values in order to compare the results to the laboratory results.

5.2.1. Falling jet

This module is based on three parameters, namely the velocity at the issuance V_i , diameter or width at issuance (D_i , B_i) and the initial jet turbulence intensity T_u . It describes the jet trajectory to jet impingement into the plunge pool from point of issuance. It outlines all the hydraulic characteristics during this trajectory. The basic theory was detailed in section 2.4.3.

The turbulence intensity T_u value was assumed based on the type of the outlet of model (structure) as summarised in Table 3.2 (Schleiss & Whittaker, 1984). In this case, it was assumed that the physical model type of outlet represented that of ski-jump outlet jets (3-5%). The reason of choosing the ski-jump case instead of a free-over fall spillway is due to the fact that uniform flow was not reached in the rectangular issuance canal (model limitation), thus the internal turbulence of the jet in the laboratory was much higher than what it would be for a normal free falling jet where the approach flow is uniform. This falling jet module also determines the location of impingement with the tailwater level X_{ult} , the width of the core at impact B_j , the outside width of the jet at impact B_{out} and the velocity at impact V_j . Table 5.3 summarises the calculated parameters of the falling jet module.

Table 5.3. Falling Jet module parameter calculations at impact with tailwater level

Discharge	Drop height	Tail water depth	Issuance width	Impact core width	Issuance velocity	Impact velocity	Turbulence Intensity	Outer jet width at impact	Trajectory length	Horizontal distance to impact
Q (l/s)	H (m)	TW (m)	B_i (m)	B_j (m)	V_i (m/s)	V_j (m/s)	T_u (%)	B_{out} (m)	L (m)	X_{ult} (m)
				Eq.26		Eq. 25		Eq. 26	Table 3.3	
Input	Input	Input	Input	Calc*	Input	Calc*	Input	Calc*	Calc*	
10	2	0.50	0.2	0.108	1.667	5.675	3%	1.786	2.333	1.208
10	2	0.25	0.2	0.104	1.667	6.09	3%	1.786	2.333	1.208
20	2	0.50	0.2	0.118	2.000	5.782	4%	2.215	2.512	1.381
20	2	0.25	0.2	0.114	2.000	6.192	4%	2.215	2.512	1.381
10	3	0.50	0.2	0.096	1.667	7.199	3%	2.893	3.355	1.479
10	3	0.25	0.2	0.094	1.667	7.532	3%	2.893	3.355	1.479
20	3	0.50	0.2	0.105	2.000	7.284	4%	3.622	3.542	1.691
20	3	0.25	0.2	0.103	2.000	7.613	4%	3.622	3.542	1.691
10	4	0.50	0.2	0.089	1.667	8.453	3%	4.310	4.418	1.708
10	4	0.25	0.2	0.087	1.667	8.738	3%	4.310	4.418	1.708
20	4	0.50	0.2	0.097	2.000	8.525	4%	5.478	4.630	1.953
20	4	0.25	0.2	0.095	2.000	8.808	4%	5.478	4.630	1.953

*Calc: Calculated value

5.2.2. Plunge pool module

This module is characterised by the tailwater depth Y . It determines the ratio of the water depth to the jet width Y/B_j , which is related to the diffusion characteristics of the jet through the plunge pool. The turbulence of jet that is described in the falling jet module above, defines the degree of turbulent pressure fluctuations of the jet at impact with the tailwater level. This model also quantifies the total dynamic pressure (P_{total}) exerted on the plunge pool floor at the center point of the jet, which is dependent on the root-mean-square (C'_{pa}) value and the mean dynamic pressure coefficient (C_{pa}).

The root-mean-square (C'_{pa}) value of the pressure fluctuations at the water-rock interface depends on the Y/B_j and H/L_b ratios. Whereas the non-dimensional mean dynamic pressure coefficient (C_{pa}) is defined by the Y/B_j ratio. The data collected were measured in the experimental facility, under the jet's centreline based on the literature review (see section 2.4.3). Bollaert (2002) proposed to calculate the dynamic pressure coefficient and root mean square value of pressure fluctuation by using the equation 36 to 39. Thus, the total dynamic pressure was calculated by equation 41. These coefficients and total dynamic pressure are summarised in

Table 5.4. The relationship between the root-mean-square value of the fluctuation part of the dynamic pressure (C'_{pa}) and the Y/B_j ratio, which are presented in Table 5.4 shows that the pressure increases with increasing the tailwater depth. The modification of the jet diameter had no significant effect on the measurement of the pressures.

Table 5.4. Dynamic pressure and RMS pressure fluctuation coefficients

Discharge (l/s)	Height (m)	Tailwater depth (m)	Water depth/jet width	Drop height/breakup length	Mean dynamic pressure coefficient	Root mean square value of pressure fluctuation	Total Pressure
Q	H	Y	Y/B_j	H/L_b	C_{pa}	C'_{pa}	P_{total}
					Eq. 36-38	Eq.39	Eq.41
10	2	0.50	4.613	1.45	0.994	0.273	36374.7
10	2	0.25	2.344	1.45	0.895	0.220	19087.3
20	2	0.50	4.251	1.16	1.068	0.269	43060.4
20	2	0.25	2.199	1.16	0.923	0.214	22162.6
10	3	0.50	5.196	2.18	0.884	0.276	49452.9
10	3	0.25	2.657	2.18	0.843	0.275	2662.56
20	3	0.50	4.771	1.74	0.963	0.274	65343.2
20	3	0.25	2.439	1.74	0.878	0.224	33237.9
10	4	0.50	5.630	2.91	0.866	0.275	74568.3
10	4	0.25	2.862	2.91	0.815	0.281	38357
20	4	0.50	5.161	2.33	0.890	0.276	82994.3
20	4	0.25	2.623	2.33	0.852	0.274	43376.7

5.2.3. The rock mass

This module outlines directly the hydrodynamic loading inside the joints. The basic parameters that describe the hydrodynamic loading inside the rock joints was explained in section 2.4.3.

5.2.3.1. Maximum dynamic pressure C_p^{max}

The maximum dynamic pressure in a closed-end rock joint was estimated using the product of root mean-square C'_{pa} by the amplification Γ^+ , where the amplification influences the fluctuation of the dynamic pressure and by superposing this product to the mean dynamic pressure value C_{pa} . Maximum dynamic pressure was computed using the equation 71 (also explained in section 2.4.3.).

$$P_{max} = \gamma C_p^{max} \frac{\phi V_j^2}{2g} = \gamma (C_{pa} + \Gamma^+ C'_{pa}) \frac{\phi V_j^2}{2g} \quad [71]$$

Where the product of Γ^+ times C'_{pa} results in the coefficient C_p^+ . The amplification value Γ^+ was defined by the curve for maximum and minimum values. For this case, the curve of maximum values is computed by $4+2Y/B_j$ and for minimum values computed by $-8+2Y/B_j$ based on the Y/B_j ratio condition (as explained in equation 49). The amplification factor Γ^+ and maximum dynamic pressure $C^{max}_p (P_{max})$ were calculated and the results are given in Table 5.5. Positive extreme pressure coefficients C_p^+ ($C_p^+ = \Gamma^+ \cdot C'_{pa}$) were computed and can be used to calculate the appropriate maximum pressure value inside the rock joint. These coefficients C_p^+ were summarised in the relationship between the positive extreme pressure coefficients C_p^+ has been defined by Bollaert (2002). These value are directly calculated to define the appropriate of maximum pressure inside the rock joints by considering the tightness of the joints by superposition of C_{pa} and C_p^+ . The amplification of pool bottom pressure fluctuations depends on the capability of the rock joints to generate peak pressure as defined by equation 72. The positive extreme pressure coefficients C_p^+ are defined as follows:

$$\begin{array}{l}
 C^+ = 2 + 0.40 \frac{Y}{B_j} \text{ for } \frac{Y}{B_j} < 8 \\
 C^+ = 10.54 - 0.66 \frac{Y}{B_j} \text{ for } \frac{Y}{B_j} \geq 8 \\
 C^+ = -2 + 0.40 \frac{Y}{B_j} \text{ for } \frac{Y}{B_j} < 8 \\
 C^+ = 6.54 - 0.66 \frac{Y}{B_j} \text{ for } \frac{Y}{B_j} \geq 8
 \end{array}
 \left. \begin{array}{l} \\ \\ \\ \end{array} \right\}
 \begin{array}{l}
 \text{Maximum} \\
 \text{value} \\
 \\ \\
 \text{Minimum} \\
 \text{Value}
 \end{array}
 \quad [70]$$

When Table 5.5 is compared with Table 5.6, it confirms the experiments of Bollaert (2002) that the scatter for the amplification factor Γ^+ and root-mean-square C'_{pa} values is higher than that of the positive extreme pressure when assuming \emptyset to be 1.

Table 5.5. Maximum and minimum pressure P_{\max} in closed rock joint calculated at different heights and with different discharges

Discharge	Drop height	Water depth	Specific weight	Amplification		Pressure	
Q (l/s)	H (m)	TW (m)	γ (N/m ³)	Γ^+ (eq. 49)		P (Pa) (eq. 48)	
				Max	Min	Max	Min
10	2	0.50	9810	13.226	1.226	74067.76	21386.23
	2	0.25	9810	8.780	-3.220	48517.29	3356.84
20	2	0.50	9810	12.501	0.501	74024.31	20110.72
	2	0.25	9810	8.399	-3.601	52149.82	2912.25
10	3	0.50	9810	14.392	2.392	125691.6	39997.08
	3	0.25	9810	9.315	-2.685	96573.45	2983.39
20	3	0.50	9810	13.542	1.542	123883.1	36735.40
	3	0.25	9810	8.878	-3.122	82967.67	5203.23
10	4	0.50	9810	15.260	3.260	181090.5	63025.08
	4	0.25	9810	9.724	-2.276	135511.8	6678.142
20	4	0.50	9810	14.323	2.323	175732.4	55607.37
	4	0.25	9810	9.246	-2.754	131254.8	3798.25

Table 5.6. The positive extreme pressure C^+ coefficients and Pressure inside the blocks results

Discharge	Drop height	Water depth	Specific weight	Extreme pressure coefficients		Pressure	
Q (l/s)	H (m)	TW (m)	γ (N/m ³)	C^+ (eq. 72)		P_{\max} (Pa) (eq. 48)	
				Max	Min	Max	Min
10	2	0.50	9810	3.845	-0.155	61924.2	-2491.35
	2	0.25	9810	2.956	-1.044	54851.4	-19374.2
20	2	0.50	9810	3.700	-0.300	61850.09	-5009.91
	2	0.25	9810	2.880	-1.120	55197.4	-21472.6
10	3	0.50	9810	4.078	0.078	105685.6	2030.054
	3	0.25	9810	3.063	-0.937	86884.23	-26581.3
20	3	0.50	9810	3.908	-0.092	103668.8	-2431.21
	3	0.25	9810	2.976	-1.024	86222.58	-29687.4
10	4	0.50	9810	4.252	0.252	151898.8	9003.239
	4	0.25	9810	3.145	-0.855	120059.3	-32646.2
20	4	0.50	9810	4.065	0.065	147685.1	2345.146
	4	0.250	9810	3.049	-0.951	118273.4	-36876.6

The combination of maximum pressure fluctuation and maximum amplification leads to the extreme coefficients, which are very high according to Bollaert (2002). This is not because of the high amplification inside the rock joint but due to the high air concentration. The characteristic pressures of the cycle (maximum and minimum) determine the characteristic amplitude according to Bollaert (2002). The minimum values are close to the standard atmospheric pressure. An average maximum pressure was

determined by counting the number of peaks and taking the average of the peak values. The number of peaks per time are equal to the resonance frequency $f_{res} = c/4L$ where L is the fissure length (m) and c is the pressure wave celerity (m/s). The mean of celerity is approximately 104 m/s for the non-aerated jets and approaches 70 m/s for jet aerations (Duarte, 2014). The total joint length of the PVC blocks representing rock in the physical model at the Stellenbosch University Hydraulic laboratory was 0.075 m (the PVC blocks' sides were 0.025 m, thus $z + x + z$ as shown in Figure 5-1).

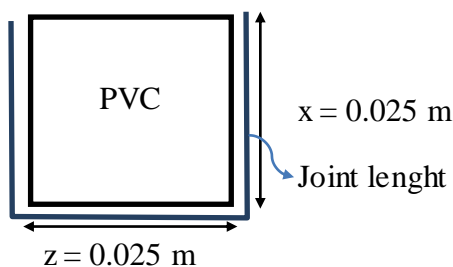


Figure 5-1: Schematic sketch of joint length

The rock mass is defined by the characteristics of the hydrodynamics loading inside open or closed end rock joint. This study deals with the failure of open-end rock joints and peeling-off of rock from their mass, thus the Dynamic Impulsion and Quasi Steady Impulsion methods could be used to predict the rock scour.

5.2.3.2. Dynamic Impulsion (DI) Methods

The side distance of block x_b was 0.025 m and the height (z) of the block was 0.025 m (model values), thus a z/x ratio of one was obtained. In addition, the total length of a joint that passes underneath is 0.075m ($L = x_b + 2z$). The thickness of the joint was neglected. The maximum net impulsion coefficient C_I was computed as defined by equation 57 and tabulated data for each scenario of recorded data was assessed.

A wave celerity c of 100 m/s was assumed as suggests by Bollaert (2002) and a time of period T of 0.0015 seconds was computed (Section 2.4.3.2). The average specific weight of a PVC block was 11520 N/m^3 . The blocks that moved had a displacement velocity of V_{up} , the displacement distance h_{up} and h_{up}/z (z is the height of a block) of different tests according to the different discharges and heights of spillway were summarised in Table 5.7. The ultimate scour depth based on DI method is given for a failure criterion of h_{up}/z ratio is less than 1 m (see Table 2.6) i.e. the ultimate scour depth is reached when the rock block displacement becomes less than the height of the block. The ultimate scour depth, which corresponds to a h_{up}/z ratio is less than 1 m, for each test scenario was determined as set out in Appendix C and is only summarised in Table 5.7.

Table 5.7. Summary of ultimate scour depths based on DI method for the different test scenarios

Discharge Q (l/s)	Drop height H (m)	Tailwater depth Y (m)	Scour depth (m)	C_I^*	I_{max}^{**} (Ns)	I_{net}^{***} (Ns)	Uplift velocity V_{up} (m/s)	Uplift height h_{up} (m)	h_{up}/z
			Annexure C	Eq 57	Eq 56	Eq 55		Eq. 58	
10	2	0.50	0	0.746	0.0015	0.0015	0.640	0.021	0.836
10	2	0.25	0.275	0.753	0.002	0.002	0.652	0.023	0.933
20	2	0.50	0.100	0.704	0.0017	0.0016	0.667	0.024	0.966
20	2	0.25	0.450	0.556	0.0016	0.0016	0.667	0.023	0.918
10	3	0.50	0.025	0.675	0.0016	0.0016	0.684	0.024	0.954
10	3	0.25	0.150	0.825	0.0016	0.0016	0.676	0.025	0.737
20	3	0.50	0.100	0.653	0.0016	0.0016	0.654	0.022	0.873
20	3	0.25	0.250	0.723	0.0016	0.0016	0.691	0.024	0.975
10	4	0.50	0.150	0.577	0.002	0.002	0.667	0.024	0.884
10	4	0.25	0.175	0.722	0.002	0.002	0.668	0.024	0.955
20	4	0.50	0.250	0.4792	0.0014	0.0014	0.643	0.021	0.842
20	4	0.25	0.275	0.477	0.002	0.002	0.641	0.022	0.902

* Maximum net impulsion coefficient

** Maximum Impulse

*** Net impulse

Comparison between model scour profiles and computation of DI were different because of the jet was partly disintegrated in the air, thus losing some of its scour potential. Moreover, the results of scour depth of the tailwater depth of 0.25 m for different drop heights show that the scour depth is much higher when compared to the scour depths obtained for the tailwater depth of 0.5 m (Table 5.8). Nevertheless, the jet impingement patterns are influenced by the shape of the plunge pool bottom.

Table 5.8. Comparison of scour depth model and empirical computation of DI method

Discharge Q (l/s)	Drop height H (m)	Tailwater depth Y (m)	Max scour depth observed (lab model) (m)	Scour depth by DI (empirical) (m)	% difference (m)*
10	2	0.50	0.075	0	0
10	2	0.25	0.173	0.225	76.9
20	2	0.50	0.129	0.100	77.5
20	2	0.25	0.312	0.450	69.3
10	3	0.50	0.052	0.025	48.07
10	3	0.25	0.175	0.100	57.14
20	3	0.50	0.075	0.100	75
20	3	0.25	0.272	0.250	91.91
10	4	0.50	0	0.150	-
10	4	0.25	0.183	0.175	95.63
20	4	0.50	0.026	0.250	0.00104
20	4	0.25	0.271	0.425	63.76

* % difference = Physical model scour depth value/DI scour depth value $\times 100$

Table 5.9 shows the comparison between the maximum scour depths computed by the DI method against the maximum scour depth measured in laboratory. It was revealed that the difference between of DI Method and laboratory results vary from 0.008 m to as much as 0.224m.

5.2.3.3. Evaluating rock scour by using Quasi-Steady Impulsion model

This method combines the quasi-steady force and brittle or fatigue fracturing methods. It occurs for rock composed of multiple, thin, near-horizontal layers based as stated in the literature review (section 2.4.3 p.33). Brittle and fatigue fracturing develop the force between the block and the underlying rock mass. Moreover, the flow deviation due to the protrusion "e" of the block along the bottom generates forces called quasi-steady forces. The velocity profile of the wall jets $V_{zbottom}$ and the up and downstream wall jet depth (h_{up} and h_{down}) for the different the scenarios were computed and are summarised in Table D 0.2 to Table D 0.12. Figure 2-16 is repeated here as Figure 5-2 for clarification purposes, shows that at the jet impingement region (green circle), the DI method is used to calculate the ultimate scour depth, while the wall jet region the QSI method is used.

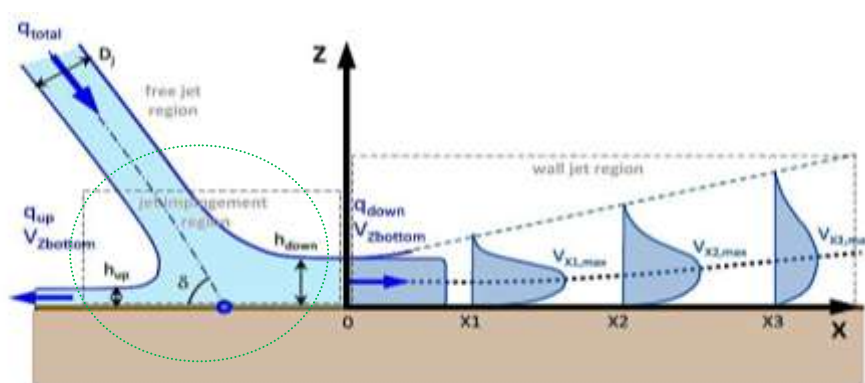


Figure 5-2. Plane jet deflection on a flat bottom (adapted from Bollaert, 2012).

From the physical model tests, it was observed that the tailwater depth for the same discharge had a significant effect on the jet wall velocity. For example, Figure 5-3 indicates that for a discharge of 10 l/s at 2 m drop height, the jet wall velocity was observed to be approximately double in magnitude for the 0.25m tailwater depth as opposed to the 0.5m tailwater depth. Figure 5-3 describe the flow velocity along the wall jet, the negative distance shows the upstream wall jet velocity and positive for the downstream wall jet velocity. It is observed that the jet velocity profile is flattened as the distance-x increases.

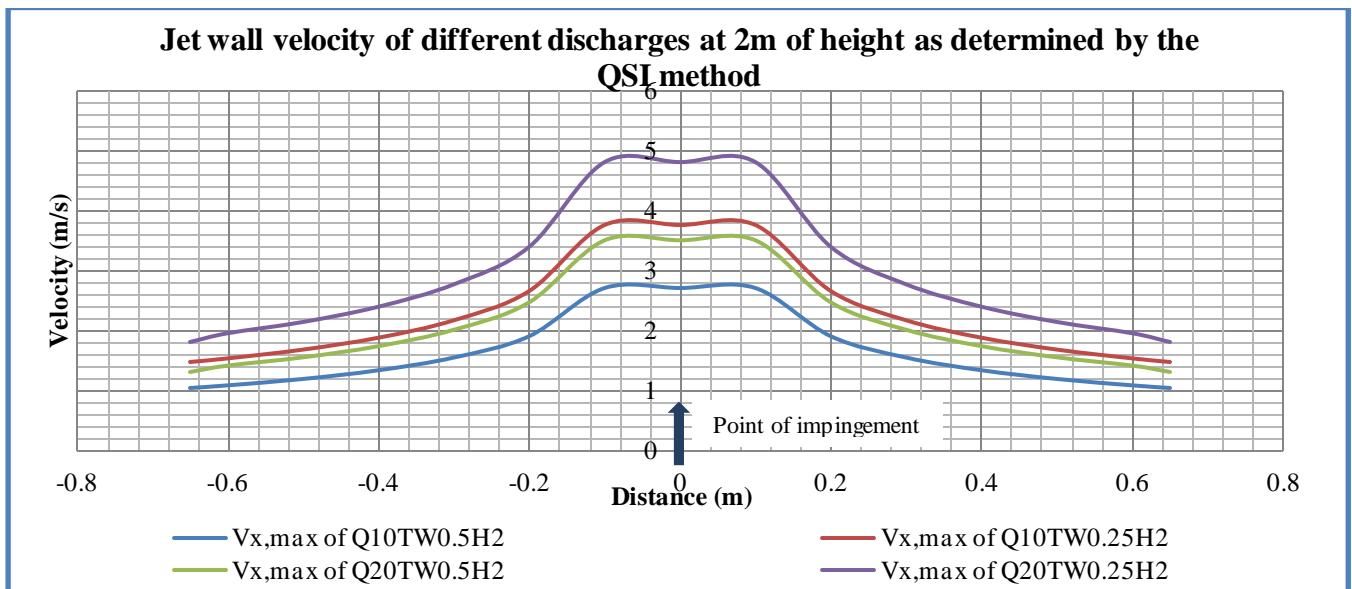


Figure 5-3. Wall jet velocity in the plunge pool for different tailwater depths for a 2 m drop height

Figure 5-4 shows the flow velocity decay (Eq.61) that takes place in the plunge pool. The flow velocity was computed from the centreline where the jets impinge with the tailwater level. It can be seen that the velocity decreases in the **Y**-direction with an increase in distance vertically.

The quasi-steady lift force F_{QSL} for different configurations of block protrusions were calculated depending on the velocity developed along wall jet. The surface pressure coefficient C_{surf} , joint pressure C_{joint} and net uplift pressure coefficient C_{uplift} were assumed to be -0.010, 0.145 and 0.155 respectively as it was mentioned in literature review (Figure 2-18). The calculated wall jet velocity and their quasi-steady lift force are summarised in Figure D 0-2 to Figure D 0-10. Refer to Appendix D for the calculated quasi-steady lift forces for all the tested scenarios.

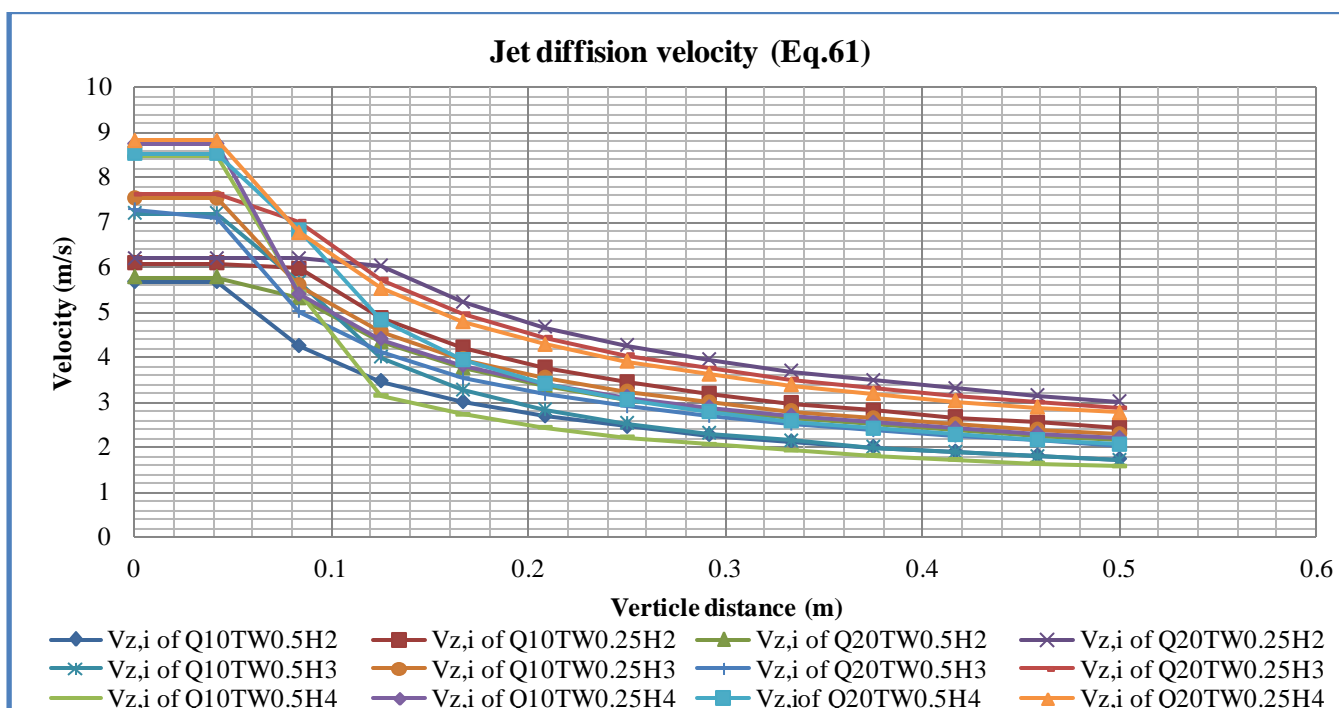


Figure 5-4. Calculated velocity decline along plunge pool centreline (y-direction)

Furthermore, it was observed as shown in Figure 5-5, that as the velocity increases, the quasi-steady forces (FQSI) also increase. It means that as the flow goes further away from the jet centreline (impingement zone); the wall jet velocity decreases which decreases the net uplift forces (assumed by calibration that uplift coefficient remains constant).

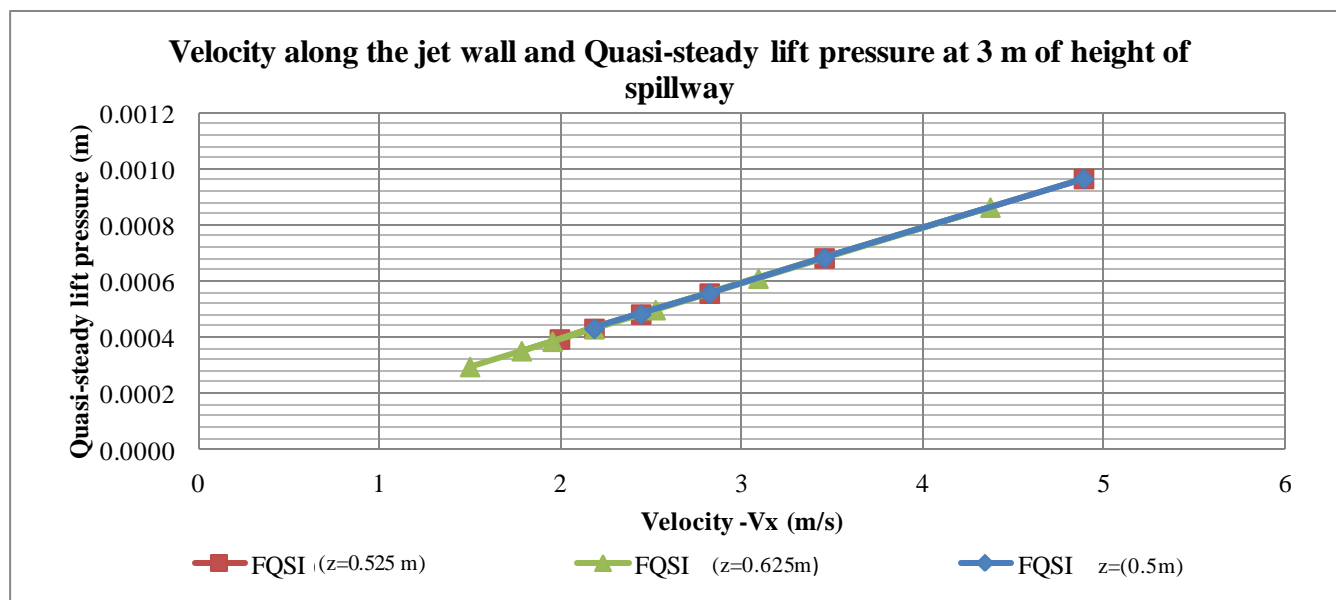


Figure 5-5. Velocity along jet wall against quasi-steady lift pressure at 3 m of height of spillway and 10 l/s for different scouring depths' z (including tailwater depth)

5.2.3.4. Results of Quasi steady scour shape against laboratory test

The quasi-steady pressure is a function of the wall jet velocity and the uplift coefficient based on the bedrock geometry in the wall jet region. The scour hole observed during the laboratory tests were compared to the scour hole determined by means of the QSI method. The computed longitudinal (as discussed in Section 2.4.3.3) scour hole cross-sections are shown in

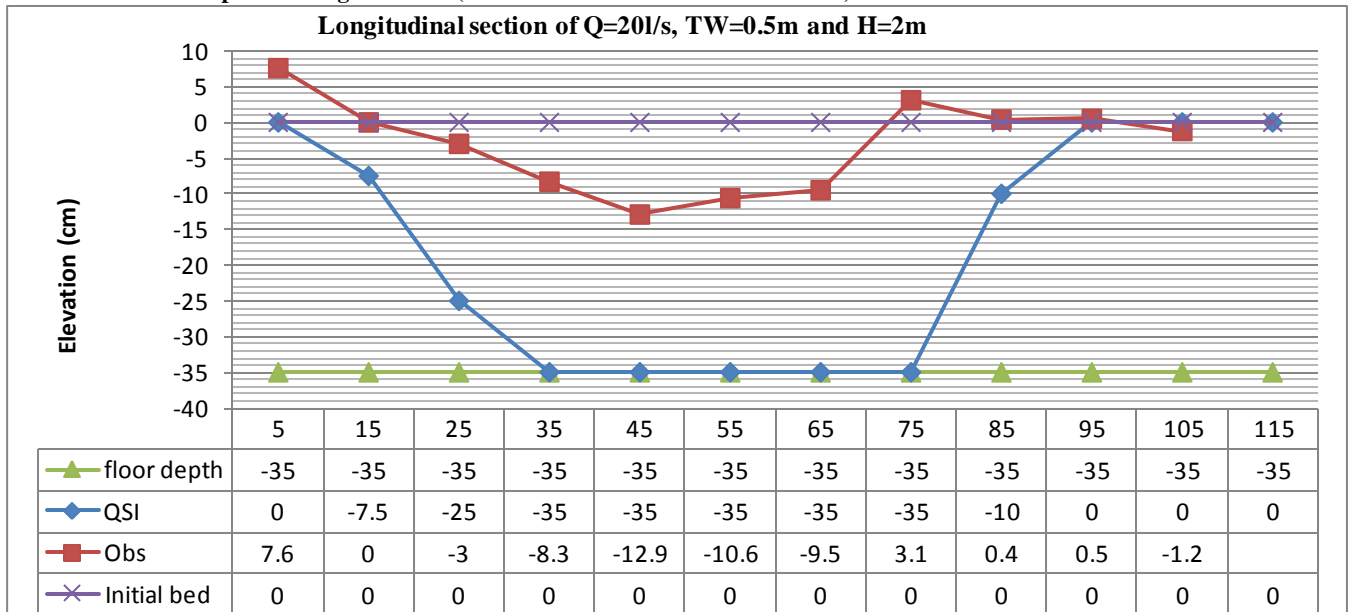


Figure 5-6 for the 20 l/s, 0.25 m tailwater depth at 2 m drop height scenario, and Figure 5-7 longitudinal scour hole cross-sections for the 10 l/s, 0.25 m tailwater depth at 4 m drop height scenario. The other scenarios are presented in Figure D 0-1 to Figure D 0-10 Appendix D. The QSI method estimates the shape of the scour hole and not just the depth. The computations of scour are performed along a vertical 2D-plane and distinct computational grid (APPENDIX D: WORK SHEET AND GRAPHS OF QSI METHOD).

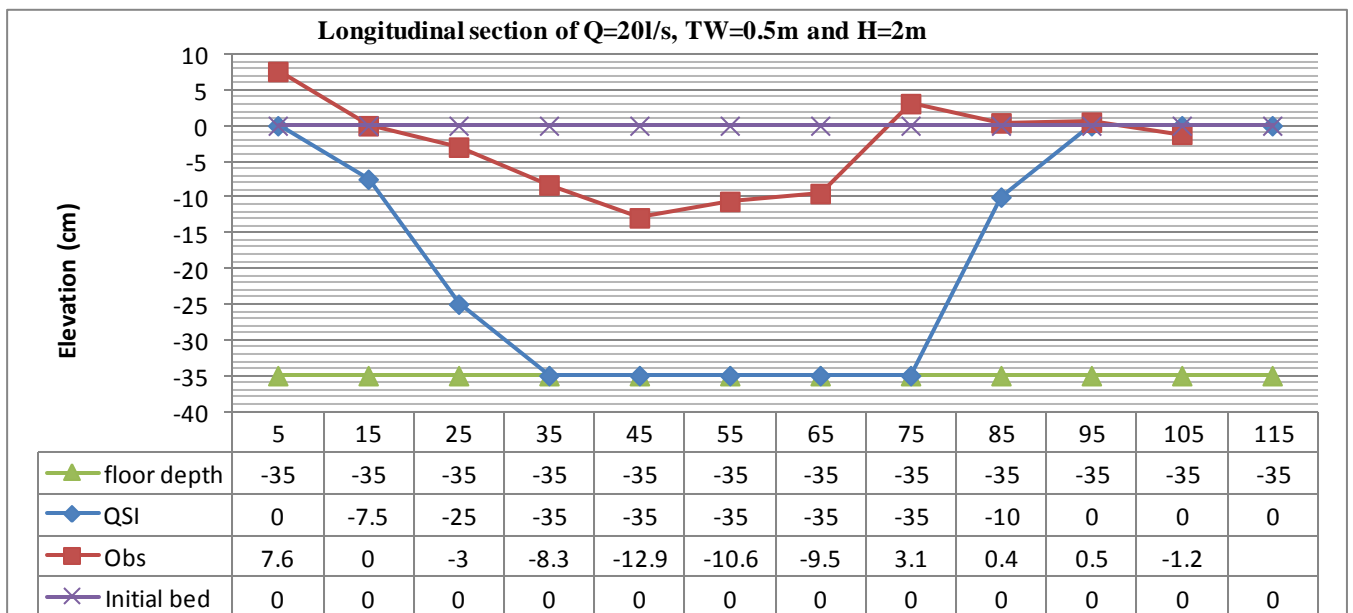


Figure 5-6. Longitudinal section for Q=20l/s, H=2m and TW=0.25m at the maximum point of observed scour profile compare to the QSI scour hole

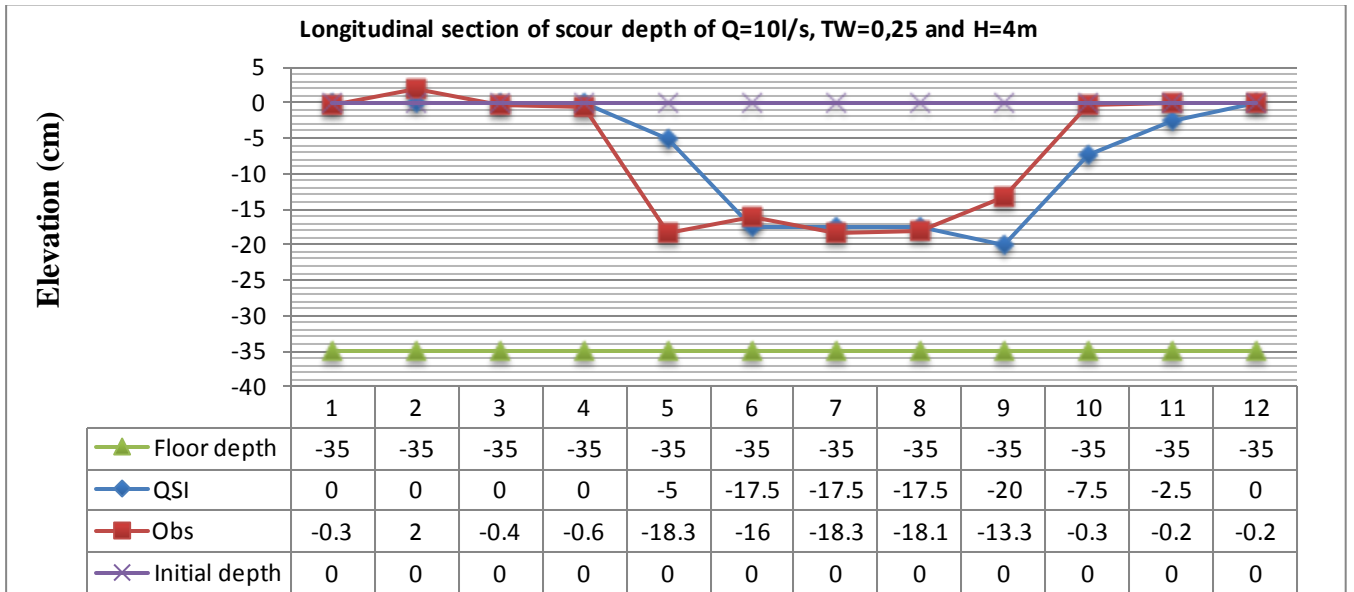


Figure 5-7. Longitudinal section for $Q=10\text{l/s}$, $H=4\text{m}$ and $TW=0.25\text{m}$ at the maximum point of observed scour profile compare to the QSI scour hole

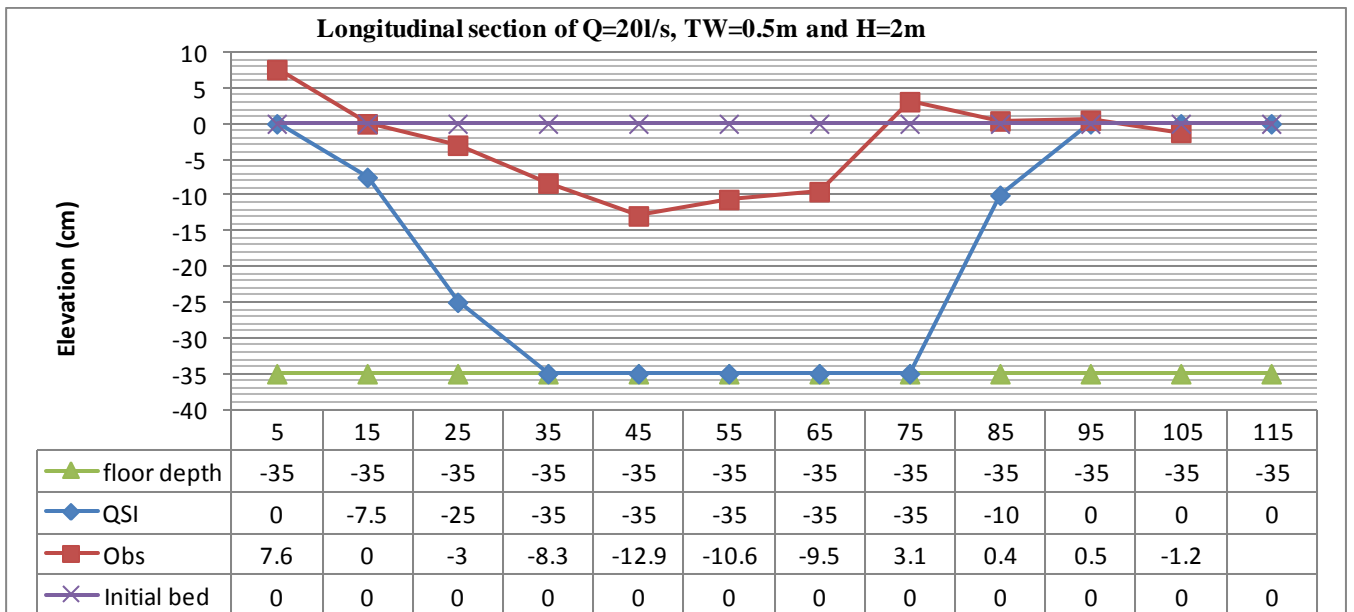


Figure 5-6 and Figure 5-7 indicated that the extent of the scour is collectively influenced by the deflection of the jet and thus the deflected velocity. It was found that there is a difference between the observed scour hole and the computed scour hole (Figure D 0-6 or Figure D 0-7), namely that the maximum scour depth for a 20 l/s discharge was much greater. The scour hole geometry calculated from the QSI method corresponded well with the measured results for only 10 l/s.

The QSI method consider the net uplift pressure and quasi-steady forces, block stability, dynamic impulsion and the discontinuity orientation of blocks. In this study, the application of QSI method presented here that the block removal depends on the deflection velocity differ varies between 6.135 m/s to 1.615 m/s for scenario of $Q=20\text{ l/s}$, $H=2\text{ m}$ and $TW=0.5\text{ m}$. This highlights that the orientation and joint of block have influence to determine the geometry of rock mass in computation of scour potential.

5.3. Summary

In this chapter, the rock scour in a plunge pool was investigated. The dynamic pressure and root mean square coefficients were introduced to estimate pressure forces generated in a plunge pool because of high-velocity jet impacts. The Erodibility Index method (EIM) and the Comprehensive Scour method (CSM) were used to determine the stability of the rock and its displacement and compared to the observed scouring.

The erodibility index (K) represents the erosive resistance of the rock material, and the stream power of the jet represents the erosive power of the overtopping water. It was indicated that the applied stream power exceeds the threshold stream power, which means that scour is deemed to occur.

The ultimate scour depth was determined by using the Dynamic Impulsion and Quasi-Steady Impulsion methods developed by Bollaert (2002). Based on the results of the DI model, Table 5.8 shows that there was a difference when comparing the results between the maximum scour depths computed by DI method against the maximum scour depth measured in laboratory. This DI model is powerful because it takes jet air entrainment in account combined with pressure coefficients, jet energy dissipation along the pool depth and the maximum impulsion coefficient on the block. However, the theoretical results had a poor correlation with the observed results.

The QSI method is a function of the wall jet velocity and the uplift coefficient based on the bedrock geometry in the wall jet region. The theoretical scour depths for a 10 l/s discharge reasonably correlated with the observed scour depths in the physical model. The great difference between the scour depth results for the 20 l/s discharge could be attributed to limitation of the laboratory, in particular the scale of the physical model, which was too small.

Chapter 6. Conclusion and Recommendation

6.1. Conclusion

The rock scour that occurs downstream of a spillway with regard to a high velocity impinging jet is a three-dimensional process consisting of “air-water-rock” phases. Underestimating the scour process may compromise the stability of hydraulic structures. Bollaert (2002; 2010; 2004) and Duarte (2014) have used physical hydraulic laboratory models to investigate rock scour. These studies have produced quantitative methods that could be used to determine the scour hole dimensions (depth and extent).

The main objective of this study was to determine the equilibrium scour hole geometry by means of constructing a physical model in the Stellenbosch University Hydraulics laboratory. The physical model investigated the hydraulic model parameters involved in the interaction between free falling jets, plunge pool aeration and turbulence, and fractured solid mass and analysis of the pressure distribution inside the rock. To assess the rock scour formation downstream, PVC blocks were used to represent a completely broken up joint system.

The scour hole geometry was affected by different parameters such as: the characteristics of the rock mass (e.g. density, shape), the plunge pool (tailwater) depth, drop height and discharge. These aforementioned parameters also influence the plunge pool bottom pressures and jet air concentration, that in turn influence the scour hole geometry. The scour hole depth decreased with an increase in drop height, decrease in discharge and increase in tailwater depth, due to the jet becoming developed, which decreases its scour potential.

The pressures in the plunge pool were measured. It was noted that the size of the pressure sensors had an effect on the rock scour profile. For this reason, the results obtained from the pressure sensors were therefore inconclusive and it was decided not to use these results.

The results related to the jet air entrainment indicated that an increase in air concentration decreased the scour depth, due to the jet core being broken up decreasing the scour potential of the jet.

The Erodibility Index method showed that the stream power of the impinging jet was greater than the erosive resistance of the rock (scour would occur) which corresponded to the model results.

The Dynamic Impulsion (DI) and Quasi-Steady Impulsion (QSI) methods were used to predict the ultimate scour depth and compared to the measured scour depths. For DI methods the ultimate scour depth is reached when $h_{up}/z < 1$. The DI model calculated that the ultimate scour depth would be deeper than obtained in the physical model.

The QSI method is a function of the wall jet velocity and the uplift coefficient based on the bedrock geometry in the wall jet region. Based on the comparison between computations and laboratory model results, the results of QSI method calculated a larger scour hole. The QSI method also calculated deeper ultimate scour holes than the DI method.

Possible reasons for the difference in calculated scour hole dimensions by the DI and QSI method and that obtained from the physical model are:

- Scale of model: The 1:40 scaled physical model was used where Bollaert (2002) recommends to use the scale of 1:20 to limit scale effects.

- Type of jet: the physical model jet was developed (it was fully aerated and no core was visible at impact with the tailwater level). The CSM was developed (Bollaert, 2004; Bollaert & Schleiss, 2005; Bollaert & Schleiss, 2003) by using undeveloped jets, which have greater scour potential.

6.2. Recommendation for the further research

Based on the results of this study, it is concluded that further investigations are desirable to improve the accuracy of predicting rock scour hole geometry. The following are recommended for further research:

- The physical model scale must be less than 1:20, as recommended by Bollaert (2002).
- The pressure sensors should be included in the model in such a way that they do not affect the scouring process.
- The influence of the turbulence intensity of the issuing jet should be quantified as proposed by Duarte (2014).

References

- Akhmedov, T. K., 1988. *Calculation of the depth of scour in rock downstream of a spillway*. pp. 25-27.
- Annandale, G. W., 1994. *Taking the scour out of water Power.*, pp. 46-49.
- Annandale, G. W., 1995. Erodibility. *Hydraulic Research*, pp. 471-494.
- Annandale, G. W., 2006. *Kalibu Dam Plunge Pool Scour*. Amsterdam, Proceedings Third international conference on scour and erosion.
- Annandale, G. W., 2006. *Scour Technology*. Denver, Colorado: McGraw-Hill Companies, Inc.
- Annandale, G. W., Wittler, R. J., Ruff, J. F. & Lewis, T. M., 1998. *Prototype Validation of erodibility Index for Scour in Fractured Rock Media*. Memphis, ASCE.
- Annandale, W. G., 1999. *Wall Jet Scour in Rock*. pp. 715-723.
- Armitage, N. P., 2002. *A unit stream power model for the prediction of local scour*, Stellenbosch.
- Attari, J., Arefi, F. & Golzari, F., 2002. *A review on physical models of scour holes below large dams in Iran*. Lausanne, pp. 73-80.
- Beltaos, S. & Rajaratnam, N., 1977. Impingement of Axisymmetric Developing Jets. *Journal of Hydraulic Research* 15, pp. 311-326.
- Bollaert, E., 2002. *Transient Water Pressures in joint and Formations of rocks scour due to high-velocity jet impact*, Lausanne: Laboratoire de constructions hydrauliques Ecole Polytechniques Federale de Lausanne.
- Bollaert, E., 2004. A comprehensive model to evaluate scour formation in plunge pools. *AquaVision Engineering Ltd*, pp. 1-9.
- Bollaert, E. F., 2010. *A Prototype-Scaled Rock Scour Prediction Model*. Sacramento. 1269-1283.
- Bollaert, E. & Mason, J. P., 2006. A physically based Model for scour prediction at Srisailem Dam. *Hydropower and Dams*, pp. 96-103.
- Bollaert, E. R., 2012. Wall jet rock scour in plunge pools: a quasi-3D prediction model. *AquaVision Engineering*, pp. 1-9.
- Bollaert, E. R., Stratford, C. S. & Lesleighter, E. J., 2015. Numerical modelling of rock scour: Case study of Wivenhoe Dam. *Taylor & Francis Group*, pp. 397-404.
- Bollaert, E. & Schleiss, A., 2001. A new approach for better assessment of rock due to high velocity jets at dam spillways. *ICOLD European Symposium*, pp. 1-11.
- Bollaert, E. & Schleiss, A., 2003. Scour of rock due to the impact of plunging high velocity jets part I. *Hydraulic Research*, pp. 1-14.
- Bollaert, E. & Schleiss, A. J., 2005. Physically based model for evaluation of rock scour due to high-velocity jet impact. *Hydraulic Engineering*, March, pp. 153-165.

- Castillo, G. L., 2003. Contribution to discussion of Bollaert and Schleiss paper " Scour of rock due to the impact of plunging jet Part 1: A state-of-art review. *Journal of Hydraulic Research*, pp. 451-464.
- Castillo, L. G., 2004. *Personal Communication*.
- Castillo, L. G. & Carrillo, J. M., 2014. *Scour Analysis downstream of Paute-Cardenillo Dam*. Porto-Portugal, 3rd IAHR Europe Congress.
- Damle, P. M., Venkatraman, C. P. & Desai, S. C., 1966. Evaluation of Scour below Ski-jump buckets of Spillways. *Proc. CWPRS Golden Jubilee Symp*, pp. 154-163.
- Dargahi, B., 2003. Scour development downstream of a spillway. *Journal of hydraulic Research Vol 41*, pp. 417-426.
- Duarte, R., 2014. *Influence of air entrainment on rock scour development and block stability in plunge pools*. Ecole Polytechnique Federale de Lausanne ed. Lausanne: Communications du Laboratoire de Constructions Hydrauliques.
- Elvine, D. A., Falvey, H. T. & Withers, W., 1997. Pressure fluctuations on plunge pool floors. *Journal of Hydraulic research*, pp. 257-279.
- Ervine, D. A., 1998. *Air Entrainment in Hydraulic structures*.
- Ervine, D. A. & Elsayy, E. M., 1975. *Effect of a falling Nappe on River Aeration*. Brazil, pp. 390-397.
- Ervine, D. A. & Falvey, H. T., 1987. Behavior of turbulent jets in the atmosphere and in plunge pools. *Proceedings of the institution of civil engineers, Part 2*, pp. 295-314.
- Fedzespiel, M., Bollaert, E. & Schleiss, A., 2011. *Dynamic response of a rock block in plunge pool due to asymmetrical impact of a high-velocity jet*. Brisbane.
- George, M. F. & Annandale, W. G., 2006. *Kariba Dam Plunge Pool Scour*. Amsterdam, The Netherlands, pp. 250-254.
- Harting, F. & Hausler, E., 1973. *Scour, Stilling basins and downstream protection Under Free Overfall Jets at Dam..* Madrid, pp. 39-56.
- Jeffrey, G. W. & Anton, S., 1984. *Scour Related to Energy Dissipators For High Head Structures*. Zurich.
- Johnson, P. L., 1974. Hydraulic Model Studies of Plunge pool Basins for Jet flow. *Engineering and Research Center*.
- Kirsten, H., 1982. Classification system for excavation in natural materials. *The civil Engineer in South Africa*, pp. 292-308.
- Kirsten, H. A., Darrel, M. T., John S, M. & Kirsten, L. H., 2000. Erodibility Criterion for Auxiliary Spillways of Dams. *International Journal of Sediment Research*, pp. 93-107.
- Lewis, M. T., Steven, R. A., Wittler, J. F. R. & Annandale, W. G., 1999. Prediction Impact Velocities of Developed Jets. pp. 255-265.

- Liu, P., 2005. A new method for calculating depth of scour pit caused by overflow of water jet. *Hydraulic Research*, pp. 693-701.
- Luis, G. C. & Jose, M. C., 2013. *Analysis of Scale ration in nappe flow case by means of CFD numerical simulation*. Beijing, pp. 1-10.
- Manso, D. A. P. F., 2006. *The influence of pool geometry and induced flow patterns on rock scour by high-velocity plunging jets*, Lausanne: Ecole polytechnique Federale de Lausanne.
- Manso, P., Fiorotto, V., Bollaert, E. & Scleiss, A., 2004. Discussion of "Effect of jet air content on plunge pool scour" by Stefano Canepa and Willi H; Hager. *Journal of Hydraulic Engineering* 130, pp. 1128-1130.
- Martins, R., 1973. *Contribution to the knowledge on the scour action of free jets on rocky river beds*. Madrid, pp. 799-814.
- Martins, R., 1975. Scouring of Rocky River Beds by Free Jet Spillways. *Water Power and Dam Construction* 27 (April): 152-153
- Mason, 1989. Effect of air entrainment on plunge pool scour. *Hydraulic engineering*, pp. 385-399.
- Mason, P., 1984. *Erosion of plunge pool downstream od Dam due to the action of free-trajectory jets*. pp. 523-537.
- Mason, P.J. 1985. Discussion on "Erosion of Plunge Pools Downstream of Dams Die to the Action of Free-Trajectory Jets" by P. J. Mason, 1984. *Proceedings of the Institution of Civil Engineers*, Part I, 78 (August):991-999.
- Mason, P. J. & Arumugan, K., 1985. Free Jets Scour below Dams and Flip Buckets. *Hydraulic Engineering*, pp. 220-235.
- McNown, J. S., 1951. *Particles in slow motion*.
- Monfette, M., 2004. Comprehensive review of plunge pool performance at four of BC hydro Dam sites and assessment of scour extent. In: *Die kolkbildung hinter uberstromten wehren im hinblick auf eine bewegliche sturzbettgestaltung*.
- Palermo, s. P. & M., 2008. plane plunge pool scour with protection srtuctures. *Hydro-environment research*, pp. 182-191.
- Rajaratnam, N. & Mazurek, K. A., 2003. Erosion of Sand by circular impinging water jets with small tailwater. *Journal of Hydraulic Engineering*, pp. 225-229.
- Sawadogo, O., 2010. *Scour of Unlined Dam Spillways*, Stellenbosch.
- Schleiss, 2002. *Scour evaluation in space and time- the challenge of dam designers*. EPFL, Lausanne, pp. 3-22.
- Schleiss, A. & Whittaker, J. G., 1984. *Scour relatad to Energy dissipators for high Head structures (Mitteilungen der Versuchsanstalt fur Wasserbau,Hydrologie und Glaziologie)*. ETH Zurich, Switzerland: s.n.

- Schleiss, B. &, 2011. *Journal of Hydraulic Research*. *Closure problem to jet scour*, pp. 276-282.
- Simons, B. D. & Senturk, F., 1992. *Sediment Transport Technology "Water and Sediment Dynamics"*. Colorado, USA: Water Resources Publications.
- Sokchay, H., Tawatchai, T. & Tadashi, S., 2009. Analysis of Plunge Pool Scour Hole formation Below a Chute Spillway with Flip Bucket using a Physical model. pp. 89-101.
- Spurr, K. J. W., 1985. *Energy approach to estimating scour downstream of a large Dam*. pp. 81-89.
- Tanchev, L., 2013. *Dams and Appurtenant hydraulic Structures*. Second edition ed. Skopje: Taylor & Francis Group.
- Tonon, F., 2006. *A Probabilistic Evaluation of Scour Threshold and Extent in Fractured Rock Plunge Pools, in Unsolicited proposal to the Bureau of Reclamation*: Department of the Interior.
- Turton, R. & Levenspiel, O., 1986. A short note on the drag correlation for sphere. In: *Powder Technology vol.47*. pp. 83-85.
- Veronese, A., 1937. *Erosioni di fondo a valle di un scarico* (Bottom Erosions Downstream of a Dam) *Annali dei Lavori Pubblici* 75(9): 717-726. In Italian.
- Whittaker, G. J. & Schleiss, A., 1984. *Scour Related to Energy Dissipators For High Head Structures*. Zurich.
- Wu, W. & Wang, S. S., 2006. Formulas for Sediment Porosity and Settling velocity. *Journal of Hydraulic Engineering*, pp. 858-862.
- Yogendra, P. & Gopalakrishnan, E., 2000. *Dams and Development*, London: World Commission on Dams.
- Yuditskii, G. A., 1963. *Action of falling jet on joint blocks of a rock and conditions of its erosion*.
- Zhao-Yin, W., Joseph, L. H. & Charles, M. S., 2015. *River Dynamics and Integrated River Management*. Beijing.

APPENDIX A GEOLOGICAL PARAMETERS**Table A 0.1. Mass strength number for rock (Annandale, 2006).**

Consistency	Uniaxial strength	Mass Strength Factor M_s
Very soft cohesive soil	0-80 kPa	0.02
Soft cohesive soil	80-140 kPa	0.04
Firm cohesive soil	140-210 kPa	0.09
Stiff cohesive soil	210-350 kPa	0.19
Very stiff cohesive rock	350-750 kPa	0.41
Very soft rock	1-3 Mpa	1-2
Soft rock	3-13 Mpa	2-8
Hard rock	13-26 Mpa	8-35
Very hard rock	26-106 Mpa	35-70
Extremely hard rock	106-212 Mpa	70-280

Table A 0.2. Joint set number (Annandale, 1995)

Number of Joint sets	J_n
Intact, no or few joints	1.00
One joint set	1.22
One joint set plus random	1.50
Two joint sets	1.83
Two joint sets plus random	2.24
Three joint sets	2.73
Three joint sets plus random	3.34
Four joint sets	4.09
Multiple joint sets	5.00

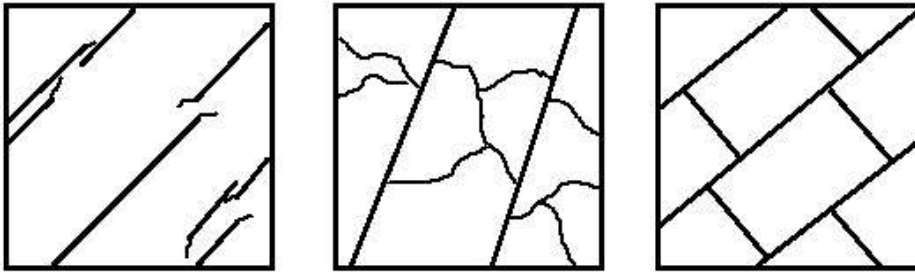


Figure A 0-1. The presentation of rock joint set (left to right: One joint set, one joint set with random joints, two joint sets)

Table A 0.3. Joint roughness number J_r (Ammandale, 2006)

Joint separation	Condition of joint	Joint roughness number
Joint tight or closing during excavation	Stepped joint	4
	Rough or irregular, undulating	3
	Smooth undulating	2
	Slickensided undulating	1.5
	Rough or irregular, planar	1.5
	Smooth planar	1
	Slickensided planer	0.5
Joint open and remain open during excavation	Joint either open or containing relatively soft gauge of sufficient thickness to prevent joint wall contact upon excavation.	1
	Shattered or micro-shattered clay	1

Table A 0.4. Joint alteration number (Annandale, 2006)

Description of gauge	Joint Alteration number for joint separation(mm)		
	1.0*	1.0-5.0 [†]	5.0 [‡]
Tightly healed, hard, non-softening impermeable filling	0.75		
Unaltered joint walls, surface staining only	1		
Slightly altered, non-softening, non-cohesive rock mineral or crushed rock filling	2	2	4
Non-softening, slightly clayey non-cohesive filling	3	6	10
Non-softening, strongly over-consolidated clay mineral filling, with or without crushed rock	3	6.0 [§]	10
Softening or low friction clay mineral coatings and small quantities of swelling clays	4	8	13
Softening moderately over-consolidated clay mineral filling, with or without crushed rock	4	8.00 [§]	13
Shattered or micro-shattered (swelling) clay gouge, with or without crushed rock	5	10.0 [§]	18

Note:

* Joint walls effectively in contact

† Joint walls come into contact after approximately 100-mm shear

‡ Joint walls do not come into contact at all upon shear

§ Also applies when crushed rock occurs in clay gouge without rock wall contact

For intact material take (**Js**) equals 1.0 and for the value of **r** greater than 8 take Js as for **r** equals to 8.

Table A 0.5. Relative ground structure number Js (Annandale, 2006).

Dip direction of closer spaced joint set (Degrees)	Dip angle of closer spaced joint set (Degrees)	Ratio of joint spacing, r			
		01:01	01:02	01:04	01:08
180/0	Vertical 90	1.14	1.2	1.24	1.26
In direction of stream flow	89	0.78	0.71	0.65	0.61
	85	0.73	0.66	0.61	0.57
	80	0.67	0.6	0.55	0.52
	70	0.56	0.5	0.46	0.43
	60	0.5	0.46	0.42	0.4
	50	0.49	0.46	0.43	0.41
	40	0.53	0.49	0.46	0.45
	30	0.63	0.59	0.55	0.53
	20	0.84	0.77	0.71	0.67
	10	1.25	1.1	0.98	0.9
	5	1.39	1.23	1.09	1.01
1	1.5	1.33	1.19	1.1	
0/180	Horizontal 0	1.14	1.09	1.05	1.02
Against direction of stream flow	-1	0.78	0.85	0.9	0.9
	-5	0.73	0.79	0.84	0.88
	-10	0.67	0.72	0.78	0.81
	-20	0.56	0.62	0.66	0.69
	-30	0.5	0.55	0.58	0.6
	-40	0.49	0.52	0.55	0.57
	-50	0.53	0.56	0.59	0.61
	-60	0.63	0.68	0.71	0.73
	-70	0.84	0.91	0.97	1.01
	-80	1.26	1.41	1.53	1.61
	-85	1.39	1.55	1.69	1.77
-89	1.5	1.68	1.82	1.91	
180/0	Vertical -90	1.14	1.2	1.24	1.26

Table A 0.6. Value of C and m various Rock Types (Annandale, 2006).

Type of rock	Fatigue exponent m	Coefficient C
Arkansas novaculite	8.5	1.00E-08
Mojave quartzite	10.2 to 12.9	3.00E-10
Ruhr sandstone	2.7 to 3.7	2.0E-6 to 1.0E-6
Tennessee sandstone	4.8	4.00E-07
Solenhofen limestone	8.8 to 9.5	1.10E-08
Carrara marble	5.1	2.50E-07
Falerans micrite	8.8	1.10E-08
St Pons marble	8.8 to 9.9	1.1E-8 to 4.0E-9
Tennessee marble	3.1	2.00E-06
Merrivale granite	13.6 to 23.1	1.5E-10 to 4.0E-14
Westerley granite	11.8 to 11.9	8.00E-10
Yugawara andesite	8.8	1.10E-08
Black gabbro	9.9 to 12.2	4.0E-9 to 5.0E-10
Kinosaki basalt	11.2	1.20E-09
Ralston basalt	8.2	1.80E-08
Whin Sill dolerite	9.9	4.00E-09

APPENDIX B SEDIMENT CHARACTERISTICS CALCULATION**Table B 0.1. Specific gravity calculation of PVC blocks**

Cube N°	Mass g	Dimensions mm			Volume mm ³	Volume m ³	PVC block Density Kg/m ³	Specific gravity -
		1	2	3				
1	0.018	25	25	25	15625	0.00001563	1152	1.152
2	0.018	25	25	25	15625	0.00001563	1152	1.152
3	0.018	25	25	25	15625	0.00001563	1152	1.152
4	0.018	25	25	25	15625	0.00001563	1152	1.152
5	0.018	25	25	25	15625	0.00001563	1152	1.152
6	0.018	25	25	25	15625	0.00001563	1152	1.152
7	0.018	25	25	25	15625	0.00001563	1152	1.152
8	0.018	25	25	25	15625	0.00001563	1152	1.152
9	0.018	25	25	25	15625	0.00001563	1152	1.152
10	0.018	25	25	25	15625	0.00001563	1152	1.152

Table B. 0.2. The Settling velocity and effective diameter of PVC blocks

Cube N°	Mass g	Distance fallen m	Time taken to fall sec	Settling velocity m/s	drag coefficient	effective diameter mm
2	0.018	0.7	2.68	0.261	1.05	36.03
3	0.018	0.7	2.75	0.254	1.05	34.22
4	0.018	0.7	2.63	0.266	1.05	37.41
5	0.018	0.7	2.43	0.288	1.05	43.82
6	0.018	0.7	2.53	0.276	1.05	40.43
7	0.018	0.7	2.72	0.257	1.05	34.98
8	0.018	0.7	2.53	0.276	1.05	40.43
9	0.018	0.7	2.72	0.257	1.05	34.98
10	0.018	0.7	2.68	0.261	1.05	36.03

APPENDIX C DYNAMIC IMPULSION COMPUTATION**Table C 0.1. The ultimate scour depth for Q=10 l/s, H=2m, TW=0.5m computed by DI**

Q = 10 l/s, H = 2m, TW = 0.5m												
Y(m)	Bottom (m)	Y/Bj	ψ	C_p	C_p^a	$C_I (-)$	$I_{max}(Ns)$	G_b (Kg/m ²)	$I_{net} (Ns)$	$V_{up} (m/s)$	$h_{up} (m)$	h_{up}/z
Measured	Measured		Eq.31	Eq. 30	Eq. 42	Eq. 57	Eq. 56	Eq. 59	Eq. 55		Eq. 58	
0.500	0.000	4.613	0.433	0.33	0.514	0.746	0.0015	0.0024	0.0015	0.6404	0.0209	0.8362
0.525	0.025	4.843	0.433	0.32	0.493	0.726	0.0014	0.0024	0.0014	0.5976	0.0182	0.7280
0.550	0.050	5.074	0.433	0.31	0.472	0.706	0.0013	0.0024	0.0013	0.5569	0.0158	0.6323
0.575	0.075	5.305	0.433	0.29	0.453	0.687	0.0013	0.0024	0.0012	0.5184	0.0137	0.5478
0.600	0.100	5.535	0.433	0.28	0.433	0.669	0.0012	0.0024	0.0011	0.4819	0.0118	0.4735
0.625	0.125	5.766	0.433	0.27	0.414	0.650	0.0011	0.0024	0.0011	0.4474	0.0102	0.4081
0.650	0.150	5.997	0.433	0.26	0.395	0.632	0.0010	0.0024	0.0010	0.4148	0.0088	0.3508
0.675	0.175	6.227	0.433	0.25	0.377	0.615	0.0009	0.0024	0.0009	0.3840	0.0075	0.3006
0.700	0.200	6.458	0.433	0.23	0.359	0.597	0.0009	0.0024	0.0008	0.3550	0.0064	0.2569
0.725	0.225	6.688	0.433	0.22	0.342	0.581	0.0008	0.0024	0.0008	0.3276	0.0055	0.2188
0.750	0.250	6.919	0.433	0.21	0.325	0.564	0.0007	0.0024	0.0007	0.3018	0.0046	0.1858
0.775	0.275	7.150	0.433	0.20	0.308	0.548	0.0007	0.0024	0.0007	0.2776	0.0039	0.1571
0.800	0.300	7.380	0.433	0.19	0.292	0.532	0.0006	0.0024	0.0006	0.2549	0.0033	0.1325

Legend: ψ : Energy Loss C_p^a : Time-average pressure coefficient C_I : Maximum dynamic impulsion coefficient

I_{max} : Maximum impulse force

G_b : Immersed weight

I_{net} : The net forces

V_{up} : Velocity of block

h_{up} : Height of the block displacement

C_p : Time-averaged coefficient

Table C 0.2. The ultimate scour depth for $Q=10$ l/s, $H=2$ m, $TW=0.25$ m computed by DI

Q = 10l/s, H = 2m, TW = 0.25m												
Y(m)	Bottom (m)	Y/Bj	ψ	C_p	C_p^a	$C_I (-)$	$I_{max}(Ns)$	$G_b (Kg/m^2)$	$I_{net} (Ns)$	$V_{up} (m/s)$	$h_{up} (m)$	h_{up}/z
Measured	Measured		Eq.31	Eq. 30	Eq. 42	Eq. 57	Eq. 56	Eq. 59	Eq. 55		Eq. 58	
0.250	0.000	2.390	0.462	0.86	1.396	0.956	0.0057	0.0024	0.0057	2.3822	0.2892	11.570
0.275	0.025	2.629	0.462	0.86	1.396	0.931	0.0055	0.0024	0.0055	2.3216	0.2747	10.988
0.300	0.050	2.867	0.462	0.86	1.396	0.908	0.0054	0.0024	0.0054	2.2619	0.2608	10.431
0.325	0.075	3.106	0.462	0.86	1.396	0.884	0.0053	0.0024	0.0052	2.2033	0.2474	9.897
0.350	0.100	3.345	0.462	0.86	1.396	0.861	0.0051	0.0024	0.0051	2.1456	0.2346	9.385
0.375	0.125	3.584	0.462	0.86	1.396	0.838	0.0050	0.0024	0.0050	2.0889	0.2224	8.896
0.400	0.150	3.823	0.462	0.86	1.396	0.816	0.0049	0.0024	0.0048	2.0333	0.2107	8.429
0.425	0.175	4.062	0.462	0.39	0.637	0.794	0.0022	0.0024	0.0021	0.8974	0.0410	1.642
0.450	0.200	4.301	0.462	0.38	0.611	0.773	0.0020	0.0024	0.0020	0.8376	0.0358	1.430
0.475	0.225	4.540	0.462	0.36	0.586	0.752	0.0019	0.0024	0.0019	0.7809	0.0311	1.243
0.500	0.250	4.779	0.462	0.35	0.562	0.731	0.0017	0.0024	0.0017	0.7272	0.0270	1.078
0.525	0.275	5.018	0.462	0.33	0.538	0.711	0.0016	0.0024	0.0016	0.6763	0.0233	0.933
0.550	0.300	5.257	0.462	0.32	0.515	0.691	0.0015	0.0024	0.0015	0.6282	0.0201	0.805

Table C 0.3. The ultimate scour depth for Q=20 l/s, H=2m, TW=0.5m computed by DI

Q = 20l/s, H = 2m, TW = 0.5m												
Y(m)	Bottom (m)	Y/Bj	ψ	C_p	C_p^a	$C_I (-)$	$I_{max}(Ns)$	G_b (Kg/m ²)	$I_{net}(Ns)$	$V_{up}(m/s)$	$h_{up}(m)$	h_{up}/z
Measured	Measured		Eq.31	Eq. 30	Eq. 42	Eq. 57	Eq. 56	Eq. 59	Eq. 55		Eq. 58	
0.500	0.000	4.251	0.519	0.43	0.659	0.777	0.0021	0.0024	0.0021	0.8871	0.0401	1.6043
0.525	0.025	4.463	0.519	0.41	0.635	0.759	0.0020	0.0024	0.0020	0.8337	0.0354	1.4171
0.550	0.050	4.676	0.519	0.40	0.612	0.740	0.0019	0.0024	0.0019	0.7829	0.0312	1.2495
0.575	0.075	4.888	0.519	0.38	0.589	0.722	0.0018	0.0024	0.0017	0.7344	0.0275	1.0996
0.600	0.100	5.101	0.519	0.37	0.566	0.704	0.0017	0.0024	0.0016	0.6882	0.0241	0.9657
0.625	0.125	5.313	0.519	0.35	0.544	0.687	0.0016	0.0024	0.0015	0.6443	0.0212	0.8464
0.650	0.150	5.526	0.519	0.34	0.523	0.669	0.0015	0.0024	0.0014	0.6026	0.0185	0.7402
0.675	0.175	5.738	0.519	0.32	0.501	0.652	0.0014	0.0024	0.0013	0.5629	0.0161	0.6460
0.700	0.200	5.951	0.519	0.31	0.481	0.636	0.0013	0.0024	0.0012	0.5252	0.0141	0.5624
0.725	0.225	6.164	0.519	0.30	0.460	0.619	0.0012	0.0024	0.0012	0.4895	0.0122	0.4885
0.750	0.250	6.376	0.519	0.29	0.440	0.604	0.0011	0.0024	0.0011	0.4556	0.0106	0.4233
0.775	0.275	6.589	0.519	0.27	0.421	0.588	0.0010	0.0024	0.0010	0.4236	0.0091	0.3658
0.800	0.300	6.801	0.519	0.26	0.402	0.573	0.0010	0.0024	0.0009	0.3933	0.0079	0.3153

Table C 0.4. The ultimate scour depth for $Q=20$ l/s, $H=2$ m, $TW=0.25$ m computed by DI

Q = 20l/s, H = 2m, TW = 0.25m												
Y(m)	Bottom (m)	Y/Bj	ψ	Cp	C_p^a	Ci	Imax	Gb	Inet	V _{up}	h _{up}	h _{up} /z
Measured	Measured		Eq.31	Eq. 30	Eq. 42	Eq. 57	Eq. 56	Eq. 59	Eq. 55		Eq. 58	
0.250	0.000	2.199	0.551	0.86	1.332	0.975	0.0047	0.0024	0.0047	1.9886	0.2016	8.0626
0.275	0.025	2.419	0.551	0.86	1.332	0.953	0.0046	0.0024	0.0046	1.9424	0.1923	7.6917
0.300	0.050	2.639	0.551	0.86	1.332	0.930	0.0045	0.0024	0.0045	1.8968	0.1834	7.3348
0.325	0.075	2.859	0.551	0.86	1.332	0.908	0.0044	0.0024	0.0044	1.8519	0.1748	6.9917
0.350	0.100	3.079	0.551	0.86	1.332	0.887	0.0043	0.0024	0.0043	1.8077	0.1665	6.6619
0.375	0.125	3.299	0.551	0.86	1.332	0.865	0.0042	0.0024	0.0042	1.7641	0.1586	6.3450
0.400	0.150	3.519	0.551	0.86	1.332	0.845	0.0041	0.0024	0.0041	1.7213	0.1510	6.0407
0.425	0.175	3.739	0.551	0.86	1.332	0.824	0.0040	0.0024	0.0040	1.6792	0.1437	5.7486
0.450	0.200	3.959	0.551	0.86	1.332	0.804	0.0039	0.0024	0.0039	1.6378	0.1367	5.4684
0.475	0.225	4.179	0.551	0.86	1.332	0.784	0.0038	0.0024	0.0038	1.5970	0.1300	5.1997
0.500	0.250	4.399	0.551	0.86	1.332	0.764	0.0037	0.0024	0.0037	1.5570	0.1236	4.9422
0.525	0.275	4.619	0.551	0.86	1.332	0.745	0.0036	0.0024	0.0036	1.5176	0.1174	4.6955
0.550	0.300	4.839	0.551	0.86	1.332	0.726	0.0035	0.0024	0.0035	1.4789	0.1115	4.4593
0.575	0.325	5.059	0.551	0.86	1.332	0.708	0.0034	0.0024	0.0034	1.4410	0.1058	4.2333
0.600	0.350	5.279	0.551	0.86	1.332	0.689	0.0034	0.0024	0.0033	1.4037	0.1004	4.0171
0.625	0.375	5.499	0.551	0.86	1.332	0.671	0.0033	0.0024	0.0032	1.3671	0.0953	3.8104
0.650	0.400	5.719	0.551	0.86	1.332	0.654	0.0032	0.0024	0.0032	1.3312	0.0903	3.6130
0.675	0.425	5.938	0.551	0.86	1.332	0.637	0.0031	0.0024	0.0031	1.2960	0.0856	3.4244
0.700	0.450	6.158	0.551	0.46	0.712	0.620	0.0016	0.0024	0.0016	0.6712	0.0230	0.9186
0.725	0.475	6.378	0.551	0.44	0.686	0.603	0.0015	0.0024	0.0015	0.6286	0.0201	0.8057
0.750	0.500	6.598	0.551	0.43	0.660	0.587	0.0014	0.0024	0.0014	0.5882	0.0176	0.7053
0.775	0.525	6.818	0.551	0.41	0.634	0.571	0.0013	0.0024	0.0013	0.5497	0.0154	0.6162
0.800	0.550	7.038	0.551	0.39	0.609	0.556	0.0012	0.0024	0.0012	0.5133	0.0134	0.5372

Table C 0.5. The ultimate scour depth for Q=10 l/s, H=3m, TW=0.5m computed by DI

Q = 10l/s, H = 3m, TW= 0.5m												
Y(m)	Bottom (m)	Y/Bj	ψ	C_p	C_p^a	$C_I(-)$	$I_{max}(Ns)$	G_b (Kg/m ²)	$I_{net}(Ns)$	$V_{up}(m/s)$	$h_{up}(m)$	h_{up}/z
Measured	Measured		Eq.31	Eq. 30	Eq. 42	Eq. 57	Eq. 56	Eq. 59	Eq. 55		Eq. 58	
0.500	0.000	5.195	0.536	0.37	0.768	0.696	0.0018	0.0024	0.0018	0.7418	0.0280	1.1220
0.525	0.025	5.455	0.536	0.35	0.732	0.675	0.0016	0.0024	0.0016	0.6841	0.0239	0.9542
0.550	0.050	5.715	0.536	0.34	0.696	0.654	0.0015	0.0024	0.0015	0.6299	0.0202	0.8089
0.575	0.075	5.975	0.536	0.32	0.661	0.634	0.0014	0.0024	0.0014	0.5790	0.0171	0.6835
0.600	0.100	6.234	0.536	0.30	0.626	0.614	0.0013	0.0024	0.0013	0.5313	0.0144	0.5755
0.625	0.125	6.494	0.536	0.29	0.593	0.595	0.0012	0.0024	0.0012	0.4866	0.0121	0.4828
0.650	0.150	6.754	0.536	0.27	0.561	0.576	0.0011	0.0024	0.0011	0.4449	0.0101	0.4035
0.675	0.175	7.014	0.536	0.26	0.529	0.558	0.0010	0.0024	0.0010	0.4059	0.0084	0.3359
0.700	0.200	7.273	0.536	0.24	0.499	0.540	0.0009	0.0024	0.0009	0.3695	0.0070	0.2784
0.725	0.225	7.533	0.536	0.23	0.469	0.522	0.0008	0.0024	0.0008	0.3357	0.0057	0.2297
0.750	0.250	7.793	0.536	0.21	0.440	0.505	0.0007	0.0024	0.0007	0.3042	0.0047	0.1887
0.775	0.275	8.053	0.536	0.20	0.413	0.489	0.0007	0.0024	0.0007	0.2750	0.0039	0.1542
0.800	0.300	8.312	0.536	0.19	0.386	0.473	0.0006	0.0024	0.0006	0.2479	0.0031	0.1253

Table C 0.6. The ultimate scour depth for Q=10 l/s, H=3m, TW=0.25m computed by DI

Q = 10l/s, H = 3m, TW = 0.25m												
Y(m)	Bottom (m)	Y/Bj	ψ	C_p	C_p^a	$C_I (-)$	$I_{max}(Ns)$	G_b (Kg/m²)	$I_{net} (Ns)$	$V_{up} (m/s)$	$h_{up} (m)$	h_{up}/z
Measured	Measured		Eq.31	Eq. 30	Eq. 42	Eq. 57	Eq. 56	Eq. 59	Eq. 55		Eq. 58	
0.250	0.000	2.657	0.557	0.86	1.520	0.929	0.0032	0.0024	0.0032	1.3530	0.0933	3.732
0.275	0.025	2.923	0.557	0.86	1.520	0.902	0.0031	0.0024	0.0031	1.3144	0.0881	3.522
0.300	0.050	3.188	0.557	0.86	1.520	0.876	0.0030	0.0024	0.0030	1.2765	0.0831	3.322
0.325	0.075	3.454	0.557	0.86	1.520	0.851	0.0030	0.0024	0.0029	1.2393	0.0783	3.131
0.350	0.100	3.720	0.557	0.86	1.520	0.826	0.0029	0.0024	0.0029	1.2029	0.0737	2.950
0.375	0.125	3.986	0.557	0.86	1.520	0.801	0.0028	0.0024	0.0028	1.1672	0.0694	2.777
0.400	0.150	4.251	0.557	0.46	0.809	0.777	0.0014	0.0024	0.0014	0.6010	0.0184	0.737
0.425	0.175	4.517	0.557	0.44	0.773	0.754	0.0013	0.0024	0.0013	0.5563	0.0158	0.631
0.450	0.200	4.783	0.557	0.42	0.737	0.731	0.0012	0.0024	0.0012	0.5142	0.0135	0.539
0.475	0.225	5.048	0.557	0.40	0.702	0.708	0.0011	0.0024	0.0011	0.4745	0.0115	0.459
0.500	0.250	5.314	0.557	0.38	0.668	0.686	0.0010	0.0024	0.0010	0.4372	0.0097	0.390
0.525	0.275	5.580	0.557	0.36	0.635	0.665	0.0010	0.0024	0.0010	0.4022	0.0082	0.330
0.550	0.300	5.845	0.557	0.34	0.603	0.644	0.0009	0.0024	0.0009	0.3694	0.0070	0.278

Table C 0.7. The ultimate scour depth for Q=20 l/s, H=3m, TW=0.5m computed by DI

Q = 20 l/s, H = 3m, TW = 0.5m												
Y(m)	Bottom (m)	Y/Bj	ψ	C_p	C_p^a	$C_I(-)$	$I_{max}(Ns)$	G_b (Kg/m ²)	$I_{net}(Ns)$	$V_{up}(m/s)$	$h_{up}(m)$	h_{up}/z
Measured	Measured		Eq.31	Eq. 30	Eq. 42	Eq. 57	Eq. 56	Eq. 59	Eq. 55		Eq. 58	
0.500	0.000	4.771	0.627	0.47	1.564	0.732	0.0021	0.0024	0.0021	0.8794	0.0394	1.5767
0.525	0.025	5.010	0.627	0.45	1.497	0.712	0.0020	0.0024	0.0019	0.8183	0.0341	1.3651
0.550	0.050	5.248	0.627	0.43	1.432	0.692	0.0018	0.0024	0.0018	0.7605	0.0295	1.1791
0.575	0.075	5.487	0.627	0.41	1.369	0.672	0.0017	0.0024	0.0017	0.7058	0.0254	1.0157
0.600	0.100	5.725	0.627	0.39	1.307	0.653	0.0016	0.0024	0.0016	0.6542	0.0218	0.8726
0.625	0.125	5.964	0.627	0.38	1.246	0.635	0.0015	0.0024	0.0014	0.6055	0.0187	0.7476
0.650	0.150	6.202	0.627	0.36	1.187	0.617	0.0013	0.0024	0.0013	0.5597	0.0160	0.6386
0.675	0.175	6.441	0.627	0.34	1.129	0.599	0.0012	0.0024	0.0012	0.5165	0.0136	0.5438
0.700	0.200	6.679	0.627	0.32	1.073	0.581	0.0011	0.0024	0.0011	0.4759	0.0115	0.4617
0.725	0.225	6.918	0.627	0.31	1.018	0.564	0.0011	0.0024	0.0010	0.4377	0.0098	0.3906
0.750	0.250	7.157	0.627	0.29	0.965	0.548	0.0010	0.0024	0.0010	0.4019	0.0082	0.3293
0.775	0.275	7.395	0.627	0.27	0.913	0.531	0.0009	0.0024	0.0009	0.3684	0.0069	0.2767
0.800	0.300	7.634	0.627	0.26	0.862	0.516	0.0008	0.0024	0.0008	0.3370	0.0058	0.2315

Table C 0.8. The ultimate scour depth for Q=20 l/s, H=3m, TW=0.25m computed by DI

Q = 20l/s, H = 3m, tw = 0.25m												
Y(m)	Bottom (m)	Y/dj	ψ	Cp	Cpa	Ci	lmax	Gb	Inet	Vup	hup	hup/z
Measured	Measured		Eq.31	Eq.30	Eq. 42	Eq.57	Eq.56	Eq. 59	Eq. 55		Eq. 58	
0.250	0.000	2.439	0.648806	0.86	2.047	0.951	0.0022	0.0024	0.0022	0.9104	0.0422	1.6897
0.275	0.025	2.683	0.648806	0.86	2.047	0.926	0.0021	0.0024	0.0021	0.8867	0.0401	1.6029
0.300	0.050	2.927	0.648806	0.86	2.047	0.902	0.0021	0.0024	0.0021	0.8634	0.0380	1.5199
0.325	0.075	3.170	0.648806	0.86	2.047	0.878	0.0020	0.0024	0.0020	0.8406	0.0360	1.4404
0.350	0.100	3.414	0.648806	0.86	2.047	0.854	0.0019	0.0024	0.0019	0.8181	0.0341	1.3644
0.375	0.125	3.658	0.648806	0.86	2.047	0.832	0.0019	0.0024	0.0019	0.7960	0.0323	1.2918
0.400	0.150	3.902	0.648806	0.86	2.047	0.809	0.0018	0.0024	0.0018	0.7743	0.0306	1.2224
0.425	0.175	4.146	0.648806	0.86	2.047	0.787	0.0018	0.0024	0.0018	0.7530	0.0289	1.1561
0.450	0.200	4.390	0.648806	0.86	2.047	0.765	0.0017	0.0024	0.0017	0.7322	0.0273	1.0929
0.475	0.225	4.634	0.648806	0.86	2.047	0.744	0.0017	0.0024	0.0017	0.7117	0.0258	1.0326
0.500	0.250	4.878	0.648806	0.86	2.047	0.723	0.0016	0.0024	0.0016	0.6916	0.0244	0.9752
0.525	0.275	5.121	0.648806	0.86	2.047	0.702	0.0016	0.0024	0.0016	0.6719	0.0230	0.9205
0.550	0.300	5.365	0.648806	0.86	2.047	0.682	0.0016	0.0024	0.0016	0.6527	0.0217	0.8684

Table C 0.9. The ultimate scour depth for Q=10 l/s, H=4m, TW=0.5m computed by DI

Q = 10 l/s, H = 4m, TW= 0.5m												
Y(m)	Bottom (m)	Y/Bj	ψ	C_p	C_p^a	$C_I(-)$	$I_{max}(Ns)$	G_b (Kg/m ²)	$I_{net}(Ns)$	$V_{up}(m/s)$	$h_{up}(m)$	h_{up}/z
Measured	Measured		Eq.31	Eq. 30	Eq. 42	Eq. 57	Eq. 56	Eq. 59	Eq. 55		Eq. 58	
0.500	0.000	5.630	0.612	0.39	0.755	0.661	0.0028	0.0024	0.0028	1.1690	0.0697	2.7860
0.525	0.025	5.911	0.612	0.37	0.714	0.639	0.0026	0.0024	0.0025	1.0680	0.0581	2.3254
0.550	0.050	6.193	0.612	0.35	0.674	0.617	0.0023	0.0024	0.0023	0.9738	0.0483	1.9333
0.575	0.075	6.474	0.612	0.33	0.636	0.596	0.0021	0.0024	0.0021	0.8861	0.0400	1.6007
0.600	0.100	6.756	0.612	0.31	0.598	0.576	0.0019	0.0024	0.0019	0.8045	0.0330	1.3196
0.625	0.125	7.037	0.612	0.29	0.562	0.556	0.0018	0.0024	0.0017	0.7288	0.0271	1.0829
0.650	0.150	7.318	0.612	0.27	0.527	0.537	0.0016	0.0024	0.0016	0.6586	0.0221	0.8844
0.675	0.175	7.600	0.612	0.26	0.493	0.518	0.0014	0.0024	0.0014	0.5937	0.0180	0.7186
0.700	0.200	7.881	0.612	0.24	0.460	0.500	0.0013	0.0024	0.0013	0.5337	0.0145	0.5807
0.725	0.225	8.163	0.612	0.22	0.428	0.482	0.0012	0.0024	0.0011	0.4784	0.0117	0.4666
0.750	0.250	8.444	0.612	0.21	0.397	0.465	0.0010	0.0024	0.0010	0.4275	0.0093	0.3726
0.775	0.275	8.726	0.612	0.19	0.368	0.448	0.0009	0.0024	0.0009	0.3808	0.0074	0.2956
0.800	0.300	9.007	0.612	0.18	0.340	0.432	0.0008	0.0024	0.0008	0.3380	0.0058	0.2329

Table C 0.10. The ultimate scour depth for Q=10 l/s, H=4m, TW=0.25m computed by DI

Q = 10l/s, H = 4m, TW = 0.25m												
Y(m)	Bottom (m)	Y/Bj	ψ	C_p	C_p^a	$C_I (-)$	$I_{max}(Ns)$	$G_b (Kg/m^2)$	$I_{net} (Ns)$	$V_{up} (m/s)$	$h_{up} (m)$	h_{up}/z
Measured	Measured		Eq.31	Eq. 30	Eq. 42	Eq. 57	Eq. 56	Eq. 59	Eq. 55		Eq. 58	
0.250	0.000	2.874	0.6277	0.86	1.946	0.907	0.0038	0.0024	0.0038	1.6019	0.1308	5.2313
0.275	0.025	3.161	0.6277	0.86	1.946	0.879	0.0037	0.0024	0.0037	1.5521	0.1228	4.9112
0.300	0.050	3.448	0.6277	0.86	1.946	0.851	0.0036	0.0024	0.0036	1.5033	0.1152	4.6074
0.325	0.075	3.736	0.6277	0.86	1.946	0.824	0.0035	0.0024	0.0035	1.4556	0.1080	4.3194
0.350	0.100	4.023	0.6277	0.54	1.217	0.798	0.0021	0.0024	0.0021	0.8794	0.0394	1.5766
0.375	0.125	4.310	0.6277	0.51	1.159	0.772	0.0019	0.0024	0.0019	0.8101	0.0335	1.3381
0.400	0.150	4.598	0.6277	0.49	1.102	0.747	0.0018	0.0024	0.0018	0.7452	0.0283	1.1320
0.425	0.175	4.885	0.6277	0.46	1.047	0.722	0.0016	0.0024	0.0016	0.6842	0.0239	0.9545
0.450	0.200	5.172	0.6277	0.44	0.993	0.698	0.0015	0.0024	0.0015	0.6272	0.0201	0.8020
0.475	0.225	5.460	0.6277	0.42	0.941	0.675	0.0014	0.0024	0.0014	0.5739	0.0168	0.6715
0.500	0.250	5.747	0.6277	0.39	0.890	0.652	0.0013	0.0024	0.0012	0.5241	0.0140	0.5601
0.525	0.275	6.034	0.6277	0.37	0.841	0.629	0.0011	0.0024	0.0011	0.4777	0.0116	0.4653
0.550	0.300	6.322	0.6277	0.35	0.793	0.608	0.0010	0.0024	0.0010	0.4345	0.0096	0.3850
0.575	0.325	6.609	0.6277	0.33	0.746	0.586	0.0009	0.0024	0.0009	0.3944	0.0079	0.3171
0.600	0.350	6.897	0.6277	0.31	0.701	0.566	0.0009	0.0024	0.0008	0.3571	0.0065	0.2600
0.625	0.375	7.184	0.6277	0.29	0.657	0.546	0.0008	0.0024	0.0008	0.3226	0.0053	0.2122
0.650	0.400	7.471	0.6277	0.27	0.615	0.526	0.0007	0.0024	0.0007	0.2907	0.0043	0.1723

Table C 0.11. The ultimate scour depth for Q=20 l/s, H=4m, TW=0.5m computed by DI

Q = 20l/s, H = 4m, TW = 0.5m												
Y(m)	Bottom (m)	Y/Bj	ψ	C_p	C_p^a	$C_I (-)$	$I_{max}(Ns)$	G_b (Kg/m ²)	$I_{net} (Ns)$	$V_{up} (m/s)$	$h_{up} (m)$	h_{up}/z
Measured	Measured		Eq.31	Eq. 30	Eq. 42	Eq. 57	Eq. 56	Eq. 59	Eq. 55		Eq. 58	
0.500	0.000	5.161	0.702	0.49	0.806	0.699	0.0037	0.0024	0.0037	1.5425	0.1213	4.8510
0.525	0.025	5.420	0.702	0.47	0.768	0.678	0.0034	0.0024	0.0034	1.4242	0.1034	4.1352
0.550	0.050	5.678	0.702	0.44	0.730	0.657	0.0031	0.0024	0.0031	1.3129	0.0879	3.5142
0.575	0.075	5.936	0.702	0.42	0.694	0.637	0.0029	0.0024	0.0029	1.2084	0.0744	2.9771
0.600	0.100	6.194	0.702	0.40	0.658	0.617	0.0027	0.0024	0.0026	1.1104	0.0628	2.5137
0.625	0.125	6.452	0.702	0.38	0.624	0.598	0.0024	0.0024	0.0024	1.0186	0.0529	2.1152
0.650	0.150	6.710	0.702	0.36	0.590	0.579	0.0022	0.0024	0.0022	0.9327	0.0443	1.7734
0.675	0.175	6.968	0.702	0.34	0.557	0.561	0.0020	0.0024	0.0020	0.8524	0.0370	1.4813
0.700	0.200	7.226	0.702	0.32	0.526	0.543	0.0019	0.0024	0.0018	0.7775	0.0308	1.2324
0.725	0.225	7.484	0.702	0.30	0.495	0.525	0.0017	0.0024	0.0017	0.7077	0.0255	1.0211
0.750	0.250	7.742	0.702	0.28	0.465	0.508	0.0015	0.0024	0.0015	0.6428	0.0211	0.8423
0.775	0.275	8.000	0.702	0.26	0.436	0.492	0.0014	0.0024	0.0014	0.5825	0.0173	0.6917
0.800	0.300	8.258	0.702	0.25	0.408	0.476	0.0013	0.0024	0.0013	0.5265	0.0141	0.5652

Table C 0.12. The ultimate scour depth for Q=20 l/s, H=4m, TW=0.25m computed by DI

Q = 20l/s, H = 4m, TW = 0.25m												
Y(m)	Bottom (m)	Y/Bj	ψ	C_p	C_p^a	$C_I (-)$	$I_{max}(Ns)$	$G_b (Kg/m^2)$	$I_{net} (Ns)$	$V_{up} (m/s)$	$h_{up} (m)$	h_{up}/z
Measured	Measured		Eq.31	Eq. 30	Eq. 42	Eq. 57	Eq. 56	Eq. 59	Eq. 55		Eq. 58	
0.250	0.000	2.623	0.717	0.86	2.632	0.932	0.0041	0.0024	0.0040	1.7024	0.1477	5.909
0.275	0.025	2.886	0.717	0.86	2.632	0.906	0.0039	0.0024	0.0039	1.6545	0.1395	5.581
0.300	0.050	3.148	0.717	0.86	2.632	0.880	0.0038	0.0024	0.0038	1.6075	0.1317	5.268
0.325	0.075	3.410	0.717	0.86	2.632	0.855	0.0037	0.0024	0.0037	1.5614	0.1243	4.970
0.350	0.100	3.672	0.717	0.86	2.632	0.830	0.0036	0.0024	0.0036	1.5161	0.1172	4.686
0.375	0.125	3.935	0.717	0.86	2.632	0.806	0.0035	0.0024	0.0035	1.4718	0.1104	4.416
0.400	0.150	4.197	0.717	0.59	1.820	0.782	0.0024	0.0024	0.0023	0.9862	0.0496	1.983
0.425	0.175	4.459	0.717	0.57	1.739	0.759	0.0022	0.0024	0.0022	0.9141	0.0426	1.703
0.450	0.200	4.722	0.717	0.54	1.660	0.736	0.0020	0.0024	0.0020	0.8461	0.0365	1.459
0.475	0.225	4.984	0.717	0.52	1.583	0.714	0.0019	0.0024	0.0019	0.7820	0.0312	1.247
0.500	0.250	5.246	0.717	0.49	1.508	0.692	0.0017	0.0024	0.0017	0.7218	0.0266	1.062
0.525	0.275	5.509	0.717	0.47	1.434	0.671	0.0016	0.0024	0.0016	0.6651	0.0225	0.902
0.550	0.300	5.771	0.717	0.45	1.363	0.650	0.0015	0.0024	0.0015	0.6120	0.0191	0.763
0.575	0.325	6.033	0.717	0.42	1.293	0.629	0.0013	0.0024	0.0013	0.5621	0.0161	0.644
0.600	0.350	6.296	0.717	0.40	1.225	0.610	0.0012	0.0024	0.0012	0.5154	0.0135	0.542
0.625	0.375	6.558	0.717	0.38	1.159	0.590	0.0011	0.0024	0.0011	0.4717	0.0113	0.454
0.650	0.400	6.820	0.717	0.36	1.095	0.571	0.0010	0.0024	0.0010	0.4309	0.0095	0.379
0.675	0.425	7.083	0.717	0.34	1.032	0.553	0.0009	0.0024	0.0009	0.3929	0.0079	0.315
0.700	0.450	7.345	0.717	0.32	0.972	0.535	0.0009	0.0024	0.0008	0.3574	0.0065	0.260
0.725	0.475	7.607	0.717	0.30	0.913	0.517	0.0008	0.0024	0.0008	0.3244	0.0054	0.215

APPENDIX D: WORK SHEET AND GRAPHS OF QSI METHOD

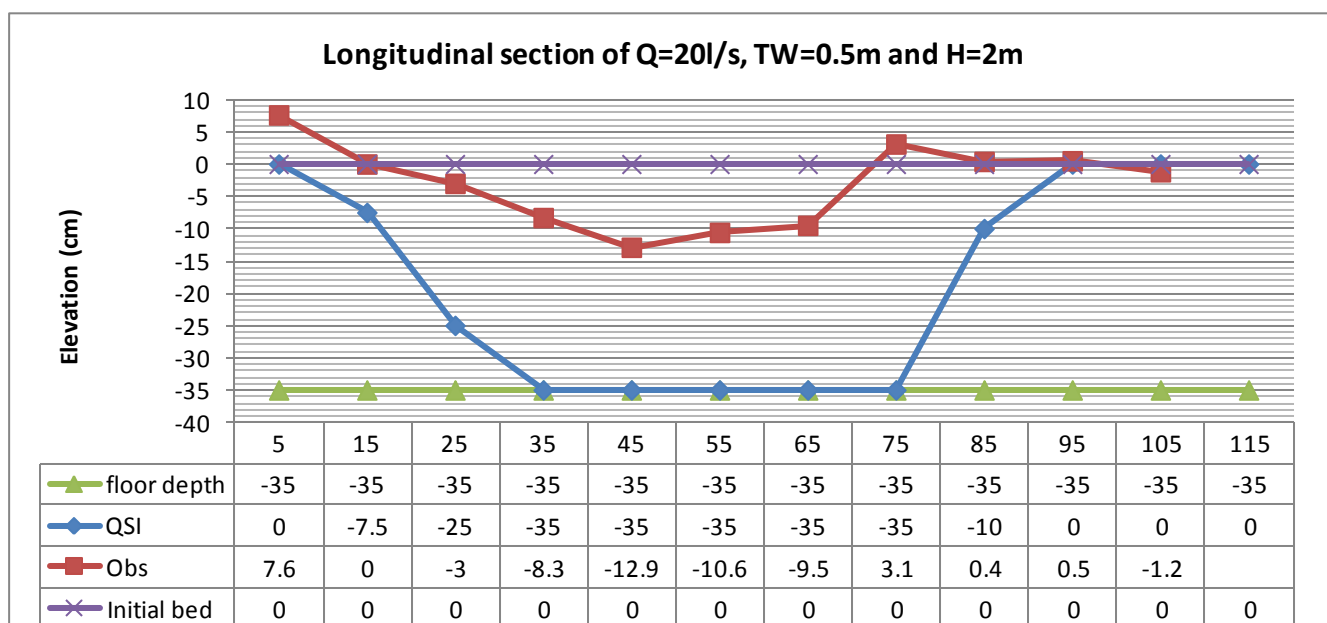


Figure D 0-1. Longitudinal section for Q=20l/s, H=2m and TW=0.5m at the maximum point of observed scour profile compare to the QSI scour hole

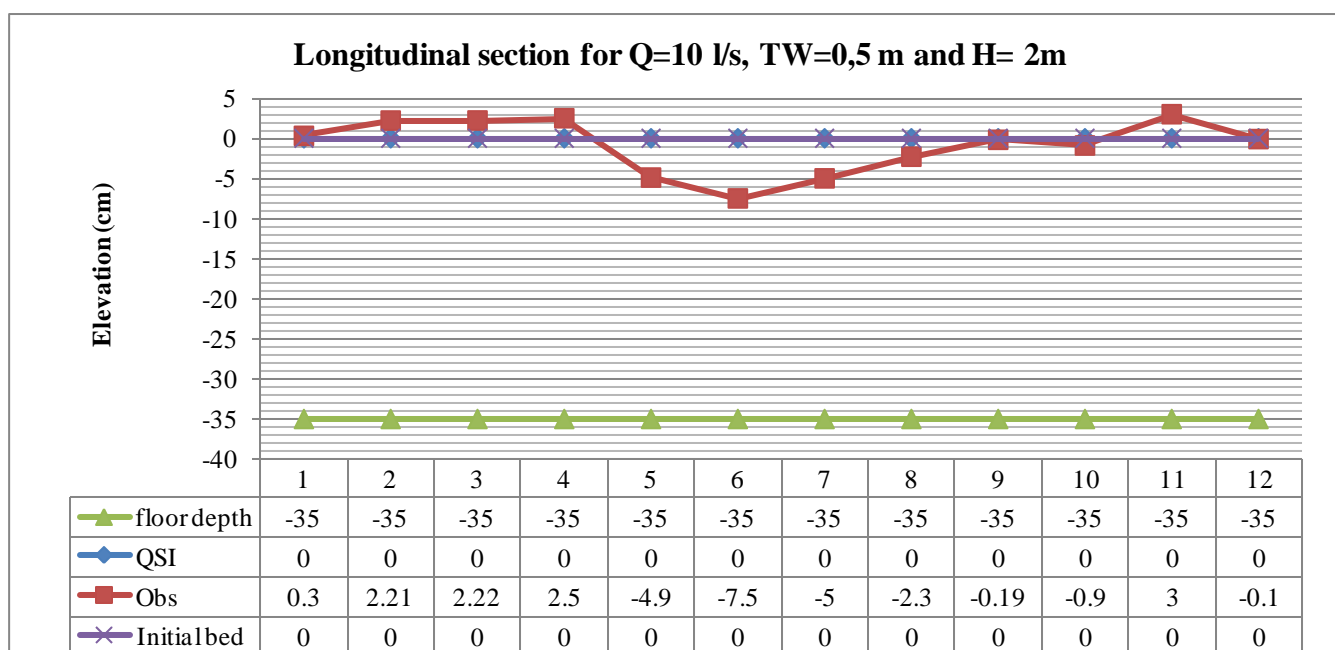


Figure D 0-2. Longitudinal section for Q=10l/s, H=2m and TW=0.5m at the maximum point of observed scour profile compare to the QSI scour hole

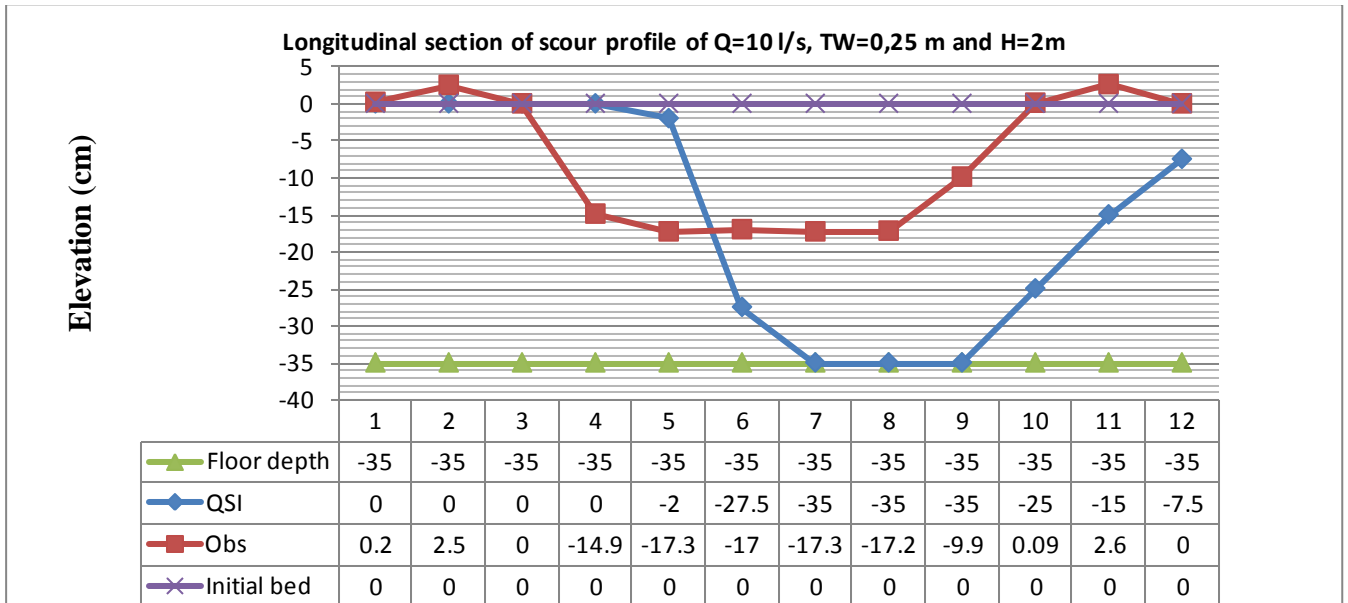


Figure D 0-3. Longitudinal section for $Q=10 \text{ l/s}$, $H=2\text{m}$ and $TW=0.25\text{m}$ at the maximum point of observed scour profile compare to the QSI scour hole.

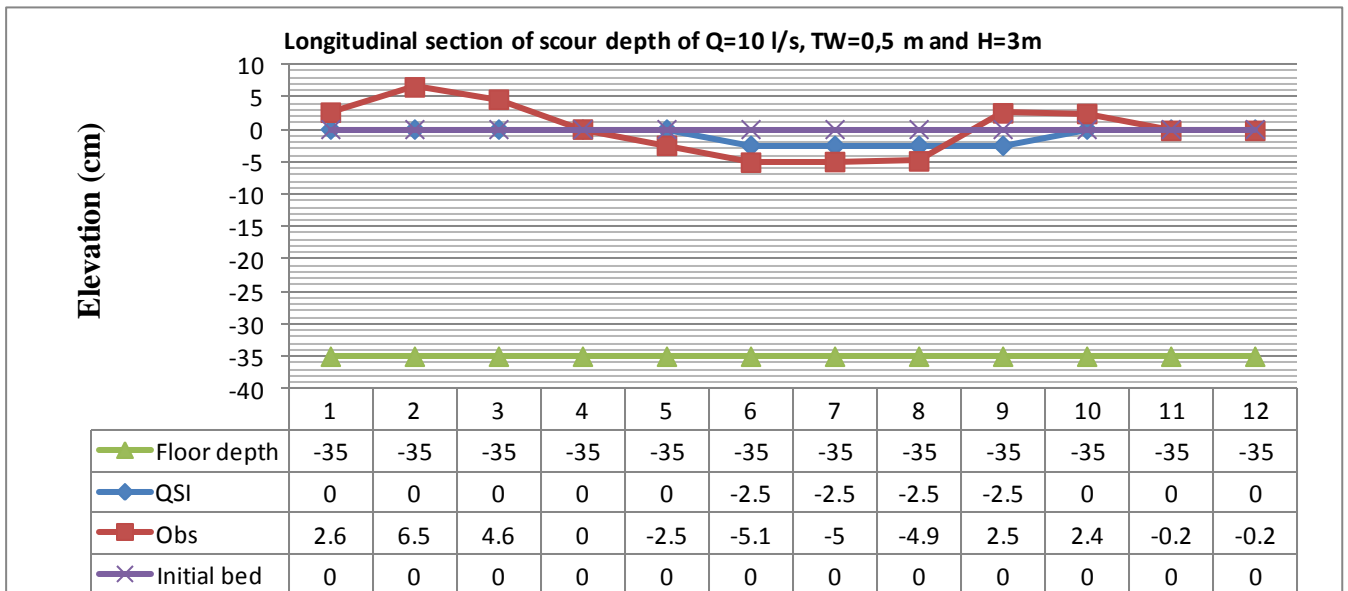


Figure D 0-4. Longitudinal section for $Q=10 \text{ l/s}$, $H=3\text{m}$ and $TW=0.5\text{m}$ at the maximum point of observed scour profile compare to the QSI scour hole.

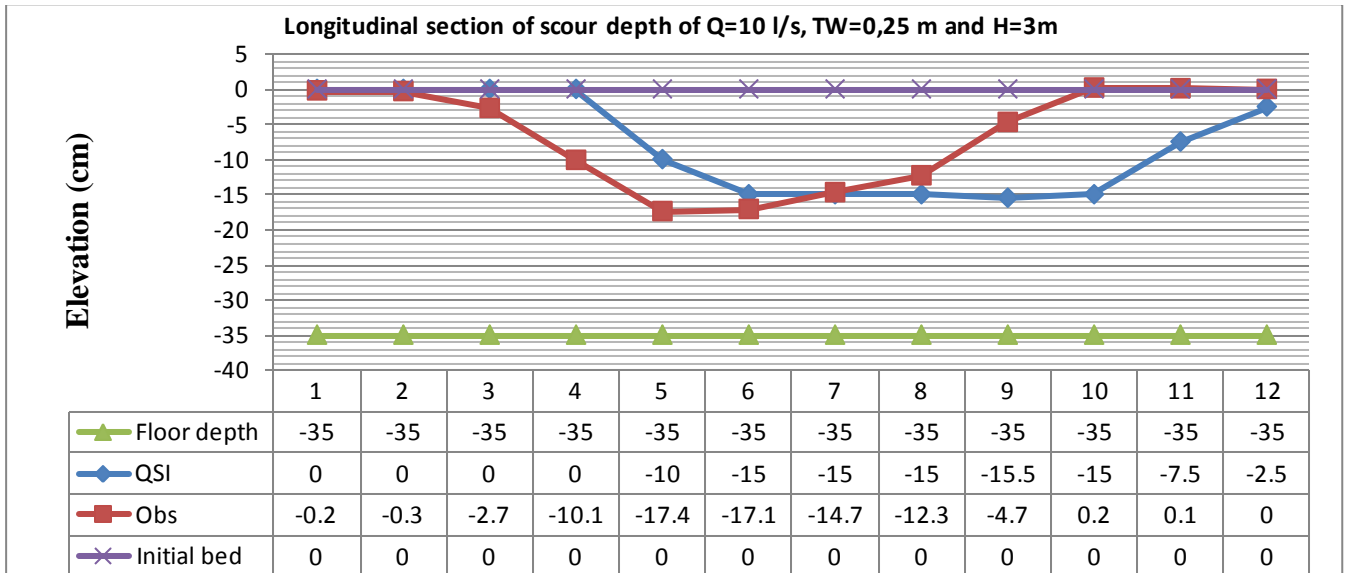


Figure D 0-5. Longitudinal section for Q=10l/s, H=3m and TW=0.25m at the maximum point of observed scour profile compare to the QSI scour hole.

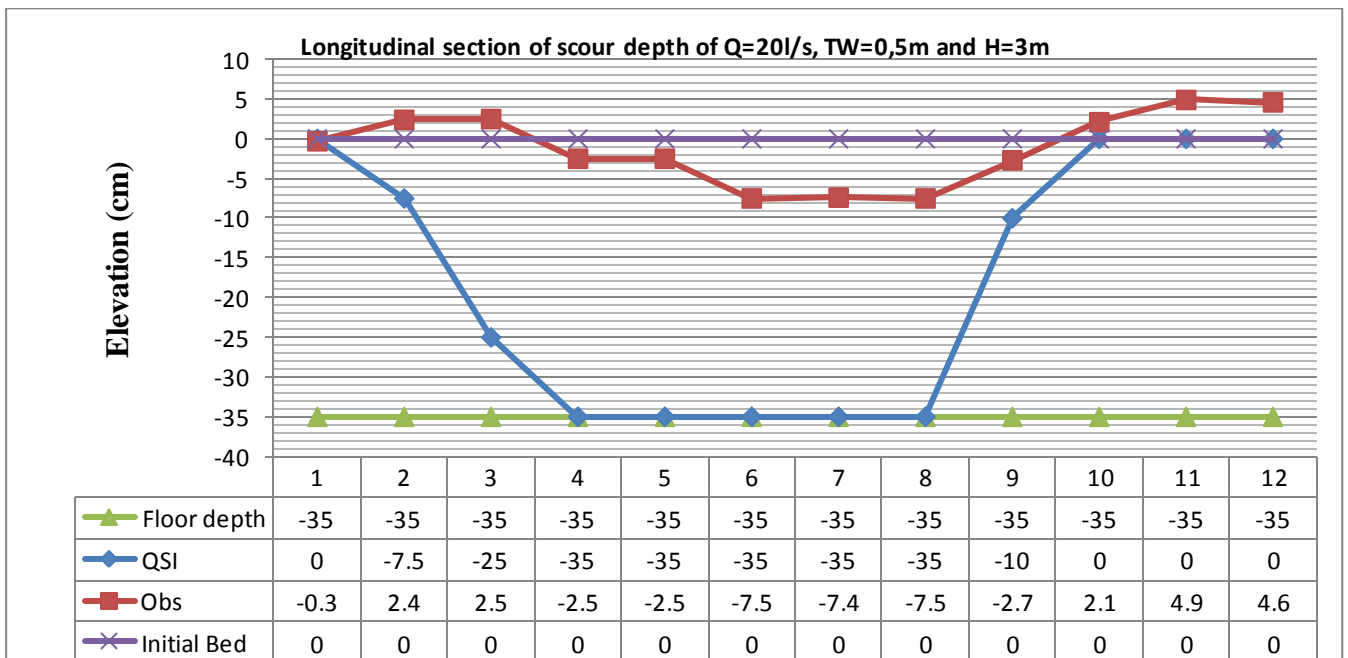


Figure D 0-6. Longitudinal section for Q=20l/s, H=3m and TW=0.5m at the maximum point of observed scour profile compare to the QSI scour hole.

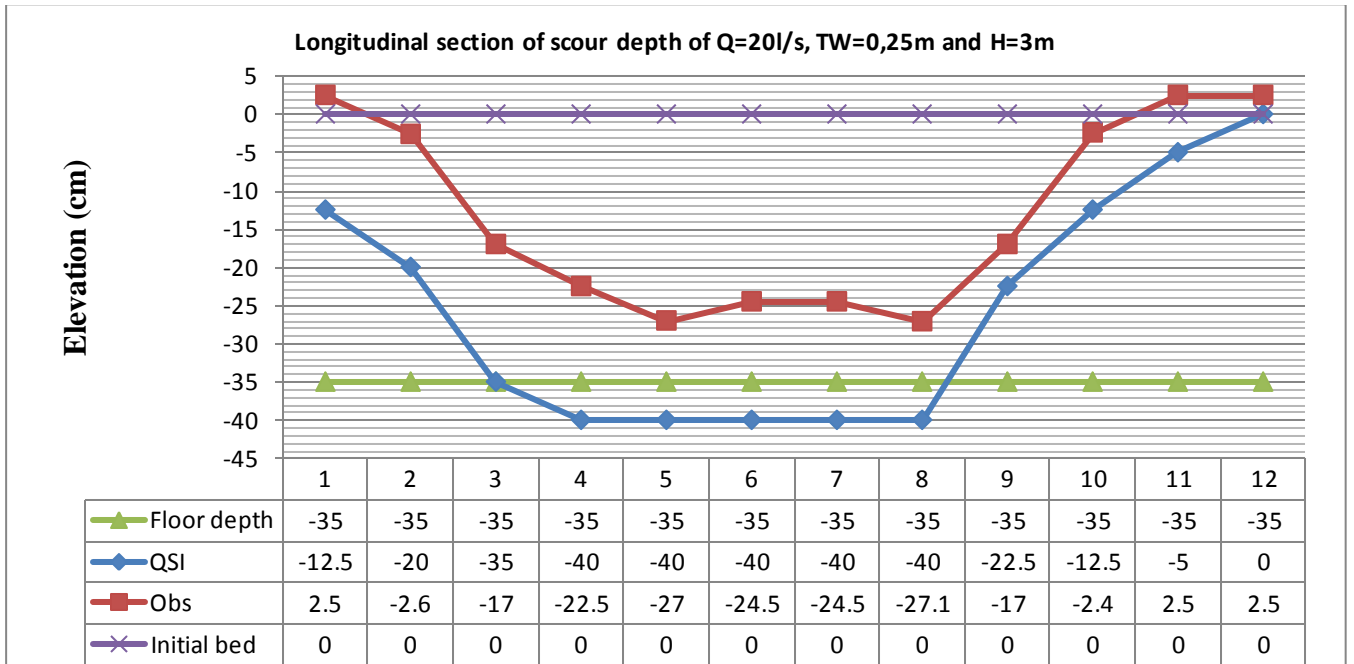


Figure D 0-7. Longitudinal section for $Q=20l/s$, $H=3m$ and $TW=0.25m$ at the maximum point of observed scour profile compare to the QSI scour hole.

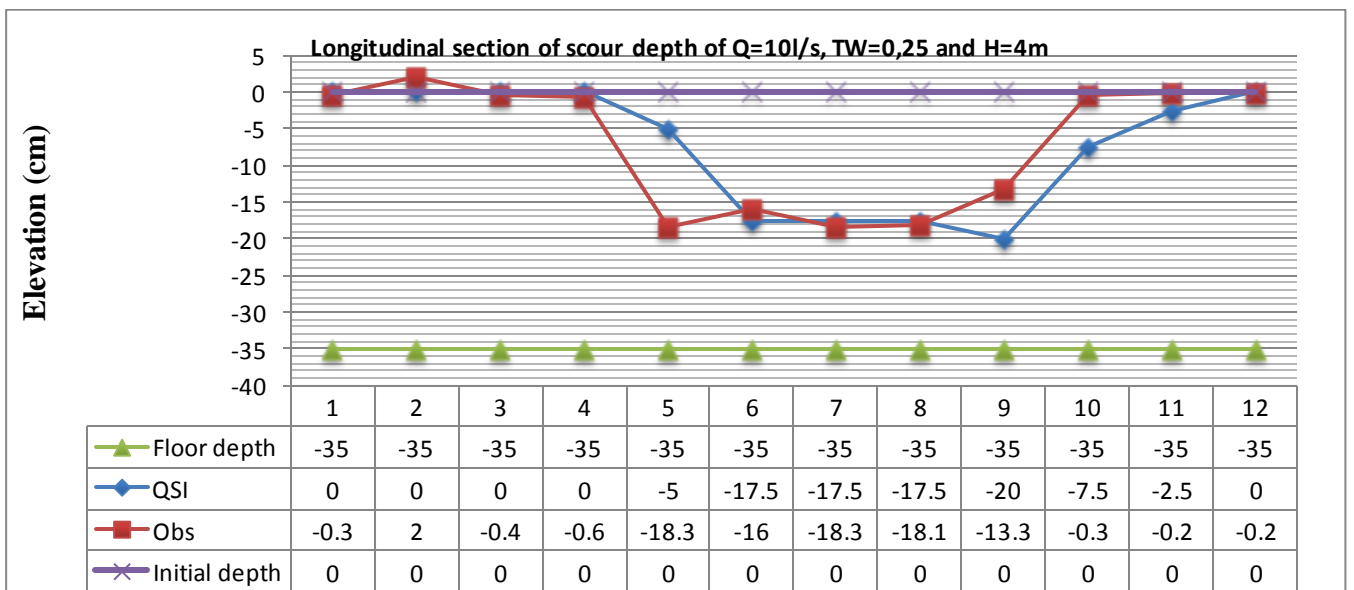


Figure D 0-8. Longitudinal section for $Q=10l/s$, $H=4m$ and $TW=0.25m$ at the maximum point of observed scour profile compare to the QSI scour hole.

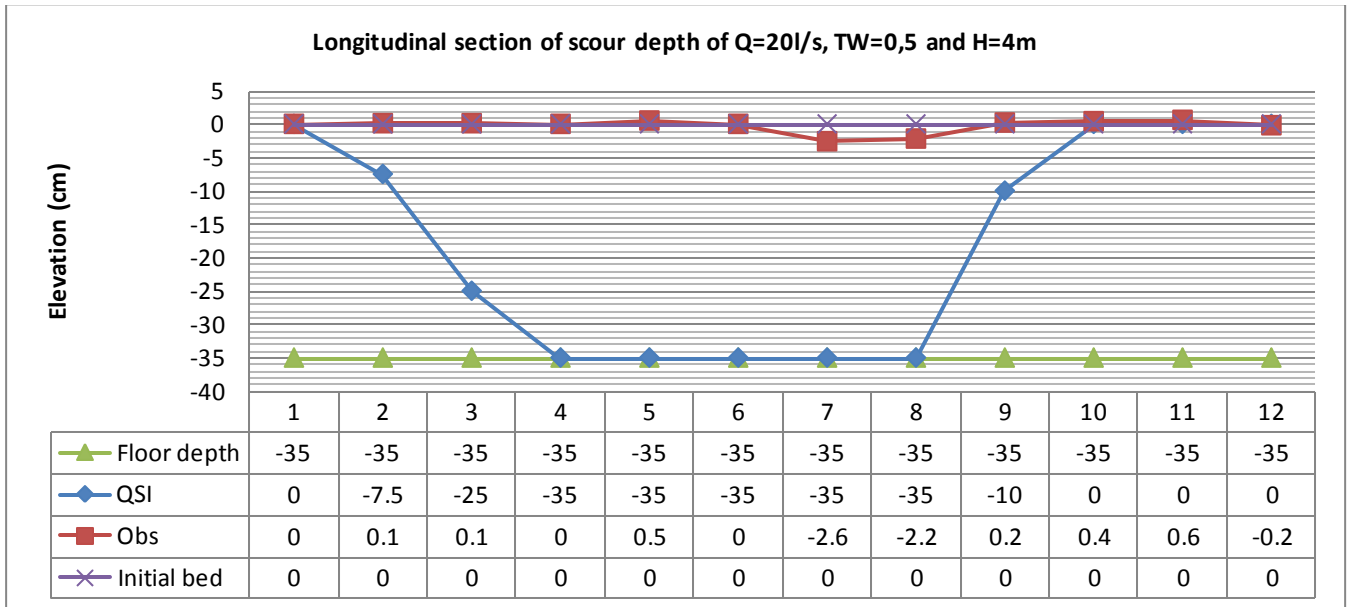


Figure D 0-9. Longitudinal section for $Q=20l/s$, $H=4m$ and $TW=0.5m$ at the maximum point of observed scour profile compare to the QSI scour hole.

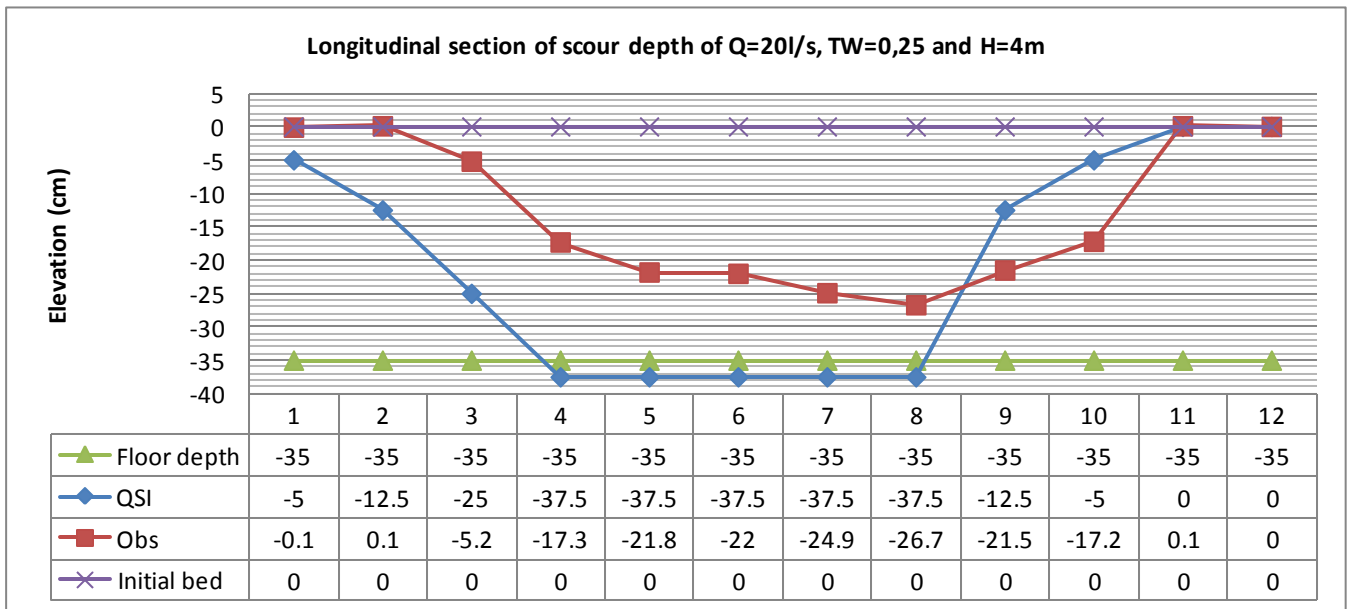
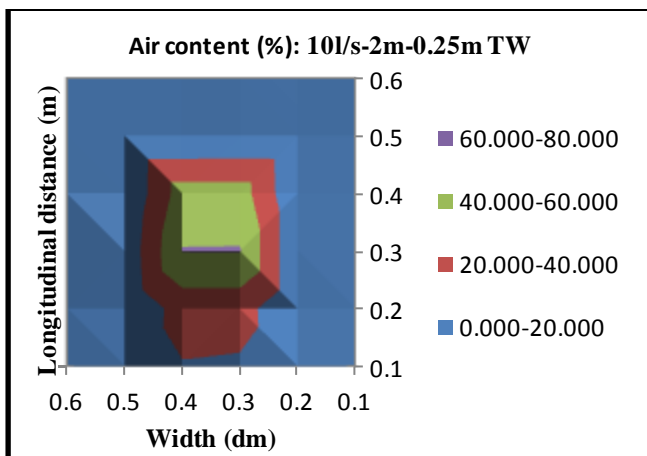
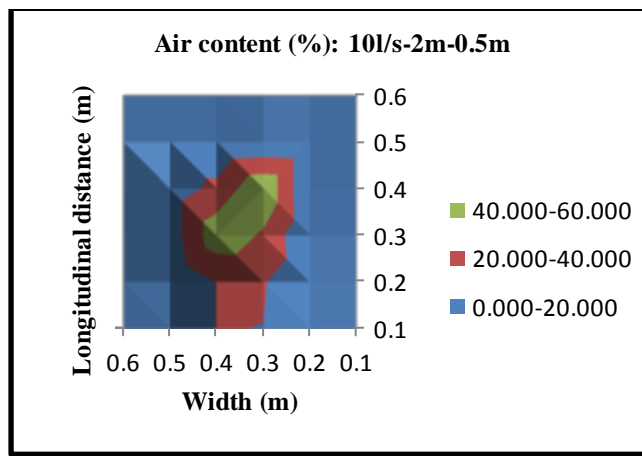


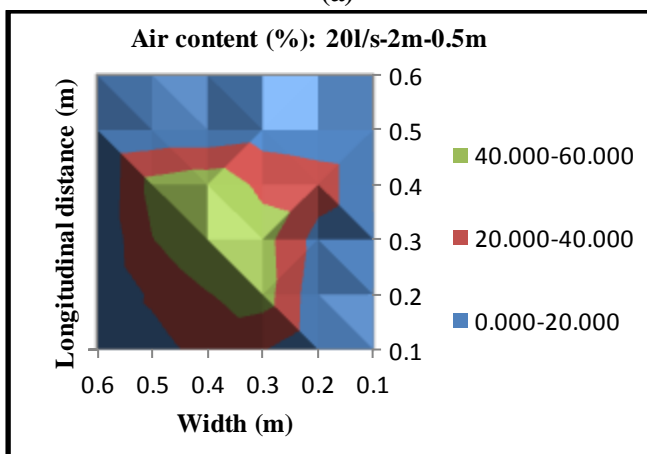
Figure D 0-10. Longitudinal section for $Q=20l/s$, $H=4m$ and $TW=0.25m$ at the maximum point of observed scour profile compare to the QSI scour hole.



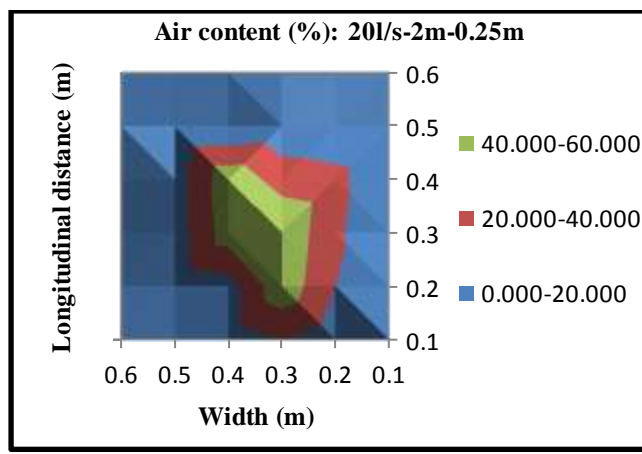
(a)



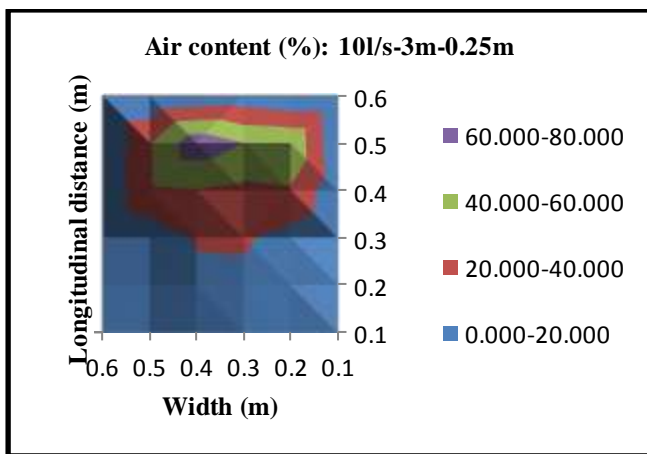
(b)



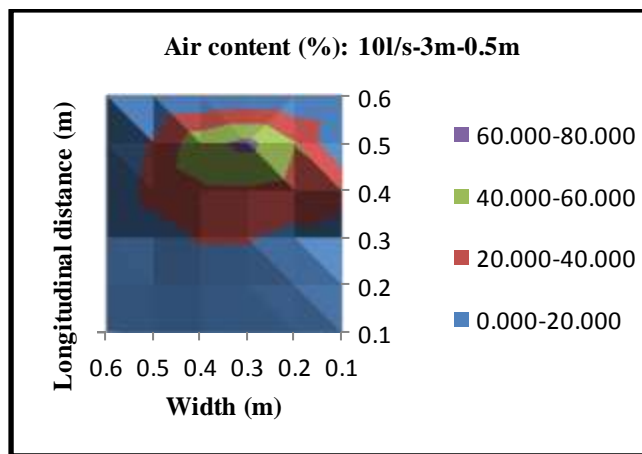
(c)



(d)



(e)



(f)

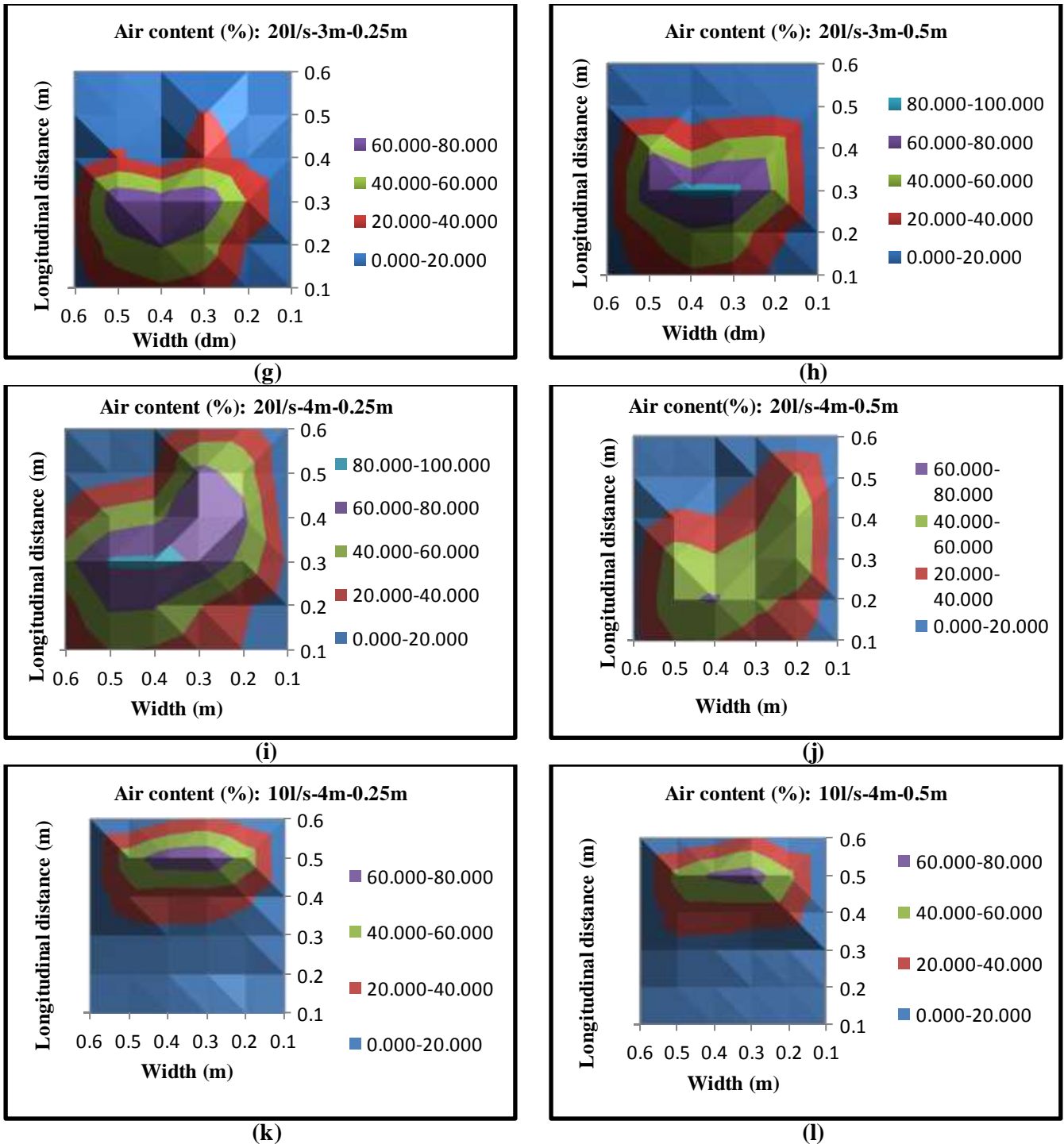


Figure D 0-11. General view of contour plot of air concentration of four scenarios

Legend:

- Q: Discharge
- X: Horizontal distance
- Z: Water depth
- V_{zi} : Velocity profile in plunge pool
- B_i : Jet width at issuance

B_j : Jet width at the impact

Z_{core} : Distance of jet to diffuse its core

δ : Jet angle with horizontal

h_{up}/d_{down} : Initial thickness of deflection flow

V_{xmax} : Maximum cross section jet velocity

q_{total} : Discharge per unit

H : Drop height

$V(z)$: Flow velocity at bottom

FQSI: Quasi steady impulsion force

G_b : Immersed weight

I_{net} : The net forces

V_{up} : Velocity of block

h_{up} : Height of the block displacement

Table D 0.1. Quasi-steady method of Q=10l/s, H=2m and TW=0.5m

Q	X	Z	V _{zi}	Z _{core}	V _{zj}	h _{down}	h _{up}	V _{xmax}	q _{up}	q _{down}	V(z)	FQSI	G _b	I _{net}	V _{up}	H _{up}	H _{up} /z
l/s	m	m	m/s	m	m/s	m	m	m/s	m ² /s	m ² /s	m/s	Ns	kg/m ²	Ns	m/s	m	
			Q=VA	Z=5*B _j	Eq. 25	Eq. 61		Eq. 63	Eq. 61&62		Eq. 60	Fig.2.1 8	Eq. 59	Eq.55		Eq. 58	
10	0.62	0	1.667	0.542	5.675	0.089	0.020	1.087	0.002	0.008	5.675						
10	0.62	0.042	1.667	0.542	5.675	0.089	0.020	1.087	0.002	0.008	6.011						
10	0.62	0.083	1.667	0.542	5.675	0.089	0.020	1.087	0.002	0.008	4.250						
10	0.62	0.125	1.667	0.542	5.675	0.089	0.020	1.087	0.002	0.008	3.470						
10	0.62	0.167	1.667	0.542	5.675	0.089	0.020	1.087	0.002	0.008	3.005						
10	0.62	0.208	1.667	0.542	5.675	0.089	0.020	1.087	0.002	0.008	2.688						
10	0.62	0.250	1.667	0.542	5.675	0.089	0.020	1.087	0.002	0.008	2.454						
10	0.62	0.292	1.667	0.542	5.675	0.089	0.020	1.087	0.002	0.008	2.272						
10	0.62	0.333	1.667	0.542	5.675	0.089	0.020	1.087	0.002	0.008	2.125						
10	0.62	0.375	1.667	0.542	5.675	0.089	0.020	1.087	0.002	0.008	2.004						
10	0.62	0.417	1.667	0.542	5.675	0.089	0.020	1.087	0.002	0.008	1.901						
10	0.62	0.458	1.667	0.542	5.675	0.089	0.020	1.087	0.002	0.008	1.812						
10	0.62	0.5	1.667	0.542	5.675	0.089	0.020	1.087	0.002	0.008	1.735						
10	0.5	0.5	1.667	0.542	5.675	0.089	0.020	1.211	0.002	0.008	1.735	0.0003	0.002	0.000	0.113	0.001	0.027
10	0.4	0.5	1.667	0.542	5.675	0.089	0.020	1.354	0.002	0.008	1.735	0.0004	0.002	0.000	0.144	0.001	0.043
10	0.3	0.5	1.667	0.542	5.675	0.089	0.020	1.563	0.002	0.008	1.735	0.0005	0.002	0.000	0.195	0.002	0.078
10	0.2	0.5	1.667	0.542	5.675	0.089	0.020	1.914	0.002	0.008	1.735	0.0007	0.002	0.001	0.296	0.004	0.180
10	0.1	0.5	1.667	0.542	5.675	0.089	0.020	2.707	0.002	0.008	1.735	0.0014	0.002	0.001	0.601	0.018	0.737
10	0.62	0.5	1.667	0.542	5.675	0.089	0.020	1.087	0.002	0.008	1.735	0.0002	0.002	0.000	0.090	0.000	0.017
10	0.1	0.5	1.667	0.542	5.675	0.089	0.020	2.707	0.002	0.008	1.735	0.0014	0.002	0.001	0.601	0.018	0.737
10	0.2	0.5	1.667	0.542	5.675	0.089	0.020	1.914	0.002	0.008	1.735	0.0007	0.002	0.001	0.296	0.004	0.180
10	0.3	0.5	1.667	0.542	5.675	0.089	0.020	1.563	0.002	0.008	1.735	0.0005	0.002	0.000	0.195	0.002	0.078
10	0.4	0.5	1.667	0.542	5.675	0.089	0.020	1.354	0.002	0.008	1.735	0.0004	0.002	0.000	0.144	0.001	0.043

Q	X	Z	V_z	Z_{core}	V_z	h_{down}	h_{up}	V_{xmax}	q_{up}	q_{down}	V(z)	FQSI	G_b	I_{net}	V_{up}	H_{up}	H_{up}/z
l/s	m	m	m/s	m	m/s	m	m	m/s	m ² /s	m ² /s	m/s	Ns	kg/m ²	Ns	m/s	m	
			Q=VA	Z=5*B _j	Eq. 25	Eq. 61		Eq. 63	Eq. 61&62		Eq. 60	Fig.2.1 8	Eq. 59	Eq.55		Eq. 58	
10	0.5	0.5	1.667	0.542	5.675	0.089	0.020	1.211	0.002	0.008	1.735	0.0003	0.002	0.000	0.113	0.001	0.027
10	0.6	0.5	1.667	0.542	5.675	0.089	0.020	1.105	0.002	0.008	1.735	0.0002	0.002	0.000	0.093	0.000	0.019
10	0.5	0.525	1.667	0.542	5.675	0.089	0.020	1.211	0.002	0.008	1.693	0.0003	0.002	0.000	0.113	0.001	0.027
10	0.4	0.525	1.667	0.542	5.675	0.089	0.020	1.354	0.002	0.008	1.693	0.0004	0.002	0.000	0.144	0.001	0.043
10	0.3	0.525	1.667	0.542	5.675	0.089	0.020	1.563	0.002	0.008	1.693	0.0005	0.002	0.000	0.195	0.002	0.078
10	0.2	0.525	1.667	0.542	5.675	0.089	0.020	1.914	0.002	0.008	1.693	0.0007	0.002	0.001	0.296	0.004	0.180
10	0.1	0.525	1.667	0.542	5.675	0.089	0.020	2.707	0.002	0.008	1.693	0.0014	0.002	0.001	0.601	0.018	0.737
10	0.62	0.525	1.667	0.542	5.675	0.089	0.020	1.087	0.002	0.008	1.693	0.0002	0.002	0.000	0.090	0.000	0.017
10	0.1	0.525	1.667	0.542	5.675	0.089	0.020	2.707	0.002	0.008	1.693	0.0014	0.002	0.001	0.601	0.018	0.737
10	0.2	0.525	1.667	0.542	5.675	0.089	0.020	1.914	0.002	0.008	1.693	0.0007	0.002	0.001	0.296	0.004	0.180
10	0.3	0.525	1.667	0.542	5.675	0.089	0.020	1.563	0.002	0.008	1.693	0.0005	0.002	0.000	0.195	0.002	0.078
10	0.4	0.525	1.667	0.542	5.675	0.089	0.020	1.354	0.002	0.008	1.693	0.0004	0.002	0.000	0.144	0.001	0.043
10	0.5	0.525	1.667	0.542	5.675	0.089	0.020	1.211	0.002	0.008	1.693	0.0003	0.002	0.000	0.113	0.001	0.027
10	0.6	0.525	1.667	0.542	5.675	0.089	0.020	1.105	0.002	0.008	1.693	0.0002	0.002	0.000	0.093	0.000	0.019
10	0.5	0.55	1.667	0.542	5.675	0.089	0.020	1.211	0.002	0.008	1.654	0.0003	0.002	0.000	0.113	0.001	0.027
10	0.4	0.55	1.667	0.542	5.675	0.089	0.020	1.354	0.002	0.008	1.654	0.0004	0.002	0.000	0.144	0.001	0.043
10	0.3	0.55	1.667	0.542	5.675	0.089	0.020	1.563	0.002	0.008	1.654	0.0005	0.002	0.000	0.195	0.002	0.078
10	0.2	0.55	1.667	0.542	5.675	0.089	0.020	1.914	0.002	0.008	1.654	0.0007	0.002	0.001	0.296	0.004	0.180
10	0.1	0.55	1.667	0.542	5.675	0.089	0.020	2.707	0.002	0.008	1.654	0.0014	0.002	0.001	0.601	0.018	0.737
10	0.62	0.55	1.667	0.542	5.675	0.089	0.020	1.087	0.002	0.008	1.654	0.0002	0.002	0.000	0.090	0.000	0.017
10	0.1	0.55	1.667	0.542	5.675	0.089	0.020	2.707	0.002	0.008	1.654	0.0014	0.002	0.001	0.601	0.018	0.737
10	0.2	0.55	1.667	0.542	5.675	0.089	0.020	1.914	0.002	0.008	1.654	0.0007	0.002	0.001	0.296	0.004	0.180
10	0.3	0.55	1.667	0.542	5.675	0.089	0.020	1.563	0.002	0.008	1.654	0.0005	0.002	0.000	0.195	0.002	0.078
10	0.4	0.55	1.667	0.542	5.675	0.089	0.020	1.354	0.002	0.008	1.654	0.0004	0.002	0.000	0.144	0.001	0.043

Q	X	Z	V _z	Z _{core}	V _{zj}	h _{down}	h _{up}	V _{xmax}	q _{up}	q _{down}	V(z)	FQSI	G _b	I _{net}	V _{up}	H _{up}	H _{up} /z
l/s	m	m	m/s	m	m/s	m	m	m/s	m ² /s	m ² /s	m/s	Ns	kg/m ²	Ns	m/s	m	
			Q=VA	Z=5*B _j	Eq. 25	Eq. 60		Eq. 63	Eq. 61&62		Eq. 60	Fig.2.1 8	Eq. 59	Eq.55		Eq. 57	
10	0.5	0.55	1.667	0.542	5.675	0.089	0.020	1.211	0.002	0.008	1.654	0.0003	0.002	0.000	0.113	0.001	0.027
10	0.6	0.55	1.667	0.542	5.675	0.089	0.020	1.105	0.002	0.008	1.654	0.0002	0.002	0.000	0.093	0.000	0.019
10	0.5	0.575	1.667	0.542	5.675	0.089	0.020	1.211	0.002	0.008	1.618	0.0003	0.002	0.000	0.113	0.001	0.027
10	0.4	0.575	1.667	0.542	5.675	0.089	0.020	1.354	0.002	0.008	1.618	0.0004	0.002	0.000	0.144	0.001	0.043
10	0.3	0.575	1.667	0.542	5.675	0.089	0.020	1.563	0.002	0.008	1.618	0.0005	0.002	0.000	0.195	0.002	0.078
10	0.2	0.575	1.667	0.542	5.675	0.089	0.020	1.914	0.002	0.008	1.618	0.0007	0.002	0.001	0.296	0.004	0.180
10	0.1	0.575	1.667	0.542	5.675	0.089	0.020	2.707	0.002	0.008	1.618	0.0014	0.002	0.001	0.601	0.018	0.737
10	0.62	0.575	1.667	0.542	5.675	0.089	0.020	1.087	0.002	0.008	1.618	0.0002	0.002	0.000	0.090	0.000	0.017
10	0.1	0.575	1.667	0.542	5.675	0.089	0.020	2.707	0.002	0.008	1.618	0.0014	0.002	0.001	0.601	0.018	0.737
10	0.2	0.575	1.667	0.542	5.675	0.089	0.020	1.914	0.002	0.008	1.618	0.0007	0.002	0.001	0.296	0.004	0.180
10	0.3	0.575	1.667	0.542	5.675	0.089	0.020	1.563	0.002	0.008	1.618	0.0005	0.002	0.000	0.195	0.002	0.078
10	0.4	0.575	1.667	0.542	5.675	0.089	0.020	1.354	0.002	0.008	1.618	0.0004	0.002	0.000	0.144	0.001	0.043
10	0.5	0.575	1.667	0.542	5.675	0.089	0.020	1.211	0.002	0.008	1.618	0.0003	0.002	0.000	0.113	0.001	0.027
10	0.6	0.575	1.667	0.542	5.675	0.089	0.020	1.105	0.002	0.008	1.618	0.0002	0.002	0.000	0.093	0.000	0.019
10	0.5	0.6	1.667	0.542	5.675	0.089	0.020	1.211	0.002	0.008	1.584	0.0003	0.002	0.000	0.113	0.001	0.027
10	0.4	0.6	1.667	0.542	5.675	0.089	0.020	1.354	0.002	0.008	1.584	0.0004	0.002	0.000	0.144	0.001	0.043
10	0.3	0.6	1.667	0.542	5.675	0.089	0.020	1.563	0.002	0.008	1.584	0.0005	0.002	0.000	0.195	0.002	0.078
10	0.2	0.6	1.667	0.542	5.675	0.089	0.020	1.914	0.002	0.008	1.584	0.0007	0.002	0.001	0.296	0.004	0.180
10	0.1	0.6	1.667	0.542	5.675	0.089	0.020	2.707	0.002	0.008	1.584	0.0014	0.002	0.001	0.601	0.018	0.737
10	0.62	0.6	1.667	0.542	5.675	0.089	0.020	1.087	0.002	0.008	1.584	0.0002	0.002	0.000	0.090	0.000	0.017
10	0.1	0.6	1.667	0.542	5.675	0.089	0.020	2.707	0.002	0.008	1.584	0.0014	0.002	0.001	0.601	0.018	0.737
10	0.2	0.6	1.667	0.542	5.675	0.089	0.020	1.914	0.002	0.008	1.584	0.0007	0.002	0.001	0.296	0.004	0.180
10	0.3	0.6	1.667	0.542	5.675	0.089	0.020	1.563	0.002	0.008	1.584	0.0005	0.002	0.000	0.195	0.002	0.078

Q	X	Z	V _z	Z _{core}	V _{zj}	h _{down}	h _{up}	V _{xmax}	q _{up}	q _{down}	V(z)	FQSI	G _b	I _{net}	V _{up}	H _{up}	H _{up} /z
l/s	m	m	m/s	m	m/s	m	m	m/s	m ² /s	m ² /s	m/s	Ns	kg/m ²	Ns	m/s	m	
			Q=VA	Z=5*B _j	Eq. 25	Eq. 61		Eq. 63	Eq. 61&62		Eq. 60	Fig.2.1 8	Eq. 59	Eq.55		Eq. 58	
10	0.4	0.6	1.667	0.542	5.675	0.089	0.020	1.354	0.002	0.008	1.584	0.0004	0.002	0.000	0.144	0.001	0.043
10	0.5	0.6	1.667	0.542	5.675	0.089	0.020	1.211	0.002	0.008	1.584	0.0003	0.002	0.000	0.113	0.001	0.027
10	0.6	0.6	1.667	0.542	5.675	0.089	0.020	1.105	0.002	0.008	1.584	0.0002	0.002	0.000	0.093	0.000	0.019
10	0.5	0.625	1.667	0.542	5.675	0.089	0.020	1.211	0.002	0.008	1.552	0.0003	0.002	0.000	0.113	0.001	0.027
10	0.4	0.625	1.667	0.542	5.675	0.089	0.020	1.354	0.002	0.008	1.552	0.0004	0.002	0.000	0.144	0.001	0.043
10	0.3	0.625	1.667	0.542	5.675	0.089	0.020	1.563	0.002	0.008	1.552	0.0005	0.002	0.000	0.195	0.002	0.078
10	0.2	0.625	1.667	0.542	5.675	0.089	0.020	1.914	0.002	0.008	1.552	0.0007	0.002	0.001	0.296	0.004	0.180
10	0.1	0.625	1.667	0.542	5.675	0.089	0.020	2.707	0.002	0.008	1.552	0.0014	0.002	0.001	0.601	0.018	0.737
10	0.62	0.625	1.667	0.542	5.675	0.089	0.020	1.087	0.002	0.008	1.552	0.0002	0.002	0.000	0.090	0.000	0.017
10	0.1	0.625	1.667	0.542	5.675	0.089	0.020	2.707	0.002	0.008	1.552	0.0014	0.002	0.001	0.601	0.018	0.737
10	0.2	0.625	1.667	0.542	5.675	0.089	0.020	1.914	0.002	0.008	1.552	0.0007	0.002	0.001	0.296	0.004	0.180
10	0.3	0.625	1.667	0.542	5.675	0.089	0.020	1.563	0.002	0.008	1.552	0.0005	0.002	0.000	0.195	0.002	0.078
10	0.4	0.625	1.667	0.542	5.675	0.089	0.020	1.354	0.002	0.008	1.552	0.0004	0.002	0.000	0.144	0.001	0.043
10	0.5	0.625	1.667	0.542	5.675	0.089	0.020	1.211	0.002	0.008	1.552	0.0003	0.002	0.000	0.113	0.001	0.027
10	0.6	0.625	1.667	0.542	5.675	0.089	0.020	1.105	0.002	0.008	1.552	0.0002	0.002	0.000	0.093	0.000	0.019
10	0.5	0.65	1.667	0.542	5.675	0.089	0.020	1.211	0.002	0.008	1.522	0.0003	0.002	0.000	0.113	0.001	0.027
10	0.4	0.65	1.667	0.542	5.675	0.089	0.020	1.354	0.002	0.008	1.522	0.0004	0.002	0.000	0.144	0.001	0.043
10	0.3	0.65	1.667	0.542	5.675	0.089	0.020	1.563	0.002	0.008	1.522	0.0005	0.002	0.000	0.195	0.002	0.078
10	0.2	0.65	1.667	0.542	5.675	0.089	0.020	1.914	0.002	0.008	1.522	0.0007	0.002	0.001	0.296	0.004	0.180
10	0.1	0.65	1.667	0.542	5.675	0.089	0.020	2.707	0.002	0.008	1.522	0.0014	0.002	0.001	0.601	0.018	0.737
10	0.62	0.65	1.667	0.542	5.675	0.089	0.020	1.087	0.002	0.008	1.522	0.0002	0.002	0.000	0.090	0.000	0.017
10	0.1	0.65	1.667	0.542	5.675	0.089	0.020	2.707	0.002	0.008	1.522	0.0014	0.002	0.001	0.601	0.018	0.737
10	0.2	0.65	1.667	0.542	5.675	0.089	0.020	1.914	0.002	0.008	1.522	0.0007	0.002	0.001	0.296	0.004	0.180

Q	X	Z	V _z	Z _{core}	V _{zj}	h _{down}	h _{up}	V _{xmax}	q _{up}	q _{down}	V(z)	FQSI	G _b	I _{net}	V _{up}	H _{up}	H _{up} /z
l/s	m	m	m/s	m	m/s	m	m	m/s	m ² /s	m ² /s	m/s	Ns	kg/m ²	Ns	m/s	m	
			Q=VA	Z=5*B _j	Eq. 25	Eq. 61		Eq. 63	Eq. 61&62		Eq. 60	Fig.2.1 8	Eq. 59	Eq.55		Eq. 58	
10	0.3	0.65	1.667	0.542	5.675	0.089	0.020	1.563	0.002	0.008	1.522	0.0005	0.002	0.000	0.195	0.002	0.078
10	0.4	0.65	1.667	0.542	5.675	0.089	0.020	1.354	0.002	0.008	1.522	0.0004	0.002	0.000	0.144	0.001	0.043
10	0.5	0.65	1.667	0.542	5.675	0.089	0.020	1.211	0.002	0.008	1.522	0.0003	0.002	0.000	0.113	0.001	0.027
10	0.6	0.65	1.667	0.542	5.675	0.089	0.020	1.105	0.002	0.008	1.522	0.0002	0.002	0.000	0.093	0.000	0.019
10	0.5	0.675	1.667	0.542	5.675	0.089	0.020	1.211	0.002	0.008	1.493	0.0003	0.002	0.000	0.113	0.001	0.027
10	0.4	0.675	1.667	0.542	5.675	0.089	0.020	1.354	0.002	0.008	1.493	0.0004	0.002	0.000	0.144	0.001	0.043
10	0.3	0.675	1.667	0.542	5.675	0.089	0.020	1.563	0.002	0.008	1.493	0.0005	0.002	0.000	0.195	0.002	0.078
10	0.2	0.675	1.667	0.542	5.675	0.089	0.020	1.914	0.002	0.008	1.493	0.0007	0.002	0.001	0.296	0.004	0.180
10	0.1	0.675	1.667	0.542	5.675	0.089	0.020	2.707	0.002	0.008	1.493	0.0014	0.002	0.001	0.601	0.018	0.737
10	0.62	0.675	1.667	0.542	5.675	0.089	0.020	1.087	0.002	0.008	1.493	0.0002	0.002	0.000	0.090	0.000	0.017
10	0.1	0.675	1.667	0.542	5.675	0.089	0.020	2.707	0.002	0.008	1.493	0.0014	0.002	0.001	0.601	0.018	0.737
10	0.2	0.675	1.667	0.542	5.675	0.089	0.020	1.914	0.002	0.008	1.493	0.0007	0.002	0.001	0.296	0.004	0.180
10	0.3	0.675	1.667	0.542	5.675	0.089	0.020	1.563	0.002	0.008	1.493	0.0005	0.002	0.000	0.195	0.002	0.078
10	0.4	0.675	1.667	0.542	5.675	0.089	0.020	1.354	0.002	0.008	1.493	0.0004	0.002	0.000	0.144	0.001	0.043
10	0.5	0.675	1.667	0.542	5.675	0.089	0.020	1.211	0.002	0.008	1.493	0.0003	0.002	0.000	0.113	0.001	0.027
10	0.6	0.675	1.667	0.542	5.675	0.089	0.020	1.105	0.002	0.008	1.493	0.0002	0.002	0.000	0.093	0.000	0.019
10	0.5	0.7	1.667	0.542	5.675	0.089	0.020	1.211	0.002	0.008	1.466	0.0003	0.002	0.000	0.113	0.001	0.026
10	0.4	0.7	1.667	0.542	5.675	0.089	0.020	1.354	0.002	0.008	1.466	0.0004	0.002	0.000	0.144	0.001	0.042
10	0.3	0.7	1.667	0.542	5.675	0.089	0.020	1.563	0.002	0.008	1.466	0.0005	0.002	0.000	0.195	0.002	0.077
10	0.2	0.7	1.667	0.542	5.675	0.089	0.020	1.914	0.002	0.008	1.466	0.0007	0.002	0.001	0.296	0.004	0.179
10	0.1	0.7	1.667	0.542	5.675	0.089	0.020	2.707	0.002	0.008	1.466	0.0014	0.002	0.001	0.601	0.018	0.736
10	0.62	0.7	1.667	0.542	5.675	0.089	0.020	1.087	0.002	0.008	1.466	0.0002	0.002	0.000	0.090	0.000	0.016
10	0.1	0.7	1.667	0.542	5.675	0.089	0.020	2.707	0.002	0.008	1.466	0.0014	0.002	0.001	0.601	0.018	0.736

Q	X	Z	V _z	Z _{core}	V _{zj}	h _{down}	h _{up}	V _{xmax}	q _{up}	q _{down}	V(z)	FQSI	G _b	I _{net}	V _{up}	H _{up}	H _{up} /z
l/s	m	m	m/s	m	m/s	m	m	m/s	m ² /s	m ² /s	m/s	Ns	kg/m ²	Ns	m/s	m	
			Q=VA	Z=5*B _j	eq. 25	Eq. 61		Eq. 63	Eq. 61&62		Eq. 60	Fig.2.1 8	Eq. 59	Eq.55		Eq. 58	
10	0.2	0.7	1.667	0.542	5.675	0.089	0.020	1.914	0.002	0.008	1.466	0.0007	0.002	0.001	0.296	0.004	0.179
10	0.3	0.7	1.667	0.542	5.675	0.089	0.020	1.563	0.002	0.008	1.466	0.0005	0.002	0.000	0.195	0.002	0.077
10	0.4	0.7	1.667	0.542	5.675	0.089	0.020	1.354	0.002	0.008	1.466	0.0004	0.002	0.000	0.144	0.001	0.042
10	0.5	0.7	1.667	0.542	5.675	0.089	0.020	1.211	0.002	0.008	1.466	0.0003	0.002	0.000	0.113	0.001	0.026
10	0.6	0.7	1.667	0.542	5.675	0.089	0.020	1.105	0.002	0.008	1.466	0.0002	0.002	0.000	0.093	0.000	0.018
10	0.5	0.725	1.667	0.542	5.675	0.089	0.020	1.211	0.002	0.008	1.441	0.0003	0.002	0.000	0.113	0.001	0.026
10	0.4	0.725	1.667	0.542	5.675	0.089	0.020	1.354	0.002	0.008	1.441	0.0004	0.002	0.000	0.144	0.001	0.042
10	0.3	0.725	1.667	0.542	5.675	0.089	0.020	1.563	0.002	0.008	1.441	0.0005	0.002	0.000	0.195	0.002	0.077
10	0.2	0.725	1.667	0.542	5.675	0.089	0.020	1.914	0.002	0.008	1.441	0.0007	0.002	0.001	0.296	0.004	0.179
10	0.1	0.725	1.667	0.542	5.675	0.089	0.020	2.707	0.002	0.008	1.441	0.0014	0.002	0.001	0.601	0.018	0.736
10	0.62	0.725	1.667	0.542	5.675	0.089	0.020	1.087	0.002	0.008	1.441	0.0002	0.002	0.000	0.090	0.000	0.016
10	0.1	0.725	1.667	0.542	5.675	0.089	0.020	2.707	0.002	0.008	1.441	0.0014	0.002	0.001	0.601	0.018	0.736
10	0.2	0.725	1.667	0.542	5.675	0.089	0.020	1.914	0.002	0.008	1.441	0.0007	0.002	0.001	0.296	0.004	0.179
10	0.3	0.725	1.667	0.542	5.675	0.089	0.020	1.563	0.002	0.008	1.441	0.0005	0.002	0.000	0.195	0.002	0.077
10	0.4	0.725	1.667	0.542	5.675	0.089	0.020	1.354	0.002	0.008	1.441	0.0004	0.002	0.000	0.144	0.001	0.042
10	0.5	0.725	1.667	0.542	5.675	0.089	0.020	1.211	0.002	0.008	1.441	0.0003	0.002	0.000	0.113	0.001	0.026
10	0.6	0.725	1.667	0.542	5.675	0.089	0.020	1.105	0.002	0.008	1.441	0.0002	0.002	0.000	0.093	0.000	0.018
10	0.5	0.75	1.667	0.542	5.675	0.089	0.020	1.211	0.002	0.008	1.417	0.0003	0.002	0.000	0.113	0.001	0.026
10	0.4	0.75	1.667	0.542	5.675	0.089	0.020	1.354	0.002	0.008	1.417	0.0004	0.002	0.000	0.144	0.001	0.042
10	0.3	0.75	1.667	0.542	5.675	0.089	0.020	1.563	0.002	0.008	1.417	0.0005	0.002	0.000	0.195	0.002	0.077
10	0.2	0.75	1.667	0.542	5.675	0.089	0.020	1.914	0.002	0.008	1.417	0.0007	0.002	0.001	0.296	0.004	0.179
10	0.1	0.75	1.667	0.542	5.675	0.089	0.020	2.707	0.002	0.008	1.417	0.0014	0.002	0.001	0.601	0.018	0.736
10	0.62	0.75	1.667	0.542	5.675	0.089	0.020	1.087	0.002	0.008	1.417	0.0002	0.002	0.000	0.090	0.000	0.016

Q	X	Z	V _z	Z _{core}	V _{zj}	h _{down}	h _{up}	V _{xmax}	q _{up}	q _{down}	V(z)	FQSI	G _b	I _{net}	V _{up}	H _{up}	H _{up} /z
l/s	m	m	m/s	m	m/s	m	m	m/s	m ² /s	m ² /s	m/s	Ns	kg/m ²	Ns	m/s	m	
			Q=VA	Z=5*B _j	Eq. 25	Eq. 61		Eq. 63	Eq. 61&62		Eq. 60	Fig.2.1 8	Eq. 59	Eq.55		Eq. 55	
10	0.1	0.75	1.667	0.542	5.675	0.089	0.020	2.707	0.002	0.008	1.417	0.0014	0.002	0.001	0.601	0.018	0.736
10	0.2	0.75	1.667	0.542	5.675	0.089	0.020	1.914	0.002	0.008	1.417	0.0007	0.002	0.001	0.296	0.004	0.179
10	0.3	0.75	1.667	0.542	5.675	0.089	0.020	1.563	0.002	0.008	1.417	0.0005	0.002	0.000	0.195	0.002	0.077
10	0.4	0.75	1.667	0.542	5.675	0.089	0.020	1.354	0.002	0.008	1.417	0.0004	0.002	0.000	0.144	0.001	0.042
10	0.5	0.75	1.667	0.542	5.675	0.089	0.020	1.211	0.002	0.008	1.417	0.0003	0.002	0.000	0.113	0.001	0.026
10	0.6	0.75	1.667	0.542	5.675	0.089	0.020	1.105	0.002	0.008	1.417	0.0002	0.002	0.000	0.093	0.000	0.018
10	0.5	0.775	1.667	0.542	5.675	0.089	0.020	1.211	0.002	0.008	1.394	0.0003	0.002	0.000	0.113	0.001	0.026
10	0.4	0.775	1.667	0.542	5.675	0.089	0.020	1.354	0.002	0.008	1.394	0.0004	0.002	0.000	0.144	0.001	0.042
10	0.3	0.775	1.667	0.542	5.675	0.089	0.020	1.563	0.002	0.008	1.394	0.0005	0.002	0.000	0.195	0.002	0.077
10	0.2	0.775	1.667	0.542	5.675	0.089	0.020	1.914	0.002	0.008	1.394	0.0007	0.002	0.001	0.296	0.004	0.179
10	0.1	0.775	1.667	0.542	5.675	0.089	0.020	2.707	0.002	0.008	1.394	0.0014	0.002	0.001	0.601	0.018	0.736
10	0.62	0.775	1.667	0.542	5.675	0.089	0.020	1.087	0.002	0.008	1.394	0.0002	0.002	0.000	0.090	0.000	0.016
10	0.1	0.775	1.667	0.542	5.675	0.089	0.020	2.707	0.002	0.008	1.394	0.0014	0.002	0.001	0.601	0.018	0.736
10	0.2	0.775	1.667	0.542	5.675	0.089	0.020	1.914	0.002	0.008	1.394	0.0007	0.002	0.001	0.296	0.004	0.179
10	0.3	0.775	1.667	0.542	5.675	0.089	0.020	1.563	0.002	0.008	1.394	0.0005	0.002	0.000	0.195	0.002	0.077
10	0.4	0.775	1.667	0.542	5.675	0.089	0.020	1.354	0.002	0.008	1.394	0.0004	0.002	0.000	0.144	0.001	0.042
10	0.5	0.775	1.667	0.542	5.675	0.089	0.020	1.211	0.002	0.008	1.394	0.0003	0.002	0.000	0.113	0.001	0.026
10	0.6	0.775	1.667	0.542	5.675	0.089	0.020	1.105	0.002	0.008	1.394	0.0002	0.002	0.000	0.093	0.000	0.018
10	0.5	0.8	1.667	0.542	5.675	0.089	0.020	1.211	0.002	0.008	1.372	0.0003	0.002	0.000	0.113	0.001	0.026
10	0.4	0.8	1.667	0.542	5.675	0.089	0.020	1.354	0.002	0.008	1.372	0.0004	0.002	0.000	0.144	0.001	0.042
10	0.3	0.8	1.667	0.542	5.675	0.089	0.020	1.563	0.002	0.008	1.372	0.0005	0.002	0.000	0.195	0.002	0.077
10	0.2	0.8	1.667	0.542	5.675	0.089	0.020	1.914	0.002	0.008	1.372	0.0007	0.002	0.001	0.296	0.004	0.179
10	0.1	0.8	1.667	0.542	5.675	0.089	0.020	2.707	0.002	0.008	1.372	0.0014	0.002	0.001	0.601	0.018	0.736

Q	X	Z	V_z	Z_{core}	V_z	h_{down}	h_{up}	V_{xmax}	q_{up}	q_{down}	V(z)	FQSI	G_b	I_{net}	V_{up}	H_{up}	H_{up}/z
l/s	m	m	m/s	m	m/s	m	m	m/s	m ² /s	m ² /s	m/s	Ns	kg/m ²	Ns	m/s	m	
			Q=VA	Z=5*B _j	Eq. 25	Eq.61		Eq. 63	Eq. 61&62		Eq. 60	Fig.2.1 8	Eq. 59	Eq.55		Eq. 58	
10	0.62	0.8	1.667	0.542	5.675	0.089	0.020	1.087	0.002	0.008	1.372	0.0002	0.002	0.000	0.090	0.000	0.016
10	0.1	0.8	1.667	0.542	5.675	0.089	0.020	2.707	0.002	0.008	1.372	0.0014	0.002	0.001	0.601	0.018	0.736
10	0.2	0.8	1.667	0.542	5.675	0.089	0.020	1.914	0.002	0.008	1.372	0.0007	0.002	0.001	0.296	0.004	0.179
10	0.3	0.8	1.667	0.542	5.675	0.089	0.020	1.563	0.002	0.008	1.372	0.0005	0.002	0.000	0.195	0.002	0.077
10	0.4	0.8	1.667	0.542	5.675	0.089	0.020	1.354	0.002	0.008	1.372	0.0004	0.002	0.000	0.144	0.001	0.042
10	0.5	0.8	1.667	0.542	5.675	0.089	0.020	1.211	0.002	0.008	1.372	0.0003	0.002	0.000	0.113	0.001	0.026
10	0.6	0.8	1.667	0.542	5.675	0.089	0.020	1.105	0.002	0.008	1.372	0.0002	0.002	0.000	0.093	0.000	0.018
10	0.5	0.825	1.667	0.542	5.675	0.089	0.020	1.211	0.002	0.008	1.351	0.0003	0.002	0.000	0.113	0.001	0.026
10	0.4	0.825	1.667	0.542	5.675	0.089	0.020	1.354	0.002	0.008	1.351	0.0004	0.002	0.000	0.144	0.001	0.042
10	0.3	0.825	1.667	0.542	5.675	0.089	0.020	1.563	0.002	0.008	1.351	0.0005	0.002	0.000	0.195	0.002	0.077
10	0.2	0.825	1.667	0.542	5.675	0.089	0.020	1.914	0.002	0.008	1.351	0.0007	0.002	0.001	0.296	0.004	0.179
10	0.1	0.825	1.667	0.542	5.675	0.089	0.020	2.707	0.002	0.008	1.351	0.0014	0.002	0.001	0.601	0.018	0.736
10	0.62	0.825	1.667	0.542	5.675	0.089	0.020	1.087	0.002	0.008	1.351	0.0002	0.002	0.000	0.090	0.000	0.016
10	0.1	0.825	1.667	0.542	5.675	0.089	0.020	2.707	0.002	0.008	1.351	0.0014	0.002	0.001	0.601	0.018	0.736
10	0.2	0.825	1.667	0.542	5.675	0.089	0.020	1.914	0.002	0.008	1.351	0.0007	0.002	0.001	0.296	0.004	0.179
10	0.3	0.825	1.667	0.542	5.675	0.089	0.020	1.563	0.002	0.008	1.351	0.0005	0.002	0.000	0.195	0.002	0.077
10	0.4	0.825	1.667	0.542	5.675	0.089	0.020	1.354	0.002	0.008	1.351	0.0004	0.002	0.000	0.144	0.001	0.042
10	0.5	0.825	1.667	0.542	5.675	0.089	0.020	1.211	0.002	0.008	1.351	0.0003	0.002	0.000	0.113	0.001	0.026
10	0.6	0.825	1.667	0.542	5.675	0.089	0.020	1.105	0.002	0.008	1.351	0.0002	0.002	0.000	0.093	0.000	0.018

Table D 0.2. Quasi-steady method of Q=20L l/s, H=2 m and TW= 0.5 m

Q	X	Z	V _{zi}	Z _{core}	V _{zj}	h _{down}	h _{up}	V _{xmax}	q _{up}	q _{down}	V(z)	FQSI	G _b	I _{net}	V _{up}	H _{up}	H _{up} /z
l/s	m	m	m/s	m	m/s	m	m	m/s	m ² /s	m ² /s	m/s	Ns	kg/m ²	Ns	m/s	m	
			Q=V A	Z=5*Bj	Eq. 25	Eq. 61		Eq. 63	Eq.61&62		Eq. 60	Fig.2.18	Eq. 59	Eq.55		Eq. 58	
20	0.7	0	2	0.59	5.78	0.052	0.065	2.319	0.011	0.009	5.782						
20	0.7	0.042	2	0.59	5.78	0.052	0.065	2.319	0.011	0.009	7.514						
20	0.7	0.083	2	0.59	5.78	0.052	0.065	2.319	0.011	0.009	5.313						
20	0.7	0.125	2	0.59	5.78	0.052	0.065	2.319	0.011	0.009	4.338						
20	0.7	0.167	2	0.59	5.78	0.052	0.065	2.319	0.011	0.009	3.757						
20	0.7	0.208	2	0.59	5.78	0.052	0.065	2.319	0.011	0.009	3.360						
20	0.7	0.250	2	0.59	5.78	0.052	0.065	2.319	0.011	0.009	3.068						
20	0.7	0.292	2	0.59	5.78	0.052	0.065	2.319	0.011	0.009	2.840						
20	0.7	0.333	2	0.59	5.78	0.052	0.065	2.319	0.011	0.009	2.657						
20	0.7	0.375	2	0.59	5.78	0.052	0.065	2.319	0.011	0.009	2.505						
20	0.7	0.417	2	0.59	5.78	0.052	0.065	2.319	0.011	0.009	2.376						
20	0.7	0.458	2	0.59	5.78	0.052	0.065	2.319	0.011	0.009	2.266						
20	0.7	0.5	2	0.59	5.78	0.052	0.065	2.319	0.011	0.009	2.169						
20	0.5	0.5	2	0.59	5.78	0.052	0.065	2.744	0.011	0.009	2.169	0.001	0.002	0.001	0.618	0.019	0.777
20	0.4	0.5	2	0.59	5.78	0.052	0.065	3.068	0.011	0.009	2.169	0.002	0.002	0.002	0.774	0.031	1.221
20	0.3	0.5	2	0.59	5.78	0.052	0.065	3.542	0.011	0.009	2.169	0.002	0.002	0.002	1.035	0.055	2.183
20	0.2	0.5	2	0.59	5.78	0.052	0.065	4.338	0.011	0.009	2.169	0.004	0.002	0.004	1.557	0.123	4.940
20	0.1	0.5	2	0.59	5.78	0.052	0.065	6.135	0.011	0.009	2.169	0.007	0.002	0.007	3.122	0.497	19.867
20	0.7	0.5	2	0.59	5.78	0.052	0.065	2.076	0.011	0.009	2.169	0.001	0.002	0.001	0.350	0.006	0.249
20	0.1	0.5	2	0.59	5.78	0.052	0.065	5.492	0.011	0.009	2.169	0.006	0.002	0.006	2.499	0.318	12.735
20	0.2	0.5	2	0.59	5.78	0.052	0.065	3.883	0.011	0.009	2.169	0.003	0.002	0.003	1.245	0.079	3.162
20	0.3	0.5	2	0.59	5.78	0.052	0.065	3.171	0.011	0.009	2.169	0.002	0.002	0.002	0.827	0.035	1.396
20	0.4	0.5	2	0.59	5.78	0.052	0.065	2.746	0.011	0.009	2.169	0.001	0.002	0.001	0.618	0.019	0.780
20	0.5	0.5	2	0.59	5.78	0.052	0.065	2.456	0.011	0.009	2.169	0.001	0.002	0.001	0.493	0.012	0.496

Q	X	Z	V _{zi}	Z _{core}	V _{zj}	h _{down}	h _{up}	V _{xmax}	q _{up}	q _{down}	V(z)	FQSI	G _b	I _{net}	V _{up}	H _{up}	H _{up} /z
l/s	m	m	m/s	m	m/s	m	m	m/s	m ² /s	m ² /s	m/s	Ns	kg/m ²	Ns	m/s	m	
			Q=V A	Z=5*Bj	Eq. 25	Eq. 61		Eq. 63	Eq.61&62		Eq. 60	Fig.2.18	Eq. 59	Eq.55		Eq. 58	
20	0.6	0.5	2	0.59	5.78	0.052	0.065	2.242	0.011	0.009	2.169	0.001	0.002	0.001	0.409	0.009	0.342
20	0.5	0.525	2	0.59	5.78	0.052	0.065	2.678	0.011	0.009	2.117	0.001	0.002	0.001	0.588	0.018	0.704
20	0.4	0.525	2	0.59	5.78	0.052	0.065	2.994	0.011	0.009	2.117	0.002	0.002	0.002	0.737	0.028	1.107
20	0.3	0.525	2	0.59	5.78	0.052	0.065	3.457	0.011	0.009	2.117	0.002	0.002	0.002	0.985	0.049	1.979
20	0.2	0.525	2	0.59	5.78	0.052	0.065	4.234	0.011	0.009	2.117	0.004	0.002	0.004	1.482	0.112	4.478
20	0.1	0.525	2	0.59	5.78	0.052	0.065	5.987	0.011	0.009	2.117	0.007	0.002	0.007	2.973	0.450	18.015
20	0.7	0.525	2	0.59	5.78	0.052	0.065	2.026	0.011	0.009	2.117	0.001	0.002	0.001	0.333	0.006	0.226
20	0.1	0.525	2	0.59	5.78	0.052	0.065	5.359	0.011	0.009	2.117	0.006	0.002	0.006	2.380	0.289	11.547
20	0.2	0.525	2	0.59	5.78	0.052	0.065	3.790	0.011	0.009	2.117	0.003	0.002	0.003	1.186	0.072	2.866
20	0.3	0.525	2	0.59	5.78	0.052	0.065	3.094	0.011	0.009	2.117	0.002	0.002	0.002	0.788	0.032	1.265
20	0.4	0.525	2	0.59	5.78	0.052	0.065	2.680	0.011	0.009	2.117	0.001	0.002	0.001	0.589	0.018	0.706
20	0.5	0.525	2	0.59	5.78	0.052	0.065	2.397	0.011	0.009	2.117	0.001	0.002	0.001	0.469	0.011	0.449
20	0.6	0.525	2	0.59	5.78	0.052	0.065	2.188	0.011	0.009	2.117	0.001	0.002	0.001	0.390	0.008	0.309
20	0.5	0.55	2	0.59	5.78	0.052	0.065	2.616	0.011	0.009	2.068	0.001	0.002	0.001	0.561	0.016	0.641
20	0.4	0.55	2	0.59	5.78	0.052	0.065	2.925	0.011	0.009	2.068	0.002	0.002	0.002	0.703	0.025	1.007
20	0.3	0.55	2	0.59	5.78	0.052	0.065	3.377	0.011	0.009	2.068	0.002	0.002	0.002	0.940	0.045	1.801
20	0.2	0.55	2	0.59	5.78	0.052	0.065	4.136	0.011	0.009	2.068	0.003	0.002	0.003	1.414	0.102	4.078
20	0.1	0.55	2	0.59	5.78	0.052	0.065	5.850	0.011	0.009	2.068	0.007	0.002	0.007	2.837	0.410	16.410
20	0.7	0.55	2	0.59	5.78	0.052	0.065	1.979	0.011	0.009	2.068	0.001	0.002	0.001	0.317	0.005	0.205
20	0.1	0.55	2	0.59	5.78	0.052	0.065	5.236	0.011	0.009	2.068	0.005	0.002	0.005	2.271	0.263	10.518
20	0.2	0.55	2	0.59	5.78	0.052	0.065	3.702	0.011	0.009	2.068	0.003	0.002	0.003	1.131	0.065	2.610
20	0.3	0.55	2	0.59	5.78	0.052	0.065	3.023	0.011	0.009	2.068	0.002	0.002	0.002	0.751	0.029	1.151
20	0.4	0.55	2	0.59	5.78	0.052	0.065	2.618	0.011	0.009	2.068	0.001	0.002	0.001	0.561	0.016	0.643
20	0.5	0.55	2	0.59	5.78	0.052	0.065	2.342	0.011	0.009	2.068	0.001	0.002	0.001	0.447	0.010	0.408

Q	X	Z	V _{zi}	Z _{core}	V _{zj}	h _{down}	h _{up}	V _{xmax}	q _{up}	q _{down}	V(z)	FQSI	G _b	I _{net}	V _{up}	H _{up}	H _{up} /z
l/s	m	m	m/s	m	m/s	m	m	m/s	m ² /s	m ² /s	m/s	Ns	kg/m ²	Ns	m/s	m	
			Q=V A	Z=5*Bj	Eq. 25	Eq. 61		Eq. 63	Eq. 61&62		Eq. 60	Fig.2.18	Eq. 59	Eq.55		Eq. 58	
20	0.6	0.55	2	0.59	5.78	0.052	0.065	2.138	0.011	0.009	2.068	0.001	0.002	0.001	0.371	0.007	0.281
20	0.5	0.575	2	0.59	5.78	0.052	0.065	2.559	0.011	0.009	2.023	0.001	0.002	0.001	0.536	0.015	0.585
20	0.4	0.575	2	0.59	5.78	0.052	0.065	2.861	0.011	0.009	2.023	0.002	0.002	0.002	0.672	0.023	0.921
20	0.3	0.575	2	0.59	5.78	0.052	0.065	3.303	0.011	0.009	2.023	0.002	0.002	0.002	0.899	0.041	1.647
20	0.2	0.575	2	0.59	5.78	0.052	0.065	4.045	0.011	0.009	2.023	0.003	0.002	0.003	1.352	0.093	3.729
20	0.1	0.575	2	0.59	5.78	0.052	0.065	5.721	0.011	0.009	2.023	0.006	0.002	0.006	2.713	0.375	15.010
20	0.7	0.575	2	0.59	5.78	0.052	0.065	1.936	0.011	0.009	2.023	0.001	0.002	0.001	0.303	0.005	0.187
20	0.1	0.575	2	0.59	5.78	0.052	0.065	5.121	0.011	0.009	2.023	0.005	0.002	0.005	2.172	0.240	9.620
20	0.2	0.575	2	0.59	5.78	0.052	0.065	3.621	0.011	0.009	2.023	0.003	0.002	0.003	1.082	0.060	2.386
20	0.3	0.575	2	0.59	5.78	0.052	0.065	2.957	0.011	0.009	2.023	0.002	0.002	0.002	0.718	0.026	1.052
20	0.4	0.575	2	0.59	5.78	0.052	0.065	2.560	0.011	0.009	2.023	0.001	0.002	0.001	0.537	0.015	0.587
20	0.5	0.575	2	0.59	5.78	0.052	0.065	2.290	0.011	0.009	2.023	0.001	0.002	0.001	0.428	0.009	0.373
20	0.6	0.575	2	0.59	5.78	0.052	0.065	2.091	0.011	0.009	2.023	0.001	0.002	0.001	0.355	0.006	0.257
20	0.5	0.6	2	0.59	5.78	0.052	0.065	2.505	0.011	0.009	1.980	0.001	0.002	0.001	0.513	0.013	0.537
20	0.4	0.6	2	0.59	5.78	0.052	0.065	2.800	0.011	0.009	1.980	0.002	0.002	0.002	0.644	0.021	0.844
20	0.3	0.6	2	0.59	5.78	0.052	0.065	3.234	0.011	0.009	1.980	0.002	0.002	0.002	0.861	0.038	1.511
20	0.2	0.6	2	0.59	5.78	0.052	0.065	3.960	0.011	0.009	1.980	0.003	0.002	0.003	1.296	0.086	3.423
20	0.1	0.6	2	0.59	5.78	0.052	0.065	5.601	0.011	0.009	1.980	0.006	0.002	0.006	2.600	0.345	13.781
20	0.7	0.6	2	0.59	5.78	0.052	0.065	1.895	0.011	0.009	1.980	0.001	0.002	0.001	0.290	0.004	0.171
20	0.1	0.6	2	0.59	5.78	0.052	0.065	5.013	0.011	0.009	1.980	0.005	0.002	0.005	2.081	0.221	8.832
20	0.2	0.6	2	0.59	5.78	0.052	0.065	3.545	0.011	0.009	1.980	0.002	0.002	0.002	1.036	0.055	2.190
20	0.3	0.6	2	0.59	5.78	0.052	0.065	2.894	0.011	0.009	1.980	0.002	0.002	0.002	0.688	0.024	0.965
20	0.4	0.6	2	0.59	5.78	0.052	0.065	2.507	0.011	0.009	1.980	0.001	0.002	0.001	0.514	0.013	0.538
20	0.5	0.6	2	0.59	5.78	0.052	0.065	2.242	0.011	0.009	1.980	0.001	0.002	0.001	0.409	0.009	0.342

Q	X	Z	V _{zi}	Z _{core}	V _{zj}	h _{down}	h _{up}	V _{xmax}	q _{up}	q _{down}	V(z)	FQSI	G _b	I _{net}	V _{up}	H _{up}	H _{up} /z
l/s	m	m	m/s	m	m/s	m	m	m/s	m ² /s	m ² /s	m/s	Ns	kg/m ²	Ns	m/s	m	
			Q=V A	Z=5*Bj	Eq. 25	Eq.61		Eq. 63	Eq.61&62		Eq. 60	Fig.2.18	Eq. 59	Eq.55		Eq. 58	
20	0.6	0.6	2	0.59	5.78	0.052	0.065	2.047	0.011	0.009	1.980	0.001	0.002	0.001	0.340	0.006	0.235
20	0.5	0.625	2	0.59	5.78	0.052	0.065	2.454	0.011	0.009	1.940	0.001	0.002	0.001	0.492	0.012	0.494
20	0.4	0.625	2	0.59	5.78	0.052	0.065	2.744	0.011	0.009	1.940	0.001	0.002	0.001	0.618	0.019	0.777
20	0.3	0.625	2	0.59	5.78	0.052	0.065	3.168	0.011	0.009	1.940	0.002	0.002	0.002	0.826	0.035	1.392
20	0.2	0.625	2	0.59	5.78	0.052	0.065	3.880	0.011	0.009	1.940	0.003	0.002	0.003	1.244	0.079	3.153
20	0.1	0.625	2	0.59	5.78	0.052	0.065	5.488	0.011	0.009	1.940	0.006	0.002	0.006	2.496	0.317	12.698
20	0.7	0.625	2	0.59	5.78	0.052	0.065	1.856	0.011	0.009	1.940	0.001	0.002	0.001	0.278	0.004	0.158
20	0.1	0.625	2	0.59	5.78	0.052	0.065	4.912	0.011	0.009	1.940	0.005	0.002	0.005	1.998	0.203	8.136
20	0.2	0.625	2	0.59	5.78	0.052	0.065	3.473	0.011	0.009	1.940	0.002	0.002	0.002	0.995	0.050	2.017
20	0.3	0.625	2	0.59	5.78	0.052	0.065	2.836	0.011	0.009	1.940	0.002	0.002	0.002	0.660	0.022	0.889
20	0.4	0.625	2	0.59	5.78	0.052	0.065	2.456	0.011	0.009	1.940	0.001	0.002	0.001	0.493	0.012	0.496
20	0.5	0.625	2	0.59	5.78	0.052	0.065	2.197	0.011	0.009	1.940	0.001	0.002	0.001	0.393	0.008	0.314
20	0.6	0.625	2	0.59	5.78	0.052	0.065	2.005	0.011	0.009	1.940	0.001	0.002	0.001	0.326	0.005	0.216
20	0.5	0.65	2	0.59	5.78	0.052	0.065	2.406	0.011	0.009	1.902	0.001	0.002	0.001	0.473	0.011	0.456
20	0.4	0.65	2	0.59	5.78	0.052	0.065	2.690	0.011	0.009	1.902	0.001	0.002	0.001	0.593	0.018	0.718
20	0.3	0.65	2	0.59	5.78	0.052	0.065	3.107	0.011	0.009	1.902	0.002	0.002	0.002	0.794	0.032	1.286
20	0.2	0.65	2	0.59	5.78	0.052	0.065	3.805	0.011	0.009	1.902	0.003	0.002	0.003	1.195	0.073	2.913
20	0.1	0.65	2	0.59	5.78	0.052	0.065	5.381	0.011	0.009	1.902	0.006	0.002	0.006	2.399	0.293	11.736
20	0.7	0.65	2	0.59	5.78	0.052	0.065	1.820	0.011	0.009	1.902	0.001	0.002	0.001	0.267	0.004	0.145
20	0.1	0.65	2	0.59	5.78	0.052	0.065	4.816	0.011	0.009	1.902	0.005	0.002	0.005	1.921	0.188	7.520
20	0.2	0.65	2	0.59	5.78	0.052	0.065	3.406	0.011	0.009	1.902	0.002	0.002	0.002	0.956	0.047	1.863
20	0.3	0.65	2	0.59	5.78	0.052	0.065	2.781	0.011	0.009	1.902	0.002	0.002	0.002	0.635	0.021	0.821
20	0.4	0.65	2	0.59	5.78	0.052	0.065	2.408	0.011	0.009	1.902	0.001	0.002	0.001	0.474	0.011	0.458
20	0.5	0.65	2	0.59	5.78	0.052	0.065	2.154	0.011	0.009	1.902	0.001	0.002	0.001	0.377	0.007	0.290

Q	X	Z	V _{zi}	Z _{core}	V _{zj}	h _{down}	h _{up}	V _{xmax}	q _{up}	q _{down}	V(z)	FQSI	G _b	I _{net}	V _{up}	H _{up}	H _{up} /z
l/s	m	m	m/s	m	m/s	m	m	m/s	m ² /s	m ² /s	m/s	Ns	kg/m ²	Ns	m/s	m	
			Q=V A	Z=5*Bj	Eq. 25	Eq.61		Eq. 63	Eq. 61&62		Eq. 60	Fig.2.18	Eq. 59	Eq.55		Eq. 58	
20	0.6	0.65	2	0.59	5.78	0.052	0.065	1.966	0.011	0.009	1.902	0.001	0.002	0.001	0.313	0.005	0.200
20	0.5	0.675	2	0.59	5.78	0.052	0.065	2.361	0.011	0.009	1.867	0.001	0.002	0.001	0.455	0.011	0.422
20	0.4	0.675	2	0.59	5.78	0.052	0.065	2.640	0.011	0.009	1.867	0.001	0.002	0.001	0.571	0.017	0.665
20	0.3	0.675	2	0.59	5.78	0.052	0.065	3.049	0.011	0.009	1.867	0.002	0.002	0.002	0.764	0.030	1.191
20	0.2	0.675	2	0.59	5.78	0.052	0.065	3.734	0.011	0.009	1.867	0.003	0.002	0.003	1.151	0.067	2.700
20	0.1	0.675	2	0.59	5.78	0.052	0.065	5.280	0.011	0.009	1.867	0.006	0.002	0.005	2.310	0.272	10.880
20	0.7	0.675	2	0.59	5.78	0.052	0.065	1.786	0.011	0.009	1.867	0.001	0.002	0.001	0.257	0.003	0.134
20	0.1	0.675	2	0.59	5.78	0.052	0.065	4.726	0.011	0.009	1.867	0.004	0.002	0.004	1.849	0.174	6.971
20	0.2	0.675	2	0.59	5.78	0.052	0.065	3.342	0.011	0.009	1.867	0.002	0.002	0.002	0.920	0.043	1.727
20	0.3	0.675	2	0.59	5.78	0.052	0.065	2.729	0.011	0.009	1.867	0.001	0.002	0.001	0.611	0.019	0.760
20	0.4	0.675	2	0.59	5.78	0.052	0.065	2.363	0.011	0.009	1.867	0.001	0.002	0.001	0.456	0.011	0.424
20	0.5	0.675	2	0.59	5.78	0.052	0.065	2.114	0.011	0.009	1.867	0.001	0.002	0.001	0.363	0.007	0.269
20	0.6	0.675	2	0.59	5.78	0.052	0.065	1.930	0.011	0.009	1.867	0.001	0.002	0.001	0.301	0.005	0.185
20	0.5	0.7	2	0.59	5.78	0.052	0.065	2.319	0.011	0.009	1.833	0.001	0.002	0.001	0.439	0.010	0.392
20	0.4	0.7	2	0.59	5.78	0.052	0.065	2.593	0.011	0.009	1.833	0.001	0.002	0.001	0.550	0.015	0.618
20	0.3	0.7	2	0.59	5.78	0.052	0.065	2.994	0.011	0.009	1.833	0.002	0.002	0.002	0.737	0.028	1.107
20	0.2	0.7	2	0.59	5.78	0.052	0.065	3.667	0.011	0.009	1.833	0.003	0.002	0.003	1.109	0.063	2.509
20	0.1	0.7	2	0.59	5.78	0.052	0.065	5.185	0.011	0.009	1.833	0.005	0.002	0.005	2.227	0.253	10.114
20	0.7	0.7	2	0.59	5.78	0.052	0.065	1.754	0.011	0.009	1.833	0.001	0.002	0.001	0.247	0.003	0.125
20	0.1	0.7	2	0.59	5.78	0.052	0.065	4.641	0.011	0.009	1.833	0.004	0.002	0.004	1.783	0.162	6.480
20	0.2	0.7	2	0.59	5.78	0.052	0.065	3.282	0.011	0.009	1.833	0.002	0.002	0.002	0.887	0.040	1.604
20	0.3	0.7	2	0.59	5.78	0.052	0.065	2.680	0.011	0.009	1.833	0.001	0.002	0.001	0.589	0.018	0.706
20	0.4	0.7	2	0.59	5.78	0.052	0.065	2.321	0.011	0.009	1.833	0.001	0.002	0.001	0.439	0.010	0.393
20	0.5	0.7	2	0.59	5.78	0.052	0.065	2.076	0.011	0.009	1.833	0.001	0.002	0.001	0.350	0.006	0.249

Q	X	Z	V _{zi}	Z _{core}	V _{zj}	h _{down}	h _{up}	V _{xmax}	q _{up}	q _{down}	V(z)	FQSI	G _b	I _{net}	V _{up}	H _{up}	H _{up} /z
l/s	m	m	m/s	m	m/s	m	m	m/s	m ² /s	m ² /s	m/s	Ns	kg/m ²	Ns	m/s	m	
			Q=V A	Z=5*Bj	Eq. 25	Eq. 61		Eq. 63	Eq.61&62		Eq. 60	Fig.2.18	Eq. 59	Eq.55		Eq. 58	
20	0.6	0.7	2	0.59	5.78	0.052	0.065	1.895	0.011	0.009	1.833	0.001	0.002	0.001	0.290	0.004	0.171
20	0.5	0.725	2	0.59	5.78	0.052	0.065	2.279	0.011	0.009	1.801	0.001	0.002	0.001	0.423	0.009	0.365
20	0.4	0.725	2	0.59	5.78	0.052	0.065	2.548	0.011	0.009	1.801	0.001	0.002	0.001	0.531	0.014	0.575
20	0.3	0.725	2	0.59	5.78	0.052	0.065	2.942	0.011	0.009	1.801	0.002	0.002	0.002	0.711	0.026	1.031
20	0.2	0.725	2	0.59	5.78	0.052	0.065	3.603	0.011	0.009	1.801	0.003	0.002	0.003	1.071	0.058	2.338
20	0.1	0.725	2	0.59	5.78	0.052	0.065	5.095	0.011	0.009	1.801	0.005	0.002	0.005	2.150	0.236	9.426
20	0.7	0.725	2	0.59	5.78	0.052	0.065	1.724	0.011	0.009	1.801	0.001	0.002	0.001	0.239	0.003	0.116
20	0.1	0.725	2	0.59	5.78	0.052	0.065	4.560	0.011	0.009	1.801	0.004	0.002	0.004	1.721	0.151	6.038
20	0.2	0.725	2	0.59	5.78	0.052	0.065	3.225	0.011	0.009	1.801	0.002	0.002	0.002	0.856	0.037	1.495
20	0.3	0.725	2	0.59	5.78	0.052	0.065	2.633	0.011	0.009	1.801	0.001	0.002	0.001	0.568	0.016	0.658
20	0.4	0.725	2	0.59	5.78	0.052	0.065	2.280	0.011	0.009	1.801	0.001	0.002	0.001	0.424	0.009	0.366
20	0.5	0.725	2	0.59	5.78	0.052	0.065	2.040	0.011	0.009	1.801	0.001	0.002	0.001	0.337	0.006	0.232
20	0.6	0.725	2	0.59	5.78	0.052	0.065	1.862	0.011	0.009	1.801	0.001	0.002	0.001	0.280	0.004	0.160
20	0.5	0.75	2	0.59	5.78	0.052	0.065	2.240	0.011	0.009	1.771	0.001	0.002	0.001	0.409	0.009	0.341
20	0.4	0.75	2	0.59	5.78	0.052	0.065	2.505	0.011	0.009	1.771	0.001	0.002	0.001	0.513	0.013	0.537
20	0.3	0.75	2	0.59	5.78	0.052	0.065	2.892	0.011	0.009	1.771	0.002	0.002	0.002	0.687	0.024	0.962
20	0.2	0.75	2	0.59	5.78	0.052	0.065	3.542	0.011	0.009	1.771	0.002	0.002	0.002	1.035	0.055	2.183
20	0.1	0.75	2	0.59	5.78	0.052	0.065	5.009	0.011	0.009	1.771	0.005	0.002	0.005	2.078	0.220	8.806
20	0.7	0.75	2	0.59	5.78	0.052	0.065	1.695	0.011	0.009	1.771	0.001	0.002	0.001	0.230	0.003	0.108
20	0.1	0.75	2	0.59	5.78	0.052	0.065	4.484	0.011	0.009	1.771	0.004	0.002	0.004	1.663	0.141	5.641
20	0.2	0.75	2	0.59	5.78	0.052	0.065	3.171	0.011	0.009	1.771	0.002	0.002	0.002	0.827	0.035	1.396
20	0.3	0.75	2	0.59	5.78	0.052	0.065	2.589	0.011	0.009	1.771	0.001	0.002	0.001	0.549	0.015	0.614
20	0.4	0.75	2	0.59	5.78	0.052	0.065	2.242	0.011	0.009	1.771	0.001	0.002	0.001	0.409	0.009	0.342
20	0.5	0.75	2	0.59	5.78	0.052	0.065	2.005	0.011	0.009	1.771	0.001	0.002	0.001	0.326	0.005	0.216

Q	X	Z	V _{zi}	Z _{core}	V _{zj}	h _{down}	h _{up}	V _{xmax}	q _{up}	q _{down}	V(z)	FQSI	G _b	I _{net}	V _{up}	H _{up}	H _{up} /z
l/s	m	m	m/s	m	m/s	m	m	m/s	m ² /s	m ² /s	m/s	Ns	kg/m ²	Ns	m/s	m	
			Q=V A	Z=5*Bj	Eq. 25	Eq. 61		Eq. 63	Eq. 61&62		Eq. 60	Fig.2.18	Eq. 59	Eq.55		Eq. 58	
20	0.6	0.75	2	0.59	5.78	0.052	0.065	1.831	0.011	0.009	1.771	0.001	0.002	0.001	0.270	0.004	0.149
20	0.5	0.775	2	0.59	5.78	0.052	0.065	2.204	0.011	0.009	1.742	0.001	0.002	0.001	0.395	0.008	0.319
20	0.4	0.775	2	0.59	5.78	0.052	0.065	2.464	0.011	0.009	1.742	0.001	0.002	0.001	0.496	0.013	0.502
20	0.3	0.775	2	0.59	5.78	0.052	0.065	2.845	0.011	0.009	1.742	0.002	0.002	0.002	0.665	0.023	0.901
20	0.2	0.775	2	0.59	5.78	0.052	0.065	3.485	0.011	0.009	1.742	0.002	0.002	0.002	1.001	0.051	2.044
20	0.1	0.775	2	0.59	5.78	0.052	0.065	4.928	0.011	0.009	1.742	0.005	0.002	0.005	2.011	0.206	8.244
20	0.7	0.775	2	0.59	5.78	0.052	0.065	1.667	0.011	0.009	1.742	0.001	0.002	0.001	0.223	0.003	0.101
20	0.1	0.775	2	0.59	5.78	0.052	0.065	4.411	0.011	0.009	1.742	0.004	0.002	0.004	1.609	0.132	5.281
20	0.2	0.775	2	0.59	5.78	0.052	0.065	3.119	0.011	0.009	1.742	0.002	0.002	0.002	0.800	0.033	1.306
20	0.3	0.775	2	0.59	5.78	0.052	0.065	2.547	0.011	0.009	1.742	0.001	0.002	0.001	0.531	0.014	0.574
20	0.4	0.775	2	0.59	5.78	0.052	0.065	2.205	0.011	0.009	1.742	0.001	0.002	0.001	0.396	0.008	0.320
20	0.5	0.775	2	0.59	5.78	0.052	0.065	1.973	0.011	0.009	1.742	0.001	0.002	0.001	0.315	0.005	0.202
20	0.6	0.775	2	0.59	5.78	0.052	0.065	1.801	0.011	0.009	1.742	0.001	0.002	0.001	0.261	0.003	0.139
20	0.5	0.8	2	0.59	5.78	0.052	0.065	2.169	0.011	0.009	1.715	0.001	0.002	0.001	0.383	0.007	0.299
20	0.4	0.8	2	0.59	5.78	0.052	0.065	2.425	0.011	0.009	1.715	0.001	0.002	0.001	0.481	0.012	0.471
20	0.3	0.8	2	0.59	5.78	0.052	0.065	2.800	0.011	0.009	1.715	0.002	0.002	0.002	0.644	0.021	0.844
20	0.2	0.8	2	0.59	5.78	0.052	0.065	3.430	0.011	0.009	1.715	0.002	0.002	0.002	0.970	0.048	1.917
20	0.1	0.8	2	0.59	5.78	0.052	0.065	4.850	0.011	0.009	1.715	0.005	0.002	0.005	1.948	0.193	7.735
20	0.7	0.8	2	0.59	5.78	0.052	0.065	1.641	0.011	0.009	1.715	0.001	0.002	0.001	0.215	0.002	0.095
20	0.1	0.8	2	0.59	5.78	0.052	0.065	4.341	0.011	0.009	1.715	0.004	0.002	0.004	1.559	0.124	4.954
20	0.2	0.8	2	0.59	5.78	0.052	0.065	3.070	0.011	0.009	1.715	0.002	0.002	0.002	0.775	0.031	1.225
20	0.3	0.8	2	0.59	5.78	0.052	0.065	2.507	0.011	0.009	1.715	0.001	0.002	0.001	0.514	0.013	0.538
20	0.4	0.8	2	0.59	5.78	0.052	0.065	2.171	0.011	0.009	1.715	0.001	0.002	0.001	0.383	0.007	0.300
20	0.5	0.8	2	0.59	5.78	0.052	0.065	1.942	0.011	0.009	1.715	0.001	0.002	0.001	0.305	0.005	0.190

Q	X	Z	V _{zi}	Z _{core}	V _{zj}	h _{down}	h _{up}	V _{xmax}	q _{up}	q _{down}	V(z)	FQSI	G _b	I _{net}	V _{up}	H _{up}	H _{up} /z
l/s	m	m	m/s	m	m/s	m	m	m/s	m ² /s	m ² /s	m/s	Ns	kg/m ²	Ns	m/s	m	
			Q=V A	Z=5*Bj	Eq. 25	Eq. 61		Eq. 63	Eq. 61&62		Eq. 60	Fig.2.18	Eq. 59	Eq.55		Eq. 58	
20	0.6	0.8	2	0.59	5.78	0.052	0.065	1.772	0.011	0.009	1.715	0.001	0.002	0.001	0.253	0.003	0.130
20	0.5	0.825	2	0.59	5.78	0.052	0.065	2.136	0.011	0.009	1.689	0.001	0.002	0.001	0.371	0.007	0.280
20	0.4	0.825	2	0.59	5.78	0.052	0.065	2.388	0.011	0.009	1.689	0.001	0.002	0.001	0.466	0.011	0.442
20	0.3	0.825	2	0.59	5.78	0.052	0.065	2.758	0.011	0.009	1.689	0.002	0.002	0.001	0.624	0.020	0.793
20	0.2	0.825	2	0.59	5.78	0.052	0.065	3.377	0.011	0.009	1.689	0.002	0.002	0.002	0.940	0.045	1.801
20	0.1	0.825	2	0.59	5.78	0.052	0.065	4.776	0.011	0.009	1.689	0.005	0.002	0.004	1.889	0.182	7.271
20	0.7	0.825	2	0.59	5.78	0.052	0.065	1.616	0.011	0.009	1.689	0.001	0.002	0.000	0.209	0.002	0.089
20	0.1	0.825	2	0.59	5.78	0.052	0.065	4.275	0.011	0.009	1.689	0.004	0.002	0.004	1.511	0.116	4.657
20	0.2	0.825	2	0.59	5.78	0.052	0.065	3.023	0.011	0.009	1.689	0.002	0.002	0.002	0.751	0.029	1.151
20	0.3	0.825	2	0.59	5.78	0.052	0.065	2.468	0.011	0.009	1.689	0.001	0.002	0.001	0.498	0.013	0.506
20	0.4	0.825	2	0.59	5.78	0.052	0.065	2.138	0.011	0.009	1.689	0.001	0.002	0.001	0.371	0.007	0.281
20	0.5	0.825	2	0.59	5.78	0.052	0.065	1.912	0.011	0.009	1.689	0.001	0.002	0.001	0.295	0.004	0.178
20	0.6	0.825	2	0.59	5.78	0.052	0.065	1.745	0.011	0.009	1.689	0.001	0.002	0.001	0.245	0.003	0.122
20	0.5	0.85	2	0.59	5.78	0.052	0.065	1.884	0.011	0.009	1.664	0.001	0.002	0.001	0.287	0.004	0.167
20	0.4	0.85	2	0.59	5.78	0.052	0.065	2.106	0.011	0.009	1.664	0.001	0.002	0.001	0.360	0.007	0.265
20	0.3	0.85	2	0.59	5.78	0.052	0.065	2.432	0.011	0.009	1.664	0.001	0.002	0.001	0.483	0.012	0.476
20	0.2	0.85	2	0.59	5.78	0.052	0.065	2.978	0.011	0.009	1.664	0.002	0.002	0.002	0.729	0.027	1.084
20	0.1	0.85	2	0.59	5.78	0.052	0.065	4.212	0.011	0.009	1.664	0.004	0.002	0.003	1.467	0.110	4.386
20	0.7	0.85	2	0.59	5.78	0.052	0.065	1.592	0.011	0.009	1.664	0.001	0.002	0.000	0.202	0.002	0.083
20	0.1	0.85	2	0.59	5.78	0.052	0.065	4.212	0.011	0.009	1.664	0.004	0.002	0.003	1.467	0.110	4.386
20	0.2	0.85	2	0.59	5.78	0.052	0.065	2.978	0.011	0.009	1.664	0.002	0.002	0.002	0.729	0.027	1.084
20	0.3	0.85	2	0.59	5.78	0.052	0.065	2.432	0.011	0.009	1.664	0.001	0.002	0.001	0.483	0.012	0.476
20	0.4	0.85	2	0.59	5.78	0.052	0.065	2.106	0.011	0.009	1.664	0.001	0.002	0.001	0.360	0.007	0.265
20	0.5	0.85	2	0.59	5.78	0.052	0.065	1.884	0.011	0.009	1.664	0.001	0.002	0.001	0.287	0.004	0.167

Q	X	Z	V _{zi}	Z _{core}	V _{zj}	h _{down}	h _{up}	V _{xmax}	q _{up}	q _{down}	V(z)	FQSI	G _b	I _{net}	V _{up}	H _{up}	H _{up} /z
l/s	m	m	m/s	m	m/s	m	m	m/s	m ² /s	m ² /s	m/s	Ns	kg/m ²	Ns	m/s	m	
			Q=V A	Z=5*B _j	Eq. 25	Eq. 61		Eq. 63	Eq. 61&62		Eq. 60	Fig.2.18	Eq. 59	Eq.55		Eq. 58	
20	0.6	0.85	2	0.59	5.78	0.052	0.065	1.719	0.011	0.009	1.664	0.001	0.002	0.001	0.237	0.003	0.115
20	0.5	0.875	2	0.59	5.78	0.052	0.065	1.856	0.011	0.009	1.640	0.001	0.002	0.001	0.278	0.004	0.158
20	0.4	0.875	2	0.59	5.78	0.052	0.065	2.076	0.011	0.009	1.640	0.001	0.002	0.001	0.350	0.006	0.249
20	0.3	0.875	2	0.59	5.78	0.052	0.065	2.397	0.011	0.009	1.640	0.001	0.002	0.001	0.469	0.011	0.449
20	0.2	0.875	2	0.59	5.78	0.052	0.065	2.935	0.011	0.009	1.640	0.002	0.002	0.002	0.708	0.026	1.022
20	0.1	0.875	2	0.59	5.78	0.052	0.065	4.151	0.011	0.009	1.640	0.003	0.002	0.003	1.425	0.103	4.137
20	0.7	0.875	2	0.59	5.78	0.052	0.065	1.569	0.011	0.009	1.640	0.000	0.002	0.000	0.196	0.002	0.078
20	0.1	0.875	2	0.59	5.78	0.052	0.065	4.151	0.011	0.009	1.640	0.003	0.002	0.003	1.425	0.103	4.137
20	0.2	0.875	2	0.59	5.78	0.052	0.065	2.935	0.011	0.009	1.640	0.002	0.002	0.002	0.708	0.026	1.022
20	0.3	0.875	2	0.59	5.78	0.052	0.065	2.397	0.011	0.009	1.640	0.001	0.002	0.001	0.469	0.011	0.449
20	0.4	0.875	2	0.59	5.78	0.052	0.065	2.076	0.011	0.009	1.640	0.001	0.002	0.001	0.350	0.006	0.249
20	0.5	0.875	2	0.59	5.78	0.052	0.065	1.856	0.011	0.009	1.640	0.001	0.002	0.001	0.278	0.004	0.158
20	0.6	0.875	2	0.59	5.78	0.052	0.065	1.695	0.011	0.009	1.640	0.001	0.002	0.001	0.230	0.003	0.108
20	0.5	0.9	2	0.59	5.78	0.052	0.065	1.831	0.011	0.009	1.617	0.001	0.002	0.001	0.270	0.004	0.149
20	0.4	0.925	2	0.59	5.78	0.052	0.065	2.019	0.011	0.009	1.595	0.001	0.002	0.001	0.330	0.006	0.223
20	0.3	0.95	2	0.59	5.78	0.052	0.065	2.300	0.011	0.009	1.574	0.001	0.002	0.001	0.431	0.009	0.379
20	0.2	0.975	2	0.59	5.78	0.052	0.065	2.781	0.011	0.009	1.553	0.002	0.002	0.002	0.635	0.021	0.821
20	0.1	1	2	0.59	5.78	0.052	0.065	3.883	0.011	0.009	1.534	0.003	0.002	0.003	1.245	0.079	3.162
20	0.7	1.025	2	0.59	5.78	0.052	0.065	1.450	0.011	0.009	1.515	0.000	0.002	0.000	0.166	0.001	0.056
20	0.1	1.05	2	0.59	5.78	0.052	0.065	3.790	0.011	0.009	1.497	0.003	0.002	0.003	1.186	0.072	2.866
20	0.2	1.075	2	0.59	5.78	0.052	0.065	2.648	0.011	0.009	1.479	0.001	0.002	0.001	0.575	0.017	0.673
20	0.3	1.1	2	0.59	5.78	0.052	0.065	2.138	0.011	0.009	1.462	0.001	0.002	0.001	0.371	0.007	0.281
20	0.4	1.125	2	0.59	5.78	0.052	0.065	1.831	0.011	0.009	1.446	0.001	0.002	0.001	0.270	0.004	0.149
20	0.5	1.15	2	0.59	5.78	0.052	0.065	1.619	0.011	0.009	1.430	0.001	0.002	0.000	0.210	0.002	0.090
20	0.6	1.175	2	0.59	5.78	0.052	0.065	1.462	0.011	0.009	1.415	0.000	0.002	0.000	0.169	0.001	0.058

Table D 0.3. Quasi-steady method of Q=10 l/s, H=2m and TW=0.25m

Q	X	Z	V _{zi}	Z _{core}	V _{zj}	h _{down}	h _{up}	V _{xmax}	q _{up}	q _{down}	V(z)	FQSI	Gb	Inet	V _{up}	H _{up}	H _{up} /z
l/s	m	m	m/s	m	m/s	m	m	m/s	m ² /s	m ² /s	m/s	Ns	kg/m ²	Ns	m/s	m	
			Q=VA	Z=5*B _j	Eq. 25	Eq. 61		Eq. 63	Eq. 61&62		Eq. 60	Fig. 2.18	Eq. 59	Eq.55		Eq. 58	
	0.62	0	1.667	0.542	5.675	0.089	0.020	1.538	0.002	0.008	5.675						
10	0.62	0.041	1.667	0.542	5.675	0.089	0.020	1.538	0.002	0.008	6.011						
10	0.62	0.083	1.667	0.542	5.675	0.089	0.020	1.538	0.002	0.008	4.250						
10	0.62	0.125	1.667	0.542	5.675	0.089	0.020	1.538	0.002	0.008	3.470						
10	0.62	0.166	1.667	0.542	5.675	0.089	0.020	1.538	0.002	0.008	3.005						
10	0.62	0.208	1.667	0.542	5.675	0.089	0.020	1.538	0.002	0.008	2.688						
10	0.62	0.25	1.667	0.542	5.675	0.089	0.020	1.538	0.002	0.008	2.454						
10	0.5	0.25	1.667	0.542	5.675	0.089	0.020	1.712	0.002	0.008	2.454	0.001	0.002	0.001	0.235	0.003	0.113
10	0.4	0.25	1.667	0.542	5.675	0.089	0.020	1.914	0.002	0.008	2.454	0.001	0.002	0.001	0.296	0.004	0.179
10	0.3	0.25	1.667	0.542	5.675	0.089	0.020	2.210	0.002	0.008	2.454	0.001	0.002	0.001	0.398	0.008	0.323
10	0.2	0.25	1.667	0.542	5.675	0.089	0.020	2.707	0.002	0.008	2.454	0.001	0.002	0.001	0.601	0.018	0.736
10	0.1	0.25	1.667	0.542	5.675	0.089	0.020	3.828	0.002	0.008	2.454	0.003	0.002	0.003	1.210	0.075	2.987
10	0.62	0.25	1.667	0.542	5.675	0.089	0.020	1.538	0.002	0.008	2.454	0.000	0.002	0.000	0.188	0.002	0.072
10	0.1	0.25	1.667	0.542	5.675	0.089	0.020	8.080	0.002	0.008	2.454	0.013	0.002	0.013	5.421	1.498	59.907
10	0.2	0.25	1.667	0.542	5.675	0.089	0.020	5.713	0.002	0.008	2.454	0.006	0.002	0.006	2.706	0.373	14.930
10	0.3	0.25	1.667	0.542	5.675	0.089	0.020	4.665	0.002	0.008	2.454	0.004	0.002	0.004	1.801	0.165	6.615
10	0.4	0.25	1.667	0.542	5.675	0.089	0.020	4.040	0.002	0.008	2.454	0.003	0.002	0.003	1.349	0.093	3.709
10	0.5	0.25	1.667	0.542	5.675	0.089	0.020	3.614	0.002	0.008	2.454	0.003	0.002	0.003	1.077	0.059	2.366
10	0.6	0.25	1.667	0.542	5.675	0.089	0.020	3.299	0.002	0.008	2.454	0.002	0.002	0.002	0.896	0.041	1.638
10	0.5	0.275	1.667	0.542	5.675	0.089	0.020	1.632	0.002	0.008	2.340	0.001	0.002	0.001	0.213	0.002	0.093
10	0.4	0.275	1.667	0.542	5.675	0.089	0.020	1.825	0.002	0.008	2.340	0.001	0.002	0.001	0.268	0.004	0.147
10	0.3	0.275	1.667	0.542	5.675	0.089	0.020	2.108	0.002	0.008	2.340	0.001	0.002	0.001	0.361	0.007	0.265
10	0.2	0.275	1.667	0.542	5.675	0.089	0.020	2.581	0.002	0.008	2.340	0.001	0.002	0.001	0.546	0.015	0.607
10	0.1	0.275	1.667	0.542	5.675	0.089	0.020	3.650	0.002	0.008	2.340	0.003	0.002	0.003	1.100	0.062	2.465
10	0.62	0.275	1.667	0.542	5.675	0.089	0.020	1.466	0.002	0.008	2.340	0.000	0.002	0.000	0.170	0.001	0.059

Q	X	Z	V _{zi}	Z _{core}	V _{zj}	h _{down}	h _{up}	V _{xmax}	q _{up}	q _{down}	V(z)	FQSI	G _b	I _{net}	V _{up}	H _{up}	H _{up} /z
l/s	m	m	m/s	m	m/s	m	m	m/s	m ² /s	m ² /s	m/s	Ns	kg/m ²	Ns	m/s	m	
			Q=VA	Z=5*Bj	Eq. 25	Eq. 61		Eq. 63	Eq.61&62		Eq. 60	Fig.2.18	Eq. 59	Eq.55		Eq. 58	
10	0.1	0.275	1.667	0.542	5.675	0.089	0.020	7.704	0.002	0.008	2.340	0.012	0.002	0.012	4.927	1.237	49.495
10	0.2	0.275	1.667	0.542	5.675	0.089	0.020	5.448	0.002	0.008	2.340	0.006	0.002	0.006	2.459	0.308	12.331
10	0.3	0.275	1.667	0.542	5.675	0.089	0.020	4.448	0.002	0.008	2.340	0.004	0.002	0.004	1.637	0.137	5.461
10	0.4	0.275	1.667	0.542	5.675	0.089	0.020	3.852	0.002	0.008	2.340	0.003	0.002	0.003	1.225	0.077	3.061
10	0.5	0.275	1.667	0.542	5.675	0.089	0.020	3.445	0.002	0.008	2.340	0.002	0.002	0.002	0.979	0.049	1.952
10	0.6	0.275	1.667	0.542	5.675	0.089	0.020	3.145	0.002	0.008	2.340	0.002	0.002	0.002	0.814	0.034	1.351
10	0.5	0.3	1.667	0.542	5.675	0.089	0.020	1.563	0.002	0.008	2.240	0.000	0.002	0.000	0.195	0.002	0.077
10	0.4	0.3	1.667	0.542	5.675	0.089	0.020	1.747	0.002	0.008	2.240	0.001	0.002	0.001	0.245	0.003	0.123
10	0.3	0.3	1.667	0.542	5.675	0.089	0.020	2.018	0.002	0.008	2.240	0.001	0.002	0.001	0.330	0.006	0.222
10	0.2	0.3	1.667	0.542	5.675	0.089	0.020	2.471	0.002	0.008	2.240	0.001	0.002	0.001	0.499	0.013	0.508
10	0.1	0.3	1.667	0.542	5.675	0.089	0.020	3.495	0.002	0.008	2.240	0.002	0.002	0.002	1.007	0.052	2.068
10	0.62	0.3	1.667	0.542	5.675	0.089	0.020	1.404	0.002	0.008	2.240	0.000	0.002	0.000	0.155	0.001	0.049
10	0.1	0.3	1.667	0.542	5.675	0.089	0.020	7.376	0.002	0.008	2.240	0.011	0.002	0.011	4.516	1.039	41.576
10	0.2	0.3	1.667	0.542	5.675	0.089	0.020	5.216	0.002	0.008	2.240	0.005	0.002	0.005	2.254	0.259	10.355
10	0.3	0.3	1.667	0.542	5.675	0.089	0.020	4.259	0.002	0.008	2.240	0.004	0.002	0.004	1.500	0.115	4.585
10	0.4	0.3	1.667	0.542	5.675	0.089	0.020	3.688	0.002	0.008	2.240	0.003	0.002	0.003	1.123	0.064	2.569
10	0.5	0.3	1.667	0.542	5.675	0.089	0.020	3.299	0.002	0.008	2.240	0.002	0.002	0.002	0.896	0.041	1.638
10	0.6	0.3	1.667	0.542	5.675	0.089	0.020	3.011	0.002	0.008	2.240	0.002	0.002	0.002	0.746	0.028	1.133
10	0.5	0.325	1.667	0.542	5.675	0.089	0.020	1.502	0.002	0.008	2.152	0.000	0.002	0.000	0.179	0.002	0.065
10	0.4	0.325	1.667	0.542	5.675	0.089	0.020	1.679	0.002	0.008	2.152	0.001	0.002	0.001	0.226	0.003	0.104
10	0.3	0.325	1.667	0.542	5.675	0.089	0.020	1.939	0.002	0.008	2.152	0.001	0.002	0.001	0.304	0.005	0.188
10	0.2	0.325	1.667	0.542	5.675	0.089	0.020	2.374	0.002	0.008	2.152	0.001	0.002	0.001	0.460	0.011	0.432
10	0.1	0.325	1.667	0.542	5.675	0.089	0.020	3.358	0.002	0.008	2.152	0.002	0.002	0.002	0.929	0.044	1.760
10	0.62	0.325	1.667	0.542	5.675	0.089	0.020	1.349	0.002	0.008	2.152	0.000	0.002	0.000	0.143	0.001	0.042
10	0.1	0.325	1.667	0.542	5.675	0.089	0.020	7.087	0.002	0.008	2.152	0.010	0.002	0.010	4.168	0.885	35.415
10	0.2	0.325	1.667	0.542	5.675	0.089	0.020	5.011	0.002	0.008	2.152	0.005	0.002	0.005	2.080	0.220	8.817

Q	X	Z	V _{zi}	Z _{core}	V _{zj}	h _{down}	h _{up}	V _{xmax}	q _{up}	q _{down}	V(z)	FQSI	G _b	I _{net}	V _{up}	H _{up}	H _{up} /z
l/s	m	m	m/s	m	m/s	m	m	m/s	m ² /s	m ² /s	m/s	Ns	kg/m ²	Ns	m/s	m	
			Q=VA	Z=5*Bj	Eq. 25	Eq. 61		Eq. 63	Eq.61&62		Eq. 60	Fig.2.18	Eq. 59	Eq.55		Eq. 58	
10	0.3	0.325	1.667	0.542	5.675	0.089	0.020	4.092	0.002	0.008	2.152	0.003	0.002	0.003	1.384	0.098	3.903
10	0.4	0.325	1.667	0.542	5.675	0.089	0.020	3.543	0.002	0.008	2.152	0.002	0.002	0.002	1.036	0.055	2.186
10	0.5	0.325	1.667	0.542	5.675	0.089	0.020	3.169	0.002	0.008	2.152	0.002	0.002	0.002	0.827	0.035	1.393
10	0.6	0.325	1.667	0.542	5.675	0.089	0.020	2.893	0.002	0.008	2.152	0.002	0.002	0.002	0.688	0.024	0.964
10	0.5	0.35	1.667	0.542	5.675	0.089	0.020	1.447	0.002	0.008	2.074	0.000	0.002	0.000	0.166	0.001	0.056
10	0.4	0.35	1.667	0.542	5.675	0.089	0.020	1.618	0.002	0.008	2.074	0.001	0.002	0.000	0.209	0.002	0.089
10	0.3	0.35	1.667	0.542	5.675	0.089	0.020	1.868	0.002	0.008	2.074	0.001	0.002	0.001	0.282	0.004	0.162
10	0.2	0.35	1.667	0.542	5.675	0.089	0.020	2.288	0.002	0.008	2.074	0.001	0.002	0.001	0.427	0.009	0.371
10	0.1	0.35	1.667	0.542	5.675	0.089	0.020	3.236	0.002	0.008	2.074	0.002	0.002	0.002	0.862	0.038	1.515
10	0.62	0.35	1.667	0.542	5.675	0.089	0.020	1.299	0.002	0.008	2.074	0.000	0.002	0.000	0.132	0.001	0.035
10	0.1	0.35	1.667	0.542	5.675	0.089	0.020	6.829	0.002	0.008	2.074	0.009	0.002	0.009	3.870	0.763	30.526
10	0.2	0.35	1.667	0.542	5.675	0.089	0.020	4.829	0.002	0.008	2.074	0.005	0.002	0.005	1.930	0.190	7.598
10	0.3	0.35	1.667	0.542	5.675	0.089	0.020	3.943	0.002	0.008	2.074	0.003	0.002	0.003	1.284	0.084	3.362
10	0.4	0.35	1.667	0.542	5.675	0.089	0.020	3.414	0.002	0.008	2.074	0.002	0.002	0.002	0.961	0.047	1.883
10	0.5	0.35	1.667	0.542	5.675	0.089	0.020	3.054	0.002	0.008	2.074	0.002	0.002	0.002	0.767	0.030	1.200
10	0.6	0.35	1.667	0.542	5.675	0.089	0.020	2.788	0.002	0.008	2.074	0.002	0.002	0.002	0.638	0.021	0.829
10	0.5	0.375	1.667	0.542	5.675	0.089	0.020	1.398	0.002	0.008	2.004	0.000	0.002	0.000	0.154	0.001	0.048
10	0.4	0.375	1.667	0.542	5.675	0.089	0.020	1.563	0.002	0.008	2.004	0.000	0.002	0.000	0.195	0.002	0.077
10	0.3	0.375	1.667	0.542	5.675	0.089	0.020	1.805	0.002	0.008	2.004	0.001	0.002	0.001	0.262	0.004	0.140
10	0.2	0.375	1.667	0.542	5.675	0.089	0.020	2.210	0.002	0.008	2.004	0.001	0.002	0.001	0.398	0.008	0.323
10	0.1	0.375	1.667	0.542	5.675	0.089	0.020	3.126	0.002	0.008	2.004	0.002	0.002	0.002	0.804	0.033	1.318
10	0.62	0.375	1.667	0.542	5.675	0.089	0.020	1.255	0.002	0.008	2.004	0.000	0.002	0.000	0.123	0.001	0.031
10	0.1	0.375	1.667	0.542	5.675	0.089	0.020	6.597	0.002	0.008	2.004	0.009	0.002	0.009	3.611	0.665	26.584
10	0.2	0.375	1.667	0.542	5.675	0.089	0.020	4.665	0.002	0.008	2.004	0.004	0.002	0.004	1.801	0.165	6.615
10	0.3	0.375	1.667	0.542	5.675	0.089	0.020	3.809	0.002	0.008	2.004	0.003	0.002	0.003	1.198	0.073	2.926
10	0.4	0.375	1.667	0.542	5.675	0.089	0.020	3.299	0.002	0.008	2.004	0.002	0.002	0.002	0.896	0.041	1.638

Q	X	Z	V _{zi}	Z _{core}	V _{zj}	h _{down}	h _{up}	V _{xmax}	q _{up}	q _{down}	V(z)	FQSI	G _b	I _{net}	V _{up}	H _{up}	H _{up} /z
l/s	m	m	m/s	m	m/s	m	m	m/s	m ² /s	m ² /s	m/s	Ns	kg/m ²	Ns	m/s	m	
			Q=VA	Z=5*Bj	Eq. 25	Eq. 61		Eq. 63	Eq. 61&62		Eq. 60	Fig.2.18	Eq. 59	Eq.55		Eq. 58	
10	0.5	0.375	1.667	0.542	5.675	0.089	0.020	2.950	0.002	0.008	2.004	0.002	0.002	0.002	0.715	0.026	1.043
10	0.6	0.375	1.667	0.542	5.675	0.089	0.020	2.693	0.002	0.008	2.004	0.001	0.002	0.001	0.595	0.018	0.721
10	0.5	0.4	1.667	0.542	5.675	0.089	0.020	1.354	0.002	0.008	1.940	0.000	0.002	0.000	0.144	0.001	0.042
10	0.4	0.4	1.667	0.542	5.675	0.089	0.020	1.513	0.002	0.008	1.940	0.000	0.002	0.000	0.182	0.002	0.067
10	0.3	0.4	1.667	0.542	5.675	0.089	0.020	1.747	0.002	0.008	1.940	0.001	0.002	0.001	0.245	0.003	0.123
10	0.2	0.4	1.667	0.542	5.675	0.089	0.020	2.140	0.002	0.008	1.940	0.001	0.002	0.001	0.372	0.007	0.283
10	0.1	0.4	1.667	0.542	5.675	0.089	0.020	3.027	0.002	0.008	1.940	0.002	0.002	0.002	0.753	0.029	1.157
10	0.62	0.4	1.667	0.542	5.675	0.089	0.020	1.216	0.002	0.008	1.940	0.000	0.002	0.000	0.114	0.001	0.027
10	0.1	0.4	1.667	0.542	5.675	0.089	0.020	6.388	0.002	0.008	1.940	0.008	0.002	0.008	3.385	0.584	23.357
10	0.2	0.4	1.667	0.542	5.675	0.089	0.020	4.517	0.002	0.008	1.940	0.004	0.002	0.004	1.688	0.145	5.810
10	0.3	0.4	1.667	0.542	5.675	0.089	0.020	3.688	0.002	0.008	1.940	0.003	0.002	0.003	1.123	0.064	2.569
10	0.4	0.4	1.667	0.542	5.675	0.089	0.020	3.194	0.002	0.008	1.940	0.002	0.002	0.002	0.840	0.036	1.438
10	0.5	0.4	1.667	0.542	5.675	0.089	0.020	2.857	0.002	0.008	1.940	0.002	0.002	0.002	0.670	0.023	0.916
10	0.6	0.4	1.667	0.542	5.675	0.089	0.020	2.608	0.002	0.008	1.940	0.001	0.002	0.001	0.557	0.016	0.633
10	0.5	0.425	1.667	0.542	5.675	0.089	0.020	1.313	0.002	0.008	1.882	0.000	0.002	0.000	0.135	0.001	0.037
10	0.4	0.425	1.667	0.542	5.675	0.089	0.020	1.468	0.002	0.008	1.882	0.000	0.002	0.000	0.171	0.001	0.059
10	0.3	0.425	1.667	0.542	5.675	0.089	0.020	1.695	0.002	0.008	1.882	0.001	0.002	0.001	0.230	0.003	0.108
10	0.2	0.425	1.667	0.542	5.675	0.089	0.020	2.076	0.002	0.008	1.882	0.001	0.002	0.001	0.350	0.006	0.250
10	0.1	0.425	1.667	0.542	5.675	0.089	0.020	2.936	0.002	0.008	1.882	0.002	0.002	0.002	0.708	0.026	1.023
10	0.62	0.425	1.667	0.542	5.675	0.089	0.020	1.179	0.002	0.008	1.882	0.000	0.002	0.000	0.107	0.001	0.023
10	0.1	0.425	1.667	0.542	5.675	0.089	0.020	6.197	0.002	0.008	1.882	0.008	0.002	0.008	3.185	0.517	20.683
10	0.2	0.425	1.667	0.542	5.675	0.089	0.020	4.382	0.002	0.008	1.882	0.004	0.002	0.004	1.588	0.129	5.143
10	0.3	0.425	1.667	0.542	5.675	0.089	0.020	3.578	0.002	0.008	1.882	0.003	0.002	0.003	1.056	0.057	2.274
10	0.4	0.425	1.667	0.542	5.675	0.089	0.020	3.099	0.002	0.008	1.882	0.002	0.002	0.002	0.790	0.032	1.272
10	0.5	0.425	1.667	0.542	5.675	0.089	0.020	2.771	0.002	0.008	1.882	0.002	0.002	0.001	0.630	0.020	0.810
10	0.6	0.425	1.667	0.542	5.675	0.089	0.020	2.530	0.002	0.008	1.882	0.001	0.002	0.001	0.524	0.014	0.559

Q	X	Z	V _{zi}	Z _{core}	V _{zj}	h _{down}	h _{up}	V _{xmax}	q _{up}	q _{down}	V(z)	FQSI	G _b	I _{net}	V _{up}	H _{up}	H _{up} /z
l/s	m	m	m/s	m	m/s	m	m	m/s	m ² /s	m ² /s	m/s	Ns	kg/m ²	Ns	m/s	m	
			Q=VA	Z=5*Bj	Eq. 25	Eq. 61		Eq. 63	Eq. 61&62		Eq. 60	Fig.2.18	Eq. 59	Eq.55		Eq. 58	
10	0.5	0.45	1.667	0.542	5.675	0.089	0.020	1.276	0.002	0.008	1.829	0.000	0.002	0.000	0.127	0.001	0.033
10	0.4	0.45	1.667	0.542	5.675	0.089	0.020	1.427	0.002	0.008	1.829	0.000	0.002	0.000	0.161	0.001	0.053
10	0.3	0.45	1.667	0.542	5.675	0.089	0.020	1.648	0.002	0.008	1.829	0.001	0.002	0.001	0.217	0.002	0.096
10	0.2	0.45	1.667	0.542	5.675	0.089	0.020	2.018	0.002	0.008	1.829	0.001	0.002	0.001	0.330	0.006	0.222
10	0.1	0.45	1.667	0.542	5.675	0.089	0.020	2.854	0.002	0.008	1.829	0.002	0.002	0.002	0.669	0.023	0.911
10	0.62	0.45	1.667	0.542	5.675	0.089	0.020	1.146	0.002	0.008	1.829	0.000	0.002	0.000	0.101	0.001	0.021
10	0.1	0.45	1.667	0.542	5.675	0.089	0.020	6.023	0.002	0.008	1.829	0.007	0.002	0.007	3.008	0.461	18.443
10	0.2	0.45	1.667	0.542	5.675	0.089	0.020	4.259	0.002	0.008	1.829	0.004	0.002	0.004	1.500	0.115	4.585
10	0.3	0.45	1.667	0.542	5.675	0.089	0.020	3.477	0.002	0.008	1.829	0.002	0.002	0.002	0.997	0.051	2.026
10	0.4	0.45	1.667	0.542	5.675	0.089	0.020	3.011	0.002	0.008	1.829	0.002	0.002	0.002	0.746	0.028	1.133
10	0.5	0.45	1.667	0.542	5.675	0.089	0.020	2.693	0.002	0.008	1.829	0.001	0.002	0.001	0.595	0.018	0.721
10	0.6	0.45	1.667	0.542	5.675	0.089	0.020	2.459	0.002	0.008	1.829	0.001	0.002	0.001	0.494	0.012	0.498
10	0.5	0.475	1.667	0.542	5.675	0.089	0.020	1.242	0.002	0.008	1.780	0.000	0.002	0.000	0.120	0.001	0.029
10	0.4	0.475	1.667	0.542	5.675	0.089	0.020	1.389	0.002	0.008	1.780	0.000	0.002	0.000	0.152	0.001	0.047
10	0.3	0.475	1.667	0.542	5.675	0.089	0.020	1.604	0.002	0.008	1.780	0.001	0.002	0.000	0.205	0.002	0.086
10	0.2	0.475	1.667	0.542	5.675	0.089	0.020	1.964	0.002	0.008	1.780	0.001	0.002	0.001	0.312	0.005	0.199
10	0.1	0.475	1.667	0.542	5.675	0.089	0.020	2.777	0.002	0.008	1.780	0.002	0.002	0.002	0.633	0.020	0.817
10	0.62	0.475	1.667	0.542	5.675	0.089	0.020	1.115	0.002	0.008	1.780	0.000	0.002	0.000	0.095	0.000	0.018
10	0.1	0.475	1.667	0.542	5.675	0.089	0.020	5.862	0.002	0.008	1.780	0.007	0.002	0.007	2.849	0.414	16.548
10	0.2	0.475	1.667	0.542	5.675	0.089	0.020	4.145	0.002	0.008	1.780	0.003	0.002	0.003	1.420	0.103	4.112
10	0.3	0.475	1.667	0.542	5.675	0.089	0.020	3.384	0.002	0.008	1.780	0.002	0.002	0.002	0.944	0.045	1.817
10	0.4	0.475	1.667	0.542	5.675	0.089	0.020	2.931	0.002	0.008	1.780	0.002	0.002	0.002	0.706	0.025	1.016
10	0.5	0.475	1.667	0.542	5.675	0.089	0.020	2.622	0.002	0.008	1.780	0.001	0.002	0.001	0.563	0.016	0.646
10	0.6	0.475	1.667	0.542	5.675	0.089	0.020	2.393	0.002	0.008	1.780	0.001	0.002	0.001	0.468	0.011	0.446
10	0.5	0.5	1.667	0.542	5.675	0.089	0.020	1.211	0.002	0.008	1.735	0.000	0.002	0.000	0.113	0.001	0.026
10	0.4	0.5	1.667	0.542	5.675	0.089	0.020	1.354	0.002	0.008	1.735	0.000	0.002	0.000	0.144	0.001	0.042

Q	X	Z	V _{zi}	Z _{core}	V _{zj}	h _{down}	h _{up}	V _{xmax}	q _{up}	q _{down}	V(z)	FQSI	G _b	I _{net}	V _{up}	H _{up}	H _{up} /z
l/s	m	m	m/s	m	m/s	m	m	m/s	m ² /s	m ² /s	m/s	Ns	kg/m ²	Ns	m/s	m	
			Q=VA	Z=5*Bj	Eq. 25	Eq. 61		Eq. 63	Eq.61&62		Eq. 60	Fig.2.18	Eq. 59	Eq.55		Eq. 58	
10	0.3	0.5	1.667	0.542	5.675	0.089	0.020	1.563	0.002	0.008	1.735	0.000	0.002	0.000	0.195	0.002	0.077
10	0.2	0.5	1.667	0.542	5.675	0.089	0.020	1.914	0.002	0.008	1.735	0.001	0.002	0.001	0.296	0.004	0.179
10	0.1	0.5	1.667	0.542	5.675	0.089	0.020	2.707	0.002	0.008	1.735	0.001	0.002	0.001	0.601	0.018	0.736
10	0.62	0.5	1.667	0.542	5.675	0.089	0.020	1.087	0.002	0.008	1.735	0.000	0.002	0.000	0.090	0.000	0.016
10	0.1	0.5	1.667	0.542	5.675	0.089	0.020	5.713	0.002	0.008	1.735	0.006	0.002	0.006	2.706	0.373	14.930
10	0.2	0.5	1.667	0.542	5.675	0.089	0.020	4.040	0.002	0.008	1.735	0.003	0.002	0.003	1.349	0.093	3.709
10	0.3	0.5	1.667	0.542	5.675	0.089	0.020	3.299	0.002	0.008	1.735	0.002	0.002	0.002	0.896	0.041	1.638
10	0.4	0.5	1.667	0.542	5.675	0.089	0.020	2.857	0.002	0.008	1.735	0.002	0.002	0.002	0.670	0.023	0.916
10	0.5	0.5	1.667	0.542	5.675	0.089	0.020	2.555	0.002	0.008	1.735	0.001	0.002	0.001	0.534	0.015	0.582
10	0.6	0.5	1.667	0.542	5.675	0.089	0.020	2.333	0.002	0.008	1.735	0.001	0.002	0.001	0.444	0.010	0.402
10	0.5	0.525	1.667	0.542	5.675	0.089	0.020	1.181	0.002	0.008	1.693	0.000	0.002	0.000	0.108	0.001	0.024
10	0.4	0.525	1.667	0.542	5.675	0.089	0.020	1.321	0.002	0.008	1.693	0.000	0.002	0.000	0.137	0.001	0.038
10	0.3	0.525	1.667	0.542	5.675	0.089	0.020	1.525	0.002	0.008	1.693	0.000	0.002	0.000	0.185	0.002	0.070
10	0.2	0.525	1.667	0.542	5.675	0.089	0.020	1.868	0.002	0.008	1.693	0.001	0.002	0.001	0.282	0.004	0.162
10	0.1	0.525	1.667	0.542	5.675	0.089	0.020	2.642	0.002	0.008	1.693	0.001	0.002	0.001	0.572	0.017	0.667
10	0.62	0.525	1.667	0.542	5.675	0.089	0.020	1.061	0.002	0.008	1.693	0.000	0.002	0.000	0.085	0.000	0.015
10	0.1	0.525	1.667	0.542	5.675	0.089	0.020	5.576	0.002	0.008	1.693	0.006	0.002	0.006	2.577	0.338	13.537
10	0.2	0.525	1.667	0.542	5.675	0.089	0.020	3.943	0.002	0.008	1.693	0.003	0.002	0.003	1.284	0.084	3.362
10	0.3	0.525	1.667	0.542	5.675	0.089	0.020	3.219	0.002	0.008	1.693	0.002	0.002	0.002	0.853	0.037	1.484
10	0.4	0.525	1.667	0.542	5.675	0.089	0.020	2.788	0.002	0.008	1.693	0.002	0.002	0.002	0.638	0.021	0.829
10	0.5	0.525	1.667	0.542	5.675	0.089	0.020	2.494	0.002	0.008	1.693	0.001	0.002	0.001	0.509	0.013	0.527
10	0.6	0.525	1.667	0.542	5.675	0.089	0.020	2.276	0.002	0.008	1.693	0.001	0.002	0.001	0.422	0.009	0.364
10	0.5	0.55	1.667	0.542	5.675	0.089	0.020	1.154	0.002	0.008	1.654	0.000	0.002	0.000	0.102	0.001	0.021
10	0.4	0.55	1.667	0.542	5.675	0.089	0.020	1.291	0.002	0.008	1.654	0.000	0.002	0.000	0.130	0.001	0.034
10	0.3	0.55	1.667	0.542	5.675	0.089	0.020	1.490	0.002	0.008	1.654	0.000	0.002	0.000	0.176	0.002	0.063
10	0.2	0.55	1.667	0.542	5.675	0.089	0.020	1.825	0.002	0.008	1.654	0.001	0.002	0.001	0.268	0.004	0.147

Q	X	Z	V _{zi}	Z _{core}	V _{zj}	h _{down}	h _{up}	V _{xmax}	q _{up}	q _{down}	V(z)	FQSI	G _b	I _{net}	V _{up}	H _{up}	H _{up} /z
l/s	m	m	m/s	m	m/s	m	m	m/s	m ² /s	m ² /s	m/s	Ns	kg/m ²	Ns	m/s	m	
			Q=VA	Z=5*Bj	Eq. 25	Eq. 61		Eq. 63	Eq.61&62		Eq. 60	Fig.2.18	Eq. 59	Eq.55		Eq. 58	
10	0.1	0.55	1.667	0.542	5.675	0.089	0.020	2.581	0.002	0.008	1.654	0.001	0.002	0.001	0.546	0.015	0.607
10	0.62	0.55	1.667	0.542	5.675	0.089	0.020	1.037	0.002	0.008	1.654	0.000	0.002	0.000	0.081	0.000	0.013
10	0.1	0.55	1.667	0.542	5.675	0.089	0.020	5.448	0.002	0.008	1.654	0.006	0.002	0.006	2.459	0.308	12.331
10	0.2	0.55	1.667	0.542	5.675	0.089	0.020	3.852	0.002	0.008	1.654	0.003	0.002	0.003	1.225	0.077	3.061
10	0.3	0.55	1.667	0.542	5.675	0.089	0.020	3.145	0.002	0.008	1.654	0.002	0.002	0.002	0.814	0.034	1.351
10	0.4	0.55	1.667	0.542	5.675	0.089	0.020	2.724	0.002	0.008	1.654	0.001	0.002	0.001	0.608	0.019	0.755
10	0.5	0.55	1.667	0.542	5.675	0.089	0.020	2.436	0.002	0.008	1.654	0.001	0.002	0.001	0.485	0.012	0.480
10	0.6	0.55	1.667	0.542	5.675	0.089	0.020	2.224	0.002	0.008	1.654	0.001	0.002	0.001	0.403	0.008	0.331
10	0.5	0.575	1.667	0.542	5.675	0.089	0.020	1.129	0.002	0.008	1.618	0.000	0.002	0.000	0.097	0.000	0.019
10	0.4	0.575	1.667	0.542	5.675	0.089	0.020	1.262	0.002	0.008	1.618	0.000	0.002	0.000	0.124	0.001	0.031
10	0.3	0.575	1.667	0.542	5.675	0.089	0.020	1.457	0.002	0.008	1.618	0.000	0.002	0.000	0.168	0.001	0.058
10	0.2	0.575	1.667	0.542	5.675	0.089	0.020	1.785	0.002	0.008	1.618	0.001	0.002	0.001	0.256	0.003	0.134
10	0.1	0.575	1.667	0.542	5.675	0.089	0.020	2.524	0.002	0.008	1.618	0.001	0.002	0.001	0.521	0.014	0.554
10	0.62	0.575	1.667	0.542	5.675	0.089	0.020	1.014	0.002	0.008	1.618	0.000	0.002	0.000	0.077	0.000	0.012
10	0.1	0.575	1.667	0.542	5.675	0.089	0.020	5.328	0.002	0.008	1.618	0.006	0.002	0.006	2.352	0.282	11.278
10	0.2	0.575	1.667	0.542	5.675	0.089	0.020	3.767	0.002	0.008	1.618	0.003	0.002	0.003	1.172	0.070	2.799
10	0.3	0.575	1.667	0.542	5.675	0.089	0.020	3.076	0.002	0.008	1.618	0.002	0.002	0.002	0.778	0.031	1.235
10	0.4	0.575	1.667	0.542	5.675	0.089	0.020	2.664	0.002	0.008	1.618	0.001	0.002	0.001	0.582	0.017	0.690
10	0.5	0.575	1.667	0.542	5.675	0.089	0.020	2.383	0.002	0.008	1.618	0.001	0.002	0.001	0.464	0.011	0.438
10	0.6	0.575	1.667	0.542	5.675	0.089	0.020	2.175	0.002	0.008	1.618	0.001	0.002	0.001	0.385	0.008	0.302
10	0.5	0.6	1.667	0.542	5.675	0.089	0.020	2.333	0.002	0.008	1.584	0.001	0.002	0.001	0.444	0.010	0.402
10	0.4	0.6	1.667	0.542	5.675	0.089	0.020	2.608	0.002	0.008	1.584	0.001	0.002	0.001	0.557	0.016	0.633
10	0.3	0.6	1.667	0.542	5.675	0.089	0.020	3.011	0.002	0.008	1.584	0.002	0.002	0.002	0.746	0.028	1.133
10	0.2	0.6	1.667	0.542	5.675	0.089	0.020	3.688	0.002	0.008	1.584	0.003	0.002	0.003	1.123	0.064	2.569
10	0.1	0.6	1.667	0.542	5.675	0.089	0.020	5.216	0.002	0.008	1.584	0.005	0.002	0.005	2.254	0.259	10.355

Q	X	Z	V _{zi}	Z _{core}	V _{zj}	h _{down}	h _{up}	V _{xmax}	q _{up}	q _{down}	V(z)	FQSI	G _b	I _{net}	V _{up}	H _{up}	H _{up} /z
l/s	m	m	m/s	m	m/s	m	m	m/s	m ² /s	m ² /s	m/s	Ns	kg/m ²	Ns	m/s	m	
			Q=VA	Z=5*Bj	Eq. 25	Eq. 61		Eq. 63	Eq. 61&62		Eq. 60	Fig.2.18	Eq. 59	Eq.55		Eq. 58	
10	0.62	0.6	1.667	0.542	5.675	0.089	0.020	2.095	0.002	0.008	1.584	0.001	0.002	0.001	0.356	0.006	0.259
10	0.1	0.6	1.667	0.542	5.675	0.089	0.020	5.216	0.002	0.008	1.584	0.005	0.002	0.005	2.254	0.259	10.355
10	0.2	0.6	1.667	0.542	5.675	0.089	0.020	3.688	0.002	0.008	1.584	0.003	0.002	0.003	1.123	0.064	2.569
10	0.3	0.6	1.667	0.542	5.675	0.089	0.020	3.011	0.002	0.008	1.584	0.002	0.002	0.002	0.746	0.028	1.133
10	0.4	0.6	1.667	0.542	5.675	0.089	0.020	2.608	0.002	0.008	1.584	0.001	0.002	0.001	0.557	0.016	0.633
10	0.5	0.6	1.667	0.542	5.675	0.089	0.020	2.333	0.002	0.008	1.584	0.001	0.002	0.001	0.444	0.010	0.402
10	0.6	0.6	1.667	0.542	5.675	0.089	0.020	2.129	0.002	0.008	1.584	0.001	0.002	0.001	0.369	0.007	0.277
10	0.5	0.625	1.667	0.542	5.675	0.089	0.020	2.285	0.002	0.008	1.552	0.001	0.002	0.001	0.426	0.009	0.370
10	0.4	0.625	1.667	0.542	5.675	0.089	0.020	2.555	0.002	0.008	1.552	0.001	0.002	0.001	0.534	0.015	0.582
10	0.3	0.625	1.667	0.542	5.675	0.089	0.020	2.950	0.002	0.008	1.552	0.002	0.002	0.002	0.715	0.026	1.043
10	0.2	0.625	1.667	0.542	5.675	0.089	0.020	3.614	0.002	0.008	1.552	0.003	0.002	0.003	1.077	0.059	2.366
10	0.1	0.625	1.667	0.542	5.675	0.089	0.020	5.110	0.002	0.008	1.552	0.005	0.002	0.005	2.163	0.238	9.540
10	0.62	0.625	1.667	0.542	5.675	0.089	0.020	2.052	0.002	0.008	1.552	0.001	0.002	0.001	0.342	0.006	0.238
10	0.1	0.625	1.667	0.542	5.675	0.089	0.020	5.110	0.002	0.008	1.552	0.005	0.002	0.005	2.163	0.238	9.540
10	0.2	0.625	1.667	0.542	5.675	0.089	0.020	3.614	0.002	0.008	1.552	0.003	0.002	0.003	1.077	0.059	2.366
10	0.3	0.625	1.667	0.542	5.675	0.089	0.020	2.950	0.002	0.008	1.552	0.002	0.002	0.002	0.715	0.026	1.043
10	0.4	0.625	1.667	0.542	5.675	0.089	0.020	2.555	0.002	0.008	1.552	0.001	0.002	0.001	0.534	0.015	0.582
10	0.5	0.625	1.667	0.542	5.675	0.089	0.020	2.285	0.002	0.008	1.552	0.001	0.002	0.001	0.426	0.009	0.370
10	0.6	0.625	1.667	0.542	5.675	0.089	0.020	2.086	0.002	0.008	1.552	0.001	0.002	0.001	0.353	0.006	0.255

Table D 0.4. Quasi-steady method of Q=10 l/s, H=3 m and TW=0.5 m

Q	X	Z	V _{zi}	Z _{core}	V _{zj}	h _{down}	h _{up}	V _{xmax}	q _{up}	q _{down}	V(z)	FQSI	Gb	Inet	Vup	Hup	Hup/z
l/s	m	m	m/s	m	m/s	m	m	m/s	m ² /s	m ² /s	m/s	Ns	kg/m ²	Ns	m/s	m	
			Q=VA	Z=5*Bj	Eq. 25	Eq.61		Eq. 63	Eq. 61&62		Eq. 60	Fig.2.18	Eq. 59	Eq.55		Eq. 58	
10	0.75	0	1.667	0.481	7.199	0.079	0.018	0.878	0.002	0.008	7.199						
10	0.75	0.042	1.667	0.481	7.199	0.079	0.018	0.878	0.002	0.008	5.664						
10	0.75	0.083	1.667	0.481	7.199	0.079	0.018	0.878	0.002	0.008	4.005						
10	0.75	0.125	1.667	0.481	7.199	0.079	0.018	0.878	0.002	0.008	3.270						
10	0.75	0.167	1.667	0.481	7.199	0.079	0.018	0.878	0.002	0.008	2.832						
10	0.75	0.208	1.667	0.481	7.199	0.079	0.018	0.878	0.002	0.008	2.533						
10	0.75	0.25	1.667	0.481	7.199	0.079	0.018	0.878	0.002	0.008	2.312						
10	0.75	0.292	1.667	0.481	7.199	0.079	0.018	0.878	0.002	0.008	2.141						
10	0.75	0.333	1.667	0.481	7.199	0.079	0.018	0.878	0.002	0.008	2.002						
10	0.75	0.375	1.667	0.481	7.199	0.079	0.018	0.878	0.002	0.008	1.888						
10	0.75	0.417	1.667	0.481	7.199	0.079	0.018	0.878	0.002	0.008	1.791						
10	0.75	0.458	1.667	0.481	7.199	0.079	0.018	0.878	0.002	0.008	1.708						
10	0.75	0.5	1.667	0.481	7.199	0.079	0.018	0.878	0.002	0.008	1.635						
10	0.5	0.5	1.667	0.481	7.199	0.079	0.018	1.075	0.002	0.008	1.635	0.000	0.002	0.000	0.088	0.000	0.016
10	0.4	0.5	1.667	0.481	7.199	0.079	0.018	1.202	0.002	0.008	1.635	0.000	0.002	0.000	0.112	0.001	0.025
10	0.3	0.5	1.667	0.481	7.199	0.079	0.018	1.388	0.002	0.008	1.635	0.000	0.002	0.000	0.152	0.001	0.047
10	0.2	0.5	1.667	0.481	7.199	0.079	0.018	1.700	0.002	0.008	1.635	0.001	0.002	0.001	0.232	0.003	0.109
10	0.1	0.5	1.667	0.481	7.199	0.079	0.018	2.404	0.002	0.008	1.635	0.001	0.002	0.001	0.472	0.011	0.454
10	0.75	0.5	1.667	0.481	7.199	0.079	0.018	0.878	0.002	0.008	1.635	0.000	0.002	0.000	0.056	0.000	0.006
10	0.1	0.5	1.667	0.481	7.199	0.079	0.018	5.073	0.002	0.008	1.635	0.005	0.002	0.005	2.131	0.232	9.262
10	0.2	0.5	1.667	0.481	7.199	0.079	0.018	3.587	0.002	0.008	1.635	0.003	0.002	0.003	1.061	0.057	2.297
10	0.3	0.5	1.667	0.481	7.199	0.079	0.018	2.929	0.002	0.008	1.635	0.002	0.002	0.002	0.705	0.025	1.013
10	0.4	0.5	1.667	0.481	7.199	0.079	0.018	2.536	0.002	0.008	1.635	0.001	0.002	0.001	0.526	0.014	0.565

Q	X	Z	V _{zi}	Z _{core}	V _{zj}	h _{down}	h _{up}	V _{xmax}	q _{up}	q _{down}	V(z)	FQSI	G _b	I _{net}	V _{up}	H _{up}	H _{up} /z
l/s	m	m	m/s	m	m/s	m	m	m/s	m ² /s	m ² /s	m/s	Ns	kg/m ²	Ns	m/s	m	
			Q=VA	Z=5*Bj	Eq. 25	Eq. 61		Eq. 63	Eq. 61&62		Eq. 60	Fig.2.18	Eq. 59	Eq.55		Eq. 58	
10	0.5	0.5	1.667	0.481	7.199	0.079	0.018	2.269	0.002	0.008	1.635	0.001	0.002	0.001	0.419	0.009	0.359
10	0.6	0.5	1.667	0.481	7.199	0.079	0.018	2.071	0.002	0.008	1.635	0.001	0.002	0.001	0.348	0.006	0.247
10	0.5	0.525	1.667	0.481	7.199	0.079	0.018	1.049	0.002	0.008	1.596	0.000	0.002	0.000	0.083	0.000	0.014
10	0.4	0.525	1.667	0.481	7.199	0.079	0.018	1.173	0.002	0.008	1.596	0.000	0.002	0.000	0.106	0.001	0.023
10	0.3	0.525	1.667	0.481	7.199	0.079	0.018	1.354	0.002	0.008	1.596	0.000	0.002	0.000	0.144	0.001	0.042
10	0.2	0.525	1.667	0.481	7.199	0.079	0.018	1.659	0.002	0.008	1.596	0.001	0.002	0.001	0.220	0.002	0.099
10	0.1	0.525	1.667	0.481	7.199	0.079	0.018	2.346	0.002	0.008	1.596	0.001	0.002	0.001	0.449	0.010	0.411
10	0.75	0.525	1.667	0.481	7.199	0.079	0.018	0.857	0.002	0.008	1.596	0.000	0.002	0.000	0.052	0.000	0.006
10	0.1	0.525	1.667	0.481	7.199	0.079	0.018	4.951	0.002	0.008	1.596	0.005	0.002	0.005	2.030	0.210	8.398
10	0.2	0.525	1.667	0.481	7.199	0.079	0.018	3.501	0.002	0.008	1.596	0.002	0.002	0.002	1.011	0.052	2.082
10	0.3	0.525	1.667	0.481	7.199	0.079	0.018	2.858	0.002	0.008	1.596	0.002	0.002	0.002	0.671	0.023	0.917
10	0.4	0.525	1.667	0.481	7.199	0.079	0.018	2.475	0.002	0.008	1.596	0.001	0.002	0.001	0.501	0.013	0.512
10	0.5	0.525	1.667	0.481	7.199	0.079	0.018	2.214	0.002	0.008	1.596	0.001	0.002	0.001	0.399	0.008	0.325
10	0.6	0.525	1.667	0.481	7.199	0.079	0.018	2.021	0.002	0.008	1.596	0.001	0.002	0.001	0.331	0.006	0.224
10	0.5	0.55	1.667	0.481	7.199	0.079	0.018	1.025	0.002	0.008	1.559	0.000	0.002	0.000	0.079	0.000	0.013
10	0.4	0.55	1.667	0.481	7.199	0.079	0.018	1.146	0.002	0.008	1.559	0.000	0.002	0.000	0.101	0.001	0.021
10	0.3	0.55	1.667	0.481	7.199	0.079	0.018	1.323	0.002	0.008	1.559	0.000	0.002	0.000	0.137	0.001	0.038
10	0.2	0.55	1.667	0.481	7.199	0.079	0.018	1.620	0.002	0.008	1.559	0.001	0.002	0.000	0.210	0.002	0.090
10	0.1	0.55	1.667	0.481	7.199	0.079	0.018	2.292	0.002	0.008	1.559	0.001	0.002	0.001	0.428	0.009	0.374
10	0.75	0.55	1.667	0.481	7.199	0.079	0.018	0.837	0.002	0.008	1.559	0.000	0.002	0.000	0.050	0.000	0.005
10	0.1	0.55	1.667	0.481	7.199	0.079	0.018	4.837	0.002	0.008	1.559	0.005	0.002	0.005	1.937	0.191	7.649
10	0.2	0.55	1.667	0.481	7.199	0.079	0.018	3.420	0.002	0.008	1.559	0.002	0.002	0.002	0.964	0.047	1.895
10	0.3	0.55	1.667	0.481	7.199	0.079	0.018	2.793	0.002	0.008	1.559	0.002	0.002	0.002	0.640	0.021	0.835
10	0.4	0.55	1.667	0.481	7.199	0.079	0.018	2.418	0.002	0.008	1.559	0.001	0.002	0.001	0.478	0.012	0.465

Q	X	Z	V _{zi}	Z _{core}	V _{zj}	h _{down}	h _{up}	V _{xmax}	q _{up}	q _{down}	V(z)	FQSI	G _b	I _{net}	V _{up}	H _{up}	H _{up} /z
l/s	m	m	m/s	m	m/s	m	m	m/s	m ² /s	m ² /s	m/s	Ns	kg/m ²	Ns	m/s	m	
			Q=VA	Z=5*Bj	Eq. 25	Eq. 61		Eq. 63	Eq. 61&62		Eq. 60	Fig.2.18	Eq. 59	Eq.55		Eq. 58	
10	0.5	0.55	1.667	0.481	7.199	0.079	0.018	2.163	0.002	0.008	1.559	0.001	0.002	0.001	0.381	0.007	0.295
10	0.6	0.55	1.667	0.481	7.199	0.079	0.018	1.975	0.002	0.008	1.559	0.001	0.002	0.001	0.316	0.005	0.203
10	0.5	0.575	1.667	0.481	7.199	0.079	0.018	1.002	0.002	0.008	1.525	0.000	0.002	0.000	0.075	0.000	0.011
10	0.4	0.575	1.667	0.481	7.199	0.079	0.018	1.121	0.002	0.008	1.525	0.000	0.002	0.000	0.096	0.000	0.019
10	0.3	0.575	1.667	0.481	7.199	0.079	0.018	1.294	0.002	0.008	1.525	0.000	0.002	0.000	0.131	0.001	0.035
10	0.2	0.575	1.667	0.481	7.199	0.079	0.018	1.585	0.002	0.008	1.525	0.000	0.002	0.000	0.200	0.002	0.082
10	0.1	0.575	1.667	0.481	7.199	0.079	0.018	2.241	0.002	0.008	1.525	0.001	0.002	0.001	0.409	0.009	0.341
10	0.75	0.575	1.667	0.481	7.199	0.079	0.018	0.818	0.002	0.008	1.525	0.000	0.002	0.000	0.047	0.000	0.005
10	0.1	0.575	1.667	0.481	7.199	0.079	0.018	4.730	0.002	0.008	1.525	0.004	0.002	0.004	1.852	0.175	6.995
10	0.2	0.575	1.667	0.481	7.199	0.079	0.018	3.345	0.002	0.008	1.525	0.002	0.002	0.002	0.922	0.043	1.733
10	0.3	0.575	1.667	0.481	7.199	0.079	0.018	2.731	0.002	0.008	1.525	0.001	0.002	0.001	0.612	0.019	0.763
10	0.4	0.575	1.667	0.481	7.199	0.079	0.018	2.365	0.002	0.008	1.525	0.001	0.002	0.001	0.457	0.011	0.425
10	0.5	0.575	1.667	0.481	7.199	0.079	0.018	2.116	0.002	0.008	1.525	0.001	0.002	0.001	0.364	0.007	0.270
10	0.6	0.575	1.667	0.481	7.199	0.079	0.018	1.931	0.002	0.008	1.525	0.001	0.002	0.001	0.302	0.005	0.185
10	0.5	0.6	1.667	0.481	7.199	0.079	0.018	0.981	0.002	0.008	1.493	0.000	0.002	0.000	0.072	0.000	0.010
10	0.4	0.6	1.667	0.481	7.199	0.079	0.018	1.097	0.002	0.008	1.493	0.000	0.002	0.000	0.092	0.000	0.017
10	0.3	0.6	1.667	0.481	7.199	0.079	0.018	1.267	0.002	0.008	1.493	0.000	0.002	0.000	0.125	0.001	0.032
10	0.2	0.6	1.667	0.481	7.199	0.079	0.018	1.552	0.002	0.008	1.493	0.000	0.002	0.000	0.192	0.002	0.075
10	0.1	0.6	1.667	0.481	7.199	0.079	0.018	2.194	0.002	0.008	1.493	0.001	0.002	0.001	0.392	0.008	0.313
10	0.75	0.6	1.667	0.481	7.199	0.079	0.018	0.801	0.002	0.008	1.493	0.000	0.002	0.000	0.045	0.000	0.004
10	0.1	0.6	1.667	0.481	7.199	0.079	0.018	4.631	0.002	0.008	1.493	0.004	0.002	0.004	1.775	0.161	6.422
10	0.2	0.6	1.667	0.481	7.199	0.079	0.018	3.275	0.002	0.008	1.493	0.002	0.002	0.002	0.883	0.040	1.590
10	0.3	0.6	1.667	0.481	7.199	0.079	0.018	2.674	0.002	0.008	1.493	0.001	0.002	0.001	0.586	0.017	0.700
10	0.4	0.6	1.667	0.481	7.199	0.079	0.018	2.315	0.002	0.008	1.493	0.001	0.002	0.001	0.437	0.010	0.390
10	0.5	0.6	1.667	0.481	7.199	0.079	0.018	2.071	0.002	0.008	1.493	0.001	0.002	0.001	0.348	0.006	0.247

Q	X	Z	V _{zi}	Z _{core}	V _{zj}	h _{down}	h _{up}	V _{xmax}	q _{up}	q _{down}	V(z)	FQSI	G _b	I _{net}	V _{up}	H _{up}	H _{up} /z
l/s	m	m	m/s	m	m/s	m	m	m/s	m ² /s	m ² /s	m/s	Ns	kg/m ²	Ns	m/s	m	
			Q=VA	Z=5*Bj	Eq. 25	Eq. 61		Eq. 63	Eq. 61&62		Eq. 60	Fig.2.18	Eq. 59	Eq.55		Eq. 58	
10	0.6	0.6	1.667	0.481	7.199	0.079	0.018	1.891	0.002	0.008	1.493	0.001	0.002	0.001	0.289	0.004	0.170
10	0.5	0.625	1.667	0.481	7.199	0.079	0.018	0.961	0.002	0.008	1.462	0.000	0.002	0.000	0.068	0.000	0.010
10	0.4	0.625	1.667	0.481	7.199	0.079	0.018	1.075	0.002	0.008	1.462	0.000	0.002	0.000	0.088	0.000	0.016
10	0.3	0.625	1.667	0.481	7.199	0.079	0.018	1.241	0.002	0.008	1.462	0.000	0.002	0.000	0.120	0.001	0.029
10	0.2	0.625	1.667	0.481	7.199	0.079	0.018	1.520	0.002	0.008	1.462	0.000	0.002	0.000	0.184	0.002	0.069
10	0.1	0.625	1.667	0.481	7.199	0.079	0.018	2.150	0.002	0.008	1.462	0.001	0.002	0.001	0.376	0.007	0.288
10	0.75	0.625	1.667	0.481	7.199	0.079	0.018	0.785	0.002	0.008	1.462	0.000	0.002	0.000	0.043	0.000	0.004
10	0.1	0.625	1.667	0.481	7.199	0.079	0.018	4.537	0.002	0.008	1.462	0.004	0.002	0.004	1.703	0.148	5.916
10	0.2	0.625	1.667	0.481	7.199	0.079	0.018	3.208	0.002	0.008	1.462	0.002	0.002	0.002	0.847	0.037	1.464
10	0.3	0.625	1.667	0.481	7.199	0.079	0.018	2.620	0.002	0.008	1.462	0.001	0.002	0.001	0.562	0.016	0.644
10	0.4	0.625	1.667	0.481	7.199	0.079	0.018	2.269	0.002	0.008	1.462	0.001	0.002	0.001	0.419	0.009	0.359
10	0.5	0.625	1.667	0.481	7.199	0.079	0.018	2.029	0.002	0.008	1.462	0.001	0.002	0.001	0.334	0.006	0.227
10	0.6	0.625	1.667	0.481	7.199	0.079	0.018	1.852	0.002	0.008	1.462	0.001	0.002	0.001	0.277	0.004	0.156
10	0.5	0.65	1.667	0.481	7.199	0.079	0.018	0.943	0.002	0.008	1.434	0.000	0.002	0.000	0.065	0.000	0.009
10	0.4	0.65	1.667	0.481	7.199	0.079	0.018	1.054	0.002	0.008	1.434	0.000	0.002	0.000	0.084	0.000	0.014
10	0.3	0.65	1.667	0.481	7.199	0.079	0.018	1.217	0.002	0.008	1.434	0.000	0.002	0.000	0.115	0.001	0.027
10	0.2	0.65	1.667	0.481	7.199	0.079	0.018	1.491	0.002	0.008	1.434	0.000	0.002	0.000	0.176	0.002	0.063
10	0.1	0.65	1.667	0.481	7.199	0.079	0.018	2.108	0.002	0.008	1.434	0.001	0.002	0.001	0.361	0.007	0.266
10	0.75	0.65	1.667	0.481	7.199	0.079	0.018	0.770	0.002	0.008	1.434	0.000	0.002	0.000	0.041	0.000	0.003
10	0.1	0.65	1.667	0.481	7.199	0.079	0.018	4.449	0.002	0.008	1.434	0.004	0.002	0.004	1.638	0.137	5.467
10	0.2	0.65	1.667	0.481	7.199	0.079	0.018	3.146	0.002	0.008	1.434	0.002	0.002	0.002	0.815	0.034	1.353
10	0.3	0.65	1.667	0.481	7.199	0.079	0.018	2.569	0.002	0.008	1.434	0.001	0.002	0.001	0.540	0.015	0.595
10	0.4	0.65	1.667	0.481	7.199	0.079	0.018	2.225	0.002	0.008	1.434	0.001	0.002	0.001	0.403	0.008	0.331
10	0.5	0.65	1.667	0.481	7.199	0.079	0.018	1.990	0.002	0.008	1.434	0.001	0.002	0.001	0.321	0.005	0.210
10	0.6	0.65	1.667	0.481	7.199	0.079	0.018	1.816	0.002	0.008	1.434	0.001	0.002	0.001	0.266	0.004	0.144

Q	X	Z	V _{zi}	Z _{core}	V _{zj}	h _{down}	h _{up}	V _{xmax}	q _{up}	q _{down}	V(z)	FQSI	G _b	I _{net}	V _{up}	H _{up}	H _{up} /z
l/s	m	m	m/s	m	m/s	m	m	m/s	m ² /s	m ² /s	m/s	Ns	kg/m ²	Ns	m/s	m	
			Q=VA	Z=5*Bj	Eq. 25	Eq. 61		Eq. 63	Eq. 61&62		Eq. 60	Fig.2.18	Eq. 59	Eq.55		Eq. 58	
10	0.5	0.675	1.667	0.481	7.199	0.079	0.018	0.925	0.002	0.008	1.407	0.000	0.002	0.000	0.063	0.000	0.008
10	0.4	0.675	1.667	0.481	7.199	0.079	0.018	1.034	0.002	0.008	1.407	0.000	0.002	0.000	0.080	0.000	0.013
10	0.3	0.675	1.667	0.481	7.199	0.079	0.018	1.194	0.002	0.008	1.407	0.000	0.002	0.000	0.110	0.001	0.025
10	0.2	0.675	1.667	0.481	7.199	0.079	0.018	1.463	0.002	0.008	1.407	0.000	0.002	0.000	0.169	0.001	0.059
10	0.1	0.675	1.667	0.481	7.199	0.079	0.018	2.069	0.002	0.008	1.407	0.001	0.002	0.001	0.347	0.006	0.246
10	0.75	0.675	1.667	0.481	7.199	0.079	0.018	0.755	0.002	0.008	1.407	0.000	0.002	0.000	0.039	0.000	0.003
10	0.1	0.675	1.667	0.481	7.199	0.079	0.018	4.366	0.002	0.008	1.407	0.004	0.002	0.004	1.577	0.127	5.068
10	0.2	0.675	1.667	0.481	7.199	0.079	0.018	3.087	0.002	0.008	1.407	0.002	0.002	0.002	0.784	0.031	1.253
10	0.3	0.675	1.667	0.481	7.199	0.079	0.018	2.521	0.002	0.008	1.407	0.001	0.002	0.001	0.520	0.014	0.551
10	0.4	0.675	1.667	0.481	7.199	0.079	0.018	2.183	0.002	0.008	1.407	0.001	0.002	0.001	0.388	0.008	0.307
10	0.5	0.675	1.667	0.481	7.199	0.079	0.018	1.953	0.002	0.008	1.407	0.001	0.002	0.001	0.309	0.005	0.194
10	0.6	0.675	1.667	0.481	7.199	0.079	0.018	1.782	0.002	0.008	1.407	0.001	0.002	0.001	0.256	0.003	0.133
10	0.5	0.7	1.667	0.481	7.199	0.079	0.018	0.908	0.002	0.008	1.382	0.000	0.002	0.000	0.060	0.000	0.007
10	0.4	0.7	1.667	0.481	7.199	0.079	0.018	1.016	0.002	0.008	1.382	0.000	0.002	0.000	0.077	0.000	0.012
10	0.3	0.7	1.667	0.481	7.199	0.079	0.018	1.173	0.002	0.008	1.382	0.000	0.002	0.000	0.106	0.001	0.023
10	0.2	0.7	1.667	0.481	7.199	0.079	0.018	1.436	0.002	0.008	1.382	0.000	0.002	0.000	0.163	0.001	0.054
10	0.1	0.7	1.667	0.481	7.199	0.079	0.018	2.031	0.002	0.008	1.382	0.001	0.002	0.001	0.335	0.006	0.228
10	0.75	0.7	1.667	0.481	7.199	0.079	0.018	0.742	0.002	0.008	1.382	0.000	0.002	0.000	0.037	0.000	0.003
10	0.1	0.7	1.667	0.481	7.199	0.079	0.018	4.287	0.002	0.008	1.382	0.004	0.002	0.004	1.520	0.118	4.710
10	0.2	0.7	1.667	0.481	7.199	0.079	0.018	3.032	0.002	0.008	1.382	0.002	0.002	0.002	0.756	0.029	1.164
10	0.3	0.7	1.667	0.481	7.199	0.079	0.018	2.475	0.002	0.008	1.382	0.001	0.002	0.001	0.501	0.013	0.512
10	0.4	0.7	1.667	0.481	7.199	0.079	0.018	2.144	0.002	0.008	1.382	0.001	0.002	0.001	0.374	0.007	0.285
10	0.5	0.7	1.667	0.481	7.199	0.079	0.018	1.917	0.002	0.008	1.382	0.001	0.002	0.001	0.297	0.005	0.180
10	0.6	0.7	1.667	0.481	7.199	0.079	0.018	1.750	0.002	0.008	1.382	0.001	0.002	0.001	0.246	0.003	0.124
10	0.5	0.725	1.667	0.481	7.199	0.079	0.018	0.893	0.002	0.008	1.358	0.000	0.002	0.000	0.058	0.000	0.007

Q	X	Z	V _{zi}	Z _{core}	V _{zj}	h _{down}	h _{up}	V _{xmax}	q _{up}	q _{down}	V(z)	FQSI	G _b	I _{net}	V _{up}	H _{up}	H _{up} /z
l/s	m	m	m/s	m	m/s	m	m	m/s	m ² /s	m ² /s	m/s	Ns	kg/m ²	Ns	m/s	m	
			Q=VA	Z=5*Bj	Eq. 25	Eq.61		Eq. 63	Eq. 61&62		Eq. 60	Fig.2.18	Eq. 59	Eq.55		Eq. 58	
10	0.4	0.725	1.667	0.481	7.199	0.079	0.018	0.998	0.002	0.008	1.358	0.000	0.002	0.000	0.074	0.000	0.011
10	0.3	0.725	1.667	0.481	7.199	0.079	0.018	1.152	0.002	0.008	1.358	0.000	0.002	0.000	0.102	0.001	0.021
10	0.2	0.725	1.667	0.481	7.199	0.079	0.018	1.411	0.002	0.008	1.358	0.000	0.002	0.000	0.157	0.001	0.050
10	0.1	0.725	1.667	0.481	7.199	0.079	0.018	1.996	0.002	0.008	1.358	0.001	0.002	0.001	0.323	0.005	0.212
10	0.75	0.725	1.667	0.481	7.199	0.079	0.018	0.729	0.002	0.008	1.358	0.000	0.002	0.000	0.036	0.000	0.003
10	0.1	0.725	1.667	0.481	7.199	0.079	0.018	4.213	0.002	0.008	1.358	0.004	0.002	0.003	1.467	0.110	4.389
10	0.2	0.725	1.667	0.481	7.199	0.079	0.018	2.979	0.002	0.008	1.358	0.002	0.002	0.002	0.729	0.027	1.085
10	0.3	0.725	1.667	0.481	7.199	0.079	0.018	2.432	0.002	0.008	1.358	0.001	0.002	0.001	0.483	0.012	0.476
10	0.4	0.725	1.667	0.481	7.199	0.079	0.018	2.106	0.002	0.008	1.358	0.001	0.002	0.001	0.360	0.007	0.265
10	0.5	0.725	1.667	0.481	7.199	0.079	0.018	1.884	0.002	0.008	1.358	0.001	0.002	0.001	0.287	0.004	0.168
10	0.6	0.725	1.667	0.481	7.199	0.079	0.018	1.720	0.002	0.008	1.358	0.001	0.002	0.001	0.237	0.003	0.115
10	0.5	0.75	1.667	0.481	7.199	0.079	0.018	0.878	0.002	0.008	1.335	0.000	0.002	0.000	0.056	0.000	0.006
10	0.4	0.75	1.667	0.481	7.199	0.079	0.018	0.981	0.002	0.008	1.335	0.000	0.002	0.000	0.072	0.000	0.010
10	0.3	0.75	1.667	0.481	7.199	0.079	0.018	1.133	0.002	0.008	1.335	0.000	0.002	0.000	0.098	0.000	0.020
10	0.2	0.75	1.667	0.481	7.199	0.079	0.018	1.388	0.002	0.008	1.335	0.000	0.002	0.000	0.152	0.001	0.047
10	0.1	0.75	1.667	0.481	7.199	0.079	0.018	1.963	0.002	0.008	1.335	0.001	0.002	0.001	0.312	0.005	0.198
10	0.75	0.75	1.667	0.481	7.199	0.079	0.018	0.717	0.002	0.008	1.335	0.000	0.002	0.000	0.034	0.000	0.002
10	0.1	0.75	1.667	0.481	7.199	0.079	0.018	4.142	0.002	0.008	1.335	0.003	0.002	0.003	1.418	0.103	4.100
10	0.2	0.75	1.667	0.481	7.199	0.079	0.018	1.388	0.002	0.008	1.335	0.000	0.002	0.000	0.152	0.001	0.047
10	0.3	0.75	1.667	0.481	7.199	0.079	0.018	1.133	0.002	0.008	1.335	0.000	0.002	0.000	0.098	0.000	0.020
10	0.4	0.75	1.667	0.481	7.199	0.079	0.018	0.981	0.002	0.008	1.335	0.000	0.002	0.000	0.072	0.000	0.010
10	0.5	0.75	1.667	0.481	7.199	0.079	0.018	0.878	0.002	0.008	1.335	0.000	0.002	0.000	0.056	0.000	0.006
10	0.6	0.75	1.667	0.481	7.199	0.079	0.018	0.801	0.002	0.008	1.335	0.000	0.002	0.000	0.045	0.000	0.004
10	0.5	0.775	1.667	0.481	7.199	0.079	0.018	0.863	0.002	0.008	1.313	0.000	0.002	0.000	0.053	0.000	0.006
10	0.4	0.775	1.667	0.481	7.199	0.079	0.018	0.965	0.002	0.008	1.313	0.000	0.002	0.000	0.069	0.000	0.010

Q	X	Z	V _{zi}	Z _{core}	V _{zj}	h _{down}	h _{up}	V _{xmax}	q _{up}	q _{down}	V(z)	FQSI	G _b	I _{net}	V _{up}	H _{up}	H _{up} /z
l/s	m	m	m/s	m	m/s	m	m	m/s	m ² /s	m ² /s	m/s	Ns	kg/m ²	Ns	m/s	m	
			Q=VA	Z=5*Bj	Eq. 25	Eq. 61		Eq. 63	Eq. 61&62		Eq. 60	Fig.2.18	Eq. 59	Eq.55		Eq. 58	
10	0.3	0.775	1.667	0.481	7.199	0.079	0.018	1.115	0.002	0.008	1.313	0.000	0.002	0.000	0.095	0.000	0.018
10	0.2	0.775	1.667	0.481	7.199	0.079	0.018	1.365	0.002	0.008	1.313	0.000	0.002	0.000	0.146	0.001	0.044
10	0.1	0.775	1.667	0.481	7.199	0.079	0.018	1.931	0.002	0.008	1.313	0.001	0.002	0.001	0.301	0.005	0.185
10	0.75	0.775	1.667	0.481	7.199	0.079	0.018	0.705	0.002	0.008	1.313	0.000	0.002	0.000	0.033	0.000	0.002
10	0.1	0.775	1.667	0.481	7.199	0.079	0.018	4.075	0.002	0.008	1.313	0.003	0.002	0.003	1.372	0.096	3.838
10	0.2	0.775	1.667	0.481	7.199	0.079	0.018	2.881	0.002	0.008	1.313	0.002	0.002	0.002	0.682	0.024	0.948
10	0.3	0.775	1.667	0.481	7.199	0.079	0.018	2.352	0.002	0.008	1.313	0.001	0.002	0.001	0.452	0.010	0.416
10	0.4	0.775	1.667	0.481	7.199	0.079	0.018	2.037	0.002	0.008	1.313	0.001	0.002	0.001	0.337	0.006	0.231
10	0.5	0.775	1.667	0.481	7.199	0.079	0.018	1.822	0.002	0.008	1.313	0.001	0.002	0.001	0.268	0.004	0.146
10	0.6	0.775	1.667	0.481	7.199	0.079	0.018	1.663	0.002	0.008	1.313	0.001	0.002	0.001	0.222	0.003	0.100
10	0.5	0.8	1.667	0.481	7.199	0.079	0.018	0.850	0.002	0.008	1.293	0.000	0.002	0.000	0.052	0.000	0.005
10	0.4	0.8	1.667	0.481	7.199	0.079	0.018	0.950	0.002	0.008	1.293	0.000	0.002	0.000	0.067	0.000	0.009
10	0.3	0.8	1.667	0.481	7.199	0.079	0.018	1.097	0.002	0.008	1.293	0.000	0.002	0.000	0.092	0.000	0.017
10	0.2	0.8	1.667	0.481	7.199	0.079	0.018	1.344	0.002	0.008	1.293	0.000	0.002	0.000	0.142	0.001	0.041
10	0.1	0.8	1.667	0.481	7.199	0.079	0.018	1.900	0.002	0.008	1.293	0.001	0.002	0.001	0.292	0.004	0.174
10	0.75	0.8	1.667	0.481	7.199	0.079	0.018	0.694	0.002	0.008	1.293	0.000	0.002	0.000	0.032	0.000	0.002
10	0.1	0.8	1.667	0.481	7.199	0.079	0.018	4.010	0.002	0.008	1.293	0.003	0.002	0.003	1.329	0.090	3.601
10	0.2	0.8	1.667	0.481	7.199	0.079	0.018	2.836	0.002	0.008	1.293	0.002	0.002	0.002	0.660	0.022	0.889
10	0.3	0.8	1.667	0.481	7.199	0.079	0.018	2.315	0.002	0.008	1.293	0.001	0.002	0.001	0.437	0.010	0.390
10	0.4	0.8	1.667	0.481	7.199	0.079	0.018	2.005	0.002	0.008	1.293	0.001	0.002	0.001	0.326	0.005	0.216
10	0.5	0.8	1.667	0.481	7.199	0.079	0.018	1.794	0.002	0.008	1.293	0.001	0.002	0.001	0.259	0.003	0.137
10	0.6	0.8	1.667	0.481	7.199	0.079	0.018	1.637	0.002	0.008	1.293	0.001	0.002	0.001	0.214	0.002	0.094
10	0.5	0.825	1.667	0.481	7.199	0.079	0.018	0.837	0.002	0.008	1.273	0.000	0.002	0.000	0.050	0.000	0.005
10	0.4	0.825	1.667	0.481	7.199	0.079	0.018	0.936	0.002	0.008	1.273	0.000	0.002	0.000	0.064	0.000	0.008
10	0.3	0.825	1.667	0.481	7.199	0.079	0.018	1.080	0.002	0.008	1.273	0.000	0.002	0.000	0.089	0.000	0.016

Q	X	Z	V_{zi}	Z_{core}	V_{zj}	h_{down}	h_{up}	V_{xmax}	q_{up}	q_{down}	V(z)	FQSI	G_b	I_{net}	V_{up}	H_{up}	H_{up}/z
l/s	m	m	m/s	m	m/s	m	m	m/s	m²/s	m²/s	m/s	Ns	kg/m²	Ns	m/s	m	
			Q=VA	Z=5*Bj	Eq. 25	Eq. 61		Eq. 63	Eq. 61&62		Eq. 60	Fig.2.18	Eq. 59	Eq.55		Eq. 58	
10	0.2	0.825	1.667	0.481	7.199	0.079	0.018	1.323	0.002	0.008	1.273	0.000	0.002	0.000	0.137	0.001	0.038
10	0.1	0.825	1.667	0.481	7.199	0.079	0.018	1.871	0.002	0.008	1.273	0.001	0.002	0.001	0.283	0.004	0.163
10	0.75	0.825	1.667	0.481	7.199	0.079	0.018	0.683	0.002	0.008	1.273	0.000	0.002	0.000	0.030	0.000	0.002
10	0.1	0.825	1.667	0.481	7.199	0.079	0.018	3.949	0.002	0.008	1.273	0.003	0.002	0.003	1.288	0.085	3.384
10	0.2	0.825	1.667	0.481	7.199	0.079	0.018	2.793	0.002	0.008	1.273	0.002	0.002	0.002	0.640	0.021	0.835
10	0.3	0.825	1.667	0.481	7.199	0.079	0.018	2.280	0.002	0.008	1.273	0.001	0.002	0.001	0.424	0.009	0.366
10	0.4	0.825	1.667	0.481	7.199	0.079	0.018	1.975	0.002	0.008	1.273	0.001	0.002	0.001	0.316	0.005	0.203
10	0.5	0.825	1.667	0.481	7.199	0.079	0.018	1.766	0.002	0.008	1.273	0.001	0.002	0.001	0.251	0.003	0.128
10	0.6	0.825	1.667	0.481	7.199	0.079	0.018	1.612	0.002	0.008	1.273	0.001	0.002	0.000	0.208	0.002	0.088

Table D0.5. Quasi-steady method of Q= 10 l/s, H=3 m and TW=0.25 m

Q	X	Z	V _{zi}	Z _{core}	V _{zj}	h _{down}	h _{up}	V _{xmax}	q _{up}	q _{down}	V(z)	FQSI	G _b	Inet	V _{up}	H _{up}	H _{up} /z
l/s	m	m	m/s	m	m/s	m	m	m/s	m ² /s	m ² /s	m/s						
			Q=VA	Z=5*Bj	Eq. 25	Eq.61		Eq. 63	Eq. 61&62		Eq. 60	Fig.2.18	Eq. 59	Eq.55		Eq. 58	
10	0.75	0	1.667	0.481	7.199	0.079	0.018	1.241	0.002	0.008	7.199						
10	0.75	0.042	1.667	0.481	7.199	0.079	0.018	1.241	0.002	0.008	5.664						
10	0.75	0.083	1.667	0.481	7.199	0.079	0.018	1.241	0.002	0.008	4.005						
10	0.75	0.125	1.667	0.481	7.199	0.079	0.018	1.241	0.002	0.008	3.270						
10	0.75	0.167	1.667	0.481	7.199	0.079	0.018	1.241	0.002	0.008	2.832						
10	0.75	0.208	1.667	0.481	7.199	0.079	0.018	1.241	0.002	0.008	2.533						
10	0.75	0.25	1.667	0.481	7.199	0.079	0.018	1.241	0.002	0.008	2.312						
10	0.5	0.25	1.667	0.481	7.199	0.079	0.018	1.520	0.002	0.008	2.312	0.000	0.002	0.000	0.184	0.002	0.069
10	0.4	0.25	1.667	0.481	7.199	0.079	0.018	1.700	0.002	0.008	2.312	0.001	0.002	0.001	0.232	0.003	0.109
10	0.3	0.25	1.667	0.481	7.199	0.079	0.018	1.963	0.002	0.008	2.312	0.001	0.002	0.001	0.312	0.005	0.198
10	0.2	0.25	1.667	0.481	7.199	0.079	0.018	2.404	0.002	0.008	2.312	0.001	0.002	0.001	0.472	0.011	0.454
10	0.1	0.25	1.667	0.481	7.199	0.079	0.018	3.399	0.002	0.008	2.312	0.002	0.002	0.002	0.952	0.046	1.849
10	0.75	0.25	1.667	0.481	7.199	0.079	0.018	1.241	0.002	0.008	2.312	0.000	0.002	0.000	0.120	0.001	0.029
10	0.1	0.25	1.667	0.481	7.199	0.079	0.018	7.174	0.002	0.008	2.312	0.010	0.002	0.010	4.271	0.930	37.197
10	0.2	0.25	1.667	0.481	7.199	0.079	0.018	5.073	0.002	0.008	2.312	0.005	0.002	0.005	2.131	0.232	9.262
10	0.3	0.25	1.667	0.481	7.199	0.079	0.018	4.142	0.002	0.008	2.312	0.003	0.002	0.003	1.418	0.103	4.100
10	0.4	0.25	1.667	0.481	7.199	0.079	0.018	3.587	0.002	0.008	2.312	0.003	0.002	0.003	1.061	0.057	2.297
10	0.5	0.25	1.667	0.481	7.199	0.079	0.018	3.208	0.002	0.008	2.312	0.002	0.002	0.002	0.847	0.037	1.464
10	0.6	0.25	1.667	0.481	7.199	0.079	0.018	2.929	0.002	0.008	2.312	0.002	0.002	0.002	0.705	0.025	1.013
10	0.5	0.275	1.667	0.481	7.199	0.079	0.018	1.449	0.002	0.008	2.205	0.000	0.002	0.000	0.166	0.001	0.056
10	0.4	0.275	1.667	0.481	7.199	0.079	0.018	1.620	0.002	0.008	2.205	0.001	0.002	0.000	0.210	0.002	0.090
10	0.3	0.275	1.667	0.481	7.199	0.079	0.018	1.871	0.002	0.008	2.205	0.001	0.002	0.001	0.283	0.004	0.163
10	0.2	0.275	1.667	0.481	7.199	0.079	0.018	2.292	0.002	0.008	2.205	0.001	0.002	0.001	0.428	0.009	0.374
10	0.1	0.275	1.667	0.481	7.199	0.079	0.018	3.241	0.002	0.008	2.205	0.002	0.002	0.002	0.865	0.038	1.525
10	0.75	0.275	1.667	0.481	7.199	0.079	0.018	1.183	0.002	0.008	2.205	0.000	0.002	0.000	0.108	0.001	0.024

Q	X	Z	V _{zi}	Z _{core}	V _{zj}	h _{down}	h _{up}	V _{xmax}	q _{up}	q _{down}	V(z)	FQSI	G _b	I _{net}	V _{up}	H _{up}	H _{up} /z
l/s	m	m	m/s	m	m/s	m	m	m/s	m ² /s	m ² /s	m/s	Ns	kg/m ²	Ns	m/s	m	
			Q=VA	Z=5*Bj	Eq. 25	Eq. 61		Eq. 63	Eq. 61&62		Eq. 60	Fig.2.18	Eq. 59	Eq.55		Eq. 58	
10	0.1	0.275	1.667	0.481	7.199	0.079	0.018	6.840	0.002	0.008	2.205	0.009	0.002	0.009	3.882	0.768	30.729
10	0.2	0.275	1.667	0.481	7.199	0.079	0.018	4.837	0.002	0.008	2.205	0.005	0.002	0.005	1.937	0.191	7.649
10	0.3	0.275	1.667	0.481	7.199	0.079	0.018	3.949	0.002	0.008	2.205	0.003	0.002	0.003	1.288	0.085	3.384
10	0.4	0.275	1.667	0.481	7.199	0.079	0.018	3.420	0.002	0.008	2.205	0.002	0.002	0.002	0.964	0.047	1.895
10	0.5	0.275	1.667	0.481	7.199	0.079	0.018	3.059	0.002	0.008	2.205	0.002	0.002	0.002	0.770	0.030	1.208
10	0.6	0.275	1.667	0.481	7.199	0.079	0.018	2.793	0.002	0.008	2.205	0.002	0.002	0.002	0.640	0.021	0.835
10	0.5	0.3	1.667	0.481	7.199	0.079	0.018	1.388	0.002	0.008	2.111	0.000	0.002	0.000	0.152	0.001	0.047
10	0.4	0.3	1.667	0.481	7.199	0.079	0.018	1.552	0.002	0.008	2.111	0.000	0.002	0.000	0.192	0.002	0.075
10	0.3	0.3	1.667	0.481	7.199	0.079	0.018	1.792	0.002	0.008	2.111	0.001	0.002	0.001	0.258	0.003	0.136
10	0.2	0.3	1.667	0.481	7.199	0.079	0.018	2.194	0.002	0.008	2.111	0.001	0.002	0.001	0.392	0.008	0.313
10	0.1	0.3	1.667	0.481	7.199	0.079	0.018	3.103	0.002	0.008	2.111	0.002	0.002	0.002	0.792	0.032	1.279
10	0.75	0.3	1.667	0.481	7.199	0.079	0.018	1.133	0.002	0.008	2.111	0.000	0.002	0.000	0.098	0.000	0.020
10	0.1	0.3	1.667	0.481	7.199	0.079	0.018	6.549	0.002	0.008	2.111	0.008	0.002	0.008	3.558	0.645	25.811
10	0.2	0.3	1.667	0.481	7.199	0.079	0.018	4.631	0.002	0.008	2.111	0.004	0.002	0.004	1.775	0.161	6.422
10	0.3	0.3	1.667	0.481	7.199	0.079	0.018	3.781	0.002	0.008	2.111	0.003	0.002	0.003	1.180	0.071	2.840
10	0.4	0.3	1.667	0.481	7.199	0.079	0.018	3.275	0.002	0.008	2.111	0.002	0.002	0.002	0.883	0.040	1.590
10	0.5	0.3	1.667	0.481	7.199	0.079	0.018	2.929	0.002	0.008	2.111	0.002	0.002	0.002	0.705	0.025	1.013
10	0.6	0.3	1.667	0.481	7.199	0.079	0.018	2.674	0.002	0.008	2.111	0.001	0.002	0.001	0.586	0.017	0.700
10	0.5	0.325	1.667	0.481	7.199	0.079	0.018	1.333	0.002	0.008	2.028	0.000	0.002	0.000	0.139	0.001	0.040
10	0.4	0.325	1.667	0.481	7.199	0.079	0.018	1.491	0.002	0.008	2.028	0.000	0.002	0.000	0.176	0.002	0.063
10	0.3	0.325	1.667	0.481	7.199	0.079	0.018	1.721	0.002	0.008	2.028	0.001	0.002	0.001	0.238	0.003	0.115
10	0.2	0.325	1.667	0.481	7.199	0.079	0.018	2.108	0.002	0.008	2.028	0.001	0.002	0.001	0.361	0.007	0.266
10	0.1	0.325	1.667	0.481	7.199	0.079	0.018	2.981	0.002	0.008	2.028	0.002	0.002	0.002	0.731	0.027	1.088
10	0.75	0.325	1.667	0.481	7.199	0.079	0.018	1.089	0.002	0.008	2.028	0.000	0.002	0.000	0.090	0.000	0.017
10	0.1	0.325	1.667	0.481	7.199	0.079	0.018	6.292	0.002	0.008	2.028	0.008	0.002	0.008	3.284	0.550	21.984
10	0.2	0.325	1.667	0.481	7.199	0.079	0.018	4.449	0.002	0.008	2.028	0.004	0.002	0.004	1.638	0.137	5.467

Q	X	Z	V _{zi}	Z _{core}	V _{zj}	h _{down}	h _{up}	V _{xmax}	q _{up}	q _{down}	V(z)	FQSI	G _b	I _{net}	V _{up}	H _{up}	H _{up} /z
l/s	m	m	m/s	m	m/s	m	m	m/s	m ² /s	m ² /s	m/s	Ns	kg/m ²	Ns	m/s	m	
			Q=VA	Z=5*Bj	Eq. 25	Eq.61		Eq. 63	Eq. 61&62		Eq. 60	Fig2.18	Eq. 59	Eq.55		Eq. 58	
10	0.3	0.325	1.667	0.481	7.199	0.079	0.018	3.633	0.002	0.008	2.028	0.003	0.002	0.003	1.089	0.060	2.417
10	0.4	0.325	1.667	0.481	7.199	0.079	0.018	3.146	0.002	0.008	2.028	0.002	0.002	0.002	0.815	0.034	1.353
10	0.5	0.325	1.667	0.481	7.199	0.079	0.018	2.814	0.002	0.008	2.028	0.002	0.002	0.002	0.650	0.022	0.861
10	0.6	0.325	1.667	0.481	7.199	0.079	0.018	2.569	0.002	0.008	2.028	0.001	0.002	0.001	0.540	0.015	0.595
10	0.5	0.35	1.667	0.481	7.199	0.079	0.018	1.285	0.002	0.008	1.954	0.000	0.002	0.000	0.129	0.001	0.034
10	0.4	0.35	1.667	0.481	7.199	0.079	0.018	1.436	0.002	0.008	1.954	0.000	0.002	0.000	0.163	0.001	0.054
10	0.3	0.35	1.667	0.481	7.199	0.079	0.018	1.659	0.002	0.008	1.954	0.001	0.002	0.001	0.220	0.002	0.099
10	0.2	0.35	1.667	0.481	7.199	0.079	0.018	2.031	0.002	0.008	1.954	0.001	0.002	0.001	0.335	0.006	0.228
10	0.1	0.35	1.667	0.481	7.199	0.079	0.018	2.873	0.002	0.008	1.954	0.002	0.002	0.002	0.678	0.023	0.937
10	0.75	0.35	1.667	0.481	7.199	0.079	0.018	1.049	0.002	0.008	1.954	0.000	0.002	0.000	0.083	0.000	0.014
10	0.1	0.35	1.667	0.481	7.199	0.079	0.018	6.063	0.002	0.008	1.954	0.007	0.002	0.007	3.049	0.474	18.948
10	0.2	0.35	1.667	0.481	7.199	0.079	0.018	4.287	0.002	0.008	1.954	0.004	0.002	0.004	1.520	0.118	4.710
10	0.3	0.35	1.667	0.481	7.199	0.079	0.018	3.501	0.002	0.008	1.954	0.002	0.002	0.002	1.011	0.052	2.082
10	0.4	0.35	1.667	0.481	7.199	0.079	0.018	3.032	0.002	0.008	1.954	0.002	0.002	0.002	0.756	0.029	1.164
10	0.5	0.35	1.667	0.481	7.199	0.079	0.018	2.712	0.002	0.008	1.954	0.001	0.002	0.001	0.603	0.019	0.741
10	0.6	0.35	1.667	0.481	7.199	0.079	0.018	2.475	0.002	0.008	1.954	0.001	0.002	0.001	0.501	0.013	0.512
10	0.5	0.375	1.667	0.481	7.199	0.079	0.018	1.241	0.002	0.008	1.888	0.000	0.002	0.000	0.120	0.001	0.029
10	0.4	0.375	1.667	0.481	7.199	0.079	0.018	1.388	0.002	0.008	1.888	0.000	0.002	0.000	0.152	0.001	0.047
10	0.3	0.375	1.667	0.481	7.199	0.079	0.018	1.602	0.002	0.008	1.888	0.001	0.002	0.000	0.205	0.002	0.086
10	0.2	0.375	1.667	0.481	7.199	0.079	0.018	1.963	0.002	0.008	1.888	0.001	0.002	0.001	0.312	0.005	0.198
10	0.1	0.375	1.667	0.481	7.199	0.079	0.018	2.775	0.002	0.008	1.888	0.002	0.002	0.002	0.632	0.020	0.814
10	0.75	0.375	1.667	0.481	7.199	0.079	0.018	1.013	0.002	0.008	1.888	0.000	0.002	0.000	0.077	0.000	0.012
10	0.1	0.375	1.667	0.481	7.199	0.079	0.018	5.858	0.002	0.008	1.888	0.007	0.002	0.007	2.845	0.412	16.499
10	0.2	0.375	1.667	0.481	7.199	0.079	0.018	4.142	0.002	0.008	1.888	0.003	0.002	0.003	1.418	0.103	4.100
10	0.3	0.375	1.667	0.481	7.199	0.079	0.018	3.382	0.002	0.008	1.888	0.002	0.002	0.002	0.943	0.045	1.811
10	0.4	0.375	1.667	0.481	7.199	0.079	0.018	2.929	0.002	0.008	1.888	0.002	0.002	0.002	0.705	0.025	1.013

Q	X	Z	V _{zi}	Z _{core}	V _{zj}	h _{down}	h _{up}	V _{xmax}	q _{up}	q _{down}	V(z)	FQSI	G _b	I _{net}	V _{up}	H _{up}	H _{up} /z
l/s	m	m	m/s	m	m/s	m	m	m/s	m ² /s	m ² /s	m/s	Ns	kg/m ²	Ns	m/s	m	
			Q=VA	Z=5*Bj	Eq. 25	Eq. 61		Eq. 63	Eq. 61&62		Eq. 60		Eq. 59	Eq.55		Eq. 58	
10	0.5	0.375	1.667	0.481	7.199	0.079	0.018	2.620	0.002	0.008	1.888	0.001	0.002	0.001	0.562	0.016	0.644
10	0.6	0.375	1.667	0.481	7.199	0.079	0.018	2.391	0.002	0.008	1.888	0.001	0.002	0.001	0.467	0.011	0.445
10	0.5	0.4	1.667	0.481	7.199	0.079	0.018	1.202	0.002	0.008	1.828	0.000	0.002	0.000	0.112	0.001	0.025
10	0.4	0.4	1.667	0.481	7.199	0.079	0.018	1.344	0.002	0.008	1.828	0.000	0.002	0.000	0.142	0.001	0.041
10	0.3	0.4	1.667	0.481	7.199	0.079	0.018	1.552	0.002	0.008	1.828	0.000	0.002	0.000	0.192	0.002	0.075
10	0.2	0.4	1.667	0.481	7.199	0.079	0.018	1.900	0.002	0.008	1.828	0.001	0.002	0.001	0.292	0.004	0.174
10	0.1	0.4	1.667	0.481	7.199	0.079	0.018	2.687	0.002	0.008	1.828	0.001	0.002	0.001	0.592	0.018	0.715
10	0.75	0.4	1.667	0.481	7.199	0.079	0.018	0.981	0.002	0.008	1.828	0.000	0.002	0.000	0.072	0.000	0.010
10	0.1	0.4	1.667	0.481	7.199	0.079	0.018	5.672	0.002	0.008	1.828	0.006	0.002	0.006	2.666	0.362	14.495
10	0.2	0.4	1.667	0.481	7.199	0.079	0.018	4.010	0.002	0.008	1.828	0.003	0.002	0.003	1.329	0.090	3.601
10	0.3	0.4	1.667	0.481	7.199	0.079	0.018	3.275	0.002	0.008	1.828	0.002	0.002	0.002	0.883	0.040	1.590
10	0.4	0.4	1.667	0.481	7.199	0.079	0.018	2.836	0.002	0.008	1.828	0.002	0.002	0.002	0.660	0.022	0.889
10	0.5	0.4	1.667	0.481	7.199	0.079	0.018	2.536	0.002	0.008	1.828	0.001	0.002	0.001	0.526	0.014	0.565
10	0.6	0.4	1.667	0.481	7.199	0.079	0.018	2.315	0.002	0.008	1.828	0.001	0.002	0.001	0.437	0.010	0.390
10	0.5	0.425	1.667	0.481	7.199	0.079	0.018	1.166	0.002	0.008	1.773	0.000	0.002	0.000	0.105	0.001	0.022
10	0.4	0.425	1.667	0.481	7.199	0.079	0.018	1.304	0.002	0.008	1.773	0.000	0.002	0.000	0.133	0.001	0.036
10	0.3	0.425	1.667	0.481	7.199	0.079	0.018	1.505	0.002	0.008	1.773	0.000	0.002	0.000	0.180	0.002	0.066
10	0.2	0.425	1.667	0.481	7.199	0.079	0.018	1.843	0.002	0.008	1.773	0.001	0.002	0.001	0.274	0.004	0.153
10	0.1	0.425	1.667	0.481	7.199	0.079	0.018	2.607	0.002	0.008	1.773	0.001	0.002	0.001	0.557	0.016	0.632
10	0.75	0.425	1.667	0.481	7.199	0.079	0.018	0.952	0.002	0.008	1.773	0.000	0.002	0.000	0.067	0.000	0.009
10	0.1	0.425	1.667	0.481	7.199	0.079	0.018	5.502	0.002	0.008	1.773	0.006	0.002	0.006	2.509	0.321	12.835
10	0.2	0.425	1.667	0.481	7.199	0.079	0.018	3.891	0.002	0.008	1.773	0.003	0.002	0.003	1.250	0.080	3.187
10	0.3	0.425	1.667	0.481	7.199	0.079	0.018	3.177	0.002	0.008	1.773	0.002	0.002	0.002	0.831	0.035	1.407
10	0.4	0.425	1.667	0.481	7.199	0.079	0.018	2.751	0.002	0.008	1.773	0.001	0.002	0.001	0.621	0.020	0.786
10	0.5	0.425	1.667	0.481	7.199	0.079	0.018	2.461	0.002	0.008	1.773	0.001	0.002	0.001	0.495	0.012	0.500
10	0.6	0.425	1.667	0.481	7.199	0.079	0.018	2.246	0.002	0.008	1.773	0.001	0.002	0.001	0.411	0.009	0.345

Q	X	Z	V _{zi}	Z _{core}	V _{zj}	h _{down}	h _{up}	V _{xmax}	q _{up}	q _{down}	V(z)	FQSI	G _b	I _{net}	V _{up}	H _{up}	H _{up} /z
l/s	m	m	m/s	m	m/s	m	m	m/s	m ² /s	m ² /s	m/s	Ns	kg/m ²	Ns	m/s	m	
			Q=VA	Z=5*Bj	Eq. 25	Eq. 61		Eq. 63	Eq. 61&62		Eq. 60		Eq. 59	Eq.55		Eq. 58	
10	0.5	0.45	1.667	0.481	7.199	0.079	0.018	1.133	0.002	0.008	1.723	0.000	0.002	0.000	0.098	0.000	0.020
10	0.4	0.45	1.667	0.481	7.199	0.079	0.018	1.267	0.002	0.008	1.723	0.000	0.002	0.000	0.125	0.001	0.032
10	0.3	0.45	1.667	0.481	7.199	0.079	0.018	1.463	0.002	0.008	1.723	0.000	0.002	0.000	0.169	0.001	0.059
10	0.2	0.45	1.667	0.481	7.199	0.079	0.018	1.792	0.002	0.008	1.723	0.001	0.002	0.001	0.258	0.003	0.136
10	0.1	0.45	1.667	0.481	7.199	0.079	0.018	2.534	0.002	0.008	1.723	0.001	0.002	0.001	0.525	0.014	0.563
10	0.75	0.45	1.667	0.481	7.199	0.079	0.018	0.925	0.002	0.008	1.723	0.000	0.002	0.000	0.063	0.000	0.008
10	0.1	0.45	1.667	0.481	7.199	0.079	0.018	5.347	0.002	0.008	1.723	0.006	0.002	0.006	2.369	0.286	11.444
10	0.2	0.45	1.667	0.481	7.199	0.079	0.018	3.781	0.002	0.008	1.723	0.003	0.002	0.003	1.180	0.071	2.840
10	0.3	0.45	1.667	0.481	7.199	0.079	0.018	3.087	0.002	0.008	1.723	0.002	0.002	0.002	0.784	0.031	1.253
10	0.4	0.45	1.667	0.481	7.199	0.079	0.018	2.674	0.002	0.008	1.723	0.001	0.002	0.001	0.586	0.017	0.700
10	0.5	0.45	1.667	0.481	7.199	0.079	0.018	2.391	0.002	0.008	1.723	0.001	0.002	0.001	0.467	0.011	0.445
10	0.6	0.45	1.667	0.481	7.199	0.079	0.018	2.183	0.002	0.008	1.723	0.001	0.002	0.001	0.388	0.008	0.307
10	0.5	0.475	1.667	0.481	7.199	0.079	0.018	1.103	0.002	0.008	1.677	0.000	0.002	0.000	0.093	0.000	0.017
10	0.4	0.475	1.667	0.481	7.199	0.079	0.018	1.233	0.002	0.008	1.677	0.000	0.002	0.000	0.118	0.001	0.028
10	0.3	0.475	1.667	0.481	7.199	0.079	0.018	1.424	0.002	0.008	1.677	0.000	0.002	0.000	0.160	0.001	0.052
10	0.2	0.475	1.667	0.481	7.199	0.079	0.018	1.744	0.002	0.008	1.677	0.001	0.002	0.001	0.244	0.003	0.122
10	0.1	0.475	1.667	0.481	7.199	0.079	0.018	2.466	0.002	0.008	1.677	0.001	0.002	0.001	0.497	0.013	0.504
10	0.75	0.475	1.667	0.481	7.199	0.079	0.018	0.900	0.002	0.008	1.677	0.000	0.002	0.000	0.059	0.000	0.007
10	0.1	0.475	1.667	0.481	7.199	0.079	0.018	5.205	0.002	0.008	1.677	0.005	0.002	0.005	2.244	0.257	10.267
10	0.2	0.475	1.667	0.481	7.199	0.079	0.018	3.680	0.002	0.008	1.677	0.003	0.002	0.003	1.118	0.064	2.547
10	0.3	0.475	1.667	0.481	7.199	0.079	0.018	3.005	0.002	0.008	1.677	0.002	0.002	0.002	0.742	0.028	1.123
10	0.4	0.475	1.667	0.481	7.199	0.079	0.018	2.602	0.002	0.008	1.677	0.001	0.002	0.001	0.555	0.016	0.627
10	0.5	0.475	1.667	0.481	7.199	0.079	0.018	2.328	0.002	0.008	1.677	0.001	0.002	0.001	0.442	0.010	0.398
10	0.6	0.475	1.667	0.481	7.199	0.079	0.018	2.125	0.002	0.008	1.677	0.001	0.002	0.001	0.367	0.007	0.274
10	0.5	0.5	1.667	0.481	7.199	0.079	0.018	1.075	0.002	0.008	1.635	0.000	0.002	0.000	0.088	0.000	0.016
10	0.4	0.5	1.667	0.481	7.199	0.079	0.018	1.202	0.002	0.008	1.635	0.000	0.002	0.000	0.112	0.001	0.025

Q	X	Z	V _{zi}	Z _{core}	V _{zj}	h _{down}	h _{up}	V _{xmax}	q _{up}	q _{down}	V(z)	FQSI	G _b	I _{net}	V _{up}	H _{up}	H _{up} /z
l/s	m	m	m/s	m	m/s	m	m	m/s	m ² /s	m ² /s	m/s	Ns	kg/m ²	Ns	m/s	m	
			Q=VA	Z=5*Bj	Eq. 25	Eq. 61		Eq. 63	Eq. 61&62		Eq. 60		Eq. 59	Eq.55		Eq. 59	
10	0.3	0.5	1.667	0.481	7.199	0.079	0.018	1.388	0.002	0.008	1.635	0.000	0.002	0.000	0.152	0.001	0.047
10	0.2	0.5	1.667	0.481	7.199	0.079	0.018	1.700	0.002	0.008	1.635	0.001	0.002	0.001	0.232	0.003	0.109
10	0.1	0.5	1.667	0.481	7.199	0.079	0.018	2.404	0.002	0.008	1.635	0.001	0.002	0.001	0.472	0.011	0.454
10	0.75	0.5	1.667	0.481	7.199	0.079	0.018	0.878	0.002	0.008	1.635	0.000	0.002	0.000	0.056	0.000	0.006
10	0.1	0.5	1.667	0.481	7.199	0.079	0.018	5.073	0.002	0.008	1.635	0.005	0.002	0.005	2.131	0.232	9.262
10	0.2	0.5	1.667	0.481	7.199	0.079	0.018	3.587	0.002	0.008	1.635	0.003	0.002	0.003	1.061	0.057	2.297
10	0.3	0.5	1.667	0.481	7.199	0.079	0.018	2.929	0.002	0.008	1.635	0.002	0.002	0.002	0.705	0.025	1.013
10	0.4	0.5	1.667	0.481	7.199	0.079	0.018	2.536	0.002	0.008	1.635	0.001	0.002	0.001	0.526	0.014	0.565
10	0.5	0.5	1.667	0.481	7.199	0.079	0.018	2.269	0.002	0.008	1.635	0.001	0.002	0.001	0.419	0.009	0.359
10	0.6	0.5	1.667	0.481	7.199	0.079	0.018	2.071	0.002	0.008	1.635	0.001	0.002	0.001	0.348	0.006	0.247
10	0.5	0.525	1.667	0.481	7.199	0.079	0.018	1.049	0.002	0.008	1.596	0.000	0.002	0.000	0.083	0.000	0.014
10	0.4	0.525	1.667	0.481	7.199	0.079	0.018	1.173	0.002	0.008	1.596	0.000	0.002	0.000	0.106	0.001	0.023
10	0.3	0.525	1.667	0.481	7.199	0.079	0.018	1.354	0.002	0.008	1.596	0.000	0.002	0.000	0.144	0.001	0.042
10	0.2	0.525	1.667	0.481	7.199	0.079	0.018	1.659	0.002	0.008	1.596	0.001	0.002	0.001	0.220	0.002	0.099
10	0.1	0.525	1.667	0.481	7.199	0.079	0.018	2.346	0.002	0.008	1.596	0.001	0.002	0.001	0.449	0.010	0.411
10	0.75	0.525	1.667	0.481	7.199	0.079	0.018	0.857	0.002	0.008	1.596	0.000	0.002	0.000	0.052	0.000	0.006
10	0.1	0.525	1.667	0.481	7.199	0.079	0.018	4.951	0.002	0.008	1.596	0.005	0.002	0.005	2.030	0.210	8.398
10	0.2	0.525	1.667	0.481	7.199	0.079	0.018	3.501	0.002	0.008	1.596	0.002	0.002	0.002	1.011	0.052	2.082
10	0.3	0.525	1.667	0.481	7.199	0.079	0.018	2.858	0.002	0.008	1.596	0.002	0.002	0.002	0.671	0.023	0.917
10	0.4	0.525	1.667	0.481	7.199	0.079	0.018	2.475	0.002	0.008	1.596	0.001	0.002	0.001	0.501	0.013	0.512
10	0.5	0.525	1.667	0.481	7.199	0.079	0.018	2.214	0.002	0.008	1.596	0.001	0.002	0.001	0.399	0.008	0.325
10	0.6	0.525	1.667	0.481	7.199	0.079	0.018	2.021	0.002	0.008	1.596	0.001	0.002	0.001	0.331	0.006	0.224
10	0.5	0.55	1.667	0.481	7.199	0.079	0.018	1.025	0.002	0.008	1.559	0.000	0.002	0.000	0.079	0.000	0.013
10	0.4	0.55	1.667	0.481	7.199	0.079	0.018	1.146	0.002	0.008	1.559	0.000	0.002	0.000	0.101	0.001	0.021
10	0.3	0.55	1.667	0.481	7.199	0.079	0.018	1.323	0.002	0.008	1.559	0.000	0.002	0.000	0.137	0.001	0.038
10	0.2	0.55	1.667	0.481	7.199	0.079	0.018	1.620	0.002	0.008	1.559	0.001	0.002	0.000	0.210	0.002	0.090

Q	X	Z	V _{zi}	Z _{core}	V _{zj}	h _{down}	h _{up}	V _{xmax}	q _{up}	q _{down}	V(z)	FQSI	G _b	I _{net}	V _{up}	H _{up}	H _{up} /z
l/s	m	m	m/s	m	m/s	m	m	m/s	m ² /s	m ² /s	m/s	Ns	kg/m ²	Ns	m/s	m	
			Q=VA	Z=5*Bj	Eq. 25	Eq. 61		Eq. 63	Eq. 61&62		Eq. 60		Eq. 59	Eq.55		Eq. 56	
10	0.1	0.55	1.667	0.481	7.199	0.079	0.018	2.292	0.002	0.008	1.559	0.001	0.002	0.001	0.428	0.009	0.374
10	0.75	0.55	1.667	0.481	7.199	0.079	0.018	0.837	0.002	0.008	1.559	0.000	0.002	0.000	0.050	0.000	0.005
10	0.1	0.55	1.667	0.481	7.199	0.079	0.018	4.837	0.002	0.008	1.559	0.005	0.002	0.005	1.937	0.191	7.649
10	0.2	0.55	1.667	0.481	7.199	0.079	0.018	3.420	0.002	0.008	1.559	0.002	0.002	0.002	0.964	0.047	1.895
10	0.3	0.55	1.667	0.481	7.199	0.079	0.018	2.793	0.002	0.008	1.559	0.002	0.002	0.002	0.640	0.021	0.835
10	0.4	0.55	1.667	0.481	7.199	0.079	0.018	2.418	0.002	0.008	1.559	0.001	0.002	0.001	0.478	0.012	0.465
10	0.5	0.55	1.667	0.481	7.199	0.079	0.018	2.163	0.002	0.008	1.559	0.001	0.002	0.001	0.381	0.007	0.295
10	0.6	0.55	1.667	0.481	7.199	0.079	0.018	1.975	0.002	0.008	1.559	0.001	0.002	0.001	0.316	0.005	0.203
10	0.5	0.575	1.667	0.481	7.199	0.079	0.018	1.002	0.002	0.008	1.525	0.000	0.002	0.000	0.075	0.000	0.011
10	0.4	0.575	1.667	0.481	7.199	0.079	0.018	1.121	0.002	0.008	1.525	0.000	0.002	0.000	0.096	0.000	0.019
10	0.3	0.575	1.667	0.481	7.199	0.079	0.018	1.294	0.002	0.008	1.525	0.000	0.002	0.000	0.131	0.001	0.035
10	0.2	0.575	1.667	0.481	7.199	0.079	0.018	1.585	0.002	0.008	1.525	0.000	0.002	0.000	0.200	0.002	0.082
10	0.1	0.575	1.667	0.481	7.199	0.079	0.018	2.241	0.002	0.008	1.525	0.001	0.002	0.001	0.409	0.009	0.341
10	0.75	0.575	1.667	0.481	7.199	0.079	0.018	0.818	0.002	0.008	1.525	0.000	0.002	0.000	0.047	0.000	0.005
10	0.1	0.575	1.667	0.481	7.199	0.079	0.018	4.730	0.002	0.008	1.525	0.004	0.002	0.004	1.852	0.175	6.995
10	0.2	0.575	1.667	0.481	7.199	0.079	0.018	3.345	0.002	0.008	1.525	0.002	0.002	0.002	0.922	0.043	1.733
10	0.3	0.575	1.667	0.481	7.199	0.079	0.018	2.731	0.002	0.008	1.525	0.001	0.002	0.001	0.612	0.019	0.763
10	0.4	0.575	1.667	0.481	7.199	0.079	0.018	2.365	0.002	0.008	1.525	0.001	0.002	0.001	0.457	0.011	0.425
10	0.5	0.575	1.667	0.481	7.199	0.079	0.018	2.116	0.002	0.008	1.525	0.001	0.002	0.001	0.364	0.007	0.270
10	0.6	0.575	1.667	0.481	7.199	0.079	0.018	1.931	0.002	0.008	1.525	0.001	0.002	0.001	0.302	0.005	0.185

Table D 0.6. Quasi-steady method of Q=10 l/s, H=4 m and TW=0.5 m

Q	X	Z	V _{zi}	Z _{core}	V _{zj}	h _{down}	h _{up}	V _{xmax}	q _{up}	q _{down}	V(z)	FQSI	G _b	Inet	V _{up}	H _{up}	H _{up} /z
l/s	m	m	m/s	m	m/s	m	m	m/s	m ² /s	m ² /s	m/s	Ns	kg/m ²	Ns	m/s	m	
			Q=VA	Z=5*B j	Eq. 25	Eq.61		Eq. 63	Eq. 61&62		Eq. 60	Fig.2.18	Eq. 59	Eq.55		Eq. 58	
10	0.85	0	1.667	0.444	8.453	0.073	0.016	0.761	0.002	0.008	8.453						
10	0.85	0.042	1.667	0.444	8.453	0.073	0.016	0.761	0.002	0.008	5.441						
10	0.85	0.083	1.667	0.444	8.453	0.073	0.016	0.761	0.002	0.008	3.847						
10	0.85	0.125	1.667	0.444	8.453	0.073	0.016	0.761	0.002	0.008	3.141						
10	0.85	0.167	1.667	0.444	8.453	0.073	0.016	0.761	0.002	0.008	2.720						
10	0.85	0.208	1.667	0.444	8.453	0.073	0.016	0.761	0.002	0.008	2.433						
10	0.85	0.250	1.667	0.444	8.453	0.073	0.016	0.761	0.002	0.008	2.221						
10	0.85	0.292	1.667	0.444	8.453	0.073	0.016	0.761	0.002	0.008	2.056						
10	0.85	0.333	1.667	0.444	8.453	0.073	0.016	0.761	0.002	0.008	1.924						
10	0.85	0.375	1.667	0.444	8.453	0.073	0.016	0.761	0.002	0.008	1.814						
10	0.85	0.417	1.667	0.444	8.453	0.073	0.016	0.761	0.002	0.008	1.721						
10	0.85	0.458	1.667	0.444	8.453	0.073	0.016	0.761	0.002	0.008	1.640						
10	0.85	0.5	1.667	0.444	8.453	0.073	0.016	0.761	0.002	0.008	1.571						
10	0.5	0.5	1.667	0.444	8.453	0.073	0.016	0.992	0.002	0.008	1.571	0.000	0.002	0.000	0.073	0.000	0.011
10	0.4	0.5	1.667	0.444	8.453	0.073	0.016	1.109	0.002	0.008	1.571	0.000	0.002	0.000	0.094	0.000	0.018
10	0.3	0.5	1.667	0.444	8.453	0.073	0.016	1.281	0.002	0.008	1.571	0.000	0.002	0.000	0.128	0.001	0.033
10	0.2	0.5	1.667	0.444	8.453	0.073	0.016	1.569	0.002	0.008	1.571	0.000	0.002	0.000	0.196	0.002	0.078
10	0.1	0.5	1.667	0.444	8.453	0.073	0.016	2.218	0.002	0.008	1.571	0.001	0.002	0.001	0.401	0.008	0.327
10	0.85	0.5	1.667	0.444	8.453	0.073	0.016	0.761	0.002	0.008	1.571	0.000	0.002	0.000	0.040	0.000	0.003
10	0.1	0.5	1.667	0.444	8.453	0.073	0.016	4.682	0.002	0.008	1.571	0.004	0.002	0.004	1.814	0.168	6.709
10	0.2	0.5	1.667	0.444	8.453	0.073	0.016	3.310	0.002	0.008	1.571	0.002	0.002	0.002	0.903	0.042	1.662
10	0.3	0.5	1.667	0.444	8.453	0.073	0.016	2.703	0.002	0.008	1.571	0.001	0.002	0.001	0.599	0.018	0.732
10	0.4	0.5	1.667	0.444	8.453	0.073	0.016	2.341	0.002	0.008	1.571	0.001	0.002	0.001	0.447	0.010	0.408
10	0.5	0.5	1.667	0.444	8.453	0.073	0.016	2.094	0.002	0.008	1.571	0.001	0.002	0.001	0.356	0.006	0.258

Q	X	Z	V _{zi}	Z _{core}	V _{zj}	h _{down}	h _{up}	V _{xmax}	q _{up}	q _{down}	V(z)	FQSI	G _b	I _{net}	V _{up}	H _{up}	H _{up} /z
l/s	m	m	m/s	m	m/s	m	m	m/s	m ² /s	m ² /s	m/s	Ns	kg/m ²	Ns	m/s	m	
			Q=VA	Z=5*B j	Eq. 25	Eq. 61		Eq. 63	Eq. 61&62		Eq. 60	Fig.2.18	Eq. 59	Eq.55		Eq. 58	
10	0.6	0.5	1.667	0.444	8.453	0.073	0.016	1.911	0.002	0.008	1.571	0.001	0.002	0.001	0.295	0.004	0.178
10	0.5	0.525	1.667	0.444	8.453	0.073	0.016	0.968	0.002	0.008	1.533	0.000	0.002	0.000	0.069	0.000	0.010
10	0.4	0.525	1.667	0.444	8.453	0.073	0.016	1.082	0.002	0.008	1.533	0.000	0.002	0.000	0.089	0.000	0.016
10	0.3	0.525	1.667	0.444	8.453	0.073	0.016	1.250	0.002	0.008	1.533	0.000	0.002	0.000	0.121	0.001	0.030
10	0.2	0.525	1.667	0.444	8.453	0.073	0.016	1.531	0.002	0.008	1.533	0.000	0.002	0.000	0.186	0.002	0.071
10	0.1	0.525	1.667	0.444	8.453	0.073	0.016	2.165	0.002	0.008	1.533	0.001	0.002	0.001	0.381	0.007	0.296
10	0.85	0.525	1.667	0.444	8.453	0.073	0.016	0.743	0.002	0.008	1.533	0.000	0.002	0.000	0.037	0.000	0.003
10	0.1	0.525	1.667	0.444	8.453	0.073	0.016	4.569	0.002	0.008	1.533	0.004	0.002	0.004	1.727	0.152	6.083
10	0.2	0.525	1.667	0.444	8.453	0.073	0.016	3.231	0.002	0.008	1.533	0.002	0.002	0.002	0.859	0.038	1.506
10	0.3	0.525	1.667	0.444	8.453	0.073	0.016	2.638	0.002	0.008	1.533	0.001	0.002	0.001	0.570	0.017	0.663
10	0.4	0.525	1.667	0.444	8.453	0.073	0.016	2.284	0.002	0.008	1.533	0.001	0.002	0.001	0.425	0.009	0.369
10	0.5	0.525	1.667	0.444	8.453	0.073	0.016	2.043	0.002	0.008	1.533	0.001	0.002	0.001	0.339	0.006	0.234
10	0.6	0.525	1.667	0.444	8.453	0.073	0.016	1.865	0.002	0.008	1.533	0.001	0.002	0.001	0.281	0.004	0.161
10	0.5	0.55	1.667	0.444	8.453	0.073	0.016	0.946	0.002	0.008	1.498	0.000	0.002	0.000	0.066	0.000	0.009
10	0.4	0.55	1.667	0.444	8.453	0.073	0.016	1.057	0.002	0.008	1.498	0.000	0.002	0.000	0.084	0.000	0.015
10	0.3	0.55	1.667	0.444	8.453	0.073	0.016	1.221	0.002	0.008	1.498	0.000	0.002	0.000	0.115	0.001	0.027
10	0.2	0.55	1.667	0.444	8.453	0.073	0.016	1.496	0.002	0.008	1.498	0.000	0.002	0.000	0.177	0.002	0.064
10	0.1	0.55	1.667	0.444	8.453	0.073	0.016	2.115	0.002	0.008	1.498	0.001	0.002	0.001	0.363	0.007	0.269
10	0.85	0.55	1.667	0.444	8.453	0.073	0.016	0.725	0.002	0.008	1.498	0.000	0.002	0.000	0.035	0.000	0.003
10	0.1	0.55	1.667	0.444	8.453	0.073	0.016	4.464	0.002	0.008	1.498	0.004	0.002	0.004	1.648	0.138	5.540
10	0.2	0.55	1.667	0.444	8.453	0.073	0.016	3.156	0.002	0.008	1.498	0.002	0.002	0.002	0.820	0.034	1.371
10	0.3	0.55	1.667	0.444	8.453	0.073	0.016	2.577	0.002	0.008	1.498	0.001	0.002	0.001	0.544	0.015	0.603
10	0.4	0.55	1.667	0.444	8.453	0.073	0.016	2.232	0.002	0.008	1.498	0.001	0.002	0.001	0.406	0.008	0.336
10	0.5	0.55	1.667	0.444	8.453	0.073	0.016	1.996	0.002	0.008	1.498	0.001	0.002	0.001	0.323	0.005	0.213
10	0.6	0.55	1.667	0.444	8.453	0.073	0.016	1.822	0.002	0.008	1.498	0.001	0.002	0.001	0.268	0.004	0.146
10	0.5	0.575	1.667	0.444	8.453	0.073	0.016	0.925	0.002	0.008	1.465	0.000	0.002	0.000	0.063	0.000	0.008
10	0.4	0.575	1.667	0.444	8.453	0.073	0.016	1.034	0.002	0.008	1.465	0.000	0.002	0.000	0.080	0.000	0.013

Q	X	Z	V _{zi}	Z _{core}	V _{zj}	h _{down}	h _{up}	V _{xmax}	q _{up}	q _{down}	V(z)	FQSI	G _b	I _{net}	V _{up}	H _{up}	H _{up} /z
l/s	m	m	m/s	m	m/s	m	m	m/s	m ² /s	m ² /s	m/s	Ns	kg/m ²	Ns	m/s	m	
			Q=VA	Z=5*B j	Eq. 25	Eq. 61		Eq. 63	Eq. 61&62		Eq. 60	Fig.2.18	Eq. 59	Eq.55		Eq. 58	
10	0.3	0.575	1.667	0.444	8.453	0.073	0.016	1.194	0.002	0.008	1.465	0.000	0.002	0.000	0.110	0.001	0.025
10	0.2	0.575	1.667	0.444	8.453	0.073	0.016	1.463	0.002	0.008	1.465	0.000	0.002	0.000	0.169	0.001	0.058
10	0.1	0.575	1.667	0.444	8.453	0.073	0.016	2.068	0.002	0.008	1.465	0.001	0.002	0.001	0.347	0.006	0.246
10	0.85	0.575	1.667	0.444	8.453	0.073	0.016	0.709	0.002	0.008	1.465	0.000	0.002	0.000	0.033	0.000	0.002
10	0.1	0.575	1.667	0.444	8.453	0.073	0.016	4.366	0.002	0.008	1.465	0.004	0.002	0.004	1.576	0.127	5.066
10	0.2	0.575	1.667	0.444	8.453	0.073	0.016	3.087	0.002	0.008	1.465	0.002	0.002	0.002	0.784	0.031	1.253
10	0.3	0.575	1.667	0.444	8.453	0.073	0.016	2.520	0.002	0.008	1.465	0.001	0.002	0.001	0.520	0.014	0.551
10	0.4	0.575	1.667	0.444	8.453	0.073	0.016	2.183	0.002	0.008	1.465	0.001	0.002	0.001	0.388	0.008	0.306
10	0.5	0.575	1.667	0.444	8.453	0.073	0.016	1.952	0.002	0.008	1.465	0.001	0.002	0.001	0.308	0.005	0.194
10	0.6	0.575	1.667	0.444	8.453	0.073	0.016	1.782	0.002	0.008	1.465	0.001	0.002	0.001	0.256	0.003	0.133
10	0.5	0.6	1.667	0.444	8.453	0.073	0.016	0.906	0.002	0.008	1.434	0.000	0.002	0.000	0.060	0.000	0.007
10	0.4	0.6	1.667	0.444	8.453	0.073	0.016	1.012	0.002	0.008	1.434	0.000	0.002	0.000	0.077	0.000	0.012
10	0.3	0.6	1.667	0.444	8.453	0.073	0.016	1.169	0.002	0.008	1.434	0.000	0.002	0.000	0.105	0.001	0.023
10	0.2	0.6	1.667	0.444	8.453	0.073	0.016	1.432	0.002	0.008	1.434	0.000	0.002	0.000	0.162	0.001	0.053
10	0.1	0.6	1.667	0.444	8.453	0.073	0.016	2.025	0.002	0.008	1.434	0.001	0.002	0.001	0.332	0.006	0.225
10	0.85	0.6	1.667	0.444	8.453	0.073	0.016	0.695	0.002	0.008	1.434	0.000	0.002	0.000	0.032	0.000	0.002
10	0.1	0.6	1.667	0.444	8.453	0.073	0.016	4.274	0.002	0.008	1.434	0.004	0.002	0.004	1.510	0.116	4.651
10	0.2	0.6	1.667	0.444	8.453	0.073	0.016	3.022	0.002	0.008	1.434	0.002	0.002	0.002	0.751	0.029	1.150
10	0.3	0.6	1.667	0.444	8.453	0.073	0.016	2.467	0.002	0.008	1.434	0.001	0.002	0.001	0.498	0.013	0.505
10	0.4	0.6	1.667	0.444	8.453	0.073	0.016	2.137	0.002	0.008	1.434	0.001	0.002	0.001	0.371	0.007	0.281
10	0.5	0.6	1.667	0.444	8.453	0.073	0.016	1.911	0.002	0.008	1.434	0.001	0.002	0.001	0.295	0.004	0.178
10	0.6	0.6	1.667	0.444	8.453	0.073	0.016	1.745	0.002	0.008	1.434	0.001	0.002	0.001	0.245	0.003	0.122
10	0.5	0.625	1.667	0.444	8.453	0.073	0.016	0.887	0.002	0.008	1.405	0.000	0.002	0.000	0.057	0.000	0.007
10	0.4	0.625	1.667	0.444	8.453	0.073	0.016	0.992	0.002	0.008	1.405	0.000	0.002	0.000	0.073	0.000	0.011
10	0.3	0.625	1.667	0.444	8.453	0.073	0.016	1.145	0.002	0.008	1.405	0.000	0.002	0.000	0.101	0.001	0.021
10	0.2	0.625	1.667	0.444	8.453	0.073	0.016	1.403	0.002	0.008	1.405	0.000	0.002	0.000	0.155	0.001	0.049
10	0.1	0.625	1.667	0.444	8.453	0.073	0.016	1.984	0.002	0.008	1.405	0.001	0.002	0.001	0.319	0.005	0.207

Q	X	Z	V _{zi}	Z _{core}	V _{zj}	h _{down}	h _{up}	V _{xmax}	q _{up}	q _{down}	V(z)	FQSI	G _b	I _{net}	V _{up}	H _{up}	H _{up} /z
l/s	m	m	m/s	m	m/s	m	m	m/s	m ² /s	m ² /s	m/s	Ns	kg/m ²	Ns	m/s	m	
			Q=VA	Z=5*B j	Eq. 25	Eq.61		Eq. 63	Eq. 61&62		Eq. 60	Fig.2.18	Eq. 57	Eq.53		Eq. 58	
10	0.85	0.625	1.667	0.444	8.453	0.073	0.016	0.681	0.002	0.008	1.405	0.000	0.002	0.000	0.030	0.000	0.002
10	0.1	0.625	1.667	0.444	8.453	0.073	0.016	4.187	0.002	0.008	1.405	0.003	0.002	0.003	1.450	0.107	4.284
10	0.2	0.625	1.667	0.444	8.453	0.073	0.016	2.961	0.002	0.008	1.405	0.002	0.002	0.002	0.721	0.026	1.058
10	0.3	0.625	1.667	0.444	8.453	0.073	0.016	2.418	0.002	0.008	1.405	0.001	0.002	0.001	0.478	0.012	0.465
10	0.4	0.625	1.667	0.444	8.453	0.073	0.016	2.094	0.002	0.008	1.405	0.001	0.002	0.001	0.356	0.006	0.258
10	0.5	0.625	1.667	0.444	8.453	0.073	0.016	1.873	0.002	0.008	1.405	0.001	0.002	0.001	0.283	0.004	0.163
10	0.6	0.625	1.667	0.444	8.453	0.073	0.016	1.709	0.002	0.008	1.405	0.001	0.002	0.001	0.234	0.003	0.112
10	0.5	0.65	1.667	0.444	8.453	0.073	0.016	0.870	0.002	0.008	1.378	0.000	0.002	0.000	0.054	0.000	0.006
10	0.4	0.65	1.667	0.444	8.453	0.073	0.016	0.973	0.002	0.008	1.378	0.000	0.002	0.000	0.070	0.000	0.010
10	0.3	0.65	1.667	0.444	8.453	0.073	0.016	1.123	0.002	0.008	1.378	0.000	0.002	0.000	0.096	0.000	0.019
10	0.2	0.65	1.667	0.444	8.453	0.073	0.016	1.376	0.002	0.008	1.378	0.000	0.002	0.000	0.149	0.001	0.045
10	0.1	0.65	1.667	0.444	8.453	0.073	0.016	1.946	0.002	0.008	1.378	0.001	0.002	0.001	0.306	0.005	0.191
10	0.85	0.65	1.667	0.444	8.453	0.073	0.016	0.667	0.002	0.008	1.378	0.000	0.002	0.000	0.028	0.000	0.002
10	0.1	0.65	1.667	0.444	8.453	0.073	0.016	4.106	0.002	0.008	1.378	0.003	0.002	0.003	1.393	0.099	3.959
10	0.2	0.65	1.667	0.444	8.453	0.073	0.016	2.903	0.002	0.008	1.378	0.002	0.002	0.002	0.692	0.024	0.978
10	0.3	0.65	1.667	0.444	8.453	0.073	0.016	2.371	0.002	0.008	1.378	0.001	0.002	0.001	0.459	0.011	0.429
10	0.4	0.65	1.667	0.444	8.453	0.073	0.016	2.053	0.002	0.008	1.378	0.001	0.002	0.001	0.342	0.006	0.238
10	0.5	0.65	1.667	0.444	8.453	0.073	0.016	1.836	0.002	0.008	1.378	0.001	0.002	0.001	0.272	0.004	0.151
10	0.6	0.65	1.667	0.444	8.453	0.073	0.016	1.676	0.002	0.008	1.378	0.001	0.002	0.001	0.225	0.003	0.103
10	0.5	0.675	1.667	0.444	8.453	0.073	0.016	0.854	0.002	0.008	1.352	0.000	0.002	0.000	0.052	0.000	0.006
10	0.4	0.675	1.667	0.444	8.453	0.073	0.016	0.955	0.002	0.008	1.352	0.000	0.002	0.000	0.067	0.000	0.009
10	0.3	0.675	1.667	0.444	8.453	0.073	0.016	1.102	0.002	0.008	1.352	0.000	0.002	0.000	0.093	0.000	0.017
10	0.2	0.675	1.667	0.444	8.453	0.073	0.016	1.350	0.002	0.008	1.352	0.000	0.002	0.000	0.143	0.001	0.042
10	0.1	0.675	1.667	0.444	8.453	0.073	0.016	1.909	0.002	0.008	1.352	0.001	0.002	0.001	0.295	0.004	0.177
10	0.85	0.675	1.667	0.444	8.453	0.073	0.016	0.655	0.002	0.008	1.352	0.000	0.002	0.000	0.027	0.000	0.002
10	0.1	0.675	1.667	0.444	8.453	0.073	0.016	4.029	0.002	0.008	1.352	0.003	0.002	0.003	1.342	0.092	3.669
10	0.2	0.675	1.667	0.444	8.453	0.073	0.016	2.849	0.002	0.008	1.352	0.002	0.002	0.002	0.667	0.023	0.906

Q	X	Z	V _{zi}	Z _{core}	V _{zj}	h _{down}	h _{up}	V _{xmax}	q _{up}	q _{down}	V(z)	FQSI	G _b	I _{net}	V _{up}	H _{up}	H _{up} /z
l/s	m	m	m/s	m	m/s	m	m	m/s	m ² /s	m ² /s	m/s	Ns	kg/m ²	Ns	m/s	m	
			Q=VA	Z=5*B j	Eq. 25	Eq. 61		Eq. 63	Eq. 61&62		Eq. 60	Fig.2.18	Eq. 59	Eq.55		Eq. 58	
10	0.3	0.675	1.667	0.444	8.453	0.073	0.016	2.326	0.002	0.008	1.352	0.001	0.002	0.001	0.442	0.010	0.397
10	0.4	0.675	1.667	0.444	8.453	0.073	0.016	2.015	0.002	0.008	1.352	0.001	0.002	0.001	0.329	0.006	0.221
10	0.5	0.675	1.667	0.444	8.453	0.073	0.016	1.802	0.002	0.008	1.352	0.001	0.002	0.001	0.261	0.003	0.139
10	0.6	0.675	1.667	0.444	8.453	0.073	0.016	1.645	0.002	0.008	1.352	0.001	0.002	0.001	0.216	0.002	0.096
10	0.5	0.7	1.667	0.444	8.453	0.073	0.016	0.838	0.002	0.008	1.327	0.000	0.002	0.000	0.050	0.000	0.005
10	0.4	0.7	1.667	0.444	8.453	0.073	0.016	0.937	0.002	0.008	1.327	0.000	0.002	0.000	0.065	0.000	0.008
10	0.3	0.7	1.667	0.444	8.453	0.073	0.016	1.082	0.002	0.008	1.327	0.000	0.002	0.000	0.089	0.000	0.016
10	0.2	0.7	1.667	0.444	8.453	0.073	0.016	1.326	0.002	0.008	1.327	0.000	0.002	0.000	0.138	0.001	0.039
10	0.1	0.7	1.667	0.444	8.453	0.073	0.016	1.875	0.002	0.008	1.327	0.001	0.002	0.001	0.284	0.004	0.164
10	0.85	0.7	1.667	0.444	8.453	0.073	0.016	0.643	0.002	0.008	1.327	0.000	0.002	0.000	0.026	0.000	0.001
10	0.1	0.7	1.667	0.444	8.453	0.073	0.016	3.957	0.002	0.008	1.327	0.003	0.002	0.003	1.293	0.085	3.410
10	0.2	0.7	1.667	0.444	8.453	0.073	0.016	2.798	0.002	0.008	1.327	0.002	0.002	0.002	0.642	0.021	0.841
10	0.3	0.7	1.667	0.444	8.453	0.073	0.016	2.284	0.002	0.008	1.327	0.001	0.002	0.001	0.425	0.009	0.369
10	0.4	0.7	1.667	0.444	8.453	0.073	0.016	1.978	0.002	0.008	1.327	0.001	0.002	0.001	0.317	0.005	0.205
10	0.5	0.7	1.667	0.444	8.453	0.073	0.016	1.769	0.002	0.008	1.327	0.001	0.002	0.001	0.252	0.003	0.129
10	0.6	0.7	1.667	0.444	8.453	0.073	0.016	1.615	0.002	0.008	1.327	0.001	0.002	0.000	0.208	0.002	0.089
10	0.5	0.725	1.667	0.444	8.453	0.073	0.016	0.824	0.002	0.008	1.304	0.000	0.002	0.000	0.048	0.000	0.005
10	0.4	0.725	1.667	0.444	8.453	0.073	0.016	0.921	0.002	0.008	1.304	0.000	0.002	0.000	0.062	0.000	0.008
10	0.3	0.725	1.667	0.444	8.453	0.073	0.016	1.064	0.002	0.008	1.304	0.000	0.002	0.000	0.086	0.000	0.015
10	0.2	0.725	1.667	0.444	8.453	0.073	0.016	1.303	0.002	0.008	1.304	0.000	0.002	0.000	0.133	0.001	0.036
10	0.1	0.725	1.667	0.444	8.453	0.073	0.016	1.842	0.002	0.008	1.304	0.001	0.002	0.001	0.274	0.004	0.153
10	0.85	0.725	1.667	0.444	8.453	0.073	0.016	0.632	0.002	0.008	1.304	0.000	0.002	0.000	0.025	0.000	0.001
10	0.1	0.725	1.667	0.444	8.453	0.073	0.016	3.888	0.002	0.008	1.304	0.003	0.002	0.003	1.248	0.079	3.178
10	0.2	0.725	1.667	0.444	8.453	0.073	0.016	2.749	0.002	0.008	1.304	0.001	0.002	0.001	0.620	0.020	0.784
10	0.3	0.725	1.667	0.444	8.453	0.073	0.016	2.245	0.002	0.008	1.304	0.001	0.002	0.001	0.410	0.009	0.343
10	0.4	0.725	1.667	0.444	8.453	0.073	0.016	1.944	0.002	0.008	1.304	0.001	0.002	0.001	0.306	0.005	0.191
10	0.5	0.725	1.667	0.444	8.453	0.073	0.016	1.739	0.002	0.008	1.304	0.001	0.002	0.001	0.243	0.003	0.120

Q	X	Z	V _{zi}	Z _{core}	V _{zj}	h _{down}	h _{up}	V _{xmax}	q _{up}	q _{down}	V(z)	FQSI	G _b	I _{net}	V _{up}	H _{up}	H _{up} /z
l/s	m	m	m/s	m	m/s	m	m	m/s	m ² /s	m ² /s	m/s	Ns	kg/m ²	Ns	m/s	m	
			Q=VA	Z=5*B j	Eq. 25	Eq. 61		Eq. 63	Eq. 61&62		Eq. 60	Fig.2.18	Eq. 59	Eq.55		Eq. 58	
10	0.6	0.725	1.667	0.444	8.453	0.073	0.016	1.587	0.002	0.008	1.304	0.000	0.002	0.000	0.201	0.002	0.082
10	0.5	0.75	1.667	0.444	8.453	0.073	0.016	0.810	0.002	0.008	1.282	0.000	0.002	0.000	0.046	0.000	0.004
10	0.4	0.75	1.667	0.444	8.453	0.073	0.016	0.906	0.002	0.008	1.282	0.000	0.002	0.000	0.060	0.000	0.007
10	0.3	0.75	1.667	0.444	8.453	0.073	0.016	1.046	0.002	0.008	1.282	0.000	0.002	0.000	0.082	0.000	0.014
10	0.2	0.75	1.667	0.444	8.453	0.073	0.016	1.281	0.002	0.008	1.282	0.000	0.002	0.000	0.128	0.001	0.033
10	0.1	0.75	1.667	0.444	8.453	0.073	0.016	1.811	0.002	0.008	1.282	0.001	0.002	0.001	0.264	0.004	0.142
10	0.85	0.75	1.667	0.444	8.453	0.073	0.016	0.621	0.002	0.008	1.282	0.000	0.002	0.000	0.024	0.000	0.001
10	0.1	0.75	1.667	0.444	8.453	0.073	0.016	3.823	0.002	0.008	1.282	0.003	0.002	0.003	1.207	0.074	2.968
10	0.2	0.75	1.667	0.444	8.453	0.073	0.016	1.281	0.002	0.008	1.282	0.000	0.002	0.000	0.128	0.001	0.033
10	0.3	0.75	1.667	0.444	8.453	0.073	0.016	1.046	0.002	0.008	1.282	0.000	0.002	0.000	0.082	0.000	0.014
10	0.4	0.75	1.667	0.444	8.453	0.073	0.016	0.906	0.002	0.008	1.282	0.000	0.002	0.000	0.060	0.000	0.007
10	0.5	0.75	1.667	0.444	8.453	0.073	0.016	0.810	0.002	0.008	1.282	0.000	0.002	0.000	0.046	0.000	0.004
10	0.6	0.75	1.667	0.444	8.453	0.073	0.016	0.739	0.002	0.008	1.282	0.000	0.002	0.000	0.037	0.000	0.003
10	0.5	0.775	1.667	0.444	8.453	0.073	0.016	0.797	0.002	0.008	1.262	0.000	0.002	0.000	0.044	0.000	0.004
10	0.4	0.775	1.667	0.444	8.453	0.073	0.016	0.891	0.002	0.008	1.262	0.000	0.002	0.000	0.057	0.000	0.007
10	0.3	0.775	1.667	0.444	8.453	0.073	0.016	1.029	0.002	0.008	1.262	0.000	0.002	0.000	0.079	0.000	0.013
10	0.2	0.775	1.667	0.444	8.453	0.073	0.016	1.260	0.002	0.008	1.262	0.000	0.002	0.000	0.123	0.001	0.031
10	0.1	0.775	1.667	0.444	8.453	0.073	0.016	1.782	0.002	0.008	1.262	0.001	0.002	0.001	0.255	0.003	0.133
10	0.85	0.775	1.667	0.444	8.453	0.073	0.016	0.611	0.002	0.008	1.262	0.000	0.002	0.000	0.023	0.000	0.001
10	0.1	0.775	1.667	0.444	8.453	0.073	0.016	3.760	0.002	0.008	1.262	0.003	0.002	0.003	1.167	0.069	2.778
10	0.2	0.775	1.667	0.444	8.453	0.073	0.016	2.659	0.002	0.008	1.262	0.001	0.002	0.001	0.579	0.017	0.684
10	0.3	0.775	1.667	0.444	8.453	0.073	0.016	2.171	0.002	0.008	1.262	0.001	0.002	0.001	0.383	0.007	0.300
10	0.4	0.775	1.667	0.444	8.453	0.073	0.016	1.880	0.002	0.008	1.262	0.001	0.002	0.001	0.285	0.004	0.166
10	0.5	0.775	1.667	0.444	8.453	0.073	0.016	1.682	0.002	0.008	1.262	0.001	0.002	0.001	0.227	0.003	0.105
10	0.6	0.775	1.667	0.444	8.453	0.073	0.016	1.535	0.002	0.008	1.262	0.000	0.002	0.000	0.187	0.002	0.072
10	0.5	0.8	1.667	0.444	8.453	0.073	0.016	0.784	0.002	0.008	1.242	0.000	0.002	0.000	0.043	0.000	0.004
10	0.4	0.8	1.667	0.444	8.453	0.073	0.016	0.877	0.002	0.008	1.242	0.000	0.002	0.000	0.055	0.000	0.006

Q	X	Z	V _{zi}	Z _{core}	V _{zj}	h _{down}	h _{up}	V _{xmax}	q _{up}	q _{down}	V(z)	FQSI	G _b	I _{net}	V _{up}	H _{up}	H _{up} /z
l/s	m	m	m/s	m	m/s	m	m	m/s	m ² /s	m ² /s	m/s	Ns	kg/m ²	Ns	m/s	m	
			Q=VA	Z=5*B j	Eq. 25	Eq. 61		Eq. 63	Eq. 61&62		Eq. 60	Fig.2.18	Eq. 59	Eq.55		Eq. 58	
10	0.3	0.8	1.667	0.444	8.453	0.073	0.016	1.012	0.002	0.008	1.242	0.000	0.002	0.000	0.077	0.000	0.012
10	0.2	0.8	1.667	0.444	8.453	0.073	0.016	1.240	0.002	0.008	1.242	0.000	0.002	0.000	0.119	0.001	0.029
10	0.1	0.8	1.667	0.444	8.453	0.073	0.016	1.754	0.002	0.008	1.242	0.001	0.002	0.001	0.247	0.003	0.125
10	0.85	0.8	1.667	0.444	8.453	0.073	0.016	0.601	0.002	0.008	1.242	0.000	0.002	0.000	0.022	0.000	0.001
10	0.1	0.8	1.667	0.444	8.453	0.073	0.016	3.701	0.002	0.008	1.242	0.003	0.002	0.003	1.131	0.065	2.606
10	0.2	0.8	1.667	0.444	8.453	0.073	0.016	2.617	0.002	0.008	1.242	0.001	0.002	0.001	0.561	0.016	0.642
10	0.3	0.8	1.667	0.444	8.453	0.073	0.016	2.137	0.002	0.008	1.242	0.001	0.002	0.001	0.371	0.007	0.281
10	0.4	0.8	1.667	0.444	8.453	0.073	0.016	1.851	0.002	0.008	1.242	0.001	0.002	0.001	0.276	0.004	0.156
10	0.5	0.8	1.667	0.444	8.453	0.073	0.016	1.655	0.002	0.008	1.242	0.001	0.002	0.001	0.219	0.002	0.098
10	0.6	0.8	1.667	0.444	8.453	0.073	0.016	1.511	0.002	0.008	1.242	0.000	0.002	0.000	0.181	0.002	0.067
10	0.5	0.825	1.667	0.444	8.453	0.073	0.016	0.772	0.002	0.008	1.223	0.000	0.002	0.000	0.041	0.000	0.003
10	0.4	0.825	1.667	0.444	8.453	0.073	0.016	0.863	0.002	0.008	1.223	0.000	0.002	0.000	0.053	0.000	0.006
10	0.3	0.825	1.667	0.444	8.453	0.073	0.016	0.997	0.002	0.008	1.223	0.000	0.002	0.000	0.074	0.000	0.011
10	0.2	0.825	1.667	0.444	8.453	0.073	0.016	1.221	0.002	0.008	1.223	0.000	0.002	0.000	0.115	0.001	0.027
10	0.1	0.825	1.667	0.444	8.453	0.073	0.016	1.727	0.002	0.008	1.223	0.001	0.002	0.001	0.239	0.003	0.117
10	0.85	0.825	1.667	0.444	8.453	0.073	0.016	0.592	0.002	0.008	1.223	0.000	0.002	0.000	0.021	0.000	0.001
10	0.1	0.825	1.667	0.444	8.453	0.073	0.016	3.645	0.002	0.008	1.223	0.003	0.002	0.003	1.096	0.061	2.449
10	0.2	0.825	1.667	0.444	8.453	0.073	0.016	2.577	0.002	0.008	1.223	0.001	0.002	0.001	0.544	0.015	0.603
10	0.3	0.825	1.667	0.444	8.453	0.073	0.016	2.104	0.002	0.008	1.223	0.001	0.002	0.001	0.360	0.007	0.264
10	0.4	0.825	1.667	0.444	8.453	0.073	0.016	1.822	0.002	0.008	1.223	0.001	0.002	0.001	0.268	0.004	0.146
10	0.5	0.825	1.667	0.444	8.453	0.073	0.016	1.630	0.002	0.008	1.223	0.001	0.002	0.001	0.212	0.002	0.092
10	0.6	0.825	1.667	0.444	8.453	0.073	0.016	1.488	0.002	0.008	1.223	0.000	0.002	0.000	0.176	0.002	0.063

Table D 0.7. Quasi-steady method of Q=10 l/s, H=4 m and TW=0.25 m

Q	X	Z	V _{zi}	Z _{core}	V _{zj}	h _{down}	h _{up}	V _{xmax}	q _{up}	q _{down}	V(z)	FQSI	G _b	I _{net}	V _{up}	H _{up}	H _{up} /z
l/s	m	m	m/s	m	m/s	m	m	m/s	m ² /s	m ² /s	m/s	Ns	kg/m ²	Ns	m/s	m	
			Q=VA	Z=5*Bj	eq. 25	Eq.61		Eq. 63	Eq. 61&62		Eq. 60	Fig.2.18	Eq. 59	Eq.55		Eq. 58	
10	0.85	0	1.667	0.444	8.453	0.073	0.016	1.076	0.002	0.008	8.453						
10	0.85	0.042	1.667	0.444	8.453	0.073	0.016	1.076	0.002	0.008	5.441						
10	0.85	0.083	1.667	0.444	8.453	0.073	0.016	1.076	0.002	0.008	3.847						
10	0.85	0.125	1.667	0.444	8.453	0.073	0.016	1.076	0.002	0.008	3.141						
10	0.85	0.167	1.667	0.444	8.453	0.073	0.016	1.076	0.002	0.008	2.720						
10	0.85	0.208	1.667	0.444	8.453	0.073	0.016	1.076	0.002	0.008	2.433						
10	0.85	0.25	1.667	0.444	8.453	0.073	0.016	1.076	0.002	0.008	2.221						
10	0.5	0.25	1.667	0.444	8.453	0.073	0.016	1.403	0.002	0.008	2.221	0.000	0.002	0.000	0.155	0.001	0.049
10	0.4	0.25	1.667	0.444	8.453	0.073	0.016	1.569	0.002	0.008	2.221	0.000	0.002	0.000	0.196	0.002	0.078
10	0.3	0.25	1.667	0.444	8.453	0.073	0.016	1.811	0.002	0.008	2.221	0.001	0.002	0.001	0.264	0.004	0.142
10	0.2	0.25	1.667	0.444	8.453	0.073	0.016	2.218	0.002	0.008	2.221	0.001	0.002	0.001	0.401	0.008	0.327
10	0.1	0.25	1.667	0.444	8.453	0.073	0.016	3.137	0.002	0.008	2.221	0.002	0.002	0.002	0.810	0.033	1.337
10	0.85	0.25	1.667	0.444	8.453	0.073	0.016	1.076	0.002	0.008	2.221	0.000	0.002	0.000	0.088	0.000	0.016
10	0.1	0.25	1.667	0.444	8.453	0.073	0.016	6.621	0.002	0.008	2.221	0.009	0.002	0.009	3.637	0.674	26.964
10	0.2	0.25	1.667	0.444	8.453	0.073	0.016	4.682	0.002	0.008	2.221	0.004	0.002	0.004	1.814	0.168	6.709
10	0.3	0.25	1.667	0.444	8.453	0.073	0.016	3.823	0.002	0.008	2.221	0.003	0.002	0.003	1.207	0.074	2.968
10	0.4	0.25	1.667	0.444	8.453	0.073	0.016	3.310	0.002	0.008	2.221	0.002	0.002	0.002	0.903	0.042	1.662
10	0.5	0.25	1.667	0.444	8.453	0.073	0.016	2.961	0.002	0.008	2.221	0.002	0.002	0.002	0.721	0.026	1.058
10	0.6	0.25	1.667	0.444	8.453	0.073	0.016	2.703	0.002	0.008	2.221	0.001	0.002	0.001	0.599	0.018	0.732
10	0.5	0.275	1.667	0.444	8.453	0.073	0.016	1.338	0.002	0.008	2.118	0.000	0.002	0.000	0.140	0.001	0.040
10	0.4	0.275	1.667	0.444	8.453	0.073	0.016	1.496	0.002	0.008	2.118	0.000	0.002	0.000	0.177	0.002	0.064
10	0.3	0.275	1.667	0.444	8.453	0.073	0.016	1.727	0.002	0.008	2.118	0.001	0.002	0.001	0.239	0.003	0.117
10	0.2	0.275	1.667	0.444	8.453	0.073	0.016	2.115	0.002	0.008	2.118	0.001	0.002	0.001	0.363	0.007	0.269
10	0.1	0.275	1.667	0.444	8.453	0.073	0.016	2.991	0.002	0.008	2.118	0.002	0.002	0.002	0.735	0.028	1.103
10	0.85	0.275	1.667	0.444	8.453	0.073	0.016	1.026	0.002	0.008	2.118	0.000	0.002	0.000	0.079	0.000	0.013

Q	X	Z	V _{zi}	Z _{core}	V _{zj}	h _{down}	h _{up}	V _{xmax}	q _{up}	q _{down}	V(z)	FQSI	G _b	I _{net}	V _{up}	H _{up}	H _{up} /z
l/s	m	m	m/s	m	m/s	m	m	m/s	m ² /s	m ² /s	m/s	Ns	kg/m ²	Ns	m/s	m	
			Q=VA	Z=5*Bj	Eq. 25	Eq. 61		Eq. 63	Eq. 61&62		Eq. 60	Fig.2.18	Eq. 59	Eq.55		Eq. 58	
10	0.1	0.275	1.667	0.444	8.453	0.073	0.016	6.313	0.002	0.008	2.118	0.008	0.002	0.008	3.305	0.557	22.274
10	0.2	0.275	1.667	0.444	8.453	0.073	0.016	4.464	0.002	0.008	2.118	0.004	0.002	0.004	1.648	0.138	5.540
10	0.3	0.275	1.667	0.444	8.453	0.073	0.016	3.645	0.002	0.008	2.118	0.003	0.002	0.003	1.096	0.061	2.449
10	0.4	0.275	1.667	0.444	8.453	0.073	0.016	3.156	0.002	0.008	2.118	0.002	0.002	0.002	0.820	0.034	1.371
10	0.5	0.275	1.667	0.444	8.453	0.073	0.016	2.823	0.002	0.008	2.118	0.002	0.002	0.002	0.654	0.022	0.873
10	0.6	0.275	1.667	0.444	8.453	0.073	0.016	2.577	0.002	0.008	2.118	0.001	0.002	0.001	0.544	0.015	0.603
10	0.5	0.3	1.667	0.444	8.453	0.073	0.016	1.281	0.002	0.008	2.028	0.000	0.002	0.000	0.128	0.001	0.033
10	0.4	0.3	1.667	0.444	8.453	0.073	0.016	1.432	0.002	0.008	2.028	0.000	0.002	0.000	0.162	0.001	0.053
10	0.3	0.3	1.667	0.444	8.453	0.073	0.016	1.653	0.002	0.008	2.028	0.001	0.002	0.001	0.219	0.002	0.098
10	0.2	0.3	1.667	0.444	8.453	0.073	0.016	2.025	0.002	0.008	2.028	0.001	0.002	0.001	0.332	0.006	0.225
10	0.1	0.3	1.667	0.444	8.453	0.073	0.016	2.864	0.002	0.008	2.028	0.002	0.002	0.002	0.673	0.023	0.925
10	0.85	0.3	1.667	0.444	8.453	0.073	0.016	0.982	0.002	0.008	2.028	0.000	0.002	0.000	0.072	0.000	0.010
10	0.1	0.3	1.667	0.444	8.453	0.073	0.016	6.044	0.002	0.008	2.028	0.007	0.002	0.007	3.029	0.468	18.707
10	0.2	0.3	1.667	0.444	8.453	0.073	0.016	4.274	0.002	0.008	2.028	0.004	0.002	0.004	1.510	0.116	4.651
10	0.3	0.3	1.667	0.444	8.453	0.073	0.016	3.489	0.002	0.008	2.028	0.002	0.002	0.002	1.004	0.051	2.055
10	0.4	0.3	1.667	0.444	8.453	0.073	0.016	3.022	0.002	0.008	2.028	0.002	0.002	0.002	0.751	0.029	1.150
10	0.5	0.3	1.667	0.444	8.453	0.073	0.016	2.703	0.002	0.008	2.028	0.001	0.002	0.001	0.599	0.018	0.732
10	0.6	0.3	1.667	0.444	8.453	0.073	0.016	2.467	0.002	0.008	2.028	0.001	0.002	0.001	0.498	0.013	0.505
10	0.5	0.325	1.667	0.444	8.453	0.073	0.016	1.230	0.002	0.008	1.948	0.000	0.002	0.000	0.117	0.001	0.028
10	0.4	0.325	1.667	0.444	8.453	0.073	0.016	1.376	0.002	0.008	1.948	0.000	0.002	0.000	0.149	0.001	0.045
10	0.3	0.325	1.667	0.444	8.453	0.073	0.016	1.588	0.002	0.008	1.948	0.000	0.002	0.000	0.201	0.002	0.083
10	0.2	0.325	1.667	0.444	8.453	0.073	0.016	1.946	0.002	0.008	1.948	0.001	0.002	0.001	0.306	0.005	0.191
10	0.1	0.325	1.667	0.444	8.453	0.073	0.016	2.751	0.002	0.008	1.948	0.001	0.002	0.001	0.621	0.020	0.786
10	0.85	0.325	1.667	0.444	8.453	0.073	0.016	0.944	0.002	0.008	1.948	0.000	0.002	0.000	0.066	0.000	0.009
10	0.1	0.325	1.667	0.444	8.453	0.073	0.016	5.807	0.002	0.008	1.948	0.007	0.002	0.007	2.796	0.398	15.932
10	0.2	0.325	1.667	0.444	8.453	0.073	0.016	4.106	0.002	0.008	1.948	0.003	0.002	0.003	1.393	0.099	3.959

Q	X	Z	V _{zi}	Z _{core}	V _{zj}	h _{down}	h _{up}	V _{xmax}	q _{up}	q _{down}	V(z)	FQSI	G _b	I _{net}	V _{up}	H _{up}	H _{up} /z
l/s	m	m	m/s	m	m/s	m	m	m/s	m ² /s	m ² /s	m/s	Ns	kg/m ²	Ns	m/s	m	
			Q=VA	Z=5*Bj	Eq. 25	Eq. 61		Eq. 63	Eq. 61&62		Eq. 60	Fig.2.18	Eq. 59	Eq.55		Eq. 58	
10	0.3	0.325	1.667	0.444	8.453	0.073	0.016	3.353	0.002	0.008	1.948	0.002	0.002	0.002	0.926	0.044	1.749
10	0.4	0.325	1.667	0.444	8.453	0.073	0.016	2.903	0.002	0.008	1.948	0.002	0.002	0.002	0.692	0.024	0.978
10	0.5	0.325	1.667	0.444	8.453	0.073	0.016	2.597	0.002	0.008	1.948	0.001	0.002	0.001	0.552	0.016	0.622
10	0.6	0.325	1.667	0.444	8.453	0.073	0.016	2.371	0.002	0.008	1.948	0.001	0.002	0.001	0.459	0.011	0.429
10	0.5	0.35	1.667	0.444	8.453	0.073	0.016	1.186	0.002	0.008	1.877	0.000	0.002	0.000	0.108	0.001	0.024
10	0.4	0.35	1.667	0.444	8.453	0.073	0.016	1.326	0.002	0.008	1.877	0.000	0.002	0.000	0.138	0.001	0.039
10	0.3	0.35	1.667	0.444	8.453	0.073	0.016	1.531	0.002	0.008	1.877	0.000	0.002	0.000	0.186	0.002	0.071
10	0.2	0.35	1.667	0.444	8.453	0.073	0.016	1.875	0.002	0.008	1.877	0.001	0.002	0.001	0.284	0.004	0.164
10	0.1	0.35	1.667	0.444	8.453	0.073	0.016	2.651	0.002	0.008	1.877	0.001	0.002	0.001	0.576	0.017	0.676
10	0.85	0.35	1.667	0.444	8.453	0.073	0.016	0.909	0.002	0.008	1.877	0.000	0.002	0.000	0.060	0.000	0.007
10	0.1	0.35	1.667	0.444	8.453	0.073	0.016	5.596	0.002	0.008	1.877	0.006	0.002	0.006	2.595	0.343	13.731
10	0.2	0.35	1.667	0.444	8.453	0.073	0.016	3.957	0.002	0.008	1.877	0.003	0.002	0.003	1.293	0.085	3.410
10	0.3	0.35	1.667	0.444	8.453	0.073	0.016	3.231	0.002	0.008	1.877	0.002	0.002	0.002	0.859	0.038	1.506
10	0.4	0.35	1.667	0.444	8.453	0.073	0.016	2.798	0.002	0.008	1.877	0.002	0.002	0.002	0.642	0.021	0.841
10	0.5	0.35	1.667	0.444	8.453	0.073	0.016	2.502	0.002	0.008	1.877	0.001	0.002	0.001	0.512	0.013	0.535
10	0.6	0.35	1.667	0.444	8.453	0.073	0.016	2.284	0.002	0.008	1.877	0.001	0.002	0.001	0.425	0.009	0.369
10	0.5	0.375	1.667	0.444	8.453	0.073	0.016	1.145	0.002	0.008	1.814	0.000	0.002	0.000	0.101	0.001	0.021
10	0.4	0.375	1.667	0.444	8.453	0.073	0.016	1.281	0.002	0.008	1.814	0.000	0.002	0.000	0.128	0.001	0.033
10	0.3	0.375	1.667	0.444	8.453	0.073	0.016	1.479	0.002	0.008	1.814	0.000	0.002	0.000	0.173	0.002	0.061
10	0.2	0.375	1.667	0.444	8.453	0.073	0.016	1.811	0.002	0.008	1.814	0.001	0.002	0.001	0.264	0.004	0.142
10	0.1	0.375	1.667	0.444	8.453	0.073	0.016	2.561	0.002	0.008	1.814	0.001	0.002	0.001	0.537	0.015	0.588
10	0.85	0.375	1.667	0.444	8.453	0.073	0.016	0.879	0.002	0.008	1.814	0.000	0.002	0.000	0.056	0.000	0.006
10	0.1	0.375	1.667	0.444	8.453	0.073	0.016	5.406	0.002	0.008	1.814	0.006	0.002	0.006	2.422	0.299	11.956
10	0.2	0.375	1.667	0.444	8.453	0.073	0.016	3.823	0.002	0.008	1.814	0.003	0.002	0.003	1.207	0.074	2.968
10	0.3	0.375	1.667	0.444	8.453	0.073	0.016	3.121	0.002	0.008	1.814	0.002	0.002	0.002	0.802	0.033	1.310
10	0.4	0.375	1.667	0.444	8.453	0.073	0.016	2.703	0.002	0.008	1.814	0.001	0.002	0.001	0.599	0.018	0.732

Q	X	Z	V _{zi}	Z _{core}	V _{zj}	h _{down}	h _{up}	V _{xmax}	q _{up}	q _{down}	V(z)	FQSI	G _b	I _{net}	V _{up}	H _{up}	H _{up} /z
l/s	m	m	m/s	m	m/s	m	m	m/s	m ² /s	m ² /s	m/s	Ns	kg/m ²	Ns	m/s	m	
			Q=VA	Z=5*Bj	Eq. 25	Eq. 61		Eq. 63	Eq. 61&62		Eq. 60	Fig.2.18	Eq. 59	Eq.55		Eq. 59	
10	0.5	0.375	1.667	0.444	8.453	0.073	0.016	2.418	0.002	0.008	1.814	0.001	0.002	0.001	0.478	0.012	0.465
10	0.6	0.375	1.667	0.444	8.453	0.073	0.016	2.207	0.002	0.008	1.814	0.001	0.002	0.001	0.396	0.008	0.321
10	0.5	0.4	1.667	0.444	8.453	0.073	0.016	1.109	0.002	0.008	1.756	0.000	0.002	0.000	0.094	0.000	0.018
10	0.4	0.4	1.667	0.444	8.453	0.073	0.016	1.240	0.002	0.008	1.756	0.000	0.002	0.000	0.119	0.001	0.029
10	0.3	0.4	1.667	0.444	8.453	0.073	0.016	1.432	0.002	0.008	1.756	0.000	0.002	0.000	0.162	0.001	0.053
10	0.2	0.4	1.667	0.444	8.453	0.073	0.016	1.754	0.002	0.008	1.756	0.001	0.002	0.001	0.247	0.003	0.125
10	0.1	0.4	1.667	0.444	8.453	0.073	0.016	2.480	0.002	0.008	1.756	0.001	0.002	0.001	0.503	0.013	0.516
10	0.85	0.4	1.667	0.444	8.453	0.073	0.016	0.851	0.002	0.008	1.756	0.000	0.002	0.000	0.052	0.000	0.005
10	0.1	0.4	1.667	0.444	8.453	0.073	0.016	5.234	0.002	0.008	1.756	0.005	0.002	0.005	2.270	0.263	10.503
10	0.2	0.4	1.667	0.444	8.453	0.073	0.016	3.701	0.002	0.008	1.756	0.003	0.002	0.003	1.131	0.065	2.606
10	0.3	0.4	1.667	0.444	8.453	0.073	0.016	3.022	0.002	0.008	1.756	0.002	0.002	0.002	0.751	0.029	1.150
10	0.4	0.4	1.667	0.444	8.453	0.073	0.016	2.617	0.002	0.008	1.756	0.001	0.002	0.001	0.561	0.016	0.642
10	0.5	0.4	1.667	0.444	8.453	0.073	0.016	2.341	0.002	0.008	1.756	0.001	0.002	0.001	0.447	0.010	0.408
10	0.6	0.4	1.667	0.444	8.453	0.073	0.016	2.137	0.002	0.008	1.756	0.001	0.002	0.001	0.371	0.007	0.281
10	0.5	0.425	1.667	0.444	8.453	0.073	0.016	1.076	0.002	0.008	1.704	0.000	0.002	0.000	0.088	0.000	0.016
10	0.4	0.425	1.667	0.444	8.453	0.073	0.016	1.203	0.002	0.008	1.704	0.000	0.002	0.000	0.112	0.001	0.025
10	0.3	0.425	1.667	0.444	8.453	0.073	0.016	1.389	0.002	0.008	1.704	0.000	0.002	0.000	0.152	0.001	0.047
10	0.2	0.425	1.667	0.444	8.453	0.073	0.016	1.701	0.002	0.008	1.704	0.001	0.002	0.001	0.232	0.003	0.110
10	0.1	0.425	1.667	0.444	8.453	0.073	0.016	2.406	0.002	0.008	1.704	0.001	0.002	0.001	0.473	0.011	0.456
10	0.85	0.425	1.667	0.444	8.453	0.073	0.016	0.825	0.002	0.008	1.704	0.000	0.002	0.000	0.048	0.000	0.005
10	0.1	0.425	1.667	0.444	8.453	0.073	0.016	5.078	0.002	0.008	1.704	0.005	0.002	0.005	2.136	0.232	9.299
10	0.2	0.425	1.667	0.444	8.453	0.073	0.016	3.591	0.002	0.008	1.704	0.003	0.002	0.003	1.064	0.058	2.306
10	0.3	0.425	1.667	0.444	8.453	0.073	0.016	2.932	0.002	0.008	1.704	0.002	0.002	0.002	0.706	0.025	1.017
10	0.4	0.425	1.667	0.444	8.453	0.073	0.016	2.539	0.002	0.008	1.704	0.001	0.002	0.001	0.528	0.014	0.567
10	0.5	0.425	1.667	0.444	8.453	0.073	0.016	2.271	0.002	0.008	1.704	0.001	0.002	0.001	0.420	0.009	0.360
10	0.6	0.425	1.667	0.444	8.453	0.073	0.016	2.073	0.002	0.008	1.704	0.001	0.002	0.001	0.349	0.006	0.248

Q	X	Z	V _{zi}	Z _{core}	V _{zj}	h _{down}	h _{up}	V _{xmax}	q _{up}	q _{down}	V(z)	FQSI	G _b	I _{net}	V _{up}	H _{up}	H _{up/z}
l/s	m	m	m/s	m	m/s	m	m	m/s	m ² /s	m ² /s	m/s	Ns	kg/m ²	Ns	m/s	m	
			Q=VA	Z=5*Bj	Eq. 25	Eq. 61		Eq. 63	Eq. 61&62		Eq. 60	Fig.2.18	Eq. 59	Eq.55		Eq. 58	
10	0.5	0.45	1.667	0.444	8.453	0.073	0.016	1.046	0.002	0.008	1.656	0.000	0.002	0.000	0.082	0.000	0.014
10	0.4	0.45	1.667	0.444	8.453	0.073	0.016	1.169	0.002	0.008	1.656	0.000	0.002	0.000	0.105	0.001	0.023
10	0.3	0.45	1.667	0.444	8.453	0.073	0.016	1.350	0.002	0.008	1.656	0.000	0.002	0.000	0.143	0.001	0.042
10	0.2	0.45	1.667	0.444	8.453	0.073	0.016	1.653	0.002	0.008	1.656	0.001	0.002	0.001	0.219	0.002	0.098
10	0.1	0.45	1.667	0.444	8.453	0.073	0.016	2.338	0.002	0.008	1.656	0.001	0.002	0.001	0.446	0.010	0.406
10	0.85	0.45	1.667	0.444	8.453	0.073	0.016	0.802	0.002	0.008	1.656	0.000	0.002	0.000	0.045	0.000	0.004
10	0.1	0.45	1.667	0.444	8.453	0.073	0.016	4.935	0.002	0.008	1.656	0.005	0.002	0.005	2.017	0.207	8.291
10	0.2	0.45	1.667	0.444	8.453	0.073	0.016	3.489	0.002	0.008	1.656	0.002	0.002	0.002	1.004	0.051	2.055
10	0.3	0.45	1.667	0.444	8.453	0.073	0.016	2.849	0.002	0.008	1.656	0.002	0.002	0.002	0.667	0.023	0.906
10	0.4	0.45	1.667	0.444	8.453	0.073	0.016	2.467	0.002	0.008	1.656	0.001	0.002	0.001	0.498	0.013	0.505
10	0.5	0.45	1.667	0.444	8.453	0.073	0.016	2.207	0.002	0.008	1.656	0.001	0.002	0.001	0.396	0.008	0.321
10	0.6	0.45	1.667	0.444	8.453	0.073	0.016	2.015	0.002	0.008	1.656	0.001	0.002	0.001	0.329	0.006	0.221
10	0.5	0.475	1.667	0.444	8.453	0.073	0.016	1.018	0.002	0.008	1.611	0.000	0.002	0.000	0.078	0.000	0.012
10	0.4	0.475	1.667	0.444	8.453	0.073	0.016	1.138	0.002	0.008	1.611	0.000	0.002	0.000	0.099	0.001	0.020
10	0.3	0.475	1.667	0.444	8.453	0.073	0.016	1.314	0.002	0.008	1.611	0.000	0.002	0.000	0.135	0.001	0.037
10	0.2	0.475	1.667	0.444	8.453	0.073	0.016	1.609	0.002	0.008	1.611	0.001	0.002	0.000	0.207	0.002	0.087
10	0.1	0.475	1.667	0.444	8.453	0.073	0.016	2.276	0.002	0.008	1.611	0.001	0.002	0.001	0.422	0.009	0.363
10	0.85	0.475	1.667	0.444	8.453	0.073	0.016	0.781	0.002	0.008	1.611	0.000	0.002	0.000	0.042	0.000	0.004
10	0.1	0.475	1.667	0.444	8.453	0.073	0.016	4.803	0.002	0.008	1.611	0.005	0.002	0.005	1.910	0.186	7.438
10	0.2	0.475	1.667	0.444	8.453	0.073	0.016	3.396	0.002	0.008	1.611	0.002	0.002	0.002	0.951	0.046	1.843
10	0.3	0.475	1.667	0.444	8.453	0.073	0.016	2.773	0.002	0.008	1.611	0.002	0.002	0.001	0.631	0.020	0.812
10	0.4	0.475	1.667	0.444	8.453	0.073	0.016	2.402	0.002	0.008	1.611	0.001	0.002	0.001	0.471	0.011	0.452
10	0.5	0.475	1.667	0.444	8.453	0.073	0.016	2.148	0.002	0.008	1.611	0.001	0.002	0.001	0.375	0.007	0.287
10	0.6	0.475	1.667	0.444	8.453	0.073	0.016	1.961	0.002	0.008	1.611	0.001	0.002	0.001	0.311	0.005	0.197
10	0.5	0.5	1.667	0.444	8.453	0.073	0.016	0.992	0.002	0.008	1.571	0.000	0.002	0.000	0.073	0.000	0.011
10	0.4	0.5	1.667	0.444	8.453	0.073	0.016	1.109	0.002	0.008	1.571	0.000	0.002	0.000	0.094	0.000	0.018

Q	X	Z	V _{zi}	Z _{core}	V _{zj}	h _{down}	h _{up}	V _{xmax}	q _{up}	q _{down}	V(z)	FQSI	G _b	I _{net}	V _{up}	H _{up}	H _{up} /z
l/s	m	m	m/s	m	m/s	m	m	m/s	m ² /s	m ² /s	m/s	Ns	kg/m ²	Ns	m/s	m	
			Q=VA	Z=5*Bj	Eq. 25	Eq. 61		Eq. 63	Eq. 61&62		Eq. 60	Fig.2.18	Eq. 59	Eq.55		Eq. 58	
10	0.3	0.5	1.667	0.444	8.453	0.073	0.016	1.281	0.002	0.008	1.571	0.000	0.002	0.000	0.128	0.001	0.033
10	0.2	0.5	1.667	0.444	8.453	0.073	0.016	1.569	0.002	0.008	1.571	0.000	0.002	0.000	0.196	0.002	0.078
10	0.1	0.5	1.667	0.444	8.453	0.073	0.016	2.218	0.002	0.008	1.571	0.001	0.002	0.001	0.401	0.008	0.327
10	0.85	0.5	1.667	0.444	8.453	0.073	0.016	0.761	0.002	0.008	1.571	0.000	0.002	0.000	0.040	0.000	0.003
10	0.1	0.5	1.667	0.444	8.453	0.073	0.016	4.682	0.002	0.008	1.571	0.004	0.002	0.004	1.814	0.168	6.709
10	0.2	0.5	1.667	0.444	8.453	0.073	0.016	3.310	0.002	0.008	1.571	0.002	0.002	0.002	0.903	0.042	1.662
10	0.3	0.5	1.667	0.444	8.453	0.073	0.016	2.703	0.002	0.008	1.571	0.001	0.002	0.001	0.599	0.018	0.732
10	0.4	0.5	1.667	0.444	8.453	0.073	0.016	2.341	0.002	0.008	1.571	0.001	0.002	0.001	0.447	0.010	0.408
10	0.5	0.5	1.667	0.444	8.453	0.073	0.016	2.094	0.002	0.008	1.571	0.001	0.002	0.001	0.356	0.006	0.258
10	0.6	0.5	1.667	0.444	8.453	0.073	0.016	1.911	0.002	0.008	1.571	0.001	0.002	0.001	0.295	0.004	0.178
10	0.5	0.525	1.667	0.444	8.453	0.073	0.016	0.968	0.002	0.008	1.533	0.000	0.002	0.000	0.069	0.000	0.010
10	0.4	0.525	1.667	0.444	8.453	0.073	0.016	1.082	0.002	0.008	1.533	0.000	0.002	0.000	0.089	0.000	0.016
10	0.3	0.525	1.667	0.444	8.453	0.073	0.016	1.250	0.002	0.008	1.533	0.000	0.002	0.000	0.121	0.001	0.030
10	0.2	0.525	1.667	0.444	8.453	0.073	0.016	1.531	0.002	0.008	1.533	0.000	0.002	0.000	0.186	0.002	0.071
10	0.1	0.525	1.667	0.444	8.453	0.073	0.016	2.165	0.002	0.008	1.533	0.001	0.002	0.001	0.381	0.007	0.296
10	0.85	0.525	1.667	0.444	8.453	0.073	0.016	0.743	0.002	0.008	1.533	0.000	0.002	0.000	0.037	0.000	0.003
10	0.1	0.525	1.667	0.444	8.453	0.073	0.016	4.569	0.002	0.008	1.533	0.004	0.002	0.004	1.727	0.152	6.083
10	0.2	0.525	1.667	0.444	8.453	0.073	0.016	3.231	0.002	0.008	1.533	0.002	0.002	0.002	0.859	0.038	1.506
10	0.3	0.525	1.667	0.444	8.453	0.073	0.016	2.638	0.002	0.008	1.533	0.001	0.002	0.001	0.570	0.017	0.663
10	0.4	0.525	1.667	0.444	8.453	0.073	0.016	2.284	0.002	0.008	1.533	0.001	0.002	0.001	0.425	0.009	0.369
10	0.5	0.525	1.667	0.444	8.453	0.073	0.016	2.043	0.002	0.008	1.533	0.001	0.002	0.001	0.339	0.006	0.234
10	0.6	0.525	1.667	0.444	8.453	0.073	0.016	1.865	0.002	0.008	1.533	0.001	0.002	0.001	0.281	0.004	0.161
10	0.5	0.55	1.667	0.444	8.453	0.073	0.016	0.946	0.002	0.008	1.498	0.000	0.002	0.000	0.066	0.000	0.009
10	0.4	0.55	1.667	0.444	8.453	0.073	0.016	1.057	0.002	0.008	1.498	0.000	0.002	0.000	0.084	0.000	0.015
10	0.3	0.55	1.667	0.444	8.453	0.073	0.016	1.221	0.002	0.008	1.498	0.000	0.002	0.000	0.115	0.001	0.027
10	0.2	0.55	1.667	0.444	8.453	0.073	0.016	1.496	0.002	0.008	1.498	0.000	0.002	0.000	0.177	0.002	0.064

Q	X	Z	V _{zi}	Z _{core}	V _{zj}	h _{down}	h _{up}	V _{xmax}	q _{up}	q _{down}	V(z)	FQSI	G _b	I _{net}	V _{up}	H _{up}	H _{up} /z
l/s	m	m	m/s	m	m/s	m	m	m/s	m ² /s	m ² /s	m/s	Ns	kg/m ²	Ns	m/s	m	
			Q=VA	Z=5*Bj	Eq. 25	Eq. 61		Eq. 63	Eq. 61&62		Eq. 60	Fig.2.18	Eq. 59	Eq.55		Eq. 58	
10	0.1	0.55	1.667	0.444	8.453	0.073	0.016	2.115	0.002	0.008	1.498	0.001	0.002	0.001	0.363	0.007	0.269
10	0.85	0.55	1.667	0.444	8.453	0.073	0.016	0.725	0.002	0.008	1.498	0.000	0.002	0.000	0.035	0.000	0.003
10	0.1	0.55	1.667	0.444	8.453	0.073	0.016	4.464	0.002	0.008	1.498	0.004	0.002	0.004	1.648	0.138	5.540
10	0.2	0.55	1.667	0.444	8.453	0.073	0.016	3.156	0.002	0.008	1.498	0.002	0.002	0.002	0.820	0.034	1.371
10	0.3	0.55	1.667	0.444	8.453	0.073	0.016	2.577	0.002	0.008	1.498	0.001	0.002	0.001	0.544	0.015	0.603
10	0.4	0.55	1.667	0.444	8.453	0.073	0.016	2.232	0.002	0.008	1.498	0.001	0.002	0.001	0.406	0.008	0.336
10	0.5	0.55	1.667	0.444	8.453	0.073	0.016	1.996	0.002	0.008	1.498	0.001	0.002	0.001	0.323	0.005	0.213
10	0.6	0.55	1.667	0.444	8.453	0.073	0.016	1.822	0.002	0.008	1.498	0.001	0.002	0.001	0.268	0.004	0.146
10	0.5	0.575	1.667	0.444	8.453	0.073	0.016	0.925	0.002	0.008	1.465	0.000	0.002	0.000	0.063	0.000	0.008
10	0.4	0.575	1.667	0.444	8.453	0.073	0.016	1.034	0.002	0.008	1.465	0.000	0.002	0.000	0.080	0.000	0.013
10	0.3	0.575	1.667	0.444	8.453	0.073	0.016	1.194	0.002	0.008	1.465	0.000	0.002	0.000	0.110	0.001	0.025
10	0.2	0.575	1.667	0.444	8.453	0.073	0.016	1.463	0.002	0.008	1.465	0.000	0.002	0.000	0.169	0.001	0.058
10	0.1	0.575	1.667	0.444	8.453	0.073	0.016	2.068	0.002	0.008	1.465	0.001	0.002	0.001	0.347	0.006	0.246
10	0.85	0.575	1.667	0.444	8.453	0.073	0.016	0.709	0.002	0.008	1.465	0.000	0.002	0.000	0.033	0.000	0.002
10	0.1	0.575	1.667	0.444	8.453	0.073	0.016	4.366	0.002	0.008	1.465	0.004	0.002	0.004	1.576	0.127	5.066
10	0.2	0.575	1.667	0.444	8.453	0.073	0.016	3.087	0.002	0.008	1.465	0.002	0.002	0.002	0.784	0.031	1.253
10	0.3	0.575	1.667	0.444	8.453	0.073	0.016	2.520	0.002	0.008	1.465	0.001	0.002	0.001	0.520	0.014	0.551
10	0.4	0.575	1.667	0.444	8.453	0.073	0.016	2.183	0.002	0.008	1.465	0.001	0.002	0.001	0.388	0.008	0.306
10	0.5	0.575	1.667	0.444	8.453	0.073	0.016	1.952	0.002	0.008	1.465	0.001	0.002	0.001	0.308	0.005	0.194
10	0.6	0.575	1.667	0.444	8.453	0.073	0.016	1.782	0.002	0.008	1.465	0.001	0.002	0.001	0.256	0.003	0.133

Table D 0.8. Quasi-steady method of Q=20 l/s, H=2 m and TW=0.25

Q	X	Z	V _{zi}	Z _{core}	V _{zj}	h _{down}	h _{up}	V _{xmax}	q _{up}	q _{down}	V(z)	FQSI	G _b	I _{net}	V _{up}	H _{up}	H _{up} /z
l/s	m	m	m/s	m	m/s	m	m	m/s	m ² /s	m ² /s	m/s	Ns	kg/m ²	Ns	m/s	m	
			Q=VA	Z=5*Bj	Eq. 25	Eq. 61		Eq. 63	Eq. 61&62		Eq. 60	Fig.2.18	Eq. 59	Eq.55		Eq. 58	
20	0.7	0	2	0.588	5.782	0.052	0.065	3.279	0.011	0.009	5.782						
20	0.7	0.042	2	0.588	5.782	0.052	0.065	3.279	0.011	0.009	7.514						
20	0.7	0.083	2	0.588	5.782	0.052	0.065	3.279	0.011	0.009	5.313						
20	0.7	0.125	2	0.588	5.782	0.052	0.065	3.279	0.011	0.009	4.338						
20	0.7	0.167	2	0.588	5.782	0.052	0.065	3.279	0.011	0.009	3.757						
20	0.7	0.208	2	0.588	5.782	0.052	0.065	3.279	0.011	0.009	3.360						
20	0.7	0.25	2	0.588	5.782	0.052	0.065	3.279	0.011	0.009	3.068						
20	0.5	0.25	2	0.588	5.782	0.052	0.065	3.880	0.011	0.009	3.068	0.003	0.002	0.003	1.244	0.079	3.153
20	0.4	0.25	2	0.588	5.782	0.052	0.065	4.338	0.011	0.009	3.068	0.004	0.002	0.004	1.557	0.123	4.940
20	0.3	0.25	2	0.588	5.782	0.052	0.065	5.009	0.011	0.009	3.068	0.005	0.002	0.005	2.078	0.220	8.806
20	0.2	0.25	2	0.588	5.782	0.052	0.065	6.135	0.011	0.009	3.068	0.007	0.002	0.007	3.122	0.497	19.867
20	0.1	0.25	2	0.588	5.782	0.052	0.065	8.677	0.011	0.009	3.068	0.015	0.002	0.015	6.252	1.992	79.686
20	0.7	0.25	2	0.588	5.782	0.052	0.065	3.279	0.011	0.009	3.068	0.002	0.002	0.002	0.886	0.040	1.600
20	0.1	0.25	2	0.588	5.782	0.052	0.065	7.766	0.011	0.009	3.068	0.012	0.002	0.012	5.007	1.278	51.114
20	0.2	0.25	2	0.588	5.782	0.052	0.065	5.492	0.011	0.009	3.068	0.006	0.002	0.006	2.499	0.318	12.735
20	0.3	0.25	2	0.588	5.782	0.052	0.065	4.484	0.011	0.009	3.068	0.004	0.002	0.004	1.663	0.141	5.641
20	0.4	0.25	2	0.588	5.782	0.052	0.065	3.883	0.011	0.009	3.068	0.003	0.002	0.003	1.245	0.079	3.162
20	0.5	0.25	2	0.588	5.782	0.052	0.065	3.473	0.011	0.009	3.068	0.002	0.002	0.002	0.995	0.050	2.017
20	0.6	0.25	2	0.588	5.782	0.052	0.065	3.171	0.011	0.009	3.068	0.002	0.002	0.002	0.827	0.035	1.396
20	0.5	0.28	2	0.588	5.782	0.052	0.065	3.700	0.011	0.009	2.925	0.003	0.002	0.003	1.130	0.065	2.602
20	0.4	0.28	2	0.588	5.782	0.052	0.065	4.136	0.011	0.009	2.925	0.003	0.002	0.003	1.414	0.102	4.078
20	0.3	0.28	2	0.588	5.782	0.052	0.065	4.776	0.011	0.009	2.925	0.005	0.002	0.004	1.889	0.182	7.271
20	0.2	0.28	2	0.588	5.782	0.052	0.065	5.850	0.011	0.009	2.925	0.007	0.002	0.007	2.837	0.410	16.410
20	0.1	0.28	2	0.588	5.782	0.052	0.065	8.273	0.011	0.009	2.925	0.014	0.002	0.013	5.683	1.646	65.838

Q	X	Z	V _{zi}	Z _{core}	V _{zj}	h _{down}	h _{up}	V _{xmax}	q _{up}	q _{down}	V(z)	FQSI	G _b	I _{net}	V _{up}	H _{up}	H _{up} /z
l/s	m	m	m/s	m	m/s	m	m	m/s	m ² /s	m ² /s	m/s	Ns	kg/m ²	Ns	m/s	m	
			Q=VA	Z=5*Bj	Eq. 25	Eq. 61		Eq. 63	Eq. 61&62		Eq. 60	Fig.2.18	Eq. 59	Eq.55		Eq. 58	
20	0.7	0.28	2	0.588	5.782	0.052	0.065	3.127	0.011	0.009	2.925	0.002	0.002	0.002	0.805	0.033	1.320
20	0.1	0.28	2	0.588	5.782	0.052	0.065	7.405	0.011	0.009	2.925	0.011	0.002	0.011	4.551	1.056	42.228
20	0.2	0.28	2	0.588	5.782	0.052	0.065	5.236	0.011	0.009	2.925	0.005	0.002	0.005	2.271	0.263	10.518
20	0.3	0.28	2	0.588	5.782	0.052	0.065	4.275	0.011	0.009	2.925	0.004	0.002	0.004	1.511	0.116	4.657
20	0.4	0.28	2	0.588	5.782	0.052	0.065	3.702	0.011	0.009	2.925	0.003	0.002	0.003	1.131	0.065	2.610
20	0.5	0.28	2	0.588	5.782	0.052	0.065	3.312	0.011	0.009	2.925	0.002	0.002	0.002	0.903	0.042	1.664
20	0.6	0.28	2	0.588	5.782	0.052	0.065	3.023	0.011	0.009	2.925	0.002	0.002	0.002	0.751	0.029	1.151
20	0.5	0.3	2	0.588	5.782	0.052	0.065	3.542	0.011	0.009	2.800	0.002	0.002	0.002	1.035	0.055	2.183
20	0.4	0.3	2	0.588	5.782	0.052	0.065	3.960	0.011	0.009	2.800	0.003	0.002	0.003	1.296	0.086	3.423
20	0.3	0.3	2	0.588	5.782	0.052	0.065	4.573	0.011	0.009	2.800	0.004	0.002	0.004	1.730	0.153	6.105
20	0.2	0.3	2	0.588	5.782	0.052	0.065	5.601	0.011	0.009	2.800	0.006	0.002	0.006	2.600	0.345	13.781
20	0.1	0.3	2	0.588	5.782	0.052	0.065	7.921	0.011	0.009	2.800	0.012	0.002	0.012	5.208	1.383	55.307
20	0.7	0.3	2	0.588	5.782	0.052	0.065	2.994	0.011	0.009	2.800	0.002	0.002	0.002	0.737	0.028	1.107
20	0.1	0.3	2	0.588	5.782	0.052	0.065	7.090	0.011	0.009	2.800	0.010	0.002	0.010	4.171	0.887	35.472
20	0.2	0.3	2	0.588	5.782	0.052	0.065	5.013	0.011	0.009	2.800	0.005	0.002	0.005	2.081	0.221	8.832
20	0.3	0.3	2	0.588	5.782	0.052	0.065	4.093	0.011	0.009	2.800	0.003	0.002	0.003	1.385	0.098	3.909
20	0.4	0.3	2	0.588	5.782	0.052	0.065	3.545	0.011	0.009	2.800	0.002	0.002	0.002	1.036	0.055	2.190
20	0.5	0.3	2	0.588	5.782	0.052	0.065	3.171	0.011	0.009	2.800	0.002	0.002	0.002	0.827	0.035	1.396
20	0.6	0.3	2	0.588	5.782	0.052	0.065	2.894	0.011	0.009	2.800	0.002	0.002	0.002	0.688	0.024	0.965
20	0.5	0.33	2	0.588	5.782	0.052	0.065	3.403	0.011	0.009	2.690	0.002	0.002	0.002	0.955	0.046	1.858
20	0.4	0.33	2	0.588	5.782	0.052	0.065	3.805	0.011	0.009	2.690	0.003	0.002	0.003	1.195	0.073	2.913
20	0.3	0.33	2	0.588	5.782	0.052	0.065	4.394	0.011	0.009	2.690	0.004	0.002	0.004	1.597	0.130	5.198
20	0.2	0.33	2	0.588	5.782	0.052	0.065	5.381	0.011	0.009	2.690	0.006	0.002	0.006	2.399	0.293	11.736
20	0.1	0.33	2	0.588	5.782	0.052	0.065	7.610	0.011	0.009	2.690	0.011	0.002	0.011	4.807	1.178	47.113
20	0.7	0.33	2	0.588	5.782	0.052	0.065	2.876	0.011	0.009	2.690	0.002	0.002	0.002	0.679	0.024	0.941
20	0.1	0.33	2	0.588	5.782	0.052	0.065	6.811	0.011	0.009	2.690	0.009	0.002	0.009	3.850	0.755	30.214

Q	X	Z	V _{zi}	Z _{core}	V _{zj}	h _{down}	h _{up}	V _{xmax}	q _{up}	q _{down}	V(z)	FQSI	G _b	I _{net}	V _{up}	H _{up}	H _{up} /z
l/s	m	m	m/s	m	m/s	m	m	m/s	m ² /s	m ² /s	m/s	Ns	kg/m ²	Ns	m/s	m	
			Q=VA	Z=5*Bj	Eq. 25	Eq. 61		Eq. 63	Eq. 61&62		Eq. 60	Fig.2.18	Eq. 59	Eq.55		Eq. 58	
20	0.2	0.33	2	0.588	5.782	0.052	0.065	4.816	0.011	0.009	2.690	0.005	0.002	0.005	1.921	0.188	7.520
20	0.3	0.33	2	0.588	5.782	0.052	0.065	3.933	0.011	0.009	2.690	0.003	0.002	0.003	1.278	0.083	3.327
20	0.4	0.33	2	0.588	5.782	0.052	0.065	3.406	0.011	0.009	2.690	0.002	0.002	0.002	0.956	0.047	1.863
20	0.5	0.33	2	0.588	5.782	0.052	0.065	3.046	0.011	0.009	2.690	0.002	0.002	0.002	0.763	0.030	1.187
20	0.6	0.33	2	0.588	5.782	0.052	0.065	2.781	0.011	0.009	2.690	0.002	0.002	0.002	0.635	0.021	0.821
20	0.5	0.35	2	0.588	5.782	0.052	0.065	3.279	0.011	0.009	2.593	0.002	0.002	0.002	0.886	0.040	1.600
20	0.4	0.35	2	0.588	5.782	0.052	0.065	3.667	0.011	0.009	2.593	0.003	0.002	0.003	1.109	0.063	2.509
20	0.3	0.35	2	0.588	5.782	0.052	0.065	4.234	0.011	0.009	2.593	0.004	0.002	0.004	1.482	0.112	4.478
20	0.2	0.35	2	0.588	5.782	0.052	0.065	5.185	0.011	0.009	2.593	0.005	0.002	0.005	2.227	0.253	10.114
20	0.1	0.35	2	0.588	5.782	0.052	0.065	7.333	0.011	0.009	2.593	0.011	0.002	0.011	4.463	1.015	40.612
20	0.7	0.35	2	0.588	5.782	0.052	0.065	2.772	0.011	0.009	2.593	0.002	0.002	0.001	0.630	0.020	0.810
20	0.1	0.35	2	0.588	5.782	0.052	0.065	6.564	0.011	0.009	2.593	0.009	0.002	0.008	3.574	0.651	26.043
20	0.2	0.35	2	0.588	5.782	0.052	0.065	4.641	0.011	0.009	2.593	0.004	0.002	0.004	1.783	0.162	6.480
20	0.3	0.35	2	0.588	5.782	0.052	0.065	3.790	0.011	0.009	2.593	0.003	0.002	0.003	1.186	0.072	2.866
20	0.4	0.35	2	0.588	5.782	0.052	0.065	3.282	0.011	0.009	2.593	0.002	0.002	0.002	0.887	0.040	1.604
20	0.5	0.35	2	0.588	5.782	0.052	0.065	2.935	0.011	0.009	2.593	0.002	0.002	0.002	0.708	0.026	1.022
20	0.6	0.35	2	0.588	5.782	0.052	0.065	2.680	0.011	0.009	2.593	0.001	0.002	0.001	0.589	0.018	0.706
20	0.5	0.38	2	0.588	5.782	0.052	0.065	3.168	0.011	0.009	2.505	0.002	0.002	0.002	0.826	0.035	1.392
20	0.4	0.38	2	0.588	5.782	0.052	0.065	3.542	0.011	0.009	2.505	0.002	0.002	0.002	1.035	0.055	2.183
20	0.3	0.38	2	0.588	5.782	0.052	0.065	4.090	0.011	0.009	2.505	0.003	0.002	0.003	1.383	0.097	3.898
20	0.2	0.38	2	0.588	5.782	0.052	0.065	5.009	0.011	0.009	2.505	0.005	0.002	0.005	2.078	0.220	8.806
20	0.1	0.38	2	0.588	5.782	0.052	0.065	7.084	0.011	0.009	2.505	0.010	0.002	0.010	4.165	0.884	35.367
20	0.7	0.38	2	0.588	5.782	0.052	0.065	2.678	0.011	0.009	2.505	0.001	0.002	0.001	0.588	0.018	0.704
20	0.1	0.38	2	0.588	5.782	0.052	0.065	6.341	0.011	0.009	2.505	0.008	0.002	0.008	3.335	0.567	22.679
20	0.2	0.38	2	0.588	5.782	0.052	0.065	4.484	0.011	0.009	2.505	0.004	0.002	0.004	1.663	0.141	5.641
20	0.3	0.38	2	0.588	5.782	0.052	0.065	3.661	0.011	0.009	2.505	0.003	0.002	0.003	1.106	0.062	2.494

Q	X	Z	V _{zi}	Z _{core}	V _{zj}	h _{down}	h _{up}	V _{xmax}	q _{up}	q _{down}	V(z)	FQSI	G _b	I _{net}	V _{up}	H _{up}	H _{up} /z
l/s	m	m	m/s	m	m/s	m	m	m/s	m ² /s	m ² /s	m/s	Ns	kg/m ²	Ns	m/s	m	
			Q=VA	Z=5*Bj	Eq. 25	Eq. 61		Eq. 63	Eq. 61&62		Eq. 60	Fig.2.18	Eq. 59	Eq.55		Eq. 59	
20	0.4	0.38	2	0.588	5.782	0.052	0.065	3.171	0.011	0.009	2.505	0.002	0.002	0.002	0.827	0.035	1.396
20	0.5	0.38	2	0.588	5.782	0.052	0.065	2.836	0.011	0.009	2.505	0.002	0.002	0.002	0.660	0.022	0.889
20	0.6	0.38	2	0.588	5.782	0.052	0.065	2.589	0.011	0.009	2.505	0.001	0.002	0.001	0.549	0.015	0.614
20	0.5	0.4	2	0.588	5.782	0.052	0.065	3.068	0.011	0.009	2.425	0.002	0.002	0.002	0.774	0.031	1.221
20	0.4	0.4	2	0.588	5.782	0.052	0.065	3.430	0.011	0.009	2.425	0.002	0.002	0.002	0.970	0.048	1.917
20	0.3	0.4	2	0.588	5.782	0.052	0.065	3.960	0.011	0.009	2.425	0.003	0.002	0.003	1.296	0.086	3.423
20	0.2	0.4	2	0.588	5.782	0.052	0.065	4.850	0.011	0.009	2.425	0.005	0.002	0.005	1.948	0.193	7.735
20	0.1	0.4	2	0.588	5.782	0.052	0.065	6.859	0.011	0.009	2.425	0.009	0.002	0.009	3.904	0.777	31.076
20	0.7	0.4	2	0.588	5.782	0.052	0.065	2.593	0.011	0.009	2.425	0.001	0.002	0.001	0.550	0.015	0.618
20	0.1	0.4	2	0.588	5.782	0.052	0.065	6.140	0.011	0.009	2.425	0.007	0.002	0.007	3.126	0.498	19.926
20	0.2	0.4	2	0.588	5.782	0.052	0.065	4.341	0.011	0.009	2.425	0.004	0.002	0.004	1.559	0.124	4.954
20	0.3	0.4	2	0.588	5.782	0.052	0.065	3.545	0.011	0.009	2.425	0.002	0.002	0.002	1.036	0.055	2.190
20	0.4	0.4	2	0.588	5.782	0.052	0.065	3.070	0.011	0.009	2.425	0.002	0.002	0.002	0.775	0.031	1.225
20	0.5	0.4	2	0.588	5.782	0.052	0.065	2.746	0.011	0.009	2.425	0.001	0.002	0.001	0.618	0.019	0.780
20	0.6	0.4	2	0.588	5.782	0.052	0.065	2.507	0.011	0.009	2.425	0.001	0.002	0.001	0.514	0.013	0.538
20	0.5	0.43	2	0.588	5.782	0.052	0.065	2.976	0.011	0.009	2.353	0.002	0.002	0.002	0.728	0.027	1.080
20	0.4	0.43	2	0.588	5.782	0.052	0.065	3.327	0.011	0.009	2.353	0.002	0.002	0.002	0.912	0.042	1.696
20	0.3	0.43	2	0.588	5.782	0.052	0.065	3.842	0.011	0.009	2.353	0.003	0.002	0.003	1.219	0.076	3.029
20	0.2	0.43	2	0.588	5.782	0.052	0.065	4.706	0.011	0.009	2.353	0.004	0.002	0.004	1.833	0.171	6.848
20	0.1	0.43	2	0.588	5.782	0.052	0.065	6.655	0.011	0.009	2.353	0.009	0.002	0.009	3.674	0.688	27.520
20	0.7	0.43	2	0.588	5.782	0.052	0.065	2.515	0.011	0.009	2.353	0.001	0.002	0.001	0.518	0.014	0.546
20	0.1	0.43	2	0.588	5.782	0.052	0.065	5.956	0.011	0.009	2.353	0.007	0.002	0.007	2.942	0.441	17.644
20	0.2	0.43	2	0.588	5.782	0.052	0.065	4.212	0.011	0.009	2.353	0.004	0.002	0.003	1.467	0.110	4.386
20	0.3	0.43	2	0.588	5.782	0.052	0.065	3.439	0.011	0.009	2.353	0.002	0.002	0.002	0.975	0.048	1.938
20	0.4	0.43	2	0.588	5.782	0.052	0.065	2.978	0.011	0.009	2.353	0.002	0.002	0.002	0.729	0.027	1.084
20	0.5	0.43	2	0.588	5.782	0.052	0.065	2.664	0.011	0.009	2.353	0.001	0.002	0.001	0.582	0.017	0.689

Q	X	Z	V _{zi}	Z _{core}	V _{zj}	h _{down}	h _{up}	V _{xmax}	q _{up}	q _{down}	V(z)	FQSI	G _b	I _{net}	V _{up}	H _{up}	H _{up} /z
l/s	m	m	m/s	m	m/s	m	m	m/s	m ² /s	m ² /s	m/s	Ns	kg/m ²	Ns	m/s	m	
			Q=VA	Z=5*Bj	Eq. 25	Eq. 61		Eq. 63	Eq. 61&62		Eq. 60	Fig.2.18	Eq. 59	Eq.55		Eq. 58	
20	0.6	0.43	2	0.588	5.782	0.052	0.065	2.432	0.011	0.009	2.353	0.001	0.002	0.001	0.483	0.012	0.476
20	0.5	0.45	2	0.588	5.782	0.052	0.065	2.892	0.011	0.009	2.286	0.002	0.002	0.002	0.687	0.024	0.962
20	0.4	0.45	2	0.588	5.782	0.052	0.065	3.234	0.011	0.009	2.286	0.002	0.002	0.002	0.861	0.038	1.511
20	0.3	0.45	2	0.588	5.782	0.052	0.065	3.734	0.011	0.009	2.286	0.003	0.002	0.003	1.151	0.067	2.700
20	0.2	0.45	2	0.588	5.782	0.052	0.065	4.573	0.011	0.009	2.286	0.004	0.002	0.004	1.730	0.153	6.105
20	0.1	0.45	2	0.588	5.782	0.052	0.065	6.467	0.011	0.009	2.286	0.008	0.002	0.008	3.469	0.614	24.541
20	0.7	0.45	2	0.588	5.782	0.052	0.065	2.444	0.011	0.009	2.286	0.001	0.002	0.001	0.488	0.012	0.486
20	0.1	0.45	2	0.588	5.782	0.052	0.065	5.789	0.011	0.009	2.286	0.007	0.002	0.007	2.778	0.393	15.733
20	0.2	0.45	2	0.588	5.782	0.052	0.065	4.093	0.011	0.009	2.286	0.003	0.002	0.003	1.385	0.098	3.909
20	0.3	0.45	2	0.588	5.782	0.052	0.065	3.342	0.011	0.009	2.286	0.002	0.002	0.002	0.920	0.043	1.727
20	0.4	0.45	2	0.588	5.782	0.052	0.065	2.894	0.011	0.009	2.286	0.002	0.002	0.002	0.688	0.024	0.965
20	0.5	0.45	2	0.588	5.782	0.052	0.065	2.589	0.011	0.009	2.286	0.001	0.002	0.001	0.549	0.015	0.614
20	0.6	0.45	2	0.588	5.782	0.052	0.065	2.363	0.011	0.009	2.286	0.001	0.002	0.001	0.456	0.011	0.424
20	0.5	0.48	2	0.588	5.782	0.052	0.065	2.815	0.011	0.009	2.225	0.002	0.002	0.002	0.650	0.022	0.863
20	0.4	0.48	2	0.588	5.782	0.052	0.065	3.147	0.011	0.009	2.225	0.002	0.002	0.002	0.815	0.034	1.355
20	0.3	0.48	2	0.588	5.782	0.052	0.065	3.634	0.011	0.009	2.225	0.003	0.002	0.003	1.090	0.061	2.421
20	0.2	0.48	2	0.588	5.782	0.052	0.065	4.451	0.011	0.009	2.225	0.004	0.002	0.004	1.639	0.137	5.476
20	0.1	0.48	2	0.588	5.782	0.052	0.065	6.295	0.011	0.009	2.225	0.008	0.002	0.008	3.286	0.550	22.019
20	0.7	0.48	2	0.588	5.782	0.052	0.065	2.379	0.011	0.009	2.225	0.001	0.002	0.001	0.462	0.011	0.435
20	0.1	0.48	2	0.588	5.782	0.052	0.065	5.634	0.011	0.009	2.225	0.006	0.002	0.006	2.631	0.353	14.116
20	0.2	0.48	2	0.588	5.782	0.052	0.065	3.984	0.011	0.009	2.225	0.003	0.002	0.003	1.311	0.088	3.506
20	0.3	0.48	2	0.588	5.782	0.052	0.065	3.253	0.011	0.009	2.225	0.002	0.002	0.002	0.871	0.039	1.548
20	0.4	0.48	2	0.588	5.782	0.052	0.065	2.817	0.011	0.009	2.225	0.002	0.002	0.002	0.651	0.022	0.865
20	0.5	0.48	2	0.588	5.782	0.052	0.065	2.520	0.011	0.009	2.225	0.001	0.002	0.001	0.519	0.014	0.550
20	0.6	0.48	2	0.588	5.782	0.052	0.065	2.300	0.011	0.009	2.225	0.001	0.002	0.001	0.431	0.009	0.379
20	0.5	0.5	2	0.588	5.782	0.052	0.065	2.744	0.011	0.009	2.169	0.001	0.002	0.001	0.618	0.019	0.777

Q	X	Z	V _{zi}	Z _{core}	V _{zj}	h _{down}	h _{up}	V _{xmax}	q _{up}	q _{down}	V(z)	FQSI	G _b	I _{net}	V _{up}	H _{up}	H _{up} /z
l/s	m	m	m/s	m	m/s	m	m	m/s	m ² /s	m ² /s	m/s	Ns	kg/m ²	Ns	m/s	m	
			Q=VA	Z=5*Bj	Eq. 25	Eq. 61		Eq. 63	Eq. 61&62		Eq. 60	Fig.2.18	Eq. 59	Eq.55		Eq. 58	
20	0.4	0.5	2	0.588	5.782	0.052	0.065	3.068	0.011	0.009	2.169	0.002	0.002	0.002	0.774	0.031	1.221
20	0.3	0.5	2	0.588	5.782	0.052	0.065	3.542	0.011	0.009	2.169	0.002	0.002	0.002	1.035	0.055	2.183
20	0.2	0.5	2	0.588	5.782	0.052	0.065	4.338	0.011	0.009	2.169	0.004	0.002	0.004	1.557	0.123	4.940
20	0.1	0.5	2	0.588	5.782	0.052	0.065	6.135	0.011	0.009	2.169	0.007	0.002	0.007	3.122	0.497	19.867
20	0.7	0.5	2	0.588	5.782	0.052	0.065	2.319	0.011	0.009	2.169	0.001	0.002	0.001	0.439	0.010	0.392
20	0.1	0.5	2	0.588	5.782	0.052	0.065	5.492	0.011	0.009	2.169	0.006	0.002	0.006	2.499	0.318	12.735
20	0.2	0.5	2	0.588	5.782	0.052	0.065	3.883	0.011	0.009	2.169	0.003	0.002	0.003	1.245	0.079	3.162
20	0.3	0.5	2	0.588	5.782	0.052	0.065	3.171	0.011	0.009	2.169	0.002	0.002	0.002	0.827	0.035	1.396
20	0.4	0.5	2	0.588	5.782	0.052	0.065	2.746	0.011	0.009	2.169	0.001	0.002	0.001	0.618	0.019	0.780
20	0.5	0.5	2	0.588	5.782	0.052	0.065	2.456	0.011	0.009	2.169	0.001	0.002	0.001	0.493	0.012	0.496
20	0.6	0.5	2	0.588	5.782	0.052	0.065	2.242	0.011	0.009	2.169	0.001	0.002	0.001	0.409	0.009	0.342
20	0.5	0.53	2	0.588	5.782	0.052	0.065	2.678	0.011	0.009	2.117	0.001	0.002	0.001	0.588	0.018	0.704
20	0.4	0.53	2	0.588	5.782	0.052	0.065	2.994	0.011	0.009	2.117	0.002	0.002	0.002	0.737	0.028	1.107
20	0.3	0.53	2	0.588	5.782	0.052	0.065	3.457	0.011	0.009	2.117	0.002	0.002	0.002	0.985	0.049	1.979
20	0.2	0.53	2	0.588	5.782	0.052	0.065	4.234	0.011	0.009	2.117	0.004	0.002	0.004	1.482	0.112	4.478
20	0.1	0.53	2	0.588	5.782	0.052	0.065	5.987	0.011	0.009	2.117	0.007	0.002	0.007	2.973	0.450	18.015
20	0.7	0.53	2	0.588	5.782	0.052	0.065	2.263	0.011	0.009	2.117	0.001	0.002	0.001	0.417	0.009	0.355
20	0.1	0.53	2	0.588	5.782	0.052	0.065	5.359	0.011	0.009	2.117	0.006	0.002	0.006	2.380	0.289	11.547
20	0.2	0.53	2	0.588	5.782	0.052	0.065	3.790	0.011	0.009	2.117	0.003	0.002	0.003	1.186	0.072	2.866
20	0.3	0.53	2	0.588	5.782	0.052	0.065	3.094	0.011	0.009	2.117	0.002	0.002	0.002	0.788	0.032	1.265
20	0.4	0.53	2	0.588	5.782	0.052	0.065	2.680	0.011	0.009	2.117	0.001	0.002	0.001	0.589	0.018	0.706
20	0.5	0.53	2	0.588	5.782	0.052	0.065	2.397	0.011	0.009	2.117	0.001	0.002	0.001	0.469	0.011	0.449
20	0.6	0.53	2	0.588	5.782	0.052	0.065	2.188	0.011	0.009	2.117	0.001	0.002	0.001	0.390	0.008	0.309
20	0.5	0.55	2	0.588	5.782	0.052	0.065	2.616	0.011	0.009	2.068	0.001	0.002	0.001	0.561	0.016	0.641
20	0.4	0.55	2	0.588	5.782	0.052	0.065	2.925	0.011	0.009	2.068	0.002	0.002	0.002	0.703	0.025	1.007
20	0.3	0.55	2	0.588	5.782	0.052	0.065	3.377	0.011	0.009	2.068	0.002	0.002	0.002	0.940	0.045	1.801

Q	X	Z	V _{zi}	Z _{core}	V _{zj}	h _{down}	h _{up}	V _{xmax}	q _{up}	q _{down}	V(z)	FQSI	G _b	I _{net}	V _{up}	H _{up}	H _{up} /z
l/s	m	m	m/s	m	m/s	m	m	m/s	m ² /s	m ² /s	m/s	Ns	kg/m ²	Ns	m/s	m	
			Q=VA	Z=5*Bj	Eq. 25	Eq. 61		Eq. 63	Eq. 61&62		Eq. 60	Fig.2.18	Eq. 59	Eq.55		Eq. 58	
20	0.2	0.55	2	0.588	5.782	0.052	0.065	4.136	0.011	0.009	2.068	0.003	0.002	0.003	1.414	0.102	4.078
20	0.1	0.55	2	0.588	5.782	0.052	0.065	5.850	0.011	0.009	2.068	0.007	0.002	0.007	2.837	0.410	16.410
20	0.7	0.55	2	0.588	5.782	0.052	0.065	2.211	0.011	0.009	2.068	0.001	0.002	0.001	0.398	0.008	0.323
20	0.1	0.55	2	0.588	5.782	0.052	0.065	5.236	0.011	0.009	2.068	0.005	0.002	0.005	2.271	0.263	10.518
20	0.2	0.55	2	0.588	5.782	0.052	0.065	3.702	0.011	0.009	2.068	0.003	0.002	0.003	1.131	0.065	2.610
20	0.3	0.55	2	0.588	5.782	0.052	0.065	3.023	0.011	0.009	2.068	0.002	0.002	0.002	0.751	0.029	1.151
20	0.4	0.55	2	0.588	5.782	0.052	0.065	2.618	0.011	0.009	2.068	0.001	0.002	0.001	0.561	0.016	0.643
20	0.5	0.55	2	0.588	5.782	0.052	0.065	2.342	0.011	0.009	2.068	0.001	0.002	0.001	0.447	0.010	0.408
20	0.6	0.55	2	0.588	5.782	0.052	0.065	2.138	0.011	0.009	2.068	0.001	0.002	0.001	0.371	0.007	0.281
20	0.5	0.58	2	0.588	5.782	0.052	0.065	2.559	0.011	0.009	2.023	0.001	0.002	0.001	0.536	0.015	0.585
20	0.4	0.58	2	0.588	5.782	0.052	0.065	2.861	0.011	0.009	2.023	0.002	0.002	0.002	0.672	0.023	0.921
20	0.3	0.58	2	0.588	5.782	0.052	0.065	3.303	0.011	0.009	2.023	0.002	0.002	0.002	0.899	0.041	1.647
20	0.2	0.58	2	0.588	5.782	0.052	0.065	4.045	0.011	0.009	2.023	0.003	0.002	0.003	1.352	0.093	3.729
20	0.1	0.58	2	0.588	5.782	0.052	0.065	5.721	0.011	0.009	2.023	0.006	0.002	0.006	2.713	0.375	15.010
20	0.7	0.58	2	0.588	5.782	0.052	0.065	2.162	0.011	0.009	2.023	0.001	0.002	0.001	0.380	0.007	0.295
20	0.1	0.58	2	0.588	5.782	0.052	0.065	5.121	0.011	0.009	2.023	0.005	0.002	0.005	2.172	0.240	9.620
20	0.2	0.58	2	0.588	5.782	0.052	0.065	3.621	0.011	0.009	2.023	0.003	0.002	0.003	1.082	0.060	2.386
20	0.3	0.58	2	0.588	5.782	0.052	0.065	2.957	0.011	0.009	2.023	0.002	0.002	0.002	0.718	0.026	1.052
20	0.4	0.58	2	0.588	5.782	0.052	0.065	2.560	0.011	0.009	2.023	0.001	0.002	0.001	0.537	0.015	0.587
20	0.5	0.58	2	0.588	5.782	0.052	0.065	2.290	0.011	0.009	2.023	0.001	0.002	0.001	0.428	0.009	0.373
20	0.6	0.58	2	0.588	5.782	0.052	0.065	2.091	0.011	0.009	2.023	0.001	0.002	0.001	0.355	0.006	0.257

Table D 0.9. Quasi-steady method of Q=20 l/s, H=3 m and TW=0.5 m

Q	X	Z	V _{zi}	Z _{core}	V _{zj}	h _{down}	h _{up}	V _{xmax}	q _{up}	q _{down}	V(z)	FQSI	G _b	I _{net}	V _{up}	H _{up}	H _{up} /z
l/s	m	m	m/s	m	m/s	m	m	m/s	m ² /s	m ² /s	m/s	Ns	kg/m ²	Ns	m/s	m	
			Q=VA	Z=5*Bj	Eq. 25	Eq.61		Eq. 63	Eq. 61&62		Eq. 60	Fig.2.18	Eq. 59	Eq.55		Eq. 58	
20	0.85	0	2	0.524	7.284	0.047	0.058	1.875	0.011	0.009	7.284						
20	0.85	0.042	2	0.524	7.284	0.047	0.058	1.875	0.011	0.009	7.093						
20	0.85	0.083	2	0.524	7.284	0.047	0.058	1.875	0.011	0.009	5.015						
20	0.85	0.125	2	0.524	7.284	0.047	0.058	1.875	0.011	0.009	4.095						
20	0.85	0.167	2	0.524	7.284	0.047	0.058	1.875	0.011	0.009	3.546						
20	0.85	0.208	2	0.524	7.284	0.047	0.058	1.875	0.011	0.009	3.172						
20	0.85	0.250	2	0.524	7.284	0.047	0.058	1.875	0.011	0.009	2.896						
20	0.85	0.292	2	0.524	7.284	0.047	0.058	1.875	0.011	0.009	2.681						
20	0.85	0.333	2	0.524	7.284	0.047	0.058	1.875	0.011	0.009	2.508						
20	0.85	0.375	2	0.524	7.284	0.047	0.058	1.875	0.011	0.009	2.364						
20	0.85	0.417	2	0.524	7.284	0.047	0.058	1.875	0.011	0.009	2.243						
20	0.85	0.458	2	0.524	7.284	0.047	0.058	1.875	0.011	0.009	2.139						
20	0.85	0.5	2	0.524	7.284	0.047	0.058	1.875	0.011	0.009	2.047						
20	0.5	0.5	2	0.524	7.284	0.047	0.058	2.445	0.011	0.009	2.047	0.001	0.002	0.001	0.488	0.012	0.486
20	0.4	0.5	2	0.524	7.284	0.047	0.058	2.733	0.011	0.009	2.047	0.001	0.002	0.001	0.613	0.019	0.765
20	0.3	0.5	2	0.524	7.284	0.047	0.058	3.156	0.011	0.009	2.047	0.002	0.002	0.002	0.820	0.034	1.370
20	0.2	0.5	2	0.524	7.284	0.047	0.058	3.865	0.011	0.009	2.047	0.003	0.002	0.003	1.234	0.078	3.104
20	0.1	0.5	2	0.524	7.284	0.047	0.058	5.466	0.011	0.009	2.047	0.006	0.002	0.006	2.476	0.313	12.502
20	0.85	0.5	2	0.524	7.284	0.047	0.058	1.678	0.011	0.009	2.047	0.001	0.002	0.001	0.226	0.003	0.104
20	0.1	0.5	2	0.524	7.284	0.047	0.058	4.893	0.011	0.009	2.047	0.005	0.002	0.005	1.982	0.200	8.011
20	0.2	0.5	2	0.524	7.284	0.047	0.058	3.460	0.011	0.009	2.047	0.002	0.002	0.002	0.987	0.050	1.986
20	0.3	0.5	2	0.524	7.284	0.047	0.058	2.825	0.011	0.009	2.047	0.002	0.002	0.002	0.655	0.022	0.875
20	0.4	0.5	2	0.524	7.284	0.047	0.058	2.446	0.011	0.009	2.047	0.001	0.002	0.001	0.489	0.012	0.488
20	0.5	0.5	2	0.524	7.284	0.047	0.058	2.188	0.011	0.009	2.047	0.001	0.002	0.001	0.390	0.008	0.309

Q	X	Z	V _{zi}	Z _{core}	V _{zj}	h _{down}	h _{up}	V _{xmax}	q _{up}	q _{down}	V(z)	FQSI	G _b	I _{net}	V _{up}	H _{up}	H _{up} /z
l/s	m	m	m/s	m	m/s	m	m	m/s	m ² /s	m ² /s	m/s	Ns	kg/m ²	Ns	m/s	m	
			Q=VA	Z=5*Bj	Eq. 25	Eq. 61		Eq. 63	Eq. 61&62		Eq. 60	Fig.2.18	Eq. 59	Eq.55		Eq. 59	
20	0.6	0.5	2	0.524	7.284	0.047	0.058	1.997	0.011	0.009	2.047	0.001	0.002	0.001	0.323	0.005	0.213
20	0.5	0.525	2	0.524	7.284	0.047	0.058	2.386	0.011	0.009	1.998	0.001	0.002	0.001	0.465	0.011	0.440
20	0.4	0.525	2	0.524	7.284	0.047	0.058	2.667	0.011	0.009	1.998	0.001	0.002	0.001	0.583	0.017	0.693
20	0.3	0.525	2	0.524	7.284	0.047	0.058	3.080	0.011	0.009	1.998	0.002	0.002	0.002	0.780	0.031	1.241
20	0.2	0.525	2	0.524	7.284	0.047	0.058	3.772	0.011	0.009	1.998	0.003	0.002	0.003	1.175	0.070	2.813
20	0.1	0.525	2	0.524	7.284	0.047	0.058	5.335	0.011	0.009	1.998	0.006	0.002	0.006	2.358	0.283	11.335
20	0.85	0.525	2	0.524	7.284	0.047	0.058	1.638	0.011	0.009	1.998	0.001	0.002	0.001	0.215	0.002	0.094
20	0.1	0.525	2	0.524	7.284	0.047	0.058	4.775	0.011	0.009	1.998	0.005	0.002	0.004	1.887	0.182	7.263
20	0.2	0.525	2	0.524	7.284	0.047	0.058	3.376	0.011	0.009	1.998	0.002	0.002	0.002	0.939	0.045	1.799
20	0.3	0.525	2	0.524	7.284	0.047	0.058	2.757	0.011	0.009	1.998	0.002	0.002	0.001	0.623	0.020	0.792
20	0.4	0.525	2	0.524	7.284	0.047	0.058	2.387	0.011	0.009	1.998	0.001	0.002	0.001	0.465	0.011	0.442
20	0.5	0.525	2	0.524	7.284	0.047	0.058	2.135	0.011	0.009	1.998	0.001	0.002	0.001	0.371	0.007	0.280
20	0.6	0.525	2	0.524	7.284	0.047	0.058	1.949	0.011	0.009	1.998	0.001	0.002	0.001	0.307	0.005	0.193
20	0.5	0.55	2	0.524	7.284	0.047	0.058	2.331	0.011	0.009	1.952	0.001	0.002	0.001	0.443	0.010	0.401
20	0.4	0.55	2	0.524	7.284	0.047	0.058	2.606	0.011	0.009	1.952	0.001	0.002	0.001	0.556	0.016	0.631
20	0.3	0.55	2	0.524	7.284	0.047	0.058	3.009	0.011	0.009	1.952	0.002	0.002	0.002	0.744	0.028	1.130
20	0.2	0.55	2	0.524	7.284	0.047	0.058	3.685	0.011	0.009	1.952	0.003	0.002	0.003	1.121	0.064	2.562
20	0.1	0.55	2	0.524	7.284	0.047	0.058	5.212	0.011	0.009	1.952	0.005	0.002	0.005	2.250	0.258	10.325
20	0.85	0.55	2	0.524	7.284	0.047	0.058	1.600	0.011	0.009	1.952	0.001	0.002	0.000	0.204	0.002	0.085
20	0.1	0.55	2	0.524	7.284	0.047	0.058	4.665	0.011	0.009	1.952	0.004	0.002	0.004	1.801	0.165	6.615
20	0.2	0.55	2	0.524	7.284	0.047	0.058	3.299	0.011	0.009	1.952	0.002	0.002	0.002	0.896	0.041	1.638
20	0.3	0.55	2	0.524	7.284	0.047	0.058	2.693	0.011	0.009	1.952	0.001	0.002	0.001	0.595	0.018	0.721
20	0.4	0.55	2	0.524	7.284	0.047	0.058	2.333	0.011	0.009	1.952	0.001	0.002	0.001	0.444	0.010	0.402
20	0.5	0.55	2	0.524	7.284	0.047	0.058	2.086	0.011	0.009	1.952	0.001	0.002	0.001	0.353	0.006	0.255
20	0.6	0.55	2	0.524	7.284	0.047	0.058	1.905	0.011	0.009	1.952	0.001	0.002	0.001	0.293	0.004	0.175
20	0.5	0.575	2	0.524	7.284	0.047	0.058	2.280	0.011	0.009	1.909	0.001	0.002	0.001	0.424	0.009	0.366

Q	X	Z	V _{zi}	Z _{core}	V _{zj}	h _{down}	h _{up}	V _{xmax}	q _{up}	q _{down}	V(z)	FQSI	G _b	I _{net}	V _{up}	H _{up}	H _{up} /z
l/s	m	m	m/s	m	m/s	m	m	m/s	m ² /s	m ² /s	m/s	Ns	kg/m ²	Ns	m/s	m	
			Q=VA	Z=5*Bj	Eq. 25	Eq. 61		Eq. 63	Eq. 61&62		Eq. 60	Fig.2.18	Eq. 59	Eq.55		Eq. 58	
20	0.4	0.575	2	0.524	7.284	0.047	0.058	2.549	0.011	0.009	1.909	0.001	0.002	0.001	0.532	0.014	0.576
20	0.3	0.575	2	0.524	7.284	0.047	0.058	2.943	0.011	0.009	1.909	0.002	0.002	0.002	0.712	0.026	1.033
20	0.2	0.575	2	0.524	7.284	0.047	0.058	3.604	0.011	0.009	1.909	0.003	0.002	0.003	1.072	0.059	2.342
20	0.1	0.575	2	0.524	7.284	0.047	0.058	5.097	0.011	0.009	1.909	0.005	0.002	0.005	2.152	0.236	9.443
20	0.85	0.575	2	0.524	7.284	0.047	0.058	1.565	0.011	0.009	1.909	0.000	0.002	0.000	0.195	0.002	0.078
20	0.1	0.575	2	0.524	7.284	0.047	0.058	4.563	0.011	0.009	1.909	0.004	0.002	0.004	1.723	0.151	6.050
20	0.2	0.575	2	0.524	7.284	0.047	0.058	3.226	0.011	0.009	1.909	0.002	0.002	0.002	0.857	0.037	1.497
20	0.3	0.575	2	0.524	7.284	0.047	0.058	2.634	0.011	0.009	1.909	0.001	0.002	0.001	0.569	0.016	0.659
20	0.4	0.575	2	0.524	7.284	0.047	0.058	2.281	0.011	0.009	1.909	0.001	0.002	0.001	0.424	0.009	0.367
20	0.5	0.575	2	0.524	7.284	0.047	0.058	2.040	0.011	0.009	1.909	0.001	0.002	0.001	0.338	0.006	0.232
20	0.6	0.575	2	0.524	7.284	0.047	0.058	1.863	0.011	0.009	1.909	0.001	0.002	0.001	0.280	0.004	0.160
20	0.5	0.6	2	0.524	7.284	0.047	0.058	2.232	0.011	0.009	1.869	0.001	0.002	0.001	0.406	0.008	0.335
20	0.4	0.6	2	0.524	7.284	0.047	0.058	2.495	0.011	0.009	1.869	0.001	0.002	0.001	0.509	0.013	0.528
20	0.3	0.6	2	0.524	7.284	0.047	0.058	2.881	0.011	0.009	1.869	0.002	0.002	0.002	0.682	0.024	0.947
20	0.2	0.6	2	0.524	7.284	0.047	0.058	3.528	0.011	0.009	1.869	0.002	0.002	0.002	1.027	0.054	2.150
20	0.1	0.6	2	0.524	7.284	0.047	0.058	4.990	0.011	0.009	1.869	0.005	0.002	0.005	2.062	0.217	8.670
20	0.85	0.6	2	0.524	7.284	0.047	0.058	1.532	0.011	0.009	1.869	0.000	0.002	0.000	0.187	0.002	0.071
20	0.1	0.6	2	0.524	7.284	0.047	0.058	4.466	0.011	0.009	1.869	0.004	0.002	0.004	1.650	0.139	5.554
20	0.2	0.6	2	0.524	7.284	0.047	0.058	3.158	0.011	0.009	1.869	0.002	0.002	0.002	0.821	0.034	1.374
20	0.3	0.6	2	0.524	7.284	0.047	0.058	2.579	0.011	0.009	1.869	0.001	0.002	0.001	0.544	0.015	0.604
20	0.4	0.6	2	0.524	7.284	0.047	0.058	2.233	0.011	0.009	1.869	0.001	0.002	0.001	0.406	0.008	0.336
20	0.5	0.6	2	0.524	7.284	0.047	0.058	1.997	0.011	0.009	1.869	0.001	0.002	0.001	0.323	0.005	0.213
20	0.6	0.6	2	0.524	7.284	0.047	0.058	1.823	0.011	0.009	1.869	0.001	0.002	0.001	0.268	0.004	0.146
20	0.5	0.625	2	0.524	7.284	0.047	0.058	2.187	0.011	0.009	1.831	0.001	0.002	0.001	0.389	0.008	0.309
20	0.4	0.625	2	0.524	7.284	0.047	0.058	2.445	0.011	0.009	1.831	0.001	0.002	0.001	0.488	0.012	0.486
20	0.3	0.625	2	0.524	7.284	0.047	0.058	2.823	0.011	0.009	1.831	0.002	0.002	0.002	0.654	0.022	0.872

Q	X	Z	V _{zi}	Z _{core}	V _{zj}	h _{down}	h _{up}	V _{xmax}	q _{up}	q _{down}	V(z)	FQSI	G _b	I _{net}	V _{up}	H _{up}	H _{up} /z
l/s	m	m	m/s	m	m/s	m	m	m/s	m ² /s	m ² /s	m/s	Ns	kg/m ²	Ns	m/s	m	
			Q=VA	Z=5*Bj	Eq. 25	Eq.61		Eq. 63	Eq.61&62		Eq. 60	Fig.2.18	Eq. 59	Eq.55		Eq. 58	
20	0.2	0.625	2	0.524	7.284	0.047	0.058	3.457	0.011	0.009	1.831	0.002	0.002	0.002	0.985	0.049	1.980
20	0.1	0.625	2	0.524	7.284	0.047	0.058	4.889	0.011	0.009	1.831	0.005	0.002	0.005	1.979	0.200	7.987
20	0.85	0.625	2	0.524	7.284	0.047	0.058	1.501	0.011	0.009	1.831	0.000	0.002	0.000	0.179	0.002	0.065
20	0.1	0.625	2	0.524	7.284	0.047	0.058	4.376	0.011	0.009	1.831	0.004	0.002	0.004	1.584	0.128	5.116
20	0.2	0.625	2	0.524	7.284	0.047	0.058	3.094	0.011	0.009	1.831	0.002	0.002	0.002	0.788	0.032	1.265
20	0.3	0.625	2	0.524	7.284	0.047	0.058	2.527	0.011	0.009	1.831	0.001	0.002	0.001	0.522	0.014	0.556
20	0.4	0.625	2	0.524	7.284	0.047	0.058	2.188	0.011	0.009	1.831	0.001	0.002	0.001	0.390	0.008	0.309
20	0.5	0.625	2	0.524	7.284	0.047	0.058	1.957	0.011	0.009	1.831	0.001	0.002	0.001	0.310	0.005	0.196
20	0.6	0.625	2	0.524	7.284	0.047	0.058	1.787	0.011	0.009	1.831	0.001	0.002	0.001	0.257	0.003	0.135
20	0.5	0.65	2	0.524	7.284	0.047	0.058	2.144	0.011	0.009	1.796	0.001	0.002	0.001	0.374	0.007	0.285
20	0.4	0.65	2	0.524	7.284	0.047	0.058	2.397	0.011	0.009	1.796	0.001	0.002	0.001	0.469	0.011	0.449
20	0.3	0.65	2	0.524	7.284	0.047	0.058	2.768	0.011	0.009	1.796	0.002	0.002	0.001	0.629	0.020	0.806
20	0.2	0.65	2	0.524	7.284	0.047	0.058	3.390	0.011	0.009	1.796	0.002	0.002	0.002	0.947	0.046	1.829
20	0.1	0.65	2	0.524	7.284	0.047	0.058	4.794	0.011	0.009	1.796	0.005	0.002	0.005	1.903	0.185	7.382
20	0.85	0.65	2	0.524	7.284	0.047	0.058	1.472	0.011	0.009	1.796	0.000	0.002	0.000	0.172	0.002	0.060
20	0.1	0.65	2	0.524	7.284	0.047	0.058	4.291	0.011	0.009	1.796	0.004	0.002	0.004	1.523	0.118	4.728
20	0.2	0.65	2	0.524	7.284	0.047	0.058	3.034	0.011	0.009	1.796	0.002	0.002	0.002	0.757	0.029	1.169
20	0.3	0.65	2	0.524	7.284	0.047	0.058	2.478	0.011	0.009	1.796	0.001	0.002	0.001	0.502	0.013	0.514
20	0.4	0.65	2	0.524	7.284	0.047	0.058	2.146	0.011	0.009	1.796	0.001	0.002	0.001	0.374	0.007	0.286
20	0.5	0.65	2	0.524	7.284	0.047	0.058	1.919	0.011	0.009	1.796	0.001	0.002	0.001	0.298	0.005	0.181
20	0.6	0.65	2	0.524	7.284	0.047	0.058	1.752	0.011	0.009	1.796	0.001	0.002	0.001	0.247	0.003	0.124
20	0.5	0.675	2	0.524	7.284	0.047	0.058	2.104	0.011	0.009	1.762	0.001	0.002	0.001	0.360	0.007	0.264
20	0.4	0.675	2	0.524	7.284	0.047	0.058	2.352	0.011	0.009	1.762	0.001	0.002	0.001	0.452	0.010	0.416
20	0.3	0.675	2	0.524	7.284	0.047	0.058	2.716	0.011	0.009	1.762	0.001	0.002	0.001	0.605	0.019	0.746
20	0.2	0.675	2	0.524	7.284	0.047	0.058	3.327	0.011	0.009	1.762	0.002	0.002	0.002	0.912	0.042	1.695
20	0.1	0.675	2	0.524	7.284	0.047	0.058	4.705	0.011	0.009	1.762	0.004	0.002	0.004	1.832	0.171	6.843

Q	X	Z	V _{zi}	Z _{core}	V _{zj}	h _{down}	h _{up}	V _{xmax}	q _{up}	q _{down}	V(z)	FQSI	G _b	I _{net}	V _{up}	H _{up}	H _{up} /z
l/s	m	m	m/s	m	m/s	m	m	m/s	m ² /s	m ² /s	m/s	Ns	kg/m ²	Ns	m/s	m	
			Q=VA	Z=5*Bj	Eq. 25	Eq. 61		Eq. 63	Eq. 61&62		Eq. 60	Fig.2.18	Eq. 59	Eq.55		Eq. 58	
20	0.85	0.675	2	0.524	7.284	0.047	0.058	1.444	0.011	0.009	1.762	0.000	0.002	0.000	0.165	0.001	0.055
20	0.1	0.675	2	0.524	7.284	0.047	0.058	4.211	0.011	0.009	1.762	0.004	0.002	0.003	1.466	0.110	4.382
20	0.2	0.675	2	0.524	7.284	0.047	0.058	2.978	0.011	0.009	1.762	0.002	0.002	0.002	0.729	0.027	1.083
20	0.3	0.675	2	0.524	7.284	0.047	0.058	2.431	0.011	0.009	1.762	0.001	0.002	0.001	0.483	0.012	0.476
20	0.4	0.675	2	0.524	7.284	0.047	0.058	2.106	0.011	0.009	1.762	0.001	0.002	0.001	0.360	0.007	0.264
20	0.5	0.675	2	0.524	7.284	0.047	0.058	1.883	0.011	0.009	1.762	0.001	0.002	0.001	0.286	0.004	0.167
20	0.6	0.675	2	0.524	7.284	0.047	0.058	1.719	0.011	0.009	1.762	0.001	0.002	0.001	0.237	0.003	0.115
20	0.5	0.7	2	0.524	7.284	0.047	0.058	2.066	0.011	0.009	1.730	0.001	0.002	0.001	0.346	0.006	0.245
20	0.4	0.7	2	0.524	7.284	0.047	0.058	2.310	0.011	0.009	1.730	0.001	0.002	0.001	0.435	0.010	0.386
20	0.3	0.7	2	0.524	7.284	0.047	0.058	2.667	0.011	0.009	1.730	0.001	0.002	0.001	0.583	0.017	0.693
20	0.2	0.7	2	0.524	7.284	0.047	0.058	3.267	0.011	0.009	1.730	0.002	0.002	0.002	0.879	0.039	1.575
20	0.1	0.7	2	0.524	7.284	0.047	0.058	4.620	0.011	0.009	1.730	0.004	0.002	0.004	1.766	0.159	6.361
20	0.85	0.7	2	0.524	7.284	0.047	0.058	1.418	0.011	0.009	1.730	0.000	0.002	0.000	0.159	0.001	0.051
20	0.1	0.7	2	0.524	7.284	0.047	0.058	4.135	0.011	0.009	1.730	0.003	0.002	0.003	1.413	0.102	4.073
20	0.2	0.7	2	0.524	7.284	0.047	0.058	2.924	0.011	0.009	1.730	0.002	0.002	0.002	0.702	0.025	1.006
20	0.3	0.7	2	0.524	7.284	0.047	0.058	2.387	0.011	0.009	1.730	0.001	0.002	0.001	0.465	0.011	0.442
20	0.4	0.7	2	0.524	7.284	0.047	0.058	2.068	0.011	0.009	1.730	0.001	0.002	0.001	0.347	0.006	0.245
20	0.5	0.7	2	0.524	7.284	0.047	0.058	1.849	0.011	0.009	1.730	0.001	0.002	0.001	0.276	0.004	0.155
20	0.6	0.7	2	0.524	7.284	0.047	0.058	1.688	0.011	0.009	1.730	0.001	0.002	0.001	0.228	0.003	0.106
20	0.5	0.725	2	0.524	7.284	0.047	0.058	2.030	0.011	0.009	1.700	0.001	0.002	0.001	0.334	0.006	0.228
20	0.4	0.725	2	0.524	7.284	0.047	0.058	2.270	0.011	0.009	1.700	0.001	0.002	0.001	0.420	0.009	0.359
20	0.3	0.725	2	0.524	7.284	0.047	0.058	2.621	0.011	0.009	1.700	0.001	0.002	0.001	0.563	0.016	0.646
20	0.2	0.725	2	0.524	7.284	0.047	0.058	3.210	0.011	0.009	1.700	0.002	0.002	0.002	0.848	0.037	1.467
20	0.1	0.725	2	0.524	7.284	0.047	0.058	4.540	0.011	0.009	1.700	0.004	0.002	0.004	1.705	0.148	5.928
20	0.85	0.725	2	0.524	7.284	0.047	0.058	1.394	0.011	0.009	1.700	0.000	0.002	0.000	0.153	0.001	0.048
20	0.1	0.725	2	0.524	7.284	0.047	0.058	4.063	0.011	0.009	1.700	0.003	0.002	0.003	1.364	0.095	3.795

Q	X	Z	V _{zi}	Z _{core}	V _{zj}	h _{down}	h _{up}	V _{xmax}	q _{up}	q _{down}	V(z)	FQSI	G _b	I _{net}	V _{up}	H _{up}	H _{up} /z
l/s	m	m	m/s	m	m/s	m	m	m/s	m ² /s	m ² /s	m/s	Ns	kg/m ²	Ns	m/s	m	
			Q=VA	Z=5*Bj	Eq. 25	Eq. 61		Eq. 63	Eq. 61&62		Eq. 60	Fig.2.18	Eq. 59	Eq.55		Eq. 58	
20	0.2	0.725	2	0.524	7.284	0.047	0.058	2.873	0.011	0.009	1.700	0.002	0.002	0.002	0.678	0.023	0.937
20	0.3	0.725	2	0.524	7.284	0.047	0.058	2.346	0.011	0.009	1.700	0.001	0.002	0.001	0.449	0.010	0.411
20	0.4	0.725	2	0.524	7.284	0.047	0.058	2.032	0.011	0.009	1.700	0.001	0.002	0.001	0.335	0.006	0.228
20	0.5	0.725	2	0.524	7.284	0.047	0.058	1.817	0.011	0.009	1.700	0.001	0.002	0.001	0.266	0.004	0.144
20	0.6	0.725	2	0.524	7.284	0.047	0.058	1.659	0.011	0.009	1.700	0.001	0.002	0.001	0.220	0.002	0.099
20	0.5	0.75	2	0.524	7.284	0.047	0.058	1.996	0.011	0.009	1.672	0.001	0.002	0.001	0.323	0.005	0.212
20	0.4	0.75	2	0.524	7.284	0.047	0.058	2.232	0.011	0.009	1.672	0.001	0.002	0.001	0.406	0.008	0.335
20	0.3	0.75	2	0.524	7.284	0.047	0.058	2.577	0.011	0.009	1.672	0.001	0.002	0.001	0.544	0.015	0.603
20	0.2	0.75	2	0.524	7.284	0.047	0.058	3.156	0.011	0.009	1.672	0.002	0.002	0.002	0.820	0.034	1.370
20	0.1	0.75	2	0.524	7.284	0.047	0.058	4.463	0.011	0.009	1.672	0.004	0.002	0.004	1.648	0.138	5.537
20	0.85	0.75	2	0.524	7.284	0.047	0.058	1.370	0.011	0.009	1.672	0.000	0.002	0.000	0.148	0.001	0.044
20	0.1	0.75	2	0.524	7.284	0.047	0.058	3.995	0.011	0.009	1.672	0.003	0.002	0.003	1.319	0.089	3.545
20	0.2	0.75	2	0.524	7.284	0.047	0.058	2.825	0.011	0.009	1.672	0.002	0.002	0.002	0.655	0.022	0.875
20	0.3	0.75	2	0.524	7.284	0.047	0.058	2.306	0.011	0.009	1.672	0.001	0.002	0.001	0.434	0.010	0.384
20	0.4	0.75	2	0.524	7.284	0.047	0.058	1.997	0.011	0.009	1.672	0.001	0.002	0.001	0.323	0.005	0.213
20	0.5	0.75	2	0.524	7.284	0.047	0.058	1.787	0.011	0.009	1.672	0.001	0.002	0.001	0.257	0.003	0.135
20	0.6	0.75	2	0.524	7.284	0.047	0.058	1.631	0.011	0.009	1.672	0.001	0.002	0.001	0.213	0.002	0.092
20	0.5	0.775	2	0.524	7.284	0.047	0.058	1.964	0.011	0.009	1.645	0.001	0.002	0.001	0.312	0.005	0.199
20	0.4	0.775	2	0.524	7.284	0.047	0.058	2.195	0.011	0.009	1.645	0.001	0.002	0.001	0.392	0.008	0.314
20	0.3	0.775	2	0.524	7.284	0.047	0.058	2.535	0.011	0.009	1.645	0.001	0.002	0.001	0.526	0.014	0.564
20	0.2	0.775	2	0.524	7.284	0.047	0.058	3.105	0.011	0.009	1.645	0.002	0.002	0.002	0.793	0.032	1.282
20	0.1	0.775	2	0.524	7.284	0.047	0.058	4.391	0.011	0.009	1.645	0.004	0.002	0.004	1.595	0.130	5.184
20	0.85	0.775	2	0.524	7.284	0.047	0.058	1.348	0.011	0.009	1.645	0.000	0.002	0.000	0.143	0.001	0.041
20	0.1	0.775	2	0.524	7.284	0.047	0.058	3.930	0.011	0.009	1.645	0.003	0.002	0.003	1.276	0.083	3.319
20	0.2	0.775	2	0.524	7.284	0.047	0.058	2.779	0.011	0.009	1.645	0.002	0.002	0.002	0.634	0.020	0.819
20	0.3	0.775	2	0.524	7.284	0.047	0.058	2.269	0.011	0.009	1.645	0.001	0.002	0.001	0.420	0.009	0.359

Q	X	Z	V _{zi}	Z _{core}	V _{zj}	h _{down}	h _{up}	V _{xmax}	q _{up}	q _{down}	V(z)	FQSI	G _b	I _{net}	V _{up}	H _{up}	H _{up} /z
l/s	m	m	m/s	m	m/s	m	m	m/s	m ² /s	m ² /s	m/s	Ns	kg/m ²	Ns	m/s	m	
			Q=VA	Z=5*Bj	Eq. 25	Eq. 61		Eq. 63	Eq. 61&62		Eq. 60	Fig.2.18	Eq. 59	Eq.55		Eq. 59	
20	0.4	0.775	2	0.524	7.284	0.047	0.058	1.965	0.011	0.009	1.645	0.001	0.002	0.001	0.313	0.005	0.199
20	0.5	0.775	2	0.524	7.284	0.047	0.058	1.758	0.011	0.009	1.645	0.001	0.002	0.001	0.248	0.003	0.126
20	0.6	0.775	2	0.524	7.284	0.047	0.058	1.604	0.011	0.009	1.645	0.001	0.002	0.000	0.206	0.002	0.086
20	0.5	0.8	2	0.524	7.284	0.047	0.058	1.933	0.011	0.009	1.619	0.001	0.002	0.001	0.302	0.005	0.186
20	0.4	0.8	2	0.524	7.284	0.047	0.058	2.161	0.011	0.009	1.619	0.001	0.002	0.001	0.380	0.007	0.294
20	0.3	0.8	2	0.524	7.284	0.047	0.058	2.495	0.011	0.009	1.619	0.001	0.002	0.001	0.509	0.013	0.528
20	0.2	0.8	2	0.524	7.284	0.047	0.058	3.056	0.011	0.009	1.619	0.002	0.002	0.002	0.768	0.030	1.202
20	0.1	0.8	2	0.524	7.284	0.047	0.058	4.321	0.011	0.009	1.619	0.004	0.002	0.004	1.544	0.122	4.863
20	0.85	0.8	2	0.524	7.284	0.047	0.058	1.327	0.011	0.009	1.619	0.000	0.002	0.000	0.138	0.001	0.039
20	0.1	0.8	2	0.524	7.284	0.047	0.058	3.868	0.011	0.009	1.619	0.003	0.002	0.003	1.236	0.078	3.113
20	0.2	0.8	2	0.524	7.284	0.047	0.058	2.735	0.011	0.009	1.619	0.001	0.002	0.001	0.614	0.019	0.768
20	0.3	0.8	2	0.524	7.284	0.047	0.058	2.233	0.011	0.009	1.619	0.001	0.002	0.001	0.406	0.008	0.336
20	0.4	0.8	2	0.524	7.284	0.047	0.058	1.934	0.011	0.009	1.619	0.001	0.002	0.001	0.303	0.005	0.187
20	0.5	0.8	2	0.524	7.284	0.047	0.058	1.730	0.011	0.009	1.619	0.001	0.002	0.001	0.240	0.003	0.118
20	0.6	0.8	2	0.524	7.284	0.047	0.058	1.579	0.011	0.009	1.619	0.000	0.002	0.000	0.199	0.002	0.081
20	0.5	0.825	2	0.524	7.284	0.047	0.058	1.903	0.011	0.009	1.594	0.001	0.002	0.001	0.293	0.004	0.175
20	0.4	0.825	2	0.524	7.284	0.047	0.058	2.128	0.011	0.009	1.594	0.001	0.002	0.001	0.368	0.007	0.276
20	0.3	0.825	2	0.524	7.284	0.047	0.058	2.457	0.011	0.009	1.594	0.001	0.002	0.001	0.493	0.012	0.496
20	0.2	0.825	2	0.524	7.284	0.047	0.058	3.009	0.011	0.009	1.594	0.002	0.002	0.002	0.744	0.028	1.130
20	0.1	0.825	2	0.524	7.284	0.047	0.058	4.256	0.011	0.009	1.594	0.004	0.002	0.004	1.497	0.114	4.571
20	0.85	0.825	2	0.524	7.284	0.047	0.058	1.306	0.011	0.009	1.594	0.000	0.002	0.000	0.133	0.001	0.036
20	0.1	0.825	2	0.524	7.284	0.047	0.058	3.809	0.011	0.009	1.594	0.003	0.002	0.003	1.198	0.073	2.926
20	0.2	0.825	2	0.524	7.284	0.047	0.058	2.693	0.011	0.009	1.594	0.001	0.002	0.001	0.595	0.018	0.721
20	0.3	0.825	2	0.524	7.284	0.047	0.058	2.199	0.011	0.009	1.594	0.001	0.002	0.001	0.394	0.008	0.316
20	0.4	0.825	2	0.524	7.284	0.047	0.058	1.905	0.011	0.009	1.594	0.001	0.002	0.001	0.293	0.004	0.175
20	0.5	0.825	2	0.524	7.284	0.047	0.058	1.703	0.011	0.009	1.594	0.001	0.002	0.001	0.233	0.003	0.110

Q	X	Z	V_{zi}	Z_{core}	V_{zj}	h_{down}	h_{up}	V_{xmax}	q_{up}	q_{down}	V(z)	FQSI	G_b	I_{net}	V_{up}	H_{up}	H_{up}/z
l/s	m	m	m/s	m	m/s	m	m	m/s	m²/s	m²/s	m/s	Ns	kg/m²	Ns	m/s	m	
			Q=VA	Z=5*Bj	Eq. 25	Eq. 61		Eq. 63	Eq. 61&62		Eq. 60	Fig.2.18	Eq. 59	Eq.55		Eq. 58	
20	0.6	0.825	2	0.524	7.284	0.047	0.058	1.555	0.011	0.009	1.594	0.000	0.002	0.000	0.193	0.002	0.076

Table D 0.10. Quasi-steady method of Q=20 l/s, H=3 m and TW=0.25 m

Q	X	Z	V _{zi}	Z _{core}	V _{zj}	h _{down}	h _{up}	V _{xmax}	q _{up}	q _{down}	V(z)	FQSI	Gb	Inet	V _{up}	H _{up}	H _{up} /z
l/s	m	m	m/s	m	m/s	m	m	m/s	m ² /s	m ² /s	m/s	Ns	kg/m ²	Ns	m/s	m	
			Q=VA	Z=5*Bj	Eq. 25	Eq.61		Eq. 63	Eq. 61&62		Eq. 60	Fig.2.18	Eq. 59	Eq.55		Eq. 58	
20	0.85	0	2	0.524	7.284	0.047	0.058	2.652	0.011	0.009	7.284						
20	0.85	0.042	2	0.524	7.284	0.047	0.058	2.652	0.011	0.009	7.093						
20	0.85	0.083	2	0.524	7.284	0.047	0.058	2.652	0.011	0.009	5.015						
20	0.85	0.125	2	0.524	7.284	0.047	0.058	2.652	0.011	0.009	4.095						
20	0.85	0.167	2	0.524	7.284	0.047	0.058	2.652	0.011	0.009	3.546						
20	0.85	0.208	2	0.524	7.284	0.047	0.058	2.652	0.011	0.009	3.172						
20	0.85	0.25	2	0.524	7.284	0.047	0.058	2.652	0.011	0.009	2.896						
20	0.5	0.25	2	0.524	7.284	0.047	0.058	3.457	0.011	0.009	2.896	0.002	0.002	0.002	0.985	0.049	1.980
20	0.4	0.25	2	0.524	7.284	0.047	0.058	3.865	0.011	0.009	2.896	0.003	0.002	0.003	1.234	0.078	3.104
20	0.3	0.25	2	0.524	7.284	0.047	0.058	4.463	0.011	0.009	2.896	0.004	0.002	0.004	1.648	0.138	5.537
20	0.2	0.25	2	0.524	7.284	0.047	0.058	5.466	0.011	0.009	2.896	0.006	0.002	0.006	2.476	0.313	12.502
20	0.1	0.25	2	0.524	7.284	0.047	0.058	7.731	0.011	0.009	2.896	0.012	0.002	0.012	4.961	1.254	50.179
20	0.85	0.25	2	0.524	7.284	0.047	0.058	2.652	0.011	0.009	2.896	0.001	0.002	0.001	0.576	0.017	0.677
20	0.1	0.25	2	0.524	7.284	0.047	0.058	6.919	0.011	0.009	2.896	0.009	0.002	0.009	3.973	0.805	32.181
20	0.2	0.25	2	0.524	7.284	0.047	0.058	4.893	0.011	0.009	2.896	0.005	0.002	0.005	1.982	0.200	8.011
20	0.3	0.25	2	0.524	7.284	0.047	0.058	3.995	0.011	0.009	2.896	0.003	0.002	0.003	1.319	0.089	3.545
20	0.4	0.25	2	0.524	7.284	0.047	0.058	3.460	0.011	0.009	2.896	0.002	0.002	0.002	0.987	0.050	1.986
20	0.5	0.25	2	0.524	7.284	0.047	0.058	3.094	0.011	0.009	2.896	0.002	0.002	0.002	0.788	0.032	1.265
20	0.6	0.25	2	0.524	7.284	0.047	0.058	2.825	0.011	0.009	2.896	0.002	0.002	0.002	0.655	0.022	0.875
20	0.5	0.275	2	0.524	7.284	0.047	0.058	3.296	0.011	0.009	2.761	0.002	0.002	0.002	0.895	0.041	1.633
20	0.4	0.275	2	0.524	7.284	0.047	0.058	3.685	0.011	0.009	2.761	0.003	0.002	0.003	1.121	0.064	2.562
20	0.3	0.275	2	0.524	7.284	0.047	0.058	4.256	0.011	0.009	2.761	0.004	0.002	0.004	1.497	0.114	4.571
20	0.2	0.275	2	0.524	7.284	0.047	0.058	5.212	0.011	0.009	2.761	0.005	0.002	0.005	2.250	0.258	10.325
20	0.1	0.275	2	0.524	7.284	0.047	0.058	7.371	0.011	0.009	2.761	0.011	0.002	0.011	4.509	1.036	41.456
20	0.85	0.275	2	0.524	7.284	0.047	0.058	2.528	0.011	0.009	2.761	0.001	0.002	0.001	0.523	0.014	0.558

Q	X	Z	V _{zi}	Z _{core}	V _{zj}	h _{down}	h _{up}	V _{xmax}	q _{up}	q _{down}	V(z)	FQSI	G _b	I _{net}	V _{up}	H _{up}	H _{up} /z
l/s	m	m	m/s	m	m/s	m	m	m/s	m ² /s	m ² /s	m/s	Ns	kg/m ²	Ns	m/s	m	
			Q=VA	Z=5*Bj	Eq. 25	Eq. 61		Eq. 63	Eq. 61&62		Eq. 60	Fig.2.18	Eq. 59	Eq.55		Eq. 58	
20	0.1	0.275	2	0.524	7.284	0.047	0.058	6.597	0.011	0.009	2.761	0.009	0.002	0.009	3.611	0.665	26.585
20	0.2	0.275	2	0.524	7.284	0.047	0.058	4.665	0.011	0.009	2.761	0.004	0.002	0.004	1.801	0.165	6.615
20	0.3	0.275	2	0.524	7.284	0.047	0.058	3.809	0.011	0.009	2.761	0.003	0.002	0.003	1.198	0.073	2.926
20	0.4	0.275	2	0.524	7.284	0.047	0.058	3.299	0.011	0.009	2.761	0.002	0.002	0.002	0.896	0.041	1.638
20	0.5	0.275	2	0.524	7.284	0.047	0.058	2.950	0.011	0.009	2.761	0.002	0.002	0.002	0.715	0.026	1.043
20	0.6	0.275	2	0.524	7.284	0.047	0.058	2.693	0.011	0.009	2.761	0.001	0.002	0.001	0.595	0.018	0.721
20	0.5	0.3	2	0.524	7.284	0.047	0.058	3.156	0.011	0.009	2.643	0.002	0.002	0.002	0.820	0.034	1.370
20	0.4	0.3	2	0.524	7.284	0.047	0.058	3.528	0.011	0.009	2.643	0.002	0.002	0.002	1.027	0.054	2.150
20	0.3	0.3	2	0.524	7.284	0.047	0.058	4.074	0.011	0.009	2.643	0.003	0.002	0.003	1.372	0.096	3.837
20	0.2	0.3	2	0.524	7.284	0.047	0.058	4.990	0.011	0.009	2.643	0.005	0.002	0.005	2.062	0.217	8.670
20	0.1	0.3	2	0.524	7.284	0.047	0.058	7.057	0.011	0.009	2.643	0.010	0.002	0.010	4.133	0.871	34.823
20	0.85	0.3	2	0.524	7.284	0.047	0.058	2.421	0.011	0.009	2.643	0.001	0.002	0.001	0.479	0.012	0.467
20	0.1	0.3	2	0.524	7.284	0.047	0.058	6.317	0.011	0.009	2.643	0.008	0.002	0.008	3.309	0.558	22.329
20	0.2	0.3	2	0.524	7.284	0.047	0.058	4.466	0.011	0.009	2.643	0.004	0.002	0.004	1.650	0.139	5.554
20	0.3	0.3	2	0.524	7.284	0.047	0.058	3.647	0.011	0.009	2.643	0.003	0.002	0.003	1.097	0.061	2.455
20	0.4	0.3	2	0.524	7.284	0.047	0.058	3.158	0.011	0.009	2.643	0.002	0.002	0.002	0.821	0.034	1.374
20	0.5	0.3	2	0.524	7.284	0.047	0.058	2.825	0.011	0.009	2.643	0.002	0.002	0.002	0.655	0.022	0.875
20	0.6	0.3	2	0.524	7.284	0.047	0.058	2.579	0.011	0.009	2.643	0.001	0.002	0.001	0.544	0.015	0.604
20	0.5	0.325	2	0.524	7.284	0.047	0.058	3.032	0.011	0.009	2.540	0.002	0.002	0.002	0.756	0.029	1.165
20	0.4	0.325	2	0.524	7.284	0.047	0.058	3.390	0.011	0.009	2.540	0.002	0.002	0.002	0.947	0.046	1.829
20	0.3	0.325	2	0.524	7.284	0.047	0.058	3.915	0.011	0.009	2.540	0.003	0.002	0.003	1.266	0.082	3.266
20	0.2	0.325	2	0.524	7.284	0.047	0.058	4.794	0.011	0.009	2.540	0.005	0.002	0.005	1.903	0.185	7.382
20	0.1	0.325	2	0.524	7.284	0.047	0.058	6.780	0.011	0.009	2.540	0.009	0.002	0.009	3.814	0.742	29.661
20	0.85	0.325	2	0.524	7.284	0.047	0.058	2.326	0.011	0.009	2.540	0.001	0.002	0.001	0.441	0.010	0.397
20	0.1	0.325	2	0.524	7.284	0.047	0.058	6.069	0.011	0.009	2.540	0.007	0.002	0.007	3.054	0.475	19.018
20	0.2	0.325	2	0.524	7.284	0.047	0.058	4.291	0.011	0.009	2.540	0.004	0.002	0.004	1.523	0.118	4.728

Q	X	Z	V _{zi}	Z _{core}	V _{zj}	h _{down}	h _{up}	V _{xmax}	q _{up}	q _{down}	V(z)	FQSI	G _b	I _{net}	V _{up}	H _{up}	H _{up} /z
l/s	m	m	m/s	m	m/s	m	m	m/s	m ² /s	m ² /s	m/s	Ns	kg/m ²	Ns	m/s	m	
			Q=VA	Z=5*Bj	Eq. 25	Eq. 61		Eq. 63	Eq. 61&62		Eq. 60	Fig.2.18	Eq. 59	Eq.55		Eq. 58	
20	0.3	0.325	2	0.524	7.284	0.047	0.058	3.504	0.011	0.009	2.540	0.002	0.002	0.002	1.012	0.052	2.090
20	0.4	0.325	2	0.524	7.284	0.047	0.058	3.034	0.011	0.009	2.540	0.002	0.002	0.002	0.757	0.029	1.169
20	0.5	0.325	2	0.524	7.284	0.047	0.058	2.714	0.011	0.009	2.540	0.001	0.002	0.001	0.604	0.019	0.744
20	0.6	0.325	2	0.524	7.284	0.047	0.058	2.478	0.011	0.009	2.540	0.001	0.002	0.001	0.502	0.013	0.514
20	0.5	0.35	2	0.524	7.284	0.047	0.058	2.922	0.011	0.009	2.447	0.002	0.002	0.002	0.701	0.025	1.003
20	0.4	0.35	2	0.524	7.284	0.047	0.058	3.267	0.011	0.009	2.447	0.002	0.002	0.002	0.879	0.039	1.575
20	0.3	0.35	2	0.524	7.284	0.047	0.058	3.772	0.011	0.009	2.447	0.003	0.002	0.003	1.175	0.070	2.813
20	0.2	0.35	2	0.524	7.284	0.047	0.058	4.620	0.011	0.009	2.447	0.004	0.002	0.004	1.766	0.159	6.361
20	0.1	0.35	2	0.524	7.284	0.047	0.058	6.533	0.011	0.009	2.447	0.008	0.002	0.008	3.541	0.639	25.566
20	0.85	0.35	2	0.524	7.284	0.047	0.058	2.241	0.011	0.009	2.447	0.001	0.002	0.001	0.409	0.009	0.341
20	0.1	0.35	2	0.524	7.284	0.047	0.058	5.848	0.011	0.009	2.447	0.007	0.002	0.007	2.835	0.410	16.391
20	0.2	0.35	2	0.524	7.284	0.047	0.058	4.135	0.011	0.009	2.447	0.003	0.002	0.003	1.413	0.102	4.073
20	0.3	0.35	2	0.524	7.284	0.047	0.058	3.376	0.011	0.009	2.447	0.002	0.002	0.002	0.939	0.045	1.799
20	0.4	0.35	2	0.524	7.284	0.047	0.058	2.924	0.011	0.009	2.447	0.002	0.002	0.002	0.702	0.025	1.006
20	0.5	0.35	2	0.524	7.284	0.047	0.058	2.615	0.011	0.009	2.447	0.001	0.002	0.001	0.560	0.016	0.640
20	0.6	0.35	2	0.524	7.284	0.047	0.058	2.387	0.011	0.009	2.447	0.001	0.002	0.001	0.465	0.011	0.442
20	0.5	0.375	2	0.524	7.284	0.047	0.058	2.823	0.011	0.009	2.364	0.002	0.002	0.002	0.654	0.022	0.872
20	0.4	0.375	2	0.524	7.284	0.047	0.058	3.156	0.011	0.009	2.364	0.002	0.002	0.002	0.820	0.034	1.370
20	0.3	0.375	2	0.524	7.284	0.047	0.058	3.644	0.011	0.009	2.364	0.003	0.002	0.003	1.096	0.061	2.448
20	0.2	0.375	2	0.524	7.284	0.047	0.058	4.463	0.011	0.009	2.364	0.004	0.002	0.004	1.648	0.138	5.537
20	0.1	0.375	2	0.524	7.284	0.047	0.058	6.312	0.011	0.009	2.364	0.008	0.002	0.008	3.305	0.557	22.263
20	0.85	0.375	2	0.524	7.284	0.047	0.058	2.165	0.011	0.009	2.364	0.001	0.002	0.001	0.381	0.007	0.296
20	0.1	0.375	2	0.524	7.284	0.047	0.058	5.650	0.011	0.009	2.364	0.006	0.002	0.006	2.646	0.357	14.272
20	0.2	0.375	2	0.524	7.284	0.047	0.058	3.995	0.011	0.009	2.364	0.003	0.002	0.003	1.319	0.089	3.545
20	0.3	0.375	2	0.524	7.284	0.047	0.058	3.262	0.011	0.009	2.364	0.002	0.002	0.002	0.876	0.039	1.565
20	0.4	0.375	2	0.524	7.284	0.047	0.058	2.825	0.011	0.009	2.364	0.002	0.002	0.002	0.655	0.022	0.875

Q	X	Z	V _{zi}	Z _{core}	V _{zj}	h _{down}	h _{up}	V _{xmax}	q _{up}	q _{down}	V(z)	FQSI	G _b	I _{net}	V _{up}	H _{up}	H _{up} /z
l/s	m	m	m/s	m	m/s	m	m	m/s	m ² /s	m ² /s	m/s	Ns	kg/m ²	Ns	m/s	m	
			Q=VA	Z=5*Bj	Eq. 25	Eq.61		Eq. 63	Eq. 61&62		Eq. 60	Fig.2.18	Eq. 59	Eq.55		Eq. 58	
20	0.5	0.375	2	0.524	7.284	0.047	0.058	2.527	0.011	0.009	2.364	0.001	0.002	0.001	0.522	0.014	0.556
20	0.6	0.375	2	0.524	7.284	0.047	0.058	2.306	0.011	0.009	2.364	0.001	0.002	0.001	0.434	0.010	0.384
20	0.5	0.4	2	0.524	7.284	0.047	0.058	2.733	0.011	0.009	2.289	0.001	0.002	0.001	0.613	0.019	0.765
20	0.4	0.4	2	0.524	7.284	0.047	0.058	3.056	0.011	0.009	2.289	0.002	0.002	0.002	0.768	0.030	1.202
20	0.3	0.4	2	0.524	7.284	0.047	0.058	3.528	0.011	0.009	2.289	0.002	0.002	0.002	1.027	0.054	2.150
20	0.2	0.4	2	0.524	7.284	0.047	0.058	4.321	0.011	0.009	2.289	0.004	0.002	0.004	1.544	0.122	4.863
20	0.1	0.4	2	0.524	7.284	0.047	0.058	6.112	0.011	0.009	2.289	0.007	0.002	0.007	3.098	0.489	19.561
20	0.85	0.4	2	0.524	7.284	0.047	0.058	2.096	0.011	0.009	2.289	0.001	0.002	0.001	0.357	0.006	0.260
20	0.1	0.4	2	0.524	7.284	0.047	0.058	5.470	0.011	0.009	2.289	0.006	0.002	0.006	2.480	0.313	12.538
20	0.2	0.4	2	0.524	7.284	0.047	0.058	3.868	0.011	0.009	2.289	0.003	0.002	0.003	1.236	0.078	3.113
20	0.3	0.4	2	0.524	7.284	0.047	0.058	3.158	0.011	0.009	2.289	0.002	0.002	0.002	0.821	0.034	1.374
20	0.4	0.4	2	0.524	7.284	0.047	0.058	2.735	0.011	0.009	2.289	0.001	0.002	0.001	0.614	0.019	0.768
20	0.5	0.4	2	0.524	7.284	0.047	0.058	2.446	0.011	0.009	2.289	0.001	0.002	0.001	0.489	0.012	0.488
20	0.6	0.4	2	0.524	7.284	0.047	0.058	2.233	0.011	0.009	2.289	0.001	0.002	0.001	0.406	0.008	0.336
20	0.5	0.425	2	0.524	7.284	0.047	0.058	2.652	0.011	0.009	2.221	0.001	0.002	0.001	0.576	0.017	0.677
20	0.4	0.425	2	0.524	7.284	0.047	0.058	2.965	0.011	0.009	2.221	0.002	0.002	0.002	0.722	0.027	1.064
20	0.3	0.425	2	0.524	7.284	0.047	0.058	3.423	0.011	0.009	2.221	0.002	0.002	0.002	0.966	0.048	1.902
20	0.2	0.425	2	0.524	7.284	0.047	0.058	4.192	0.011	0.009	2.221	0.003	0.002	0.003	1.453	0.108	4.305
20	0.1	0.425	2	0.524	7.284	0.047	0.058	5.929	0.011	0.009	2.221	0.007	0.002	0.007	2.915	0.433	17.321
20	0.85	0.425	2	0.524	7.284	0.047	0.058	2.034	0.011	0.009	2.221	0.001	0.002	0.001	0.335	0.006	0.229
20	0.1	0.425	2	0.524	7.284	0.047	0.058	5.307	0.011	0.009	2.221	0.006	0.002	0.006	2.334	0.278	11.102
20	0.2	0.425	2	0.524	7.284	0.047	0.058	3.753	0.011	0.009	2.221	0.003	0.002	0.003	1.163	0.069	2.755
20	0.3	0.425	2	0.524	7.284	0.047	0.058	3.064	0.011	0.009	2.221	0.002	0.002	0.002	0.772	0.030	1.216
20	0.4	0.425	2	0.524	7.284	0.047	0.058	2.653	0.011	0.009	2.221	0.001	0.002	0.001	0.577	0.017	0.679
20	0.5	0.425	2	0.524	7.284	0.047	0.058	2.373	0.011	0.009	2.221	0.001	0.002	0.001	0.460	0.011	0.431
20	0.6	0.425	2	0.524	7.284	0.047	0.058	2.167	0.011	0.009	2.221	0.001	0.002	0.001	0.382	0.007	0.297

Q	X	Z	V _{zi}	Z _{core}	V _{zj}	h _{down}	h _{up}	V _{xmax}	q _{up}	q _{down}	V(z)	FQSI	G _b	I _{net}	V _{up}	H _{up}	H _{up} /z
l/s	m	m	m/s	m	m/s	m	m	m/s	m ² /s	m ² /s	m/s	Ns	kg/m ²	Ns	m/s	m	
			Q=VA	Z=5*Bj	Eq. 25	Eq. 61		Eq. 63	Eq. 61&62		Eq. 60	Fig.2.18	Eq. 59	Eq.55		Eq. 58	
20	0.5	0.45	2	0.524	7.284	0.047	0.058	2.577	0.011	0.009	2.158	0.001	0.002	0.001	0.544	0.015	0.603
20	0.4	0.45	2	0.524	7.284	0.047	0.058	2.881	0.011	0.009	2.158	0.002	0.002	0.002	0.682	0.024	0.947
20	0.3	0.45	2	0.524	7.284	0.047	0.058	3.327	0.011	0.009	2.158	0.002	0.002	0.002	0.912	0.042	1.695
20	0.2	0.45	2	0.524	7.284	0.047	0.058	4.074	0.011	0.009	2.158	0.003	0.002	0.003	1.372	0.096	3.837
20	0.1	0.45	2	0.524	7.284	0.047	0.058	5.762	0.011	0.009	2.158	0.007	0.002	0.007	2.752	0.386	15.445
20	0.85	0.45	2	0.524	7.284	0.047	0.058	1.976	0.011	0.009	2.158	0.001	0.002	0.001	0.316	0.005	0.204
20	0.1	0.45	2	0.524	7.284	0.047	0.058	5.157	0.011	0.009	2.158	0.005	0.002	0.005	2.203	0.247	9.898
20	0.2	0.45	2	0.524	7.284	0.047	0.058	3.647	0.011	0.009	2.158	0.003	0.002	0.003	1.097	0.061	2.455
20	0.3	0.45	2	0.524	7.284	0.047	0.058	2.978	0.011	0.009	2.158	0.002	0.002	0.002	0.729	0.027	1.083
20	0.4	0.45	2	0.524	7.284	0.047	0.058	2.579	0.011	0.009	2.158	0.001	0.002	0.001	0.544	0.015	0.604
20	0.5	0.45	2	0.524	7.284	0.047	0.058	2.306	0.011	0.009	2.158	0.001	0.002	0.001	0.434	0.010	0.384
20	0.6	0.45	2	0.524	7.284	0.047	0.058	2.106	0.011	0.009	2.158	0.001	0.002	0.001	0.360	0.007	0.264
20	0.5	0.475	2	0.524	7.284	0.047	0.058	2.508	0.011	0.009	2.101	0.001	0.002	0.001	0.515	0.013	0.540
20	0.4	0.475	2	0.524	7.284	0.047	0.058	2.804	0.011	0.009	2.101	0.002	0.002	0.002	0.645	0.021	0.849
20	0.3	0.475	2	0.524	7.284	0.047	0.058	3.238	0.011	0.009	2.101	0.002	0.002	0.002	0.863	0.038	1.520
20	0.2	0.475	2	0.524	7.284	0.047	0.058	3.966	0.011	0.009	2.101	0.003	0.002	0.003	1.299	0.086	3.442
20	0.1	0.475	2	0.524	7.284	0.047	0.058	5.608	0.011	0.009	2.101	0.006	0.002	0.006	2.607	0.346	13.857
20	0.85	0.475	2	0.524	7.284	0.047	0.058	1.924	0.011	0.009	2.101	0.001	0.002	0.001	0.299	0.005	0.182
20	0.1	0.475	2	0.524	7.284	0.047	0.058	5.020	0.011	0.009	2.101	0.005	0.002	0.005	2.087	0.222	8.880
20	0.2	0.475	2	0.524	7.284	0.047	0.058	3.550	0.011	0.009	2.101	0.002	0.002	0.002	1.039	0.055	2.202
20	0.3	0.475	2	0.524	7.284	0.047	0.058	2.898	0.011	0.009	2.101	0.002	0.002	0.002	0.690	0.024	0.971
20	0.4	0.475	2	0.524	7.284	0.047	0.058	2.510	0.011	0.009	2.101	0.001	0.002	0.001	0.515	0.014	0.541
20	0.5	0.475	2	0.524	7.284	0.047	0.058	2.245	0.011	0.009	2.101	0.001	0.002	0.001	0.411	0.009	0.344
20	0.6	0.475	2	0.524	7.284	0.047	0.058	2.049	0.011	0.009	2.101	0.001	0.002	0.001	0.341	0.006	0.237
20	0.5	0.5	2	0.524	7.284	0.047	0.058	2.445	0.011	0.009	2.047	0.001	0.002	0.001	0.488	0.012	0.486
20	0.4	0.5	2	0.524	7.284	0.047	0.058	2.733	0.011	0.009	2.047	0.001	0.002	0.001	0.613	0.019	0.765

Q	X	Z	V _{zi}	Z _{core}	V _{zj}	h _{down}	h _{up}	V _{xmax}	q _{up}	q _{down}	V(z)	FQSI	G _b	I _{net}	V _{up}	H _{up}	H _{up} /z
l/s	m	m	m/s	m	m/s	m	m	m/s	m ² /s	m ² /s	m/s	Ns	kg/m ²	Ns	m/s	m	
			Q=VA	Z=5*Bj	Eq. 25	Eq. 61		Eq. 63	Eq.61&62		Eq. 60	Fig.2.18	Eq. 59	Eq.55		Eq. 58	
20	0.3	0.5	2	0.524	7.284	0.047	0.058	3.156	0.011	0.009	2.047	0.002	0.002	0.002	0.820	0.034	1.370
20	0.2	0.5	2	0.524	7.284	0.047	0.058	3.865	0.011	0.009	2.047	0.003	0.002	0.003	1.234	0.078	3.104
20	0.1	0.5	2	0.524	7.284	0.047	0.058	5.466	0.011	0.009	2.047	0.006	0.002	0.006	2.476	0.313	12.502
20	0.85	0.5	2	0.524	7.284	0.047	0.058	1.875	0.011	0.009	2.047	0.001	0.002	0.001	0.284	0.004	0.164
20	0.1	0.5	2	0.524	7.284	0.047	0.058	4.893	0.011	0.009	2.047	0.005	0.002	0.005	1.982	0.200	8.011
20	0.2	0.5	2	0.524	7.284	0.047	0.058	3.460	0.011	0.009	2.047	0.002	0.002	0.002	0.987	0.050	1.986
20	0.3	0.5	2	0.524	7.284	0.047	0.058	2.825	0.011	0.009	2.047	0.002	0.002	0.002	0.655	0.022	0.875
20	0.4	0.5	2	0.524	7.284	0.047	0.058	2.446	0.011	0.009	2.047	0.001	0.002	0.001	0.489	0.012	0.488
20	0.5	0.5	2	0.524	7.284	0.047	0.058	2.188	0.011	0.009	2.047	0.001	0.002	0.001	0.390	0.008	0.309
20	0.6	0.5	2	0.524	7.284	0.047	0.058	1.997	0.011	0.009	2.047	0.001	0.002	0.001	0.323	0.005	0.213
20	0.5	0.525	2	0.524	7.284	0.047	0.058	2.386	0.011	0.009	1.998	0.001	0.002	0.001	0.465	0.011	0.440
20	0.4	0.525	2	0.524	7.284	0.047	0.058	2.667	0.011	0.009	1.998	0.001	0.002	0.001	0.583	0.017	0.693
20	0.3	0.525	2	0.524	7.284	0.047	0.058	3.080	0.011	0.009	1.998	0.002	0.002	0.002	0.780	0.031	1.241
20	0.2	0.525	2	0.524	7.284	0.047	0.058	3.772	0.011	0.009	1.998	0.003	0.002	0.003	1.175	0.070	2.813
20	0.1	0.525	2	0.524	7.284	0.047	0.058	5.335	0.011	0.009	1.998	0.006	0.002	0.006	2.358	0.283	11.335
20	0.85	0.525	2	0.524	7.284	0.047	0.058	1.830	0.011	0.009	1.998	0.001	0.002	0.001	0.270	0.004	0.148
20	0.1	0.525	2	0.524	7.284	0.047	0.058	4.775	0.011	0.009	1.998	0.005	0.002	0.004	1.887	0.182	7.263
20	0.2	0.525	2	0.524	7.284	0.047	0.058	3.376	0.011	0.009	1.998	0.002	0.002	0.002	0.939	0.045	1.799
20	0.3	0.525	2	0.524	7.284	0.047	0.058	2.757	0.011	0.009	1.998	0.002	0.002	0.001	0.623	0.020	0.792
20	0.4	0.525	2	0.524	7.284	0.047	0.058	2.387	0.011	0.009	1.998	0.001	0.002	0.001	0.465	0.011	0.442
20	0.5	0.525	2	0.524	7.284	0.047	0.058	2.135	0.011	0.009	1.998	0.001	0.002	0.001	0.371	0.007	0.280
20	0.6	0.525	2	0.524	7.284	0.047	0.058	1.949	0.011	0.009	1.998	0.001	0.002	0.001	0.307	0.005	0.193
20	0.5	0.55	2	0.524	7.284	0.047	0.058	2.331	0.011	0.009	1.952	0.001	0.002	0.001	0.443	0.010	0.401
20	0.4	0.55	2	0.524	7.284	0.047	0.058	2.606	0.011	0.009	1.952	0.001	0.002	0.001	0.556	0.016	0.631
20	0.3	0.55	2	0.524	7.284	0.047	0.058	3.009	0.011	0.009	1.952	0.002	0.002	0.002	0.744	0.028	1.130
20	0.2	0.55	2	0.524	7.284	0.047	0.058	3.685	0.011	0.009	1.952	0.003	0.002	0.003	1.121	0.064	2.562

Q	X	Z	V _{zi}	Z _{core}	V _{zj}	h _{down}	h _{up}	V _{xmax}	q _{up}	q _{down}	V(z)	FQSI	G _b	I _{net}	V _{up}	H _{up}	H _{up} /z
l/s	m	m	m/s	m	m/s	m	m	m/s	m ² /s	m ² /s	m/s	Ns	kg/m ²	Ns	m/s	m	
			Q=VA	Z=5*Bj	Eq. 25	Eq. 61		Eq. 63	Eq. 61&62		Eq. 60	Fig.2.18	Eq. 59	Eq.55		Eq. 58	
20	0.1	0.55	2	0.524	7.284	0.047	0.058	5.212	0.011	0.009	1.952	0.005	0.002	0.005	2.250	0.258	10.325
20	0.85	0.55	2	0.524	7.284	0.047	0.058	1.788	0.011	0.009	1.952	0.001	0.002	0.001	0.257	0.003	0.135
20	0.1	0.55	2	0.524	7.284	0.047	0.058	4.665	0.011	0.009	1.952	0.004	0.002	0.004	1.801	0.165	6.615
20	0.2	0.55	2	0.524	7.284	0.047	0.058	3.299	0.011	0.009	1.952	0.002	0.002	0.002	0.896	0.041	1.638
20	0.3	0.55	2	0.524	7.284	0.047	0.058	2.693	0.011	0.009	1.952	0.001	0.002	0.001	0.595	0.018	0.721
20	0.4	0.55	2	0.524	7.284	0.047	0.058	2.333	0.011	0.009	1.952	0.001	0.002	0.001	0.444	0.010	0.402
20	0.5	0.55	2	0.524	7.284	0.047	0.058	2.086	0.011	0.009	1.952	0.001	0.002	0.001	0.353	0.006	0.255
20	0.6	0.55	2	0.524	7.284	0.047	0.058	1.905	0.011	0.009	1.952	0.001	0.002	0.001	0.293	0.004	0.175
20	0.5	0.575	2	0.524	7.284	0.047	0.058	2.280	0.011	0.009	1.909	0.001	0.002	0.001	0.424	0.009	0.366
20	0.4	0.575	2	0.524	7.284	0.047	0.058	2.549	0.011	0.009	1.909	0.001	0.002	0.001	0.532	0.014	0.576
20	0.3	0.575	2	0.524	7.284	0.047	0.058	2.943	0.011	0.009	1.909	0.002	0.002	0.002	0.712	0.026	1.033
20	0.2	0.575	2	0.524	7.284	0.047	0.058	3.604	0.011	0.009	1.909	0.003	0.002	0.003	1.072	0.059	2.342
20	0.1	0.575	2	0.524	7.284	0.047	0.058	5.097	0.011	0.009	1.909	0.005	0.002	0.005	2.152	0.236	9.443
20	0.85	0.575	2	0.524	7.284	0.047	0.058	1.748	0.011	0.009	1.909	0.001	0.002	0.001	0.246	0.003	0.123
20	0.1	0.575	2	0.524	7.284	0.047	0.058	4.563	0.011	0.009	1.909	0.004	0.002	0.004	1.723	0.151	6.050
20	0.2	0.575	2	0.524	7.284	0.047	0.058	3.226	0.011	0.009	1.909	0.002	0.002	0.002	0.857	0.037	1.497
20	0.3	0.575	2	0.524	7.284	0.047	0.058	2.634	0.011	0.009	1.909	0.001	0.002	0.001	0.569	0.016	0.659
20	0.4	0.575	2	0.524	7.284	0.047	0.058	2.281	0.011	0.009	1.909	0.001	0.002	0.001	0.424	0.009	0.367
20	0.5	0.575	2	0.524	7.284	0.047	0.058	2.040	0.011	0.009	1.909	0.001	0.002	0.001	0.338	0.006	0.232
20	0.6	0.575	2	0.524	7.284	0.047	0.058	1.863	0.011	0.009	1.909	0.001	0.002	0.001	0.280	0.004	0.160

Table D 0.11. Quasi-steady method of Q=20 l/s, H=4 m and TW=0.5 m

Q	X	Z	Vzi	Zcore	Vzj	hdown	hup	Vxmax	qup	qdown	V(z)	FQSI	Gb	Inet	Vup	Hup	Hup/z
l/s	m	m	m/s	m	m/s	m	m	m/s	m ² /s	m ² /s	m/s	Ns	kg/m ²	Ns	m/s	m	
Measured	Measured		Q=VA	Z=5*Bj	eq. 25	Eq61		Eq. 63	Eq. 61&62		Eq. 60	Fig.2.18	Eq. 59	Eq.55		Eq. 58	
20	0.95	0	2	0.484	8.525	0.043	0.054	1.639	0.011	0.009	8.525						
20	0.95	0.042	2	0.484	8.525	0.043	0.054	1.639	0.011	0.009	6.819						
20	0.95	0.083	2	0.484	8.525	0.043	0.054	1.639	0.011	0.009	4.822						
20	0.95	0.125	2	0.484	8.525	0.043	0.054	1.639	0.011	0.009	3.937						
20	0.95	0.167	2	0.484	8.525	0.043	0.054	1.639	0.011	0.009	3.410						
20	0.95	0.208	2	0.484	8.525	0.043	0.054	1.639	0.011	0.009	3.050						
20	0.95	0.250	2	0.484	8.525	0.043	0.054	1.639	0.011	0.009	2.784						
20	0.95	0.292	2	0.484	8.525	0.043	0.054	1.639	0.011	0.009	2.577						
20	0.95	0.333	2	0.484	8.525	0.043	0.054	1.639	0.011	0.009	2.411						
20	0.95	0.375	2	0.484	8.525	0.043	0.054	1.639	0.011	0.009	2.273						
20	0.95	0.417	2	0.484	8.525	0.043	0.054	1.639	0.011	0.009	2.156						
20	0.95	0.458	2	0.484	8.525	0.043	0.054	1.639	0.011	0.009	2.056						
20	0.95	0.5	2	0.484	8.525	0.043	0.054	1.639	0.011	0.009	1.968						
20	0.5	0.5	2	0.484	8.525	0.043	0.054	2.260	0.011	0.009	1.968	0.001	0.002	0.001	0.416	0.009	0.353
20	0.4	0.5	2	0.484	8.525	0.043	0.054	2.526	0.011	0.009	1.968	0.001	0.002	0.001	0.522	0.014	0.556
20	0.3	0.5	2	0.484	8.525	0.043	0.054	2.917	0.011	0.009	1.968	0.002	0.002	0.002	0.699	0.025	0.997
20	0.2	0.5	2	0.484	8.525	0.043	0.054	3.573	0.011	0.009	1.968	0.003	0.002	0.003	1.053	0.057	2.261
20	0.1	0.5	2	0.484	8.525	0.043	0.054	5.053	0.011	0.009	1.968	0.005	0.002	0.005	2.115	0.228	9.116
20	0.95	0.5	2	0.484	8.525	0.043	0.054	1.467	0.011	0.009	1.968	0.000	0.002	0.000	0.171	0.001	0.059
20	0.1	0.5	2	0.484	8.525	0.043	0.054	4.523	0.011	0.009	1.968	0.004	0.002	0.004	1.692	0.146	5.839
20	0.2	0.5	2	0.484	8.525	0.043	0.054	3.198	0.011	0.009	1.968	0.002	0.002	0.002	0.842	0.036	1.445
20	0.3	0.5	2	0.484	8.525	0.043	0.054	2.611	0.011	0.009	1.968	0.001	0.002	0.001	0.558	0.016	0.636
20	0.4	0.5	2	0.484	8.525	0.043	0.054	2.261	0.011	0.009	1.968	0.001	0.002	0.001	0.417	0.009	0.354
20	0.5	0.5	2	0.484	8.525	0.043	0.054	2.023	0.011	0.009	1.968	0.001	0.002	0.001	0.332	0.006	0.224
20	0.6	0.5	2	0.484	8.525	0.043	0.054	1.846	0.011	0.009	1.968	0.001	0.002	0.001	0.275	0.004	0.154

Q	X	Z	V _{zi}	Z _{core}	V _{zj}	h _{down}	h _{up}	V _{xmax}	q _{up}	q _{down}	V(z)	FQSI	G _b	I _{net}	V _{up}	H _{up}	H _{up} /z
l/s	m	m	m/s	m	m/s	m	m	m/s	m ² /s	m ² /s	m/s	Ns	kg/m ²	Ns	m/s	m	
			Q=VA	Z=5*Bj	Eq. 25	Eq.61		Eq. 63	Eq. 61&62		Eq. 60	Fig.2.18	Eq. 59	Eq.55		Eq. 58	
20	0.5	0.525	2	0.484	8.525	0.043	0.054	2.205	0.011	0.009	1.921	0.001	0.002	0.001	0.396	0.008	0.319
20	0.4	0.525	2	0.484	8.525	0.043	0.054	2.465	0.011	0.009	1.921	0.001	0.002	0.001	0.497	0.013	0.504
20	0.3	0.525	2	0.484	8.525	0.043	0.054	2.847	0.011	0.009	1.921	0.002	0.002	0.002	0.665	0.023	0.903
20	0.2	0.525	2	0.484	8.525	0.043	0.054	3.487	0.011	0.009	1.921	0.002	0.002	0.002	1.002	0.051	2.049
20	0.1	0.525	2	0.484	8.525	0.043	0.054	4.931	0.011	0.009	1.921	0.005	0.002	0.005	2.013	0.207	8.265
20	0.95	0.525	2	0.484	8.525	0.043	0.054	1.432	0.011	0.009	1.921	0.000	0.002	0.000	0.162	0.001	0.053
20	0.1	0.525	2	0.484	8.525	0.043	0.054	4.414	0.011	0.009	1.921	0.004	0.002	0.004	1.611	0.132	5.294
20	0.2	0.525	2	0.484	8.525	0.043	0.054	3.121	0.011	0.009	1.921	0.002	0.002	0.002	0.801	0.033	1.309
20	0.3	0.525	2	0.484	8.525	0.043	0.054	2.548	0.011	0.009	1.921	0.001	0.002	0.001	0.531	0.014	0.576
20	0.4	0.525	2	0.484	8.525	0.043	0.054	2.207	0.011	0.009	1.921	0.001	0.002	0.001	0.396	0.008	0.320
20	0.5	0.525	2	0.484	8.525	0.043	0.054	1.974	0.011	0.009	1.921	0.001	0.002	0.001	0.315	0.005	0.203
20	0.6	0.525	2	0.484	8.525	0.043	0.054	1.802	0.011	0.009	1.921	0.001	0.002	0.001	0.261	0.003	0.139
20	0.5	0.55	2	0.484	8.525	0.043	0.054	2.154	0.011	0.009	1.877	0.001	0.002	0.001	0.377	0.007	0.291
20	0.4	0.55	2	0.484	8.525	0.043	0.054	2.409	0.011	0.009	1.877	0.001	0.002	0.001	0.474	0.011	0.458
20	0.3	0.55	2	0.484	8.525	0.043	0.054	2.781	0.011	0.009	1.877	0.002	0.002	0.002	0.635	0.021	0.822
20	0.2	0.55	2	0.484	8.525	0.043	0.054	3.407	0.011	0.009	1.877	0.002	0.002	0.002	0.956	0.047	1.865
20	0.1	0.55	2	0.484	8.525	0.043	0.054	4.818	0.011	0.009	1.877	0.005	0.002	0.005	1.922	0.188	7.528
20	0.95	0.55	2	0.484	8.525	0.043	0.054	1.399	0.011	0.009	1.877	0.000	0.002	0.000	0.154	0.001	0.049
20	0.1	0.55	2	0.484	8.525	0.043	0.054	4.312	0.011	0.009	1.877	0.004	0.002	0.004	1.538	0.121	4.821
20	0.2	0.55	2	0.484	8.525	0.043	0.054	3.049	0.011	0.009	1.877	0.002	0.002	0.002	0.765	0.030	1.192
20	0.3	0.55	2	0.484	8.525	0.043	0.054	2.490	0.011	0.009	1.877	0.001	0.002	0.001	0.507	0.013	0.524
20	0.4	0.55	2	0.484	8.525	0.043	0.054	2.156	0.011	0.009	1.877	0.001	0.002	0.001	0.378	0.007	0.291
20	0.5	0.55	2	0.484	8.525	0.043	0.054	1.928	0.011	0.009	1.877	0.001	0.002	0.001	0.301	0.005	0.184
20	0.6	0.55	2	0.484	8.525	0.043	0.054	1.760	0.011	0.009	1.877	0.001	0.002	0.001	0.249	0.003	0.127
20	0.5	0.575	2	0.484	8.525	0.043	0.054	2.107	0.011	0.009	1.836	0.001	0.002	0.001	0.361	0.007	0.265
20	0.4	0.575	2	0.484	8.525	0.043	0.054	2.356	0.011	0.009	1.836	0.001	0.002	0.001	0.453	0.010	0.418

Q	X	Z	V _{zi}	Z _{core}	V _{zj}	h _{down}	h _{up}	V _{xmax}	q _{up}	q _{down}	V(z)	FQSI	G _b	I _{net}	V _{up}	H _{up}	H _{up} /z
l/s	m	m	m/s	m	m/s	m	m	m/s	m ² /s	m ² /s	m/s	Ns	kg/m ²	Ns	m/s	m	
			Q=VA	Z=5*Bj	Eq. 25	Eq. 61		Eq. 63	Eq. 61&62		Eq. 60	Fig.2.18	Eq. 59	Eq.55		Eq. 58	
20	0.3	0.575	2	0.484	8.525	0.043	0.054	2.720	0.011	0.009	1.836	0.001	0.002	0.001	0.607	0.019	0.751
20	0.2	0.575	2	0.484	8.525	0.043	0.054	3.332	0.011	0.009	1.836	0.002	0.002	0.002	0.915	0.043	1.705
20	0.1	0.575	2	0.484	8.525	0.043	0.054	4.712	0.011	0.009	1.836	0.004	0.002	0.004	1.838	0.172	6.884
20	0.95	0.575	2	0.484	8.525	0.043	0.054	1.368	0.011	0.009	1.836	0.000	0.002	0.000	0.147	0.001	0.044
20	0.1	0.575	2	0.484	8.525	0.043	0.054	4.217	0.011	0.009	1.836	0.004	0.002	0.003	1.471	0.110	4.409
20	0.2	0.575	2	0.484	8.525	0.043	0.054	2.982	0.011	0.009	1.836	0.002	0.002	0.002	0.731	0.027	1.089
20	0.3	0.575	2	0.484	8.525	0.043	0.054	2.435	0.011	0.009	1.836	0.001	0.002	0.001	0.484	0.012	0.479
20	0.4	0.575	2	0.484	8.525	0.043	0.054	2.109	0.011	0.009	1.836	0.001	0.002	0.001	0.361	0.007	0.266
20	0.5	0.575	2	0.484	8.525	0.043	0.054	1.886	0.011	0.009	1.836	0.001	0.002	0.001	0.287	0.004	0.168
20	0.6	0.575	2	0.484	8.525	0.043	0.054	1.722	0.011	0.009	1.836	0.001	0.002	0.001	0.238	0.003	0.115
20	0.5	0.6	2	0.484	8.525	0.043	0.054	2.063	0.011	0.009	1.797	0.001	0.002	0.001	0.345	0.006	0.243
20	0.4	0.6	2	0.484	8.525	0.043	0.054	2.306	0.011	0.009	1.797	0.001	0.002	0.001	0.434	0.010	0.384
20	0.3	0.6	2	0.484	8.525	0.043	0.054	2.663	0.011	0.009	1.797	0.001	0.002	0.001	0.581	0.017	0.689
20	0.2	0.6	2	0.484	8.525	0.043	0.054	3.262	0.011	0.009	1.797	0.002	0.002	0.002	0.876	0.039	1.565
20	0.1	0.6	2	0.484	8.525	0.043	0.054	4.612	0.011	0.009	1.797	0.004	0.002	0.004	1.761	0.158	6.320
20	0.95	0.6	2	0.484	8.525	0.043	0.054	1.339	0.011	0.009	1.797	0.000	0.002	0.000	0.141	0.001	0.040
20	0.1	0.6	2	0.484	8.525	0.043	0.054	4.129	0.011	0.009	1.797	0.003	0.002	0.003	1.409	0.101	4.047
20	0.2	0.6	2	0.484	8.525	0.043	0.054	2.919	0.011	0.009	1.797	0.002	0.002	0.002	0.700	0.025	1.000
20	0.3	0.6	2	0.484	8.525	0.043	0.054	2.384	0.011	0.009	1.797	0.001	0.002	0.001	0.464	0.011	0.439
20	0.4	0.6	2	0.484	8.525	0.043	0.054	2.064	0.011	0.009	1.797	0.001	0.002	0.001	0.346	0.006	0.244
20	0.5	0.6	2	0.484	8.525	0.043	0.054	1.846	0.011	0.009	1.797	0.001	0.002	0.001	0.275	0.004	0.154
20	0.6	0.6	2	0.484	8.525	0.043	0.054	1.685	0.011	0.009	1.797	0.001	0.002	0.001	0.228	0.003	0.106
20	0.5	0.625	2	0.484	8.525	0.043	0.054	2.021	0.011	0.009	1.761	0.001	0.002	0.001	0.331	0.006	0.224
20	0.4	0.625	2	0.484	8.525	0.043	0.054	2.260	0.011	0.009	1.761	0.001	0.002	0.001	0.416	0.009	0.353
20	0.3	0.625	2	0.484	8.525	0.043	0.054	2.609	0.011	0.009	1.761	0.001	0.002	0.001	0.558	0.016	0.634
20	0.2	0.625	2	0.484	8.525	0.043	0.054	3.196	0.011	0.009	1.761	0.002	0.002	0.002	0.841	0.036	1.441

Q	X	Z	V _{zi}	Z _{core}	V _{zj}	h _{down}	h _{up}	V _{xmax}	q _{up}	q _{down}	V(z)	FQSI	G _b	I _{net}	V _{up}	H _{up}	H _{up} /z
l/s	m	m	m/s	m	m/s	m	m	m/s	m ² /s	m ² /s	m/s	Ns	kg/m ²	Ns	m/s	m	
			Q=VA	Z=5*Bj	Eq. 25	Eq. 61		Eq. 63	Eq. 61&62		Eq. 60	Fig.2.18	Eq. 59	Eq.53		Eq. 58	
20	0.1	0.625	2	0.484	8.525	0.043	0.054	4.519	0.011	0.009	1.761	0.004	0.002	0.004	1.690	0.146	5.822
20	0.95	0.625	2	0.484	8.525	0.043	0.054	1.312	0.011	0.009	1.761	0.000	0.002	0.000	0.135	0.001	0.037
20	0.1	0.625	2	0.484	8.525	0.043	0.054	4.045	0.011	0.009	1.761	0.003	0.002	0.003	1.352	0.093	3.728
20	0.2	0.625	2	0.484	8.525	0.043	0.054	2.860	0.011	0.009	1.761	0.002	0.002	0.002	0.672	0.023	0.920
20	0.3	0.625	2	0.484	8.525	0.043	0.054	2.335	0.011	0.009	1.761	0.001	0.002	0.001	0.445	0.010	0.404
20	0.4	0.625	2	0.484	8.525	0.043	0.054	2.023	0.011	0.009	1.761	0.001	0.002	0.001	0.332	0.006	0.224
20	0.5	0.625	2	0.484	8.525	0.043	0.054	1.809	0.011	0.009	1.761	0.001	0.002	0.001	0.264	0.004	0.142
20	0.6	0.625	2	0.484	8.525	0.043	0.054	1.651	0.011	0.009	1.761	0.001	0.002	0.001	0.218	0.002	0.097
20	0.5	0.65	2	0.484	8.525	0.043	0.054	1.982	0.011	0.009	1.726	0.001	0.002	0.001	0.318	0.005	0.206
20	0.4	0.65	2	0.484	8.525	0.043	0.054	2.216	0.011	0.009	1.726	0.001	0.002	0.001	0.400	0.008	0.326
20	0.3	0.65	2	0.484	8.525	0.043	0.054	2.559	0.011	0.009	1.726	0.001	0.002	0.001	0.536	0.015	0.585
20	0.2	0.65	2	0.484	8.525	0.043	0.054	3.134	0.011	0.009	1.726	0.002	0.002	0.002	0.808	0.033	1.331
20	0.1	0.65	2	0.484	8.525	0.043	0.054	4.432	0.011	0.009	1.726	0.004	0.002	0.004	1.625	0.135	5.381
20	0.95	0.65	2	0.484	8.525	0.043	0.054	1.287	0.011	0.009	1.726	0.000	0.002	0.000	0.129	0.001	0.034
20	0.1	0.65	2	0.484	8.525	0.043	0.054	3.967	0.011	0.009	1.726	0.003	0.002	0.003	1.300	0.086	3.445
20	0.2	0.65	2	0.484	8.525	0.043	0.054	2.805	0.011	0.009	1.726	0.002	0.002	0.002	0.646	0.021	0.850
20	0.3	0.65	2	0.484	8.525	0.043	0.054	2.290	0.011	0.009	1.726	0.001	0.002	0.001	0.428	0.009	0.373
20	0.4	0.65	2	0.484	8.525	0.043	0.054	1.983	0.011	0.009	1.726	0.001	0.002	0.001	0.319	0.005	0.207
20	0.5	0.65	2	0.484	8.525	0.043	0.054	1.774	0.011	0.009	1.726	0.001	0.002	0.001	0.253	0.003	0.131
20	0.6	0.65	2	0.484	8.525	0.043	0.054	1.619	0.011	0.009	1.726	0.001	0.002	0.000	0.210	0.002	0.090
20	0.5	0.675	2	0.484	8.525	0.043	0.054	1.945	0.011	0.009	1.694	0.001	0.002	0.001	0.306	0.005	0.191
20	0.4	0.675	2	0.484	8.525	0.043	0.054	2.174	0.011	0.009	1.694	0.001	0.002	0.001	0.385	0.008	0.302
20	0.3	0.675	2	0.484	8.525	0.043	0.054	2.511	0.011	0.009	1.694	0.001	0.002	0.001	0.516	0.014	0.542
20	0.2	0.675	2	0.484	8.525	0.043	0.054	3.075	0.011	0.009	1.694	0.002	0.002	0.002	0.778	0.031	1.233
20	0.1	0.675	2	0.484	8.525	0.043	0.054	4.349	0.011	0.009	1.694	0.004	0.002	0.004	1.564	0.125	4.988
20	0.95	0.675	2	0.484	8.525	0.043	0.054	1.263	0.011	0.009	1.694	0.000	0.002	0.000	0.124	0.001	0.031

Q	X	Z	V _{zi}	Z _{core}	V _{zj}	h _{down}	h _{up}	V _{xmax}	q _{up}	q _{down}	V(z)	FQSI	G _b	I _{net}	V _{up}	H _{up}	H _{up} /z
l/s	m	m	m/s	m	m/s	m	m	m/s	m ² /s	m ² /s	m/s	Ns	kg/m ²	Ns	m/s	m	
			Q=VA	Z=5*Bj	Eq. 25	Eq. 61		Eq. 63	Eq. 61&62		Eq. 58	Fig.2.17	Eq. 57	Eq.53		Eq. 56	
20	0.1	0.675	2	0.484	8.525	0.043	0.054	3.892	0.011	0.009	1.694	0.003	0.002	0.003	1.251	0.080	3.193
20	0.2	0.675	2	0.484	8.525	0.043	0.054	2.752	0.011	0.009	1.694	0.001	0.002	0.001	0.621	0.020	0.787
20	0.3	0.675	2	0.484	8.525	0.043	0.054	2.247	0.011	0.009	1.694	0.001	0.002	0.001	0.411	0.009	0.345
20	0.4	0.675	2	0.484	8.525	0.043	0.054	1.946	0.011	0.009	1.694	0.001	0.002	0.001	0.306	0.005	0.191
20	0.5	0.675	2	0.484	8.525	0.043	0.054	1.741	0.011	0.009	1.694	0.001	0.002	0.001	0.243	0.003	0.121
20	0.6	0.675	2	0.484	8.525	0.043	0.054	1.589	0.011	0.009	1.694	0.000	0.002	0.000	0.201	0.002	0.083
20	0.5	0.7	2	0.484	8.525	0.043	0.054	1.910	0.011	0.009	1.664	0.001	0.002	0.001	0.295	0.004	0.177
20	0.4	0.7	2	0.484	8.525	0.043	0.054	2.135	0.011	0.009	1.664	0.001	0.002	0.001	0.371	0.007	0.280
20	0.3	0.7	2	0.484	8.525	0.043	0.054	2.465	0.011	0.009	1.664	0.001	0.002	0.001	0.497	0.013	0.504
20	0.2	0.7	2	0.484	8.525	0.043	0.054	3.020	0.011	0.009	1.664	0.002	0.002	0.002	0.750	0.029	1.146
20	0.1	0.7	2	0.484	8.525	0.043	0.054	4.270	0.011	0.009	1.664	0.004	0.002	0.004	1.508	0.116	4.636
20	0.95	0.7	2	0.484	8.525	0.043	0.054	1.240	0.011	0.009	1.664	0.000	0.002	0.000	0.119	0.001	0.029
20	0.1	0.7	2	0.484	8.525	0.043	0.054	3.822	0.011	0.009	1.664	0.003	0.002	0.003	1.206	0.074	2.967
20	0.2	0.7	2	0.484	8.525	0.043	0.054	2.703	0.011	0.009	1.664	0.001	0.002	0.001	0.599	0.018	0.731
20	0.3	0.7	2	0.484	8.525	0.043	0.054	2.207	0.011	0.009	1.664	0.001	0.002	0.001	0.396	0.008	0.320
20	0.4	0.7	2	0.484	8.525	0.043	0.054	1.911	0.011	0.009	1.664	0.001	0.002	0.001	0.295	0.004	0.178
20	0.5	0.7	2	0.484	8.525	0.043	0.054	1.709	0.011	0.009	1.664	0.001	0.002	0.001	0.234	0.003	0.112
20	0.6	0.7	2	0.484	8.525	0.043	0.054	1.560	0.011	0.009	1.664	0.000	0.002	0.000	0.194	0.002	0.077
20	0.5	0.725	2	0.484	8.525	0.043	0.054	1.877	0.011	0.009	1.635	0.001	0.002	0.001	0.284	0.004	0.165
20	0.4	0.725	2	0.484	8.525	0.043	0.054	2.098	0.011	0.009	1.635	0.001	0.002	0.001	0.358	0.007	0.261
20	0.3	0.725	2	0.484	8.525	0.043	0.054	2.423	0.011	0.009	1.635	0.001	0.002	0.001	0.480	0.012	0.469
20	0.2	0.725	2	0.484	8.525	0.043	0.054	2.967	0.011	0.009	1.635	0.002	0.002	0.002	0.724	0.027	1.067
20	0.1	0.725	2	0.484	8.525	0.043	0.054	4.196	0.011	0.009	1.635	0.003	0.002	0.003	1.456	0.108	4.320
20	0.95	0.725	2	0.484	8.525	0.043	0.054	1.219	0.011	0.009	1.635	0.000	0.002	0.000	0.115	0.001	0.027
20	0.1	0.725	2	0.484	8.525	0.043	0.054	3.756	0.011	0.009	1.635	0.003	0.002	0.003	1.165	0.069	2.765
20	0.2	0.725	2	0.484	8.525	0.043	0.054	2.656	0.011	0.009	1.635	0.001	0.002	0.001	0.578	0.017	0.681

Q	X	Z	V _{zi}	Z _{core}	V _{zj}	h _{down}	h _{up}	V _{xmax}	q _{up}	q _{down}	V(z)	FQSI	G _b	I _{net}	V _{up}	H _{up}	H _{up} /z
l/s	m	m	m/s	m	m/s	m	m	m/s	m ² /s	m ² /s	m/s	Ns	kg/m ²	Ns	m/s	m	
			Q=VA	Z=5*Bj	Eq. 25	Eq. 61		Eq. 63	Eq. 61&62		Eq. 60	Fig.2.18	Eq. 59	Eq.55		Eq. 58	
20	0.3	0.725	2	0.484	8.525	0.043	0.054	2.168	0.011	0.009	1.635	0.001	0.002	0.001	0.382	0.007	0.298
20	0.4	0.725	2	0.484	8.525	0.043	0.054	1.878	0.011	0.009	1.635	0.001	0.002	0.001	0.285	0.004	0.165
20	0.5	0.725	2	0.484	8.525	0.043	0.054	1.680	0.011	0.009	1.635	0.001	0.002	0.001	0.226	0.003	0.104
20	0.6	0.725	2	0.484	8.525	0.043	0.054	1.533	0.011	0.009	1.635	0.000	0.002	0.000	0.187	0.002	0.071
20	0.5	0.75	2	0.484	8.525	0.043	0.054	1.845	0.011	0.009	1.607	0.001	0.002	0.001	0.275	0.004	0.154
20	0.4	0.75	2	0.484	8.525	0.043	0.054	2.063	0.011	0.009	1.607	0.001	0.002	0.001	0.345	0.006	0.243
20	0.3	0.75	2	0.484	8.525	0.043	0.054	2.382	0.011	0.009	1.607	0.001	0.002	0.001	0.463	0.011	0.438
20	0.2	0.75	2	0.484	8.525	0.043	0.054	2.917	0.011	0.009	1.607	0.002	0.002	0.002	0.699	0.025	0.997
20	0.1	0.75	2	0.484	8.525	0.043	0.054	4.126	0.011	0.009	1.607	0.003	0.002	0.003	1.407	0.101	4.035
20	0.95	0.75	2	0.484	8.525	0.043	0.054	1.198	0.011	0.009	1.607	0.000	0.002	0.000	0.111	0.001	0.025
20	0.1	0.75	2	0.484	8.525	0.043	0.054	3.693	0.011	0.009	1.607	0.003	0.002	0.003	1.125	0.065	2.582
20	0.2	0.75	2	0.484	8.525	0.043	0.054	2.611	0.011	0.009	1.607	0.001	0.002	0.001	0.558	0.016	0.636
20	0.3	0.75	2	0.484	8.525	0.043	0.054	2.132	0.011	0.009	1.607	0.001	0.002	0.001	0.369	0.007	0.278
20	0.4	0.75	2	0.484	8.525	0.043	0.054	1.846	0.011	0.009	1.607	0.001	0.002	0.001	0.275	0.004	0.154
20	0.5	0.75	2	0.484	8.525	0.043	0.054	1.651	0.011	0.009	1.607	0.001	0.002	0.001	0.218	0.002	0.097
20	0.6	0.75	2	0.484	8.525	0.043	0.054	1.508	0.011	0.009	1.607	0.000	0.002	0.000	0.180	0.002	0.066
20	0.5	0.775	2	0.484	8.525	0.043	0.054	1.815	0.011	0.009	1.581	0.001	0.002	0.001	0.265	0.004	0.144
20	0.4	0.775	2	0.484	8.525	0.043	0.054	2.029	0.011	0.009	1.581	0.001	0.002	0.001	0.334	0.006	0.227
20	0.3	0.775	2	0.484	8.525	0.043	0.054	2.343	0.011	0.009	1.581	0.001	0.002	0.001	0.448	0.010	0.409
20	0.2	0.775	2	0.484	8.525	0.043	0.054	2.870	0.011	0.009	1.581	0.002	0.002	0.002	0.676	0.023	0.933
20	0.1	0.775	2	0.484	8.525	0.043	0.054	4.058	0.011	0.009	1.581	0.003	0.002	0.003	1.361	0.094	3.777
20	0.95	0.775	2	0.484	8.525	0.043	0.054	1.179	0.011	0.009	1.581	0.000	0.002	0.000	0.107	0.001	0.023
20	0.1	0.775	2	0.484	8.525	0.043	0.054	3.633	0.011	0.009	1.581	0.003	0.002	0.003	1.089	0.060	2.417
20	0.2	0.775	2	0.484	8.525	0.043	0.054	2.569	0.011	0.009	1.581	0.001	0.002	0.001	0.540	0.015	0.595
20	0.3	0.775	2	0.484	8.525	0.043	0.054	2.097	0.011	0.009	1.581	0.001	0.002	0.001	0.357	0.007	0.260
20	0.4	0.775	2	0.484	8.525	0.043	0.054	1.816	0.011	0.009	1.581	0.001	0.002	0.001	0.266	0.004	0.144

Q	X	Z	V _{zi}	Z _{core}	V _{zj}	h _{down}	h _{up}	V _{xmax}	q _{up}	q _{down}	V(z)	FQSI	G _b	I _{net}	V _{up}	H _{up}	H _{up} /z
l/s	m	m	m/s	m	m/s	m	m	m/s	m ² /s	m ² /s	m/s	Ns	kg/m ²	Ns	m/s	m	
			Q=VA	Z=5*Bj	Eq. 25	Eq. 61		Eq. 63	Eq. 61&62		Eq. 60	Fig.2.18	Eq. 59	Eq.55		Eq. 58	
20	0.5	0.775	2	0.484	8.525	0.043	0.054	1.625	0.011	0.009	1.581	0.001	0.002	0.001	0.211	0.002	0.091
20	0.6	0.775	2	0.484	8.525	0.043	0.054	1.483	0.011	0.009	1.581	0.000	0.002	0.000	0.174	0.002	0.062
20	0.5	0.8	2	0.484	8.525	0.043	0.054	1.786	0.011	0.009	1.556	0.001	0.002	0.001	0.257	0.003	0.135
20	0.4	0.8	2	0.484	8.525	0.043	0.054	1.997	0.011	0.009	1.556	0.001	0.002	0.001	0.323	0.005	0.213
20	0.3	0.8	2	0.484	8.525	0.043	0.054	2.306	0.011	0.009	1.556	0.001	0.002	0.001	0.434	0.010	0.384
20	0.2	0.8	2	0.484	8.525	0.043	0.054	2.825	0.011	0.009	1.556	0.002	0.002	0.002	0.655	0.022	0.874
20	0.1	0.8	2	0.484	8.525	0.043	0.054	3.995	0.011	0.009	1.556	0.003	0.002	0.003	1.318	0.089	3.544
20	0.95	0.8	2	0.484	8.525	0.043	0.054	1.160	0.011	0.009	1.556	0.000	0.002	0.000	0.103	0.001	0.022
20	0.1	0.8	2	0.484	8.525	0.043	0.054	3.575	0.011	0.009	1.556	0.003	0.002	0.003	1.055	0.057	2.267
20	0.2	0.8	2	0.484	8.525	0.043	0.054	2.528	0.011	0.009	1.556	0.001	0.002	0.001	0.523	0.014	0.558
20	0.3	0.8	2	0.484	8.525	0.043	0.054	2.064	0.011	0.009	1.556	0.001	0.002	0.001	0.346	0.006	0.244
20	0.4	0.8	2	0.484	8.525	0.043	0.054	1.788	0.011	0.009	1.556	0.001	0.002	0.001	0.257	0.003	0.135
20	0.5	0.8	2	0.484	8.525	0.043	0.054	1.599	0.011	0.009	1.556	0.001	0.002	0.000	0.204	0.002	0.085
20	0.6	0.8	2	0.484	8.525	0.043	0.054	1.460	0.011	0.009	1.556	0.000	0.002	0.000	0.169	0.001	0.058
20	0.5	0.825	2	0.484	8.525	0.043	0.054	1.759	0.011	0.009	1.532	0.001	0.002	0.001	0.249	0.003	0.126
20	0.4	0.825	2	0.484	8.525	0.043	0.054	1.967	0.011	0.009	1.532	0.001	0.002	0.001	0.313	0.005	0.200
20	0.3	0.825	2	0.484	8.525	0.043	0.054	2.271	0.011	0.009	1.532	0.001	0.002	0.001	0.420	0.009	0.360
20	0.2	0.825	2	0.484	8.525	0.043	0.054	2.781	0.011	0.009	1.532	0.002	0.002	0.002	0.635	0.021	0.822
20	0.1	0.825	2	0.484	8.525	0.043	0.054	3.934	0.011	0.009	1.532	0.003	0.002	0.003	1.278	0.083	3.331
20	0.95	0.825	2	0.484	8.525	0.043	0.054	1.142	0.011	0.009	1.532	0.000	0.002	0.000	0.100	0.001	0.020
20	0.1	0.825	2	0.484	8.525	0.043	0.054	3.521	0.011	0.009	1.532	0.002	0.002	0.002	1.022	0.053	2.131
20	0.2	0.825	2	0.484	8.525	0.043	0.054	2.490	0.011	0.009	1.532	0.001	0.002	0.001	0.507	0.013	0.524
20	0.3	0.825	2	0.484	8.525	0.043	0.054	2.033	0.011	0.009	1.532	0.001	0.002	0.001	0.335	0.006	0.229
20	0.4	0.825	2	0.484	8.525	0.043	0.054	1.760	0.011	0.009	1.532	0.001	0.002	0.001	0.249	0.003	0.127
20	0.5	0.825	2	0.484	8.525	0.043	0.054	1.575	0.011	0.009	1.532	0.000	0.002	0.000	0.198	0.002	0.080
20	0.6	0.825	2	0.484	8.525	0.043	0.054	1.437	0.011	0.009	1.532	0.000	0.002	0.000	0.163	0.001	0.054

Table D 0.12. Quasi-steady method of Q=20 l/s, H=4 m and TW=0.25 m

Q	X	Z	V _{zi}	Z _{core}	V _{zj}	h _{down}	h _{up}	V _{xmax}	q _{up}	q _{down}	V _(z)	FQSI	Gb	Inet	V _{up}	H _{up}	H _{up} /z
l/s	m	m	m/s	m	m/s	m	m	m/s	m ² /s	m ² /s	m/s	Ns	kg/m ²	Ns	m/s	m	
Measured	Measured		Q=VA	Z=5*Bj	Eq. 25	Eq.61		Eq. 63	Eq. 61&62		Eq. 60	Fig.2.18	Eq. 59	Eq.55		Eq. 58	
20	0.95	0	2	0.484	8.525	0.043	0.054	2.318	0.011	0.009	8.525						
20	0.95	0.042	2	0.484	8.525	0.043	0.054	2.318	0.011	0.009	6.819						
20	0.95	0.083	2	0.484	8.525	0.043	0.054	2.318	0.011	0.009	4.822						
20	0.95	0.125	2	0.484	8.525	0.043	0.054	2.318	0.011	0.009	3.937						
20	0.95	0.167	2	0.484	8.525	0.043	0.054	2.318	0.011	0.009	3.410						
20	0.95	0.208	2	0.484	8.525	0.043	0.054	2.318	0.011	0.009	3.050						
20	0.95	0.25	2	0.484	8.525	0.043	0.054	2.318	0.011	0.009	2.784						
20	0.5	0.25	2	0.484	8.525	0.043	0.054	3.196	0.011	0.009	2.784	0.002	0.002	0.002	0.841	0.036	1.441
20	0.4	0.25	2	0.484	8.525	0.043	0.054	3.573	0.011	0.009	2.784	0.003	0.002	0.003	1.053	0.057	2.261
20	0.3	0.25	2	0.484	8.525	0.043	0.054	4.126	0.011	0.009	2.784	0.003	0.002	0.003	1.407	0.101	4.035
20	0.2	0.25	2	0.484	8.525	0.043	0.054	5.053	0.011	0.009	2.784	0.005	0.002	0.005	2.115	0.228	9.116
20	0.1	0.25	2	0.484	8.525	0.043	0.054	7.146	0.011	0.009	2.784	0.010	0.002	0.010	4.238	0.915	36.610
20	0.95	0.25	2	0.484	8.525	0.043	0.054	2.318	0.011	0.009	2.784	0.001	0.002	0.001	0.438	0.010	0.392
20	0.1	0.25	2	0.484	8.525	0.043	0.054	6.396	0.011	0.009	2.784	0.008	0.002	0.008	3.393	0.587	23.476
20	0.2	0.25	2	0.484	8.525	0.043	0.054	4.523	0.011	0.009	2.784	0.004	0.002	0.004	1.692	0.146	5.839
20	0.3	0.25	2	0.484	8.525	0.043	0.054	3.693	0.011	0.009	2.784	0.003	0.002	0.003	1.125	0.065	2.582
20	0.4	0.25	2	0.484	8.525	0.043	0.054	3.198	0.011	0.009	2.784	0.002	0.002	0.002	0.842	0.036	1.445
20	0.5	0.25	2	0.484	8.525	0.043	0.054	2.860	0.011	0.009	2.784	0.002	0.002	0.002	0.672	0.023	0.920
20	0.6	0.25	2	0.484	8.525	0.043	0.054	2.611	0.011	0.009	2.784	0.001	0.002	0.001	0.558	0.016	0.636
20	0.5	0.28	2	0.484	8.525	0.043	0.054	3.047	0.011	0.009	2.654	0.002	0.002	0.002	0.763	0.030	1.188
20	0.4	0.28	2	0.484	8.525	0.043	0.054	3.407	0.011	0.009	2.654	0.002	0.002	0.002	0.956	0.047	1.865
20	0.3	0.28	2	0.484	8.525	0.043	0.054	3.934	0.011	0.009	2.654	0.003	0.002	0.003	1.278	0.083	3.331

Q	X	Z	V _{zi}	Z _{core}	V _{zj}	h _{down}	h _{up}	V _{xmax}	q _{up}	q _{down}	V(z)	FQSI	G _b	I _{net}	V _{up}	H _{up}	H _{up} /z
l/s	m	m	m/s	m	m/s	m	m	m/s	m ² /s	m ² /s	m/s	Ns	kg/m ²	Ns	m/s	m	
			Q=VA	Z=5*Bj	Eq. 25	Eq. 61		Eq. 63	Eq. 61&62		Eq. 60	Fig.2.18	Eq. 59	Eq.55		Eq. 58	
20	0.2	0.28	2	0.484	8.525	0.043	0.054	4.818	0.011	0.009	2.654	0.005	0.002	0.005	1.922	0.188	7.528
20	0.1	0.28	2	0.484	8.525	0.043	0.054	6.813	0.011	0.009	2.654	0.009	0.002	0.009	3.852	0.756	30.244
20	0.95	0.28	2	0.484	8.525	0.043	0.054	2.210	0.011	0.009	2.654	0.001	0.002	0.001	0.398	0.008	0.323
20	0.1	0.28	2	0.484	8.525	0.043	0.054	6.098	0.011	0.009	2.654	0.007	0.002	0.007	3.084	0.485	19.392
20	0.2	0.28	2	0.484	8.525	0.043	0.054	4.312	0.011	0.009	2.654	0.004	0.002	0.004	1.538	0.121	4.821
20	0.3	0.28	2	0.484	8.525	0.043	0.054	3.521	0.011	0.009	2.654	0.002	0.002	0.002	1.022	0.053	2.131
20	0.4	0.28	2	0.484	8.525	0.043	0.054	3.049	0.011	0.009	2.654	0.002	0.002	0.002	0.765	0.030	1.192
20	0.5	0.28	2	0.484	8.525	0.043	0.054	2.727	0.011	0.009	2.654	0.001	0.002	0.001	0.610	0.019	0.759
20	0.6	0.28	2	0.484	8.525	0.043	0.054	2.490	0.011	0.009	2.654	0.001	0.002	0.001	0.507	0.013	0.524
20	0.5	0.3	2	0.484	8.525	0.043	0.054	2.917	0.011	0.009	2.541	0.002	0.002	0.002	0.699	0.025	0.997
20	0.4	0.3	2	0.484	8.525	0.043	0.054	3.262	0.011	0.009	2.541	0.002	0.002	0.002	0.876	0.039	1.565
20	0.3	0.3	2	0.484	8.525	0.043	0.054	3.766	0.011	0.009	2.541	0.003	0.002	0.003	1.171	0.070	2.795
20	0.2	0.3	2	0.484	8.525	0.043	0.054	4.612	0.011	0.009	2.541	0.004	0.002	0.004	1.761	0.158	6.320
20	0.1	0.3	2	0.484	8.525	0.043	0.054	6.523	0.011	0.009	2.541	0.008	0.002	0.008	3.530	0.635	25.403
20	0.95	0.3	2	0.484	8.525	0.043	0.054	2.116	0.011	0.009	2.541	0.001	0.002	0.001	0.364	0.007	0.270
20	0.1	0.3	2	0.484	8.525	0.043	0.054	5.839	0.011	0.009	2.541	0.007	0.002	0.007	2.826	0.407	16.286
20	0.2	0.3	2	0.484	8.525	0.043	0.054	4.129	0.011	0.009	2.541	0.003	0.002	0.003	1.409	0.101	4.047
20	0.3	0.3	2	0.484	8.525	0.043	0.054	3.371	0.011	0.009	2.541	0.002	0.002	0.002	0.936	0.045	1.788
20	0.4	0.3	2	0.484	8.525	0.043	0.054	2.919	0.011	0.009	2.541	0.002	0.002	0.002	0.700	0.025	1.000
20	0.5	0.3	2	0.484	8.525	0.043	0.054	2.611	0.011	0.009	2.541	0.001	0.002	0.001	0.558	0.016	0.636
20	0.6	0.3	2	0.484	8.525	0.043	0.054	2.384	0.011	0.009	2.541	0.001	0.002	0.001	0.464	0.011	0.439
20	0.5	0.33	2	0.484	8.525	0.043	0.054	2.803	0.011	0.009	2.442	0.002	0.002	0.002	0.645	0.021	0.847
20	0.4	0.33	2	0.484	8.525	0.043	0.054	3.134	0.011	0.009	2.442	0.002	0.002	0.002	0.808	0.033	1.331
20	0.3	0.33	2	0.484	8.525	0.043	0.054	3.618	0.011	0.009	2.442	0.003	0.002	0.003	1.080	0.059	2.379

Q	X	Z	V _{zi}	Z _{core}	V _{zj}	h _{down}	h _{up}	V _{xmax}	q _{up}	q _{down}	V(z)	FQSI	G _b	I _{net}	V _{up}	H _{up}	H _{up} /z
l/s	m	m	m/s	m	m/s	m	m	m/s	m ² /s	m ² /s	m/s	Ns	kg/m ²	Ns	m/s	m	
			Q=VA	Z=5*Bj	Eq. 25	Eq. 61		Eq. 63	Eq. 61&62		Eq. 60	Fig.2.18	Eq. 59	Eq.55		Eq. 58	
20	0.2	0.33	2	0.484	8.525	0.043	0.054	4.432	0.011	0.009	2.442	0.004	0.002	0.004	1.625	0.135	5.381
20	0.1	0.33	2	0.484	8.525	0.043	0.054	6.267	0.011	0.009	2.442	0.008	0.002	0.008	3.258	0.541	21.636
20	0.95	0.33	2	0.484	8.525	0.043	0.054	2.033	0.011	0.009	2.442	0.001	0.002	0.001	0.335	0.006	0.229
20	0.1	0.33	2	0.484	8.525	0.043	0.054	5.610	0.011	0.009	2.442	0.006	0.002	0.006	2.608	0.347	13.870
20	0.2	0.33	2	0.484	8.525	0.043	0.054	3.967	0.011	0.009	2.442	0.003	0.002	0.003	1.300	0.086	3.445
20	0.3	0.33	2	0.484	8.525	0.043	0.054	3.239	0.011	0.009	2.442	0.002	0.002	0.002	0.864	0.038	1.521
20	0.4	0.33	2	0.484	8.525	0.043	0.054	2.805	0.011	0.009	2.442	0.002	0.002	0.002	0.646	0.021	0.850
20	0.5	0.33	2	0.484	8.525	0.043	0.054	2.509	0.011	0.009	2.442	0.001	0.002	0.001	0.515	0.014	0.540
20	0.6	0.33	2	0.484	8.525	0.043	0.054	2.290	0.011	0.009	2.442	0.001	0.002	0.001	0.428	0.009	0.373
20	0.5	0.35	2	0.484	8.525	0.043	0.054	2.701	0.011	0.009	2.353	0.001	0.002	0.001	0.598	0.018	0.729
20	0.4	0.35	2	0.484	8.525	0.043	0.054	3.020	0.011	0.009	2.353	0.002	0.002	0.002	0.750	0.029	1.146
20	0.3	0.35	2	0.484	8.525	0.043	0.054	3.487	0.011	0.009	2.353	0.002	0.002	0.002	1.002	0.051	2.049
20	0.2	0.35	2	0.484	8.525	0.043	0.054	4.270	0.011	0.009	2.353	0.004	0.002	0.004	1.508	0.116	4.636
20	0.1	0.35	2	0.484	8.525	0.043	0.054	6.039	0.011	0.009	2.353	0.007	0.002	0.007	3.024	0.466	18.648
20	0.95	0.35	2	0.484	8.525	0.043	0.054	1.959	0.011	0.009	2.353	0.001	0.002	0.001	0.311	0.005	0.197
20	0.1	0.35	2	0.484	8.525	0.043	0.054	5.406	0.011	0.009	2.353	0.006	0.002	0.006	2.421	0.299	11.953
20	0.2	0.35	2	0.484	8.525	0.043	0.054	3.822	0.011	0.009	2.353	0.003	0.002	0.003	1.206	0.074	2.967
20	0.3	0.35	2	0.484	8.525	0.043	0.054	3.121	0.011	0.009	2.353	0.002	0.002	0.002	0.801	0.033	1.309
20	0.4	0.35	2	0.484	8.525	0.043	0.054	2.703	0.011	0.009	2.353	0.001	0.002	0.001	0.599	0.018	0.731
20	0.5	0.35	2	0.484	8.525	0.043	0.054	2.417	0.011	0.009	2.353	0.001	0.002	0.001	0.477	0.012	0.465
20	0.6	0.35	2	0.484	8.525	0.043	0.054	2.207	0.011	0.009	2.353	0.001	0.002	0.001	0.396	0.008	0.320
20	0.5	0.38	2	0.484	8.525	0.043	0.054	2.609	0.011	0.009	2.273	0.001	0.002	0.001	0.558	0.016	0.634
20	0.4	0.38	2	0.484	8.525	0.043	0.054	2.917	0.011	0.009	2.273	0.002	0.002	0.002	0.699	0.025	0.997
20	0.3	0.38	2	0.484	8.525	0.043	0.054	3.368	0.011	0.009	2.273	0.002	0.002	0.002	0.935	0.045	1.783

Q	X	Z	V _{zi}	Z _{core}	V _{zj}	h _{down}	h _{up}	V _{xmax}	q _{up}	q _{down}	V(z)	FQSI	G _b	I _{net}	V _{up}	H _{up}	H _{up} /z
l/s	m	m	m/s	m	m/s	m	m	m/s	m ² /s	m ² /s	m/s	Ns	kg/m ²	Ns	m/s	m	
			Q=VA	Z=5*Bj	Eq. 25	Eq.61		Eq. 63	Eq. 61&62		Eq. 60	Fig.2.18	Eq. 59	Eq.55		Eq. 58	
20	0.2	0.38	2	0.484	8.525	0.043	0.054	4.126	0.011	0.009	2.273	0.003	0.002	0.003	1.407	0.101	4.035
20	0.1	0.38	2	0.484	8.525	0.043	0.054	5.834	0.011	0.009	2.273	0.007	0.002	0.007	2.822	0.406	16.238
20	0.95	0.38	2	0.484	8.525	0.043	0.054	1.893	0.011	0.009	2.273	0.001	0.002	0.001	0.289	0.004	0.171
20	0.1	0.38	2	0.484	8.525	0.043	0.054	5.222	0.011	0.009	2.273	0.005	0.002	0.005	2.259	0.260	10.407
20	0.2	0.38	2	0.484	8.525	0.043	0.054	3.693	0.011	0.009	2.273	0.003	0.002	0.003	1.125	0.065	2.582
20	0.3	0.38	2	0.484	8.525	0.043	0.054	3.015	0.011	0.009	2.273	0.002	0.002	0.002	0.747	0.028	1.139
20	0.4	0.38	2	0.484	8.525	0.043	0.054	2.611	0.011	0.009	2.273	0.001	0.002	0.001	0.558	0.016	0.636
20	0.5	0.38	2	0.484	8.525	0.043	0.054	2.335	0.011	0.009	2.273	0.001	0.002	0.001	0.445	0.010	0.404
20	0.6	0.38	2	0.484	8.525	0.043	0.054	2.132	0.011	0.009	2.273	0.001	0.002	0.001	0.369	0.007	0.278
20	0.5	0.4	2	0.484	8.525	0.043	0.054	2.526	0.011	0.009	2.201	0.001	0.002	0.001	0.522	0.014	0.556
20	0.4	0.4	2	0.484	8.525	0.043	0.054	2.825	0.011	0.009	2.201	0.002	0.002	0.002	0.655	0.022	0.874
20	0.3	0.4	2	0.484	8.525	0.043	0.054	3.262	0.011	0.009	2.201	0.002	0.002	0.002	0.876	0.039	1.565
20	0.2	0.4	2	0.484	8.525	0.043	0.054	3.995	0.011	0.009	2.201	0.003	0.002	0.003	1.318	0.089	3.544
20	0.1	0.4	2	0.484	8.525	0.043	0.054	5.649	0.011	0.009	2.201	0.006	0.002	0.006	2.645	0.357	14.266
20	0.95	0.4	2	0.484	8.525	0.043	0.054	1.833	0.011	0.009	2.201	0.001	0.002	0.001	0.271	0.004	0.150
20	0.1	0.4	2	0.484	8.525	0.043	0.054	5.056	0.011	0.009	2.201	0.005	0.002	0.005	2.118	0.229	9.143
20	0.2	0.4	2	0.484	8.525	0.043	0.054	3.575	0.011	0.009	2.201	0.003	0.002	0.003	1.055	0.057	2.267
20	0.3	0.4	2	0.484	8.525	0.043	0.054	2.919	0.011	0.009	2.201	0.002	0.002	0.002	0.700	0.025	1.000
20	0.4	0.4	2	0.484	8.525	0.043	0.054	2.528	0.011	0.009	2.201	0.001	0.002	0.001	0.523	0.014	0.558
20	0.5	0.4	2	0.484	8.525	0.043	0.054	2.261	0.011	0.009	2.201	0.001	0.002	0.001	0.417	0.009	0.354
20	0.6	0.4	2	0.484	8.525	0.043	0.054	2.064	0.011	0.009	2.201	0.001	0.002	0.001	0.346	0.006	0.244
20	0.5	0.43	2	0.484	8.525	0.043	0.054	2.451	0.011	0.009	2.135	0.001	0.002	0.001	0.491	0.012	0.492
20	0.4	0.43	2	0.484	8.525	0.043	0.054	2.740	0.011	0.009	2.135	0.001	0.002	0.001	0.616	0.019	0.773
20	0.3	0.43	2	0.484	8.525	0.043	0.054	3.164	0.011	0.009	2.135	0.002	0.002	0.002	0.824	0.035	1.384

Q	X	Z	V _{zi}	Z _{core}	V _{zj}	h _{down}	h _{up}	V _{xmax}	q _{up}	q _{down}	V(z)	FQSI	G _b	I _{net}	V _{up}	H _{up}	H _{up} /z
l/s	m	m	m/s	m	m/s	m	m	m/s	m ² /s	m ² /s	m/s	Ns	kg/m ²	Ns	m/s	m	
			Q=VA	Z=5*Bj	Eq. 25	Eq. 61		Eq. 63	Eq. 61&62		Eq. 60	Fig.2.18	Eq. 59	Eq.55		Eq. 58	
20	0.2	0.43	2	0.484	8.525	0.043	0.054	3.875	0.011	0.009	2.135	0.003	0.002	0.003	1.240	0.078	3.136
20	0.1	0.43	2	0.484	8.525	0.043	0.054	5.480	0.011	0.009	2.135	0.006	0.002	0.006	2.489	0.316	12.632
20	0.95	0.43	2	0.484	8.525	0.043	0.054	1.778	0.011	0.009	2.135	0.001	0.002	0.001	0.254	0.003	0.132
20	0.1	0.43	2	0.484	8.525	0.043	0.054	4.905	0.011	0.009	2.135	0.005	0.002	0.005	1.993	0.202	8.094
20	0.2	0.43	2	0.484	8.525	0.043	0.054	3.469	0.011	0.009	2.135	0.002	0.002	0.002	0.992	0.050	2.006
20	0.3	0.43	2	0.484	8.525	0.043	0.054	2.832	0.011	0.009	2.135	0.002	0.002	0.002	0.659	0.022	0.884
20	0.4	0.43	2	0.484	8.525	0.043	0.054	2.453	0.011	0.009	2.135	0.001	0.002	0.001	0.492	0.012	0.493
20	0.5	0.43	2	0.484	8.525	0.043	0.054	2.194	0.011	0.009	2.135	0.001	0.002	0.001	0.392	0.008	0.313
20	0.6	0.43	2	0.484	8.525	0.043	0.054	2.003	0.011	0.009	2.135	0.001	0.002	0.001	0.325	0.005	0.215
20	0.5	0.45	2	0.484	8.525	0.043	0.054	2.382	0.011	0.009	2.075	0.001	0.002	0.001	0.463	0.011	0.438
20	0.4	0.45	2	0.484	8.525	0.043	0.054	2.663	0.011	0.009	2.075	0.001	0.002	0.001	0.581	0.017	0.689
20	0.3	0.45	2	0.484	8.525	0.043	0.054	3.075	0.011	0.009	2.075	0.002	0.002	0.002	0.778	0.031	1.233
20	0.2	0.45	2	0.484	8.525	0.043	0.054	3.766	0.011	0.009	2.075	0.003	0.002	0.003	1.171	0.070	2.795
20	0.1	0.45	2	0.484	8.525	0.043	0.054	5.326	0.011	0.009	2.075	0.006	0.002	0.006	2.350	0.282	11.263
20	0.95	0.45	2	0.484	8.525	0.043	0.054	1.728	0.011	0.009	2.075	0.001	0.002	0.001	0.240	0.003	0.117
20	0.1	0.45	2	0.484	8.525	0.043	0.054	4.767	0.011	0.009	2.075	0.004	0.002	0.004	1.881	0.180	7.216
20	0.2	0.45	2	0.484	8.525	0.043	0.054	3.371	0.011	0.009	2.075	0.002	0.002	0.002	0.936	0.045	1.788
20	0.3	0.45	2	0.484	8.525	0.043	0.054	2.752	0.011	0.009	2.075	0.001	0.002	0.001	0.621	0.020	0.787
20	0.4	0.45	2	0.484	8.525	0.043	0.054	2.384	0.011	0.009	2.075	0.001	0.002	0.001	0.464	0.011	0.439
20	0.5	0.45	2	0.484	8.525	0.043	0.054	2.132	0.011	0.009	2.075	0.001	0.002	0.001	0.369	0.007	0.278
20	0.6	0.45	2	0.484	8.525	0.043	0.054	1.946	0.011	0.009	2.075	0.001	0.002	0.001	0.306	0.005	0.191
20	0.5	0.48	2	0.484	8.525	0.043	0.054	2.318	0.011	0.009	2.020	0.001	0.002	0.001	0.438	0.010	0.392
20	0.4	0.48	2	0.484	8.525	0.043	0.054	2.592	0.011	0.009	2.020	0.001	0.002	0.001	0.550	0.015	0.617
20	0.3	0.48	2	0.484	8.525	0.043	0.054	2.993	0.011	0.009	2.020	0.002	0.002	0.002	0.736	0.028	1.106

Q	X	Z	V _{zi}	Z _{core}	V _{zj}	h _{down}	h _{up}	V _{xmax}	q _{up}	q _{down}	V(z)	FQSI	G _b	I _{net}	V _{up}	H _{up}	H _{up} /z
l/s	m	m	m/s	m	m/s	m	m	m/s	m ² /s	m ² /s	m/s	Ns	kg/m ²	Ns	m/s	m	
			Q=VA	Z=5*Bj	Eq. 25	Eq. 61		Eq. 63	Eq. 61&62		Eq. 60	Fig.2.18	Eq. 59	Eq.55		Eq. 59	
20	0.2	0.48	2	0.484	8.525	0.043	0.054	3.666	0.011	0.009	2.020	0.003	0.002	0.003	1.109	0.063	2.507
20	0.1	0.48	2	0.484	8.525	0.043	0.054	5.184	0.011	0.009	2.020	0.005	0.002	0.005	2.226	0.253	10.105
20	0.95	0.48	2	0.484	8.525	0.043	0.054	1.682	0.011	0.009	2.020	0.001	0.002	0.001	0.227	0.003	0.105
20	0.1	0.48	2	0.484	8.525	0.043	0.054	4.640	0.011	0.009	2.020	0.004	0.002	0.004	1.782	0.162	6.474
20	0.2	0.48	2	0.484	8.525	0.043	0.054	3.281	0.011	0.009	2.020	0.002	0.002	0.002	0.887	0.040	1.603
20	0.3	0.48	2	0.484	8.525	0.043	0.054	2.679	0.011	0.009	2.020	0.001	0.002	0.001	0.588	0.018	0.706
20	0.4	0.48	2	0.484	8.525	0.043	0.054	2.320	0.011	0.009	2.020	0.001	0.002	0.001	0.439	0.010	0.393
20	0.5	0.48	2	0.484	8.525	0.043	0.054	2.075	0.011	0.009	2.020	0.001	0.002	0.001	0.350	0.006	0.249
20	0.6	0.48	2	0.484	8.525	0.043	0.054	1.894	0.011	0.009	2.020	0.001	0.002	0.001	0.290	0.004	0.171
20	0.5	0.5	2	0.484	8.525	0.043	0.054	2.260	0.011	0.009	1.968	0.001	0.002	0.001	0.416	0.009	0.353
20	0.4	0.5	2	0.484	8.525	0.043	0.054	2.526	0.011	0.009	1.968	0.001	0.002	0.001	0.522	0.014	0.556
20	0.3	0.5	2	0.484	8.525	0.043	0.054	2.917	0.011	0.009	1.968	0.002	0.002	0.002	0.699	0.025	0.997
20	0.2	0.5	2	0.484	8.525	0.043	0.054	3.573	0.011	0.009	1.968	0.003	0.002	0.003	1.053	0.057	2.261
20	0.1	0.5	2	0.484	8.525	0.043	0.054	5.053	0.011	0.009	1.968	0.005	0.002	0.005	2.115	0.228	9.116
20	0.95	0.5	2	0.484	8.525	0.043	0.054	1.639	0.011	0.009	1.968	0.001	0.002	0.001	0.215	0.002	0.094
20	0.1	0.5	2	0.484	8.525	0.043	0.054	4.523	0.011	0.009	1.968	0.004	0.002	0.004	1.692	0.146	5.839
20	0.2	0.5	2	0.484	8.525	0.043	0.054	3.198	0.011	0.009	1.968	0.002	0.002	0.002	0.842	0.036	1.445
20	0.3	0.5	2	0.484	8.525	0.043	0.054	2.611	0.011	0.009	1.968	0.001	0.002	0.001	0.558	0.016	0.636
20	0.4	0.5	2	0.484	8.525	0.043	0.054	2.261	0.011	0.009	1.968	0.001	0.002	0.001	0.417	0.009	0.354
20	0.5	0.5	2	0.484	8.525	0.043	0.054	2.023	0.011	0.009	1.968	0.001	0.002	0.001	0.332	0.006	0.224
20	0.6	0.5	2	0.484	8.525	0.043	0.054	1.846	0.011	0.009	1.968	0.001	0.002	0.001	0.275	0.004	0.154
20	0.5	0.53	2	0.484	8.525	0.043	0.054	2.205	0.011	0.009	1.921	0.001	0.002	0.001	0.396	0.008	0.319
20	0.4	0.53	2	0.484	8.525	0.043	0.054	2.465	0.011	0.009	1.921	0.001	0.002	0.001	0.497	0.013	0.504
20	0.3	0.53	2	0.484	8.525	0.043	0.054	2.847	0.011	0.009	1.921	0.002	0.002	0.002	0.665	0.023	0.903

Q	X	Z	V _{zi}	Z _{core}	V _{zj}	h _{down}	h _{up}	V _{xmax}	q _{up}	q _{down}	V(z)	FQSI	G _b	I _{net}	V _{up}	H _{up}	H _{up} /z
l/s	m	m	m/s	m	m/s	m	m	m/s	m ² /s	m ² /s	m/s	Ns	kg/m ²	Ns	m/s	m	
			Q=VA	Z=5*Bj	Eq. 25	Eq.61		Eq. 63	Eq. 61&62		Eq. 60	Fig.2.18	Eq. 59	Eq.55		Eq. 58	
20	0.2	0.53	2	0.484	8.525	0.043	0.054	3.487	0.011	0.009	1.921	0.002	0.002	0.002	1.002	0.051	2.049
20	0.1	0.53	2	0.484	8.525	0.043	0.054	4.931	0.011	0.009	1.921	0.005	0.002	0.005	2.013	0.207	8.265
20	0.95	0.53	2	0.484	8.525	0.043	0.054	1.600	0.011	0.009	1.921	0.001	0.002	0.000	0.204	0.002	0.085
20	0.1	0.53	2	0.484	8.525	0.043	0.054	4.414	0.011	0.009	1.921	0.004	0.002	0.004	1.611	0.132	5.294
20	0.2	0.53	2	0.484	8.525	0.043	0.054	3.121	0.011	0.009	1.921	0.002	0.002	0.002	0.801	0.033	1.309
20	0.3	0.53	2	0.484	8.525	0.043	0.054	2.548	0.011	0.009	1.921	0.001	0.002	0.001	0.531	0.014	0.576
20	0.4	0.53	2	0.484	8.525	0.043	0.054	2.207	0.011	0.009	1.921	0.001	0.002	0.001	0.396	0.008	0.320
20	0.5	0.53	2	0.484	8.525	0.043	0.054	1.974	0.011	0.009	1.921	0.001	0.002	0.001	0.315	0.005	0.203
20	0.6	0.53	2	0.484	8.525	0.043	0.054	1.802	0.011	0.009	1.921	0.001	0.002	0.001	0.261	0.003	0.139
20	0.5	0.55	2	0.484	8.525	0.043	0.054	2.154	0.011	0.009	1.877	0.001	0.002	0.001	0.377	0.007	0.291
20	0.4	0.55	2	0.484	8.525	0.043	0.054	2.409	0.011	0.009	1.877	0.001	0.002	0.001	0.474	0.011	0.458
20	0.3	0.55	2	0.484	8.525	0.043	0.054	2.781	0.011	0.009	1.877	0.002	0.002	0.002	0.635	0.021	0.822
20	0.2	0.55	2	0.484	8.525	0.043	0.054	3.407	0.011	0.009	1.877	0.002	0.002	0.002	0.956	0.047	1.865
20	0.1	0.55	2	0.484	8.525	0.043	0.054	4.818	0.011	0.009	1.877	0.005	0.002	0.005	1.922	0.188	7.528
20	0.95	0.55	2	0.484	8.525	0.043	0.054	1.563	0.011	0.009	1.877	0.000	0.002	0.000	0.195	0.002	0.077
20	0.1	0.55	2	0.484	8.525	0.043	0.054	4.312	0.011	0.009	1.877	0.004	0.002	0.004	1.538	0.121	4.821
20	0.2	0.55	2	0.484	8.525	0.043	0.054	3.049	0.011	0.009	1.877	0.002	0.002	0.002	0.765	0.030	1.192
20	0.3	0.55	2	0.484	8.525	0.043	0.054	2.490	0.011	0.009	1.877	0.001	0.002	0.001	0.507	0.013	0.524
20	0.4	0.55	2	0.484	8.525	0.043	0.054	2.156	0.011	0.009	1.877	0.001	0.002	0.001	0.378	0.007	0.291
20	0.5	0.55	2	0.484	8.525	0.043	0.054	1.928	0.011	0.009	1.877	0.001	0.002	0.001	0.301	0.005	0.184
20	0.6	0.55	2	0.484	8.525	0.043	0.054	1.760	0.011	0.009	1.877	0.001	0.002	0.001	0.249	0.003	0.127
20	0.5	0.58	2	0.484	8.525	0.043	0.054	2.107	0.011	0.009	1.836	0.001	0.002	0.001	0.361	0.007	0.265
20	0.4	0.58	2	0.484	8.525	0.043	0.054	2.356	0.011	0.009	1.836	0.001	0.002	0.001	0.453	0.010	0.418
20	0.3	0.58	2	0.484	8.525	0.043	0.054	2.720	0.011	0.009	1.836	0.001	0.002	0.001	0.607	0.019	0.751

Q	X	Z	V_{zi}	Z_{core}	V_{zj}	h_{down}	h_{up}	V_{xmax}	q_{up}	q_{down}	V(z)	FQSI	G_b	I_{net}	V_{up}	H_{up}	H_{up}/z
l/s	m	m	m/s	m	m/s	m	m	m/s	m²/s	m²/s	m/s	Ns	kg/m²	Ns	m/s	m	
			Q=VA	Z=5*Bj	Eq. 25	Eq. 61		Eq. 63	Eq. 61&62		Eq. 60	Fig.2.18	Eq. 59	Eq.55		Eq. 58	
20	0.2	0.58	2	0.484	8.525	0.043	0.054	3.332	0.011	0.009	1.836	0.002	0.002	0.002	0.915	0.043	1.705
20	0.1	0.58	2	0.484	8.525	0.043	0.054	4.712	0.011	0.009	1.836	0.004	0.002	0.004	1.838	0.172	6.884
20	0.95	0.58	2	0.484	8.525	0.043	0.054	1.529	0.011	0.009	1.836	0.000	0.002	0.000	0.186	0.002	0.070
20	0.1	0.58	2	0.484	8.525	0.043	0.054	4.217	0.011	0.009	1.836	0.004	0.002	0.003	1.471	0.110	4.409
20	0.2	0.58	2	0.484	8.525	0.043	0.054	2.982	0.011	0.009	1.836	0.002	0.002	0.002	0.731	0.027	1.089
20	0.3	0.58	2	0.484	8.525	0.043	0.054	2.435	0.011	0.009	1.836	0.001	0.002	0.001	0.484	0.012	0.479
20	0.4	0.58	2	0.484	8.525	0.043	0.054	2.109	0.011	0.009	1.836	0.001	0.002	0.001	0.361	0.007	0.266
20	0.5	0.58	2	0.484	8.525	0.043	0.054	1.886	0.011	0.009	1.836	0.001	0.002	0.001	0.287	0.004	0.168
20	0.6	0.58	2	0.484	8.525	0.043	0.054	1.722	0.011	0.009	1.836	0.001	0.002	0.001	0.238	0.003	0.115

APPENDIX E PARAMETERS, WORK SHEET OF PRACTICAL APPLICATION OF DI METHOD AND ADDITION FORMULA**Table E 0.1. Parameters used for calculation of DI method for Kariba Dam.**

Input parameters			Symbol
Max flood level	489.5	m.a.s.l	-
Tailwater level at impact	402	m.a.s.l	-
sluice height	9.14	m	-
sluice width	8.87	m	-
sluice discharge	1500	m ³ /s	-
sluice altitude	462.3	m.a.s.l	-
jet fall length	60.3	m	L
block width	1	m	x _b
block length	1	m	x _b
Block height	2	m	Z
Celerity	100	m/s	C
block density	2650	kg/m ³	-
water density	1000	kg/m ³	ρ _w
air density	1.2	kg/m ³	ρ _a
Intermediate results			
Jet velocity at issuance	18.5	m/s	V _i
Jet velocity at impact	41.4	m/s	V _j
Jet diameter at impact	6.3	m	D _j
Reynolds number at impact	2.30E+08	-	Re
Froude number at impact	5.30E+00	-	Fr
jet aeration	90%	-	β
jet air concentration	48%	-	Ca
jet mean density	526	kg/m ³	ρ _{aw}
core development length (Equation ???)	49.1	m	Y _c

The maximum dynamic impulsion coefficient and pressure coefficient can thus be computed with the following expression:

$$C_I^{max} = \frac{I^{max} c}{x_b^2 \rho_{aw} V_i^2 L_f} \quad [71]$$

$$\psi = \frac{1}{1 + \exp\left\{-5.37 \times 10^{-6} \left(\frac{V_i B_j}{v} - 6.63 \times 10^5\right)\right\}} \quad [72]$$

$$C_p = \psi \left(0.926 - 0.0779 \frac{Y - Y_c}{B_j}\right)^2 \quad \text{if } Y > Y_c \quad [73]$$

$$\rho_{aw} = \frac{1}{1 + \beta} \rho_w + \frac{\beta}{1 + \beta} \rho_a \quad [74]$$

$$C_a = \frac{Q_a}{Q_a + Q_w} = \frac{\beta}{1 + \beta} \quad [75]$$

$$C_p^a = C_p(1 + 0.4\beta) \quad [76]$$

$$I^{max} = C_I^{max} C_p^a \frac{\rho_{aw} V_i^2}{2} x_b^2 \Delta_p \quad [77]$$

Table E.0.2. The ultimate scour depth of Kariba Dam based on the adapted DI method

Kariba Dam												
Y(m)	Bottom (m)	Y/Bj	ψ	Cp	C_p^a	Ci	Imax	Gb	Inet	V _{up}	h _{up}	h _{up} /z
Measured	Measured		Eq.31	Eq. 30	Eq. 42	Eq. 57	Eq. 56	Eq. 59	Eq. 55		Eq. 58	
56	346	8.889	1	0.71	0.961	0.439	5440.6596	250.0000	5370.5882	21.4824	23.5215	47.0430
58	344	9.206	1	0.67	0.905	0.421	4918.8455	250.0000	4848.7741	19.3951	19.1728	38.3455
60	342	9.524	1	0.63	0.851	0.404	4438.8431	250.0000	4368.7717	17.4751	15.5647	31.1293
62	340	9.841	1	0.59	0.799	0.388	3998.0841	250.0000	3928.0127	15.7121	12.5825	25.1650
64	338	10.159	1	0.55	0.748	0.372	3594.0913	250.0000	3524.0198	14.0961	10.1274	20.2548
66	336	10.476	1	0.51	0.699	0.357	3224.4780	250.0000	3154.4066	12.6176	8.1144	16.2288
68	334	10.794	1	0.48	0.652	0.343	2886.9486	250.0000	2816.8772	11.2675	6.4708	12.9416
70	332	11.111	1	0.45	0.606	0.330	2579.2984	250.0000	2509.2270	10.0369	5.1345	10.2691
72	330	11.429	1	0.41	0.562	0.317	2299.4132	250.0000	2229.3418	8.9174	4.0530	8.1060
74	328	11.746	1	0.38	0.520	0.305	2045.2700	250.0000	1975.1986	7.9008	3.1816	6.3632
76	326	12.063	1	0.35	0.479	0.294	1814.9364	250.0000	1744.8650	6.9795	2.4828	4.9656
78	324	12.381	1	0.32	0.440	0.283	1606.5710	250.0000	1536.4995	6.1460	1.9252	3.8505
80	322	12.698	1	0.30	0.402	0.273	1418.4230	250.0000	1348.3516	5.3934	1.4826	2.9652
82	320	13.016	1	0.27	0.367	0.264	1248.8327	250.0000	1178.7613	4.7150	1.1331	2.2662
84	318	13.333	1	0.24	0.333	0.256	1096.2312	250.0000	1026.1598	4.1046	0.8587	1.7174
86	316	13.651	1	0.22	0.300	0.248	959.1403	250.0000	889.0688	3.5563	0.6446	1.2892
88	314	13.968	1	0.20	0.269	0.241	836.1727	250.0000	766.1012	3.0644	0.4786	0.9572
90	312	14.286	1	0.18	0.240	0.234	726.0319	250.0000	655.9605	2.6238	0.3509	0.7018
92	310	14.603	1	0.16	0.213	0.229	627.5124	250.0000	557.4410	2.2298	0.2534	0.5068
94	308	14.921	1	0.14	0.187	0.224	539.4994	250.0000	469.4280	1.8777	0.1797	0.3594
96	306	15.238	1	0.12	0.163	0.219	460.9689	250.0000	390.8975	1.5636	0.1246	0.2492
98	304	15.556	1	0.10	0.140	0.216	390.9879	250.0000	320.9165	1.2837	0.0840	0.1680

APPENDIX F SURVEYING DATA GRAPHS

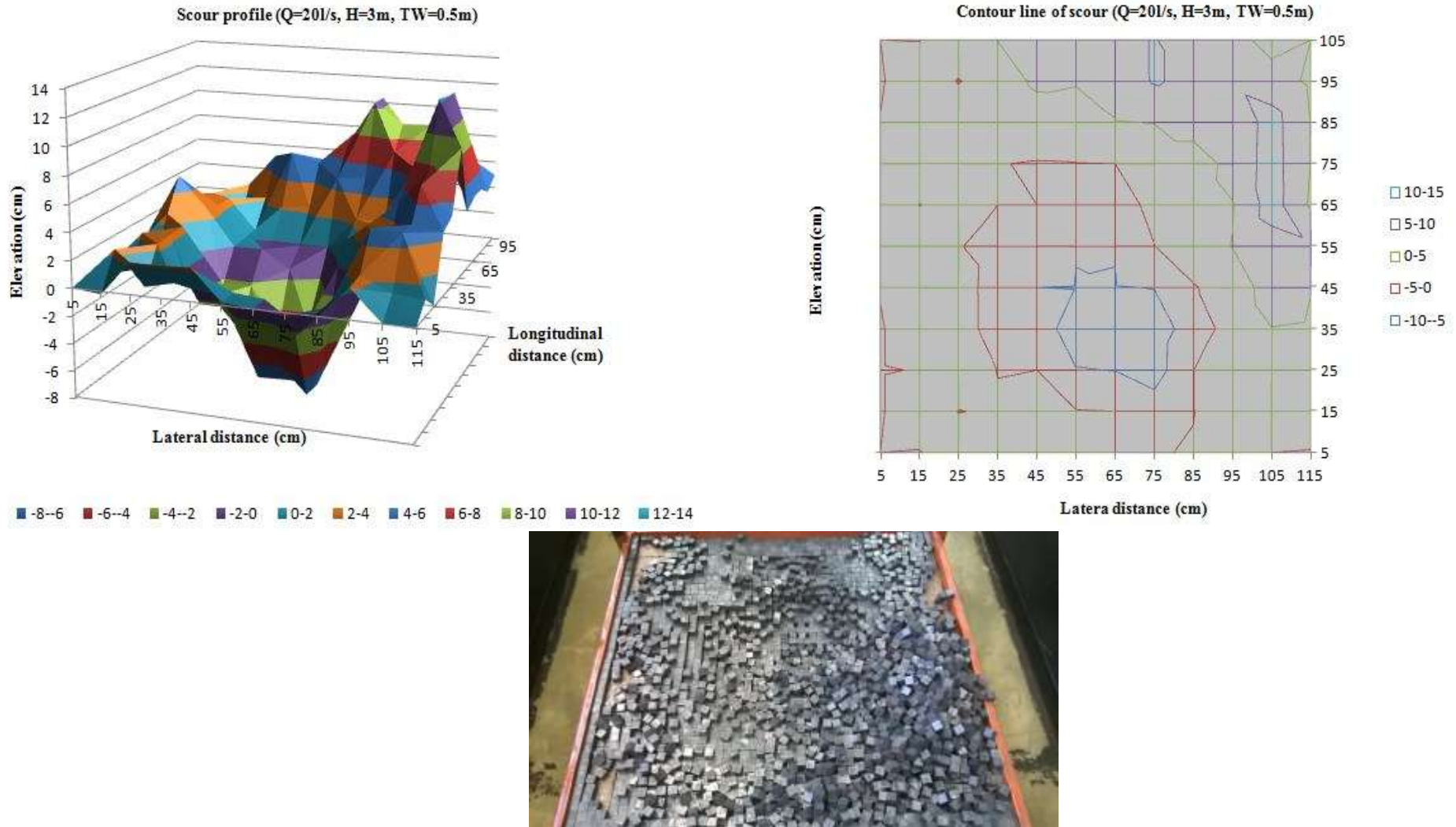


Figure F. 0-1. Scour profile and contour line of 20 l/s, H=3m and TW=0.5m

Determine plunge pool scour hole geometry

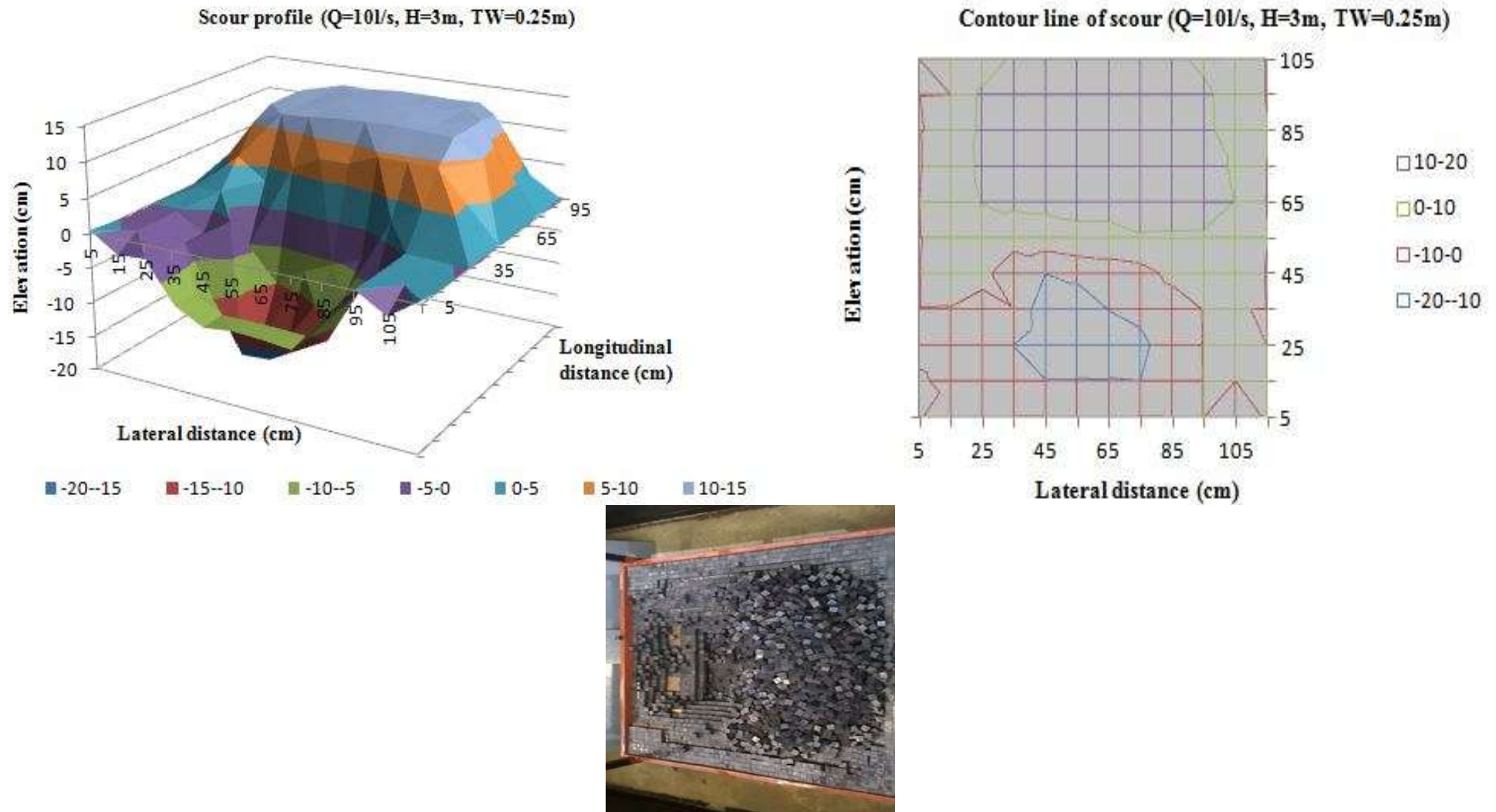


Figure F. 0-2. Scour profile and contour line of 10 l/s, H=3m and TW=0.25m

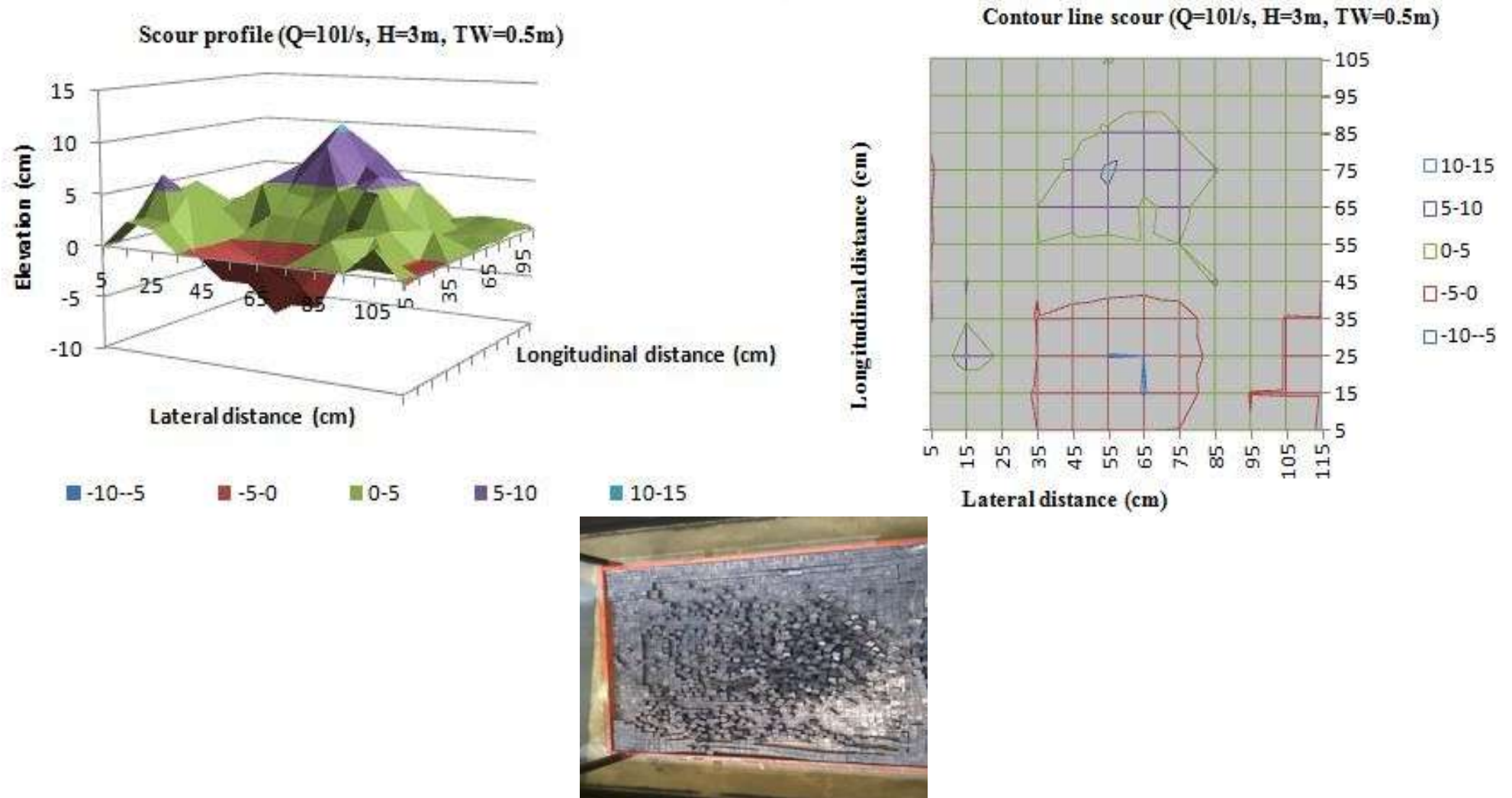


Figure F.0-3. Scour profile and contour line of 10 l/s, H=3m and TW=0.5m

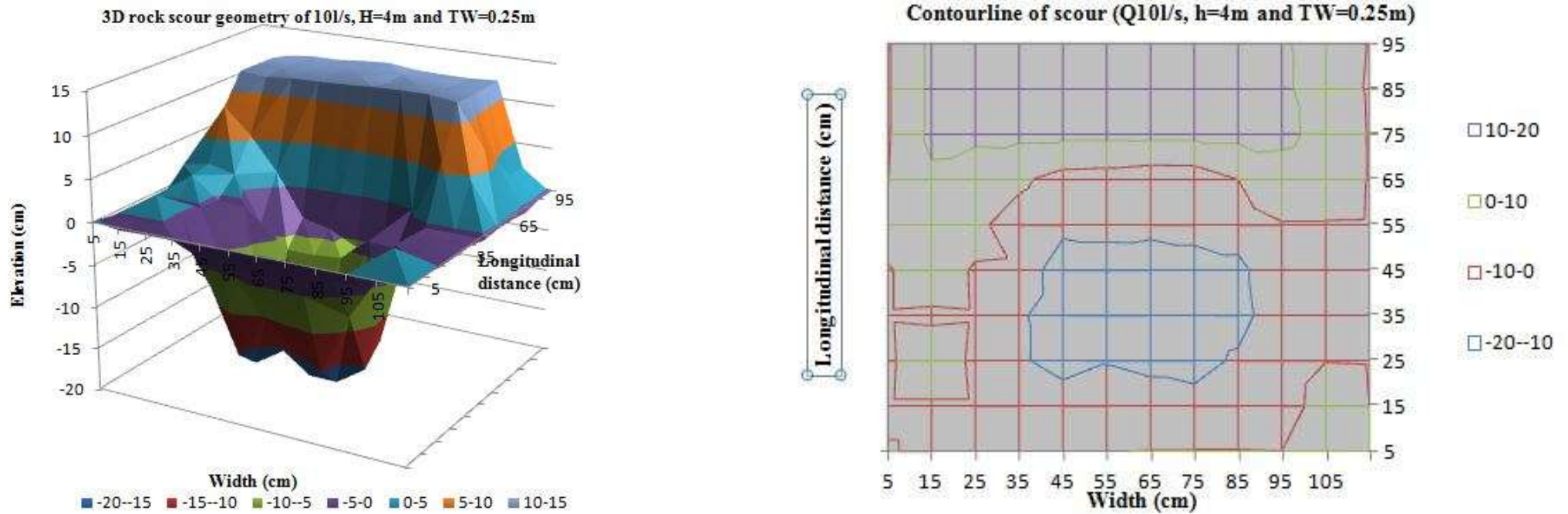


Figure F. 0-4. Scour profile and contour line of 10 l/s, H=4m and TW=0.25m

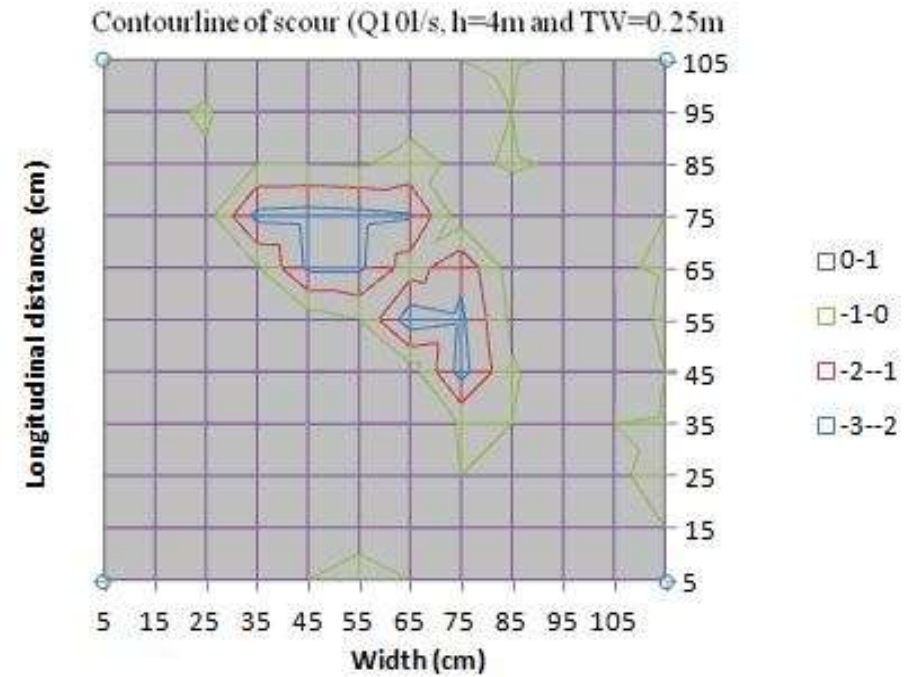
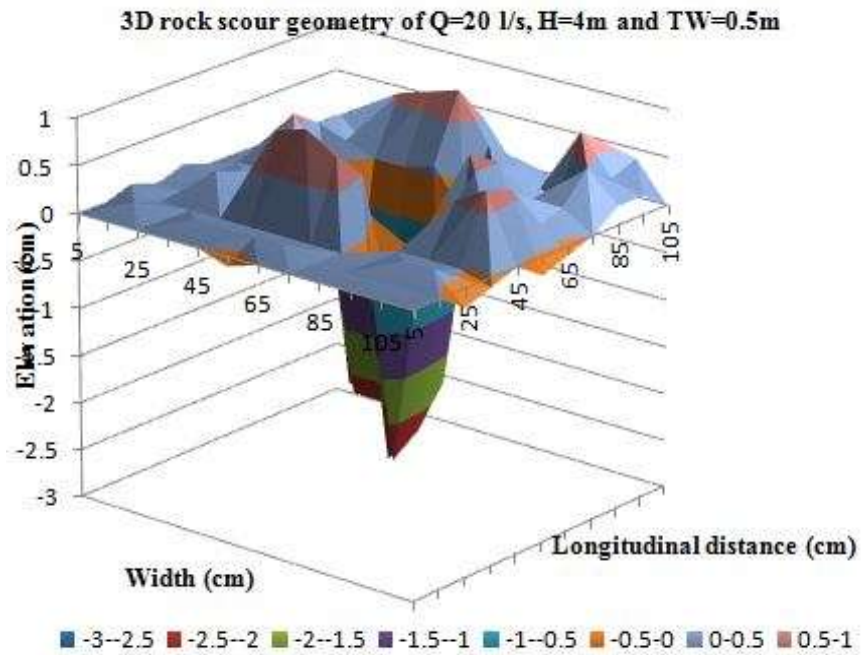


Figure F 0-5. Scour profile and contour line of 20 l/s, $H=4$ m and $TW=0.5$ m

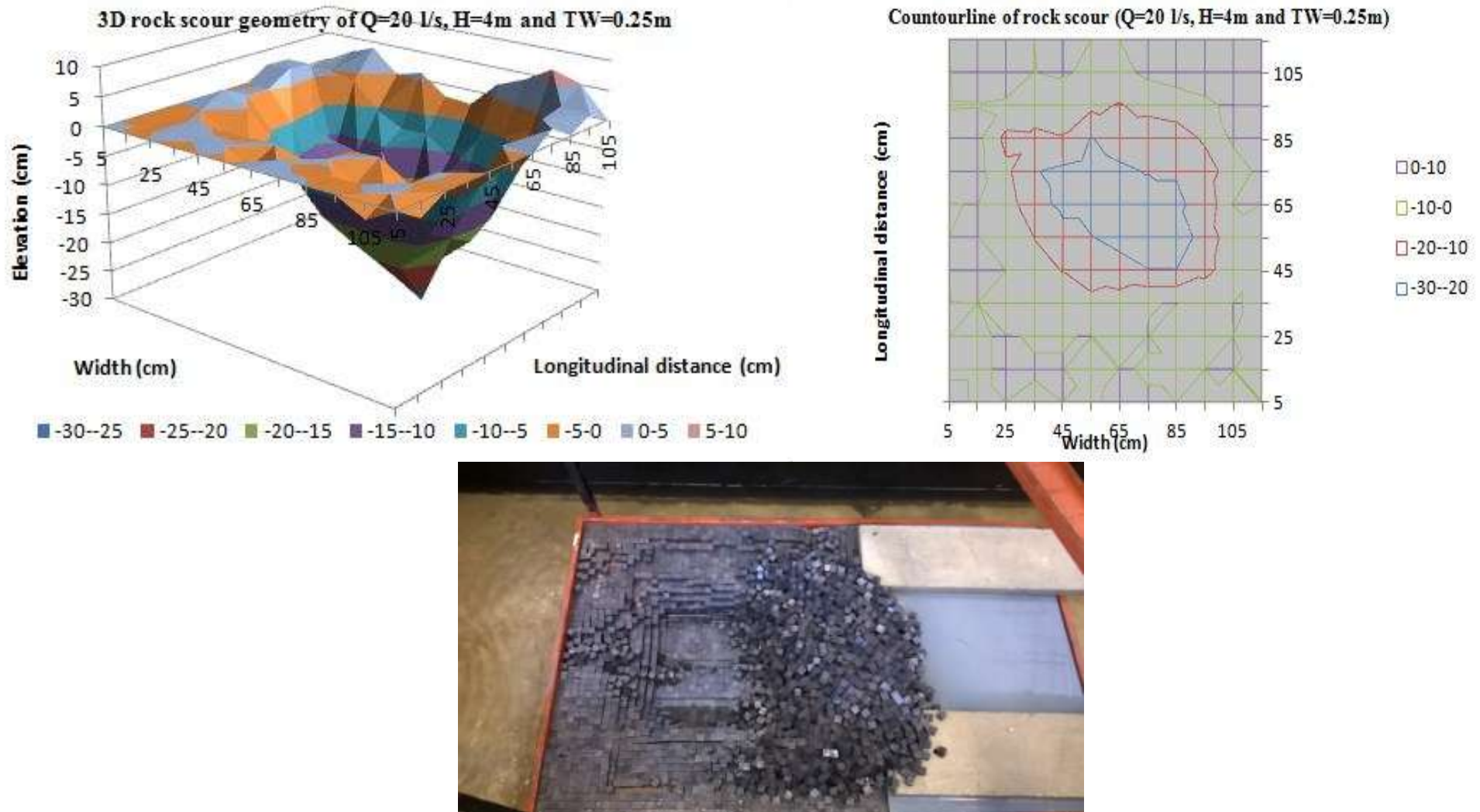


Figure F. 0-6. Scour profile and contour line of 20 l/s, H=4m and TW=0.25m

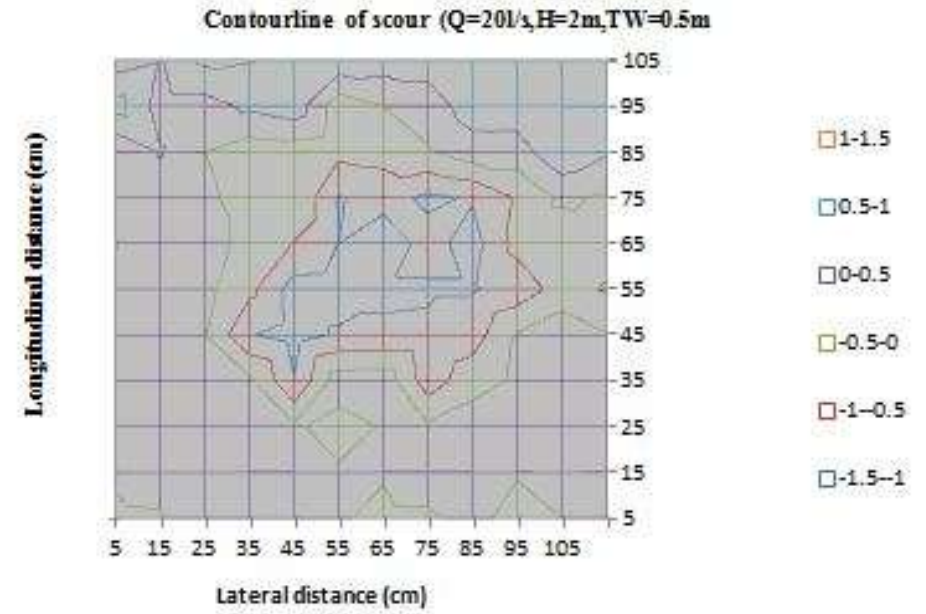
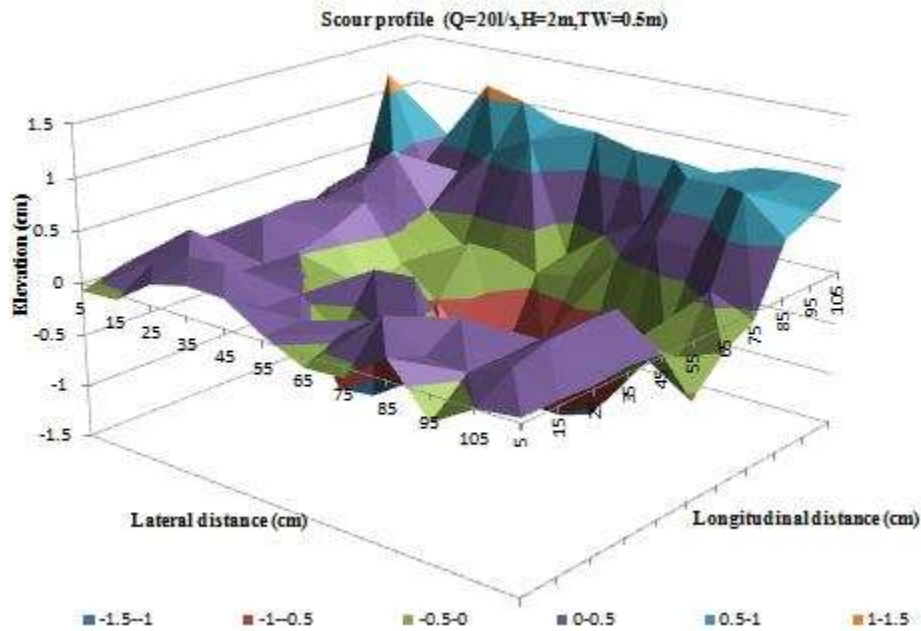


Figure F.0-7. Scour profile and contour line of 20 l/s, H=2 m and TW=0.5 m.

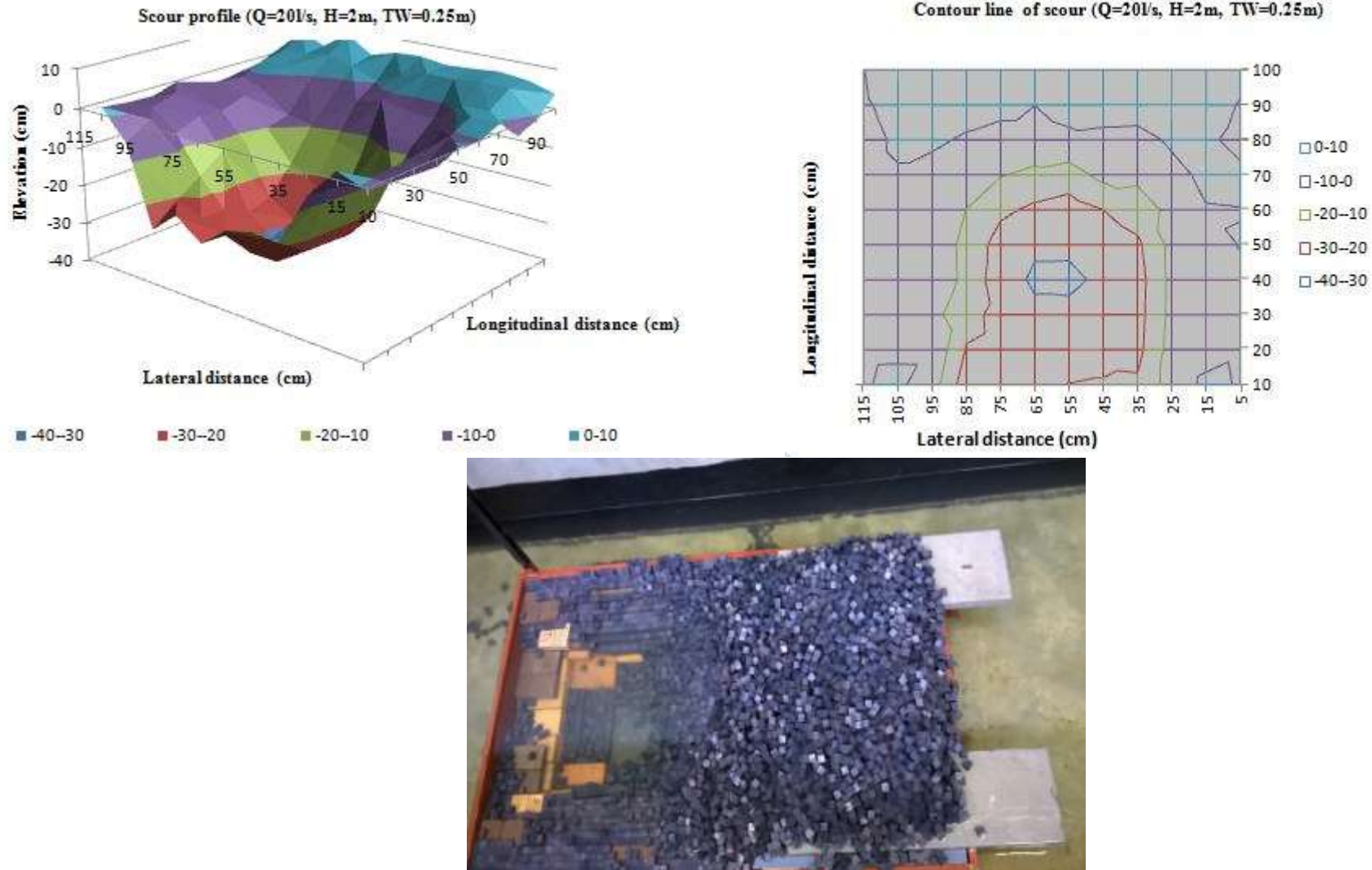


Figure F. 0-8. Scour profile and contour line of 20 l/s, H=2 m and TW=0.25 m.

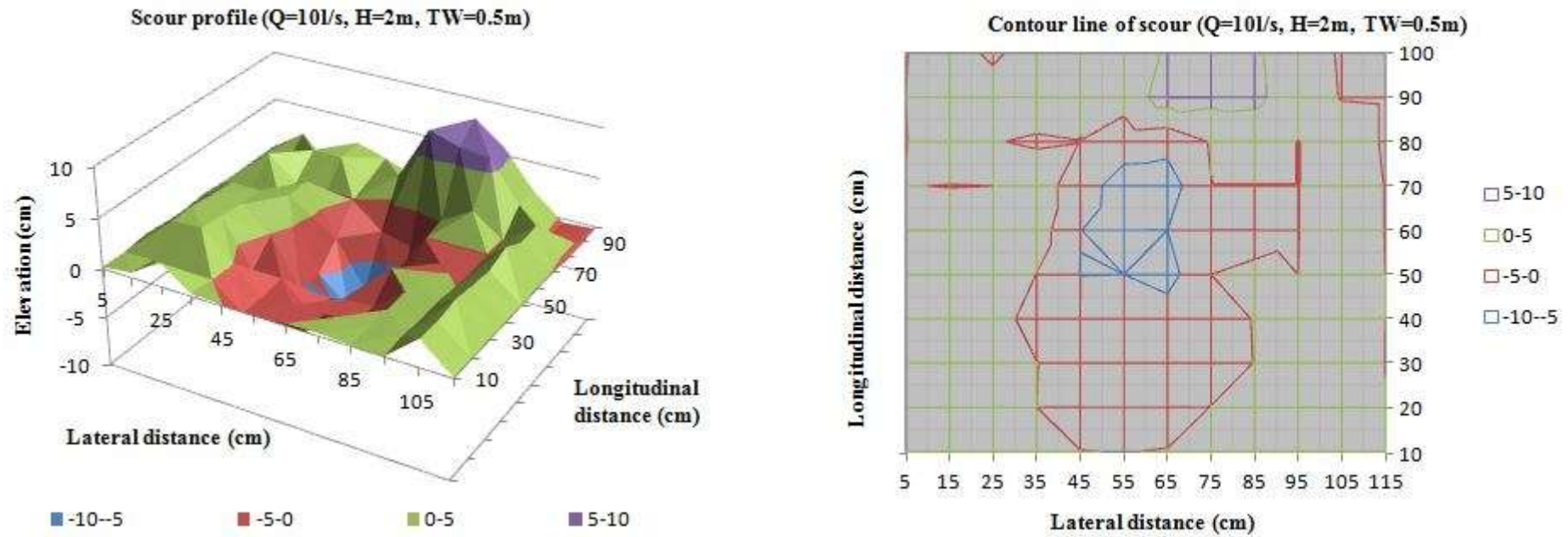


Figure F.0-9. Scour profile and contour line of 10 l/s, H=2m and TW=0.5m.

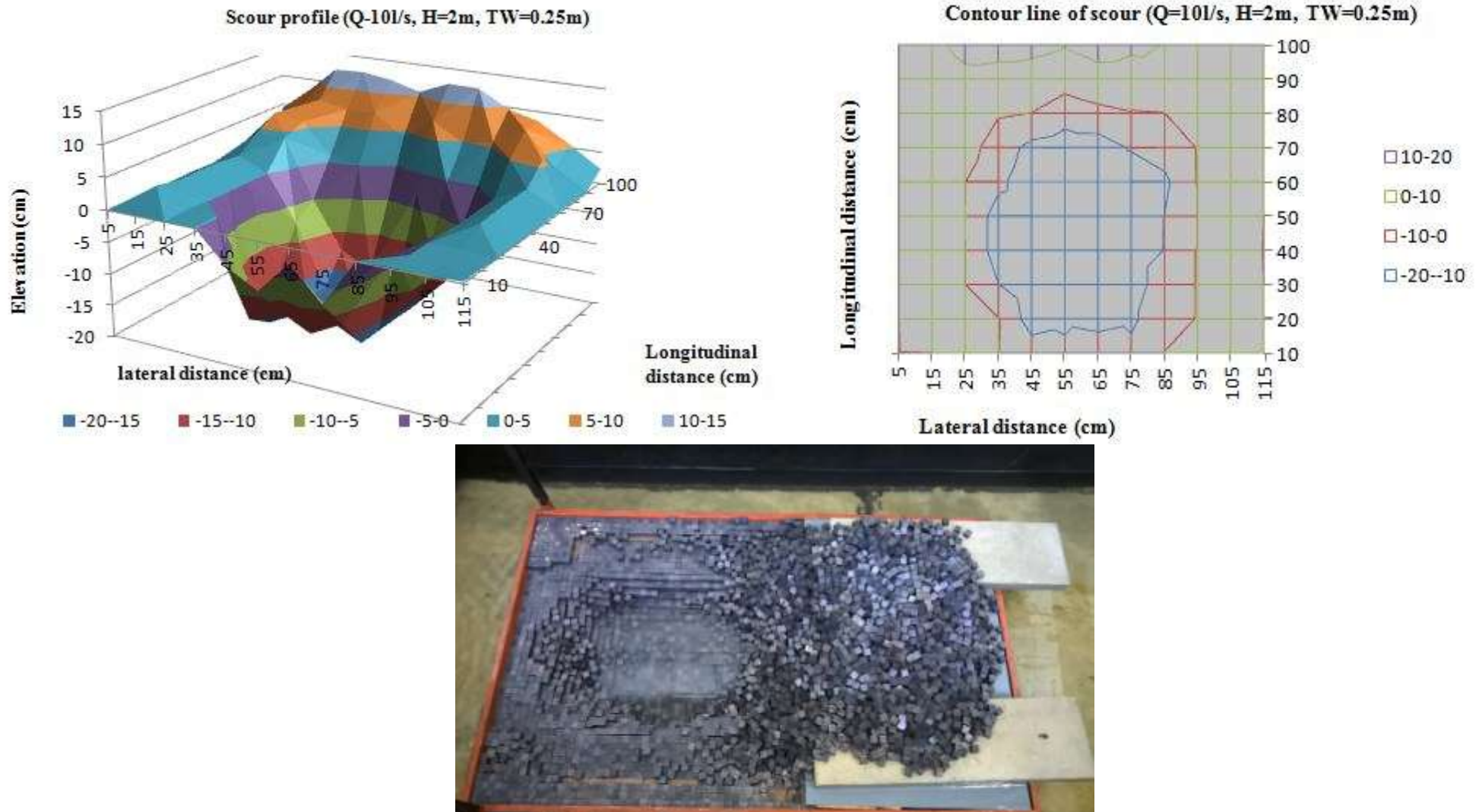


Figure F.0-10. Scour profile and contour line of 10 l/s, H=2m and TW=0.25m.